Finite element modelling of blowouts in compressed air tunnels

Peck, James G.

FINITE ELEMENT MODELLING OF BLOWOUTS IN COMPRESSED AIR TUNNELS

by

James G. Peck

A Thesis submitted for the degree of Master of Science

School of Engineering and Applied Sciences

The University of Durham
1990

Acknowledgements

I am most grateful to Prof. P.B. Attewell and Dr. D.G. Toll at the University of Durham for their valuable advice concerning various aspects of the project. I am indebted to the Committee of Vice Chancellors and Principals for the partial remission of tuition fees through the Overseas Research Students Awards scheme, and to Ian Farmer Associates Ltd., whose financial assistance made it all possible.

Principal symbols:

C	Depth of cover
c_u	Cohesive strength
c, ϕ	Shear strength parameters
c	Sonic velocity
c_∞	Far field sonic velocity
C_{d_i}	Incompressible coefficient of discharge
C_{d_c}	Compressible coefficient of discharge
D	a.) Tunnel diameter
	b.) Transmission constant
[D]	Matrix of first derivatives
E	Energy
e	Void ratio
F.O.S.	Overall factor of safety
f.o.s.	Factor of safety at a point
F.O.S.D.	Design factor of safety
G_s	Specific gravity
h	Potential head
i	Hydraulic gradient
J	Seepage force
j	Seepage pressure
K	Absolute coefficient of permeability
k	Effective coefficient of permeability
K_i	Permeability for incompressible flow
K_a	Permeability for air
k_r	Relative permeability
m	a.) Unit mass
	b.) Thermodynamic constant
m_a	Total stress ratio
m_w	Suction strength ratio
M_∞	Uniform mach number
N	Stability ratio
[N]	Interpolation function matrix
P	a.) Unsupported span
	b.) Absolute pressure
$\bar{P}$	Mean pressure
PBL	Pressure balance level
p,q	Stress invariants
Q	Fluid flux
q	Fluid flow
R	Universal gas constant
S_i	Irreducible saturation
S_r	Relative saturation
S_{r_u}	Residual saturation
T	a.) Absolute temperature
	b.) Surface tension
T_c, T_γ, T_s	Stability parameters
T_o	Tensile strength
u	Pore pressure
u_a	Pore air pressure
u_w	Pore water pressure
V_∞	Far field velocity
z_w	Depth below water table
z_r	River depth
z_s	Soil cover
γ	Unit weight
γ_w	Unit weight of water
ϵ	Expansion coefficient
θ	Contact angle
μ	Viscosity
Π	Potential energy
ρ	Fluid density
σ	Total stress
σ'	Effective stress
σ_a	Air pressure in tunnel
σ_s	Surcharge pressure
τ_f	Shear strength
ϕ	Fluid potential
$[\Phi]$	Potential matrix
$\{\phi\}$	Compressible nodal potentials
$\{\phi^{(0)}\}$	Incompressible nodal potentials
$\{\phi^{(1)}\}$	Compressibility correction
χ	Strength saturation factor
∇	Differential operator

Abstract

This study develops criteria for predicting blowouts in compressed air tunnels through an integrated design approach using empirical laboratory test data in a finite element model.

Compressed air tunnelling is first reviewed in the context of temporary works, and the relative merits of compressed air as a support system are compared with that of other methods commonly used. Design methods for estimating the stability of tunnel faces in general are discussed along with the particular problems of stability against a blowout.

The various mechanical processes that contribute to the formation of blowouts are then discussed, including unsaturated shear strength, desaturation processes, and seepage forces. A plausible mechanism which can be used analytically in studying blowouts is presented, whereby the flow of air desaturates the soil causing mechanical failure, which is the result of serious reductions in effective stress due to increased pore pressures and seepage forces. The failure self propagates with changes in the soil properties.

The permeability of soils with respect to compressible fluids is a complex property not only dependent on the soil properties but on fluid properties and pressures as well. Permeability with respect to air is presented as an empirical power function of pressure. Laboratory methods of measuring permeability with respect to air is discussed along with a description of all relevant apparatus.

A finite element package developed by NAg software was used as the basic model of potential flow. The model was adapted to account for the progressive desaturation of the soil and its influence on permeability. The model was also modified to account for compressible flow using the Rayleigh-Janzen method of

linearizing the compressible potential equation. The model was run for subaqueous tunnels of various diameters in sands of different silt contents beneath rivers of various depth. The amount of excess air pressure was varied and provision was made for a forepoling hood on the shield.

Results show compressible flow and incompressible flow are essentially the same except at the crown of the tunnel face. Blowouts demonstrate the unique feature of propagating from the surface down as well as from the tunnel up, a phenomenon which is attributed to high seepage forces and negligible total stresses at the ground surface. The overall factor of safety is most sensitive under shallow rivers, and critical tunnel depth is independent of river depth.

The data satisfy a linear relationship between critical depth and tunnel diameter, with smaller diameter tunnels requiring more cover relative to tunnel diameter than large diameter tunnels. The effect of a hood is most significant at high air pressures and in clean sands.

The critical tunnel depth is directly proportional to air pressure and is slightly more sensitive for small tunnels than for large tunnels. The critical depth generally is not influenced by silt content. A significant exception is a large drop in critical depth for silt contents between 5% and 10%.

The results of the study were summed up in a set of nomographs to provide practical aid to the design of tunnels against blowouts. They can be used to estimate safe cover depths and operating pressures, or to estimate factors of safety for a given set of operating conditions.

Contents

Chapter I

Introduction: The use of temporary works

1.1 Need for temporary works

When constructing tunnels two items that are commonly of fundamental importance are the control of groundwater and the support of the excavation face. This is particularly true in soil tunnelling where the face is characteristically unstable. Often it is necessary for the contractor to undertake special measures or temporary works to make ground conditions suitable for safe excavation.

Temporary works include a wide range of processes which are normally subcontracted out to specialists under the responsibility and risk of the contractor. As they are often employed outside the main tunnel contract, temporary works commonly become an issue of legal controversy between engineers and contractors. Although the main focus of this thesis concerns compressed air, it is important to understand the advantages and disadvantages of all the available methods in order to make proper judgements concerning ground support requirements. The primary methods used for tunnels in soft ground include dewatering, ground treatment, ground freezing, pipe piling, compressed air, and pressure balance shields (Haswell & Gutteridge, 1990).

1.2 Ground dewatering

With ground dewatering, the water table surrounding the tunnel excavation is lowered by pumping or other means. This lowering of the water table reduces the amount of pumping required in the tunnel, improves working conditions, and improves face stability by reducing water flow through the face. Dewatering is suitable for tunnels in permeable materials such as fine sands; however in very permeable materials the recharge to the dewatered area may be too large to be adequately dealt with by a dewatering program.

A serious drawback to dewatering is it accentuates consolidation settlement above and to the sides of the tunnel by increasing effective stresses upon dewatering. This can be controlled to some degree by recharging the water further away from the tunnel than the pumping wells, as shown in fig. 1.1. However lowering the water table should be avoided in areas which are sensitive to settlement such as urban areas or near large structures on clay rich or organic soils.

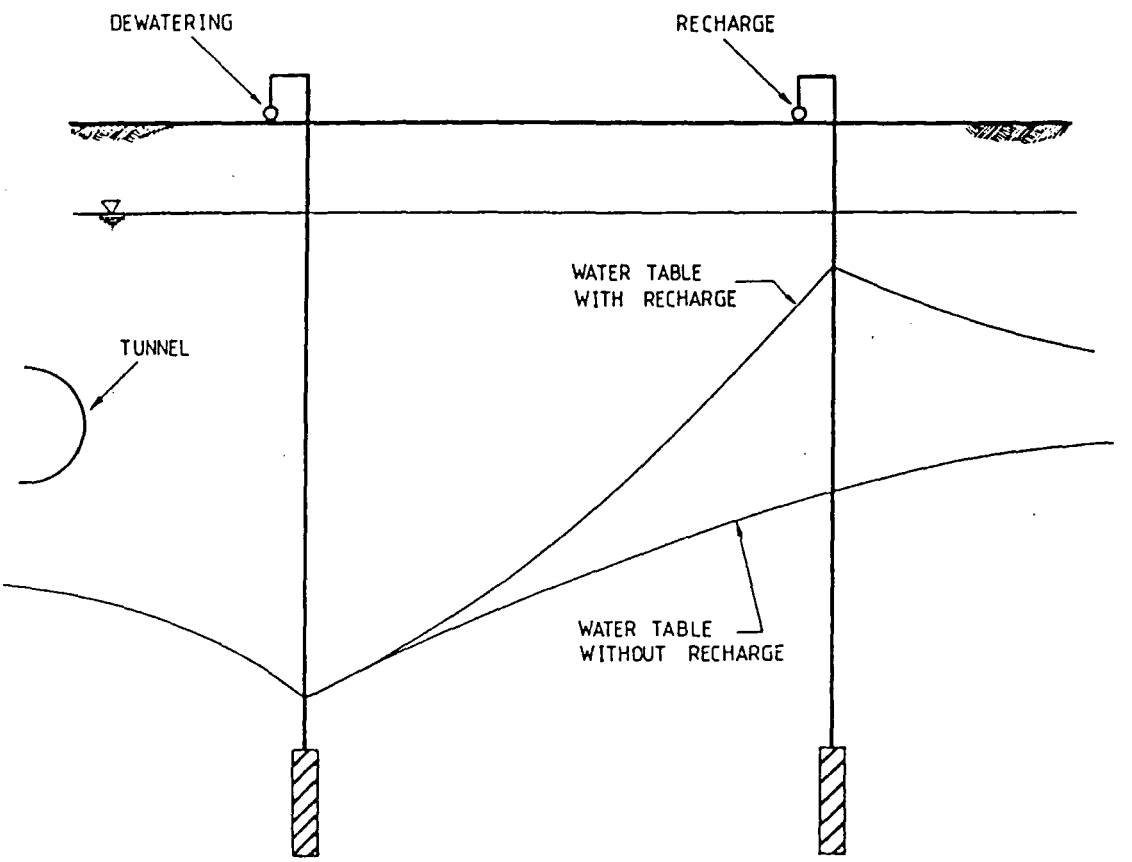

Figure 1.1 — Effects of dewatering on water table

1.3 Ground treatment

Ground treatment involves injecting a grout or other substance directly into the soil from a borehole to increase the strength and decrease the permeability of the medium. Several types of grout materials are available for different types of

soil conditions. For coarse granular soils and fissured rocks, cement based grouts mixed with fine sands are used, while for more silty materials various resin based and chemical grouts are available. Care must be taken when grouting very fine grained materials as fissuring which may actually increase the permeability of the ground can occur.

Grouting can be carried out from boreholes either within the tunnel or on the ground surface, where they won't interfere with other tunnelling works. There are several methods of grouting including stage grouting, point groutng, circulation grouting, and jet grouting.

1.3.1 Stage grouting

Stage grouting consists of dividing the soil into several substrata and grouting them sequentially. There are two ways of accomplishing this, either from the bottom of the hole up by packing off and grouting the lowest substrata and repeating for each substrata in the borehole, or from the top down by extending the borehole progressively after grouting each substata.

1.3.2 Point grouting

Point grouting is a cost effective method for grouting shallow depths by driving a lance and injecting grout as the lance is progressively raised. Point grouting usually requires close spacing patterns and is most effective when using chemical grouts.

1.3.3 Circulation grouting

This method employs a similar proceedure to stage grouting from the top down, where the grout is pumped down the grout pipe and returned up the drill hole reducing clogging (see fig. 1.2). The hole is then deepened and the procedure repeated.

1.3.4 Jet grouting

Jet grouting has the advantage over convential grouting methods by mixing the grout with the soil medium making the treatment much more thorough. Mixing

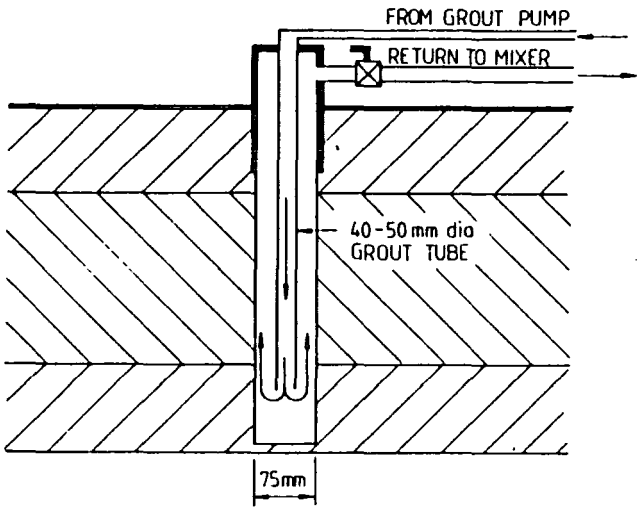

Figure 1.2 — Circulation grouting method

is accomplished by means of high pressure jet nozzles fixed on a drillpipe specially designed to convey pressurized air and water along with the grout fluid. The drill pipe is lowered to the bottom of the drillhole and slowly raised and rotated, with one jet of high pressure water cutting the soil and another jet 500 mm below the first supplying high pressure grout displacing the excavated material and forcing it to the surface (see fig. 1.3). Pillars of grouted material up to 1.5 m in diameter can be formed by jet grouting.

1.4 Ground freezing

Ground freezing provides support to the soil medium by freezing the water in the voids, converting it to the equivalent of a soft to medium strength rock. The process is carried out by circulating a primary or secondary brine coolant or liquid nitrogen through a system of tubes in the ground. Liquid nitrogen tends to be much more expensive than standard industrial coolants, but is much quicker requiring days as opposed to weeks to effectively freeze the ground, and can also be stored on site in pressure vessels, eliminating the need for a large refrigeration plant on site.

Ground freezing is typically used for short drives through very difficult material

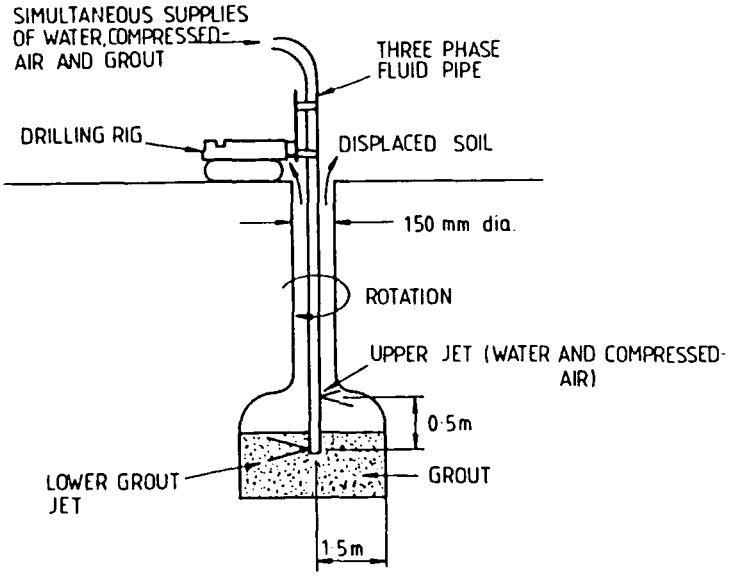

Figure 1.3 — Jet grouting method

as the method is usually too costly and time consuming for long drives. Ground freezing is particularly effective in silty materials which may be too fine for grouts to penetrate effectively. Excavation is best accomplished if the ground is not solidly frozen at excavation depth.

1.5 Pipe piling

Pipe piling is a recent development in temporary works being derived from pipe piling used in shoring operations. The method consists of driving pipe piles 20 cm or so in diameter horizontally along the crown of the tunnel. As the excavation proceeds, H-frames are installed to provide support to the piling arrangement (see fig. 1.4). The piles are often filled with concrete to provide additional stiffness to the system. Pipe piling is particularly useful when tunnelling beneath roads or other structures at shallow depths and for short distances.

1.6 Compressed air

Using compressed air represents a different theory of temporary works than the methods previously discussed. Where other methods try to alter the engineering

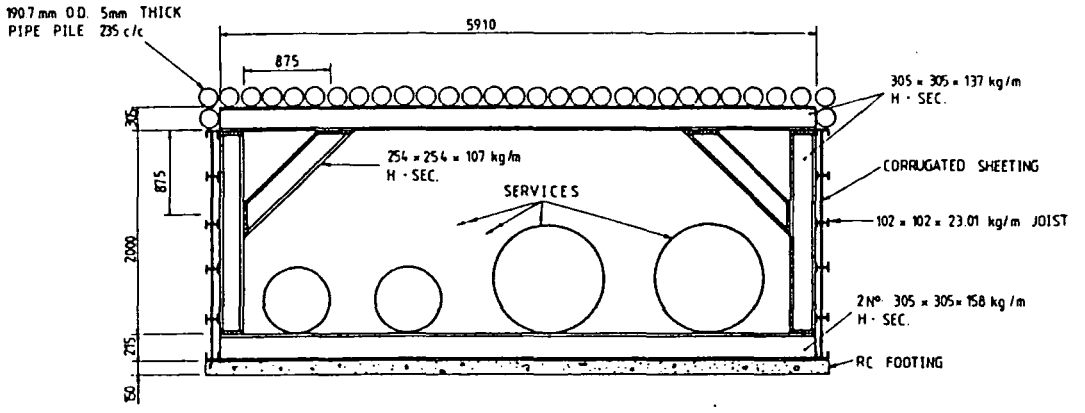

Figure 1.4 — Pipe piling arrangement

properties of the ground material immediately surrounding an excavation, compressed air provides support directly to the excavation face without deliberately altering the ground conditions. Compressed air can be used in a variety of soil types, from silts and clays to coarse sands. The method is primarily used to provide a balance to pore water pressure in saturated ground conditions, preventing excessive water inflow from the face. Thus, it is ideal for short subaqueous drives.

Compressed air complicates the logistics of tunnelling operations, as a pressure bulkhead must be installed through which all services must pass to and from the face. The bulkhead must be a sturdy structure, especially in large diameter tunnels as the large area of a bulkhead will usually be subjected to forces in the hundreds of tonnes. It is advisable to construct the bulkhead of concrete of thickness 0.4 to 0.6 times the tunnel diameter (Megaw & Bartlett, 1981). Except for small diameter tunnels under low air pressures, at least two air locks should be provided, one for materials and another for personnel. Often an emergency escape lock is provided for in as high a position as possible to provide an escape route in the event of a sudden inundation from the face (see fig. 1.5).

Also of engineering importance is the design of a compressor plant to ensure an adequate supply of compressed air. It is best to use an array of low pressure compressors both in series and in parallel to avoid sudden fluctuations in output due to equipment breakdown. The total amount of compressed air available from

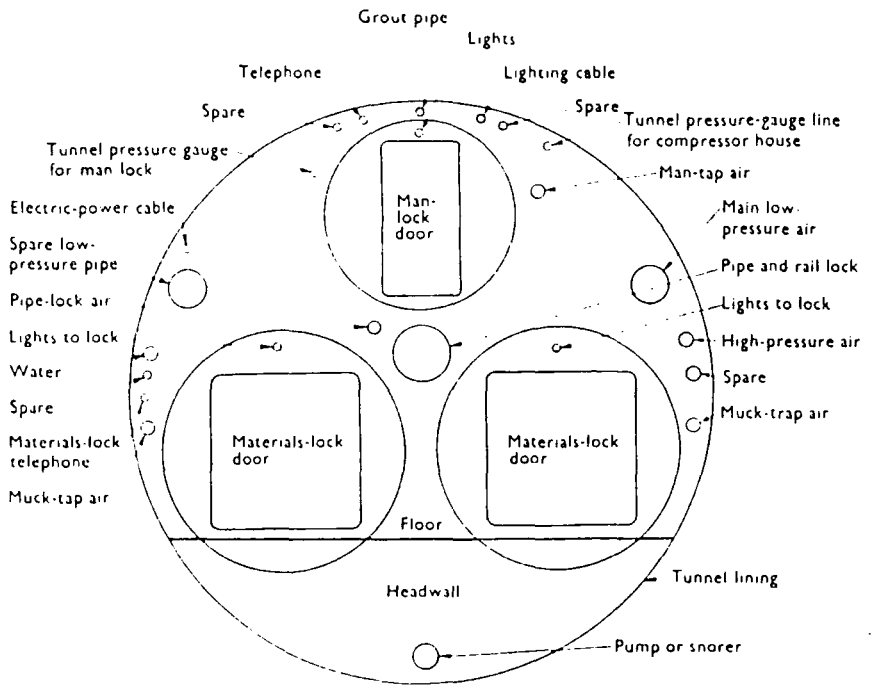

Figure 1.5 — Typical bulkhead lock arrangement

the plant should be adequate to ensure the maximum necessary pressure providing for air loss at the face and through the lining and bulkhead. A reservoir is often included to accommodate for changes in air loss (see fig. 1.6).

A possible physiological consequence of working in compressed air is decompression sickness or 'the bends', which is brought on by the formation of nitrogen bubbles in the blood stream which can occur when decompression is too sudden. To avoid decompression sickness the crew must undergo gradual decompression in an airlock. Under conditions of very high pressures a medical lock complete with trained staff may be required.

Technical problems associated with compressed air include the partial desaturation of the ground above the face which can lead to consolidation or collapse of swelling clays, and the possibility of blowouts, where due to excessive imbalance of supporting pressure, escaping air forms a channel to the surface causing a sudden loss of air pressure. A blowout will quickly remove supporting pressure and can result in collapse of the face and rapid inundation of the tunnel excavation.

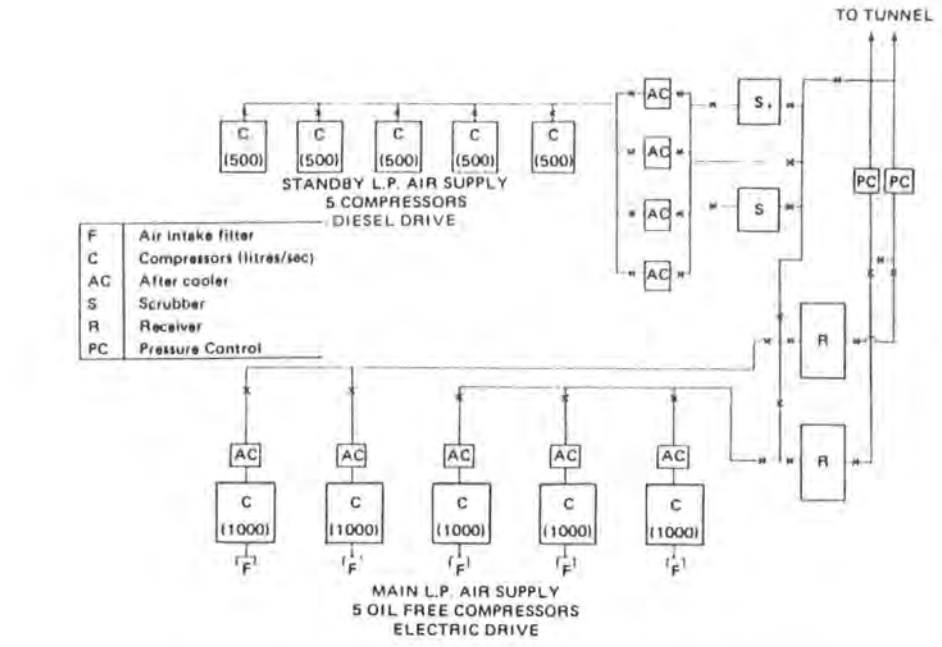

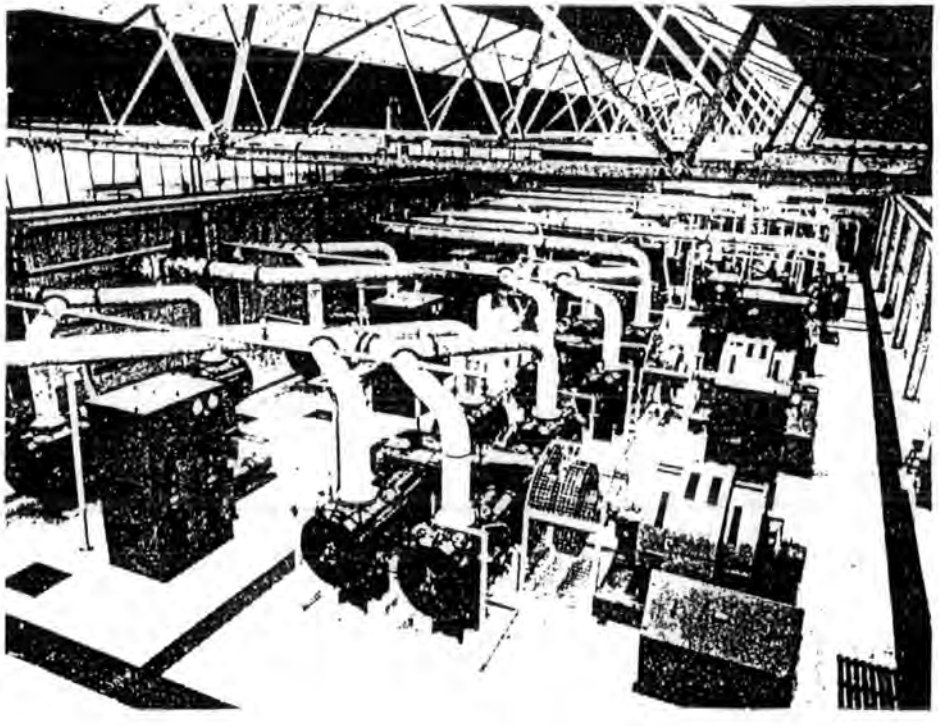

Figure 1.6 — Compressor plant design. (a) Standard array; (b) Typical compressor house

1.7 Pressure balance shields

In the late 60's, the Japanese began developing shields with a pressure balance

mechanism that more closely balances out the ground stresses in the face than compressed air. There are two basic pressure balance shield types, the bentonite slurry shield and the earth pressure balance shield. Both types of shield use a full face cutter head along with a slurry medium to support the face. With the bentonite slurry shield, pressurized bentonite slurry is injected through the bottom of a bulkhead into a chamber at the face providing a balancing force. Muck is removed as a slurry from the top of the chamber and pumped to the surface. The bentonite slurry shield is well suited for gravels and soft sands. The shield requires a slurry treatment plant on site, but creates free space in the tunnel by eliminating the need for muck haulage systems.

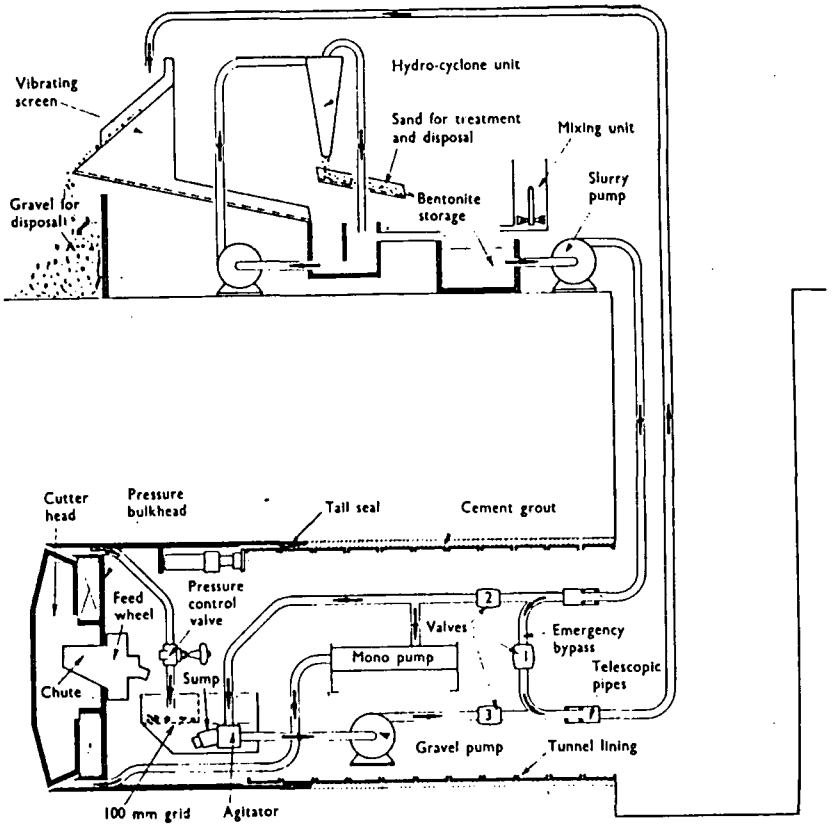

Figure 1.7 — Bentonite slurry shield

The earth pressure balance shield uses the same principle as the slurry shield, only the excavated earth is used as a supporting medium in the face chamber,

being removed from the face chamber via a screw conveyor at the same rate as material is excavated. Water is often added to ensure proper consistancy of the muck. Its use is limited to silty and clayey soils.

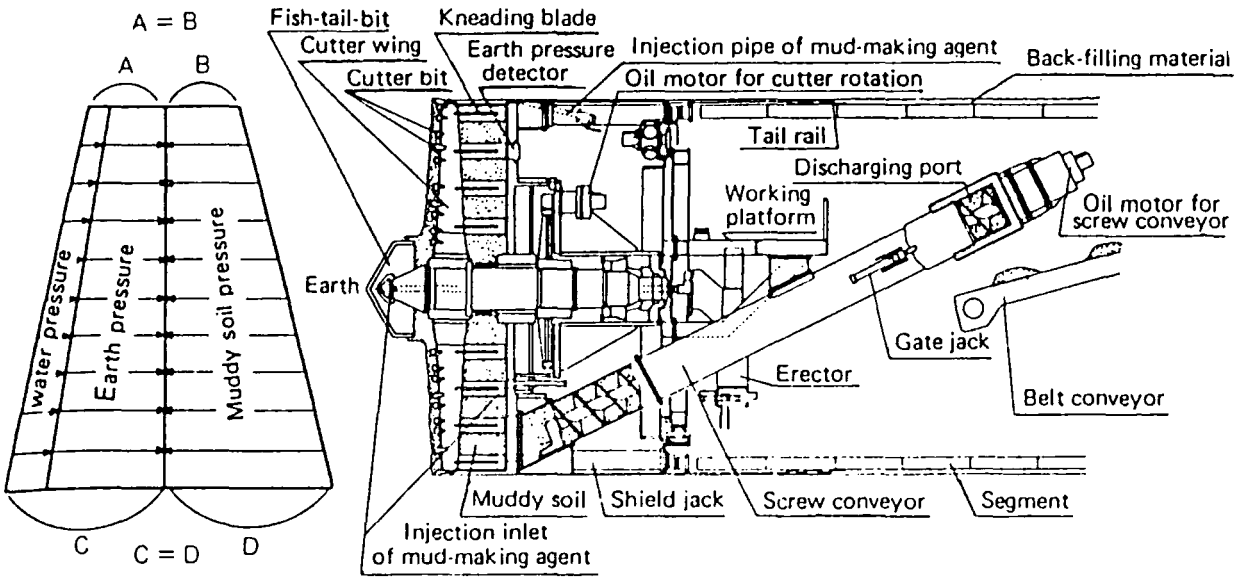

Figure 1.8 — Earth pressure balance shield

Chapter II

Stability of a tunnel face in compressed air

2.1 Pressure imbalance

As previously mentioned, compressed air as a temporary works measure is used to directly apply support to the tunnel face. However, not only does compressed air act to support the soil material in the face, it acts as a pore pressure effectively reducing the pore water pressure with an increased pore air pressure. A problem arises in that the air pressure is evenly distributed across the face of the tunnel whereas the pore water pressure increases linearly with depth, forcing an imbalance of pore pressures somewhere in the face. The level at which the two pressures balance out relative to the full tunnel diameter is known as the pressure balance level (PBL) (see fig. 2.1). If the PBL is low in the face, the tunnel will be kept reasonably dry but air will be lost through the upper portion of the face increasing the air consumption and the risk of a blowout. If the PBL is high in the face, water will be allowed to flow into the tunnel from the bottom of the face which could wash out ground material destabilizing the face and making lining operations at the invert more difficult. Thus it is important when constructing a tunnel with compressed air to choose an apppropriate PBL that consumes as little air as possible yet ensures the stability of the face.

2.2 Face stability against collapse

2.2.1 General principles

In determining what air pressures should be used during construction it is important to determine the stability of the tunnel face and what air pressures will be necessary to prevent collapse as well as the maximum pressures allowable to avoid the possibility of a blowout. In analysing the stability of the face against collapse, various methods have been developed according to material type, drainage conditions, and mechanism of failure. Some of the methods relevant to compressed

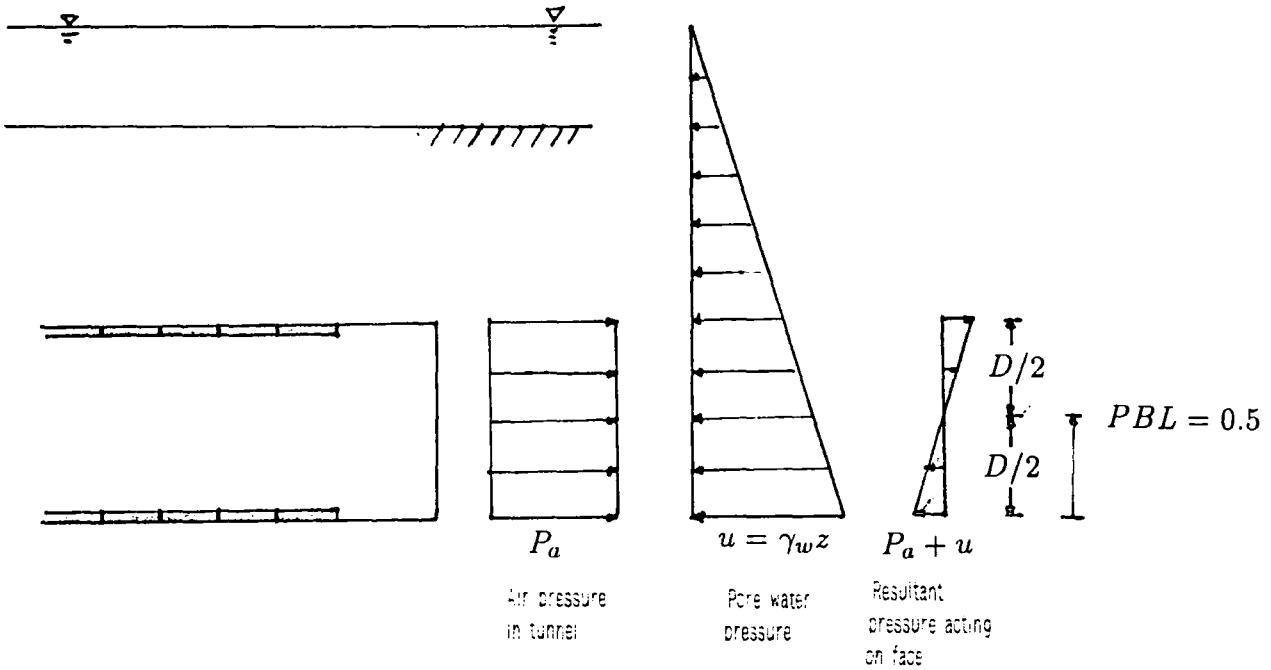

Figure 2.1 — Illustration of the pressure balance level, PBL

air tunneling will be discussed using a standard dimensional reference as shown in fig 2.2 with D being the tunnel diameter, C the depth of cover, P the unsupported span in cohesive soils, and σ_T the air pressure applied to the face.

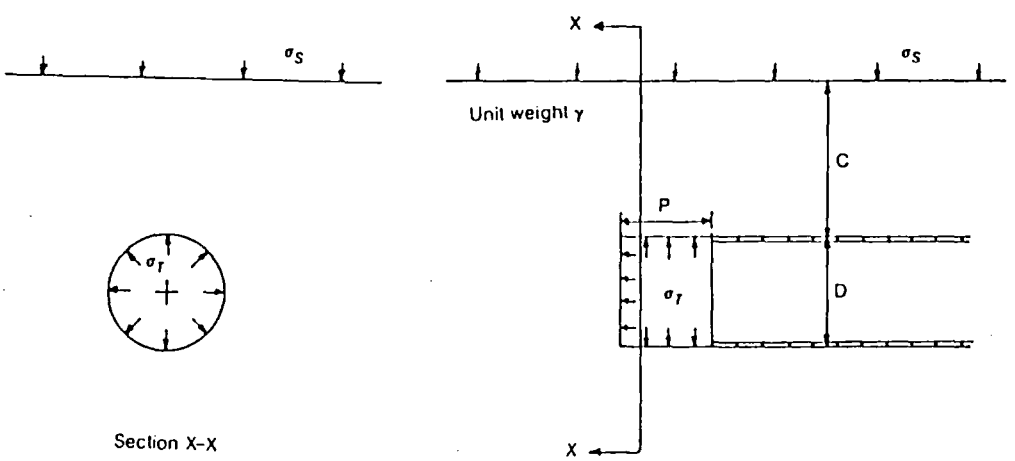

Figure 2.2 — Dimensions used in stability analyses

2.2.2 Limiting bound solutions

Davis et. al. (1980) presents a method of determining support requirements for a tunnel in cohesive material in undrained conditions. A dimensionless stability ratio N is used for determining necessary air pressure as defined by Broms and Bennermark (1967)

$$N = \frac{\sigma_s - \sigma_T + \gamma(C + D/2)}{c_u}. \tag{1}$$

The method approaches the problem using both the lower and upper bound limiting theorems of plasticity to bracket a true solution. The lower bound theorem states that if a given applied stress field supports the loads without yield being exceeded at any point in the system, then the applied stress field is equal to or greater than what would prevent collapse, and is hence conservative. The upper bound theorem states that the support loads deduced from a mechanism will be equal to or lower than what would be required to prevent collapse, and so would not provide a safe solution.

Two stress fields are analysed for the lower bound solution. In the first case, the soil is treated as a thick cylinder with an inner diameter equal to the tunnel diameter and an outer diameter equal to the tunnel depth $C + D/2$ (see fig. 2.3a). The internal pressure in the cylinder normal to the axis is $\sigma_T + 2c_u$ and external to the cylinder is an isotropic stress field σ_s equal to any surface surcharge (fig 2.3a). The lower bound solution for the stability ratio in this case is

$$N = 2 + 2\ln\left(\frac{2C}{D} + 1\right). \tag{2}$$

In a second case, the soil is treated as a thick sphere of the same dimensions (fig 2.3b). The resulting solution for stability ratio in this case is

$$N = 4\ln\left(2\frac{C}{D} + 1\right). \tag{3}$$

For an upper limit solution, a mechanism of sliding blocks of soil with elliptical cross sections as shown in fig. 2.4 is used in the work energy calculations from which

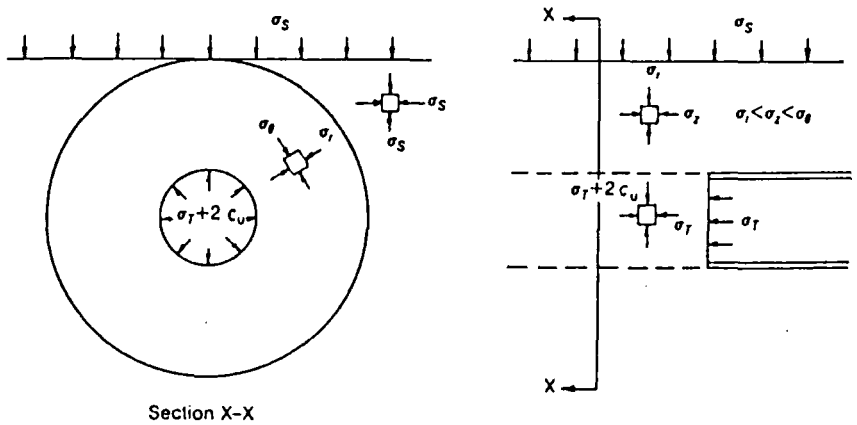

Figure 2.3 — Face stability - Lower bound solution stress fields

a solution for stability ratio can be defined by optimising the three variable angles α, β, δ.

The solutions for these cases is plotted in fig. 2.5. As can be seen, there is a large gap between upper and lower bound solutions which results from the three dimensional approach in the limiting theorems. It can also be seen that the thick cylinder offers a better lower bound solution for shallow tunnels where $C/D < 0.86$ whereas the thick sphere is a better approximation for deeper tunnels.

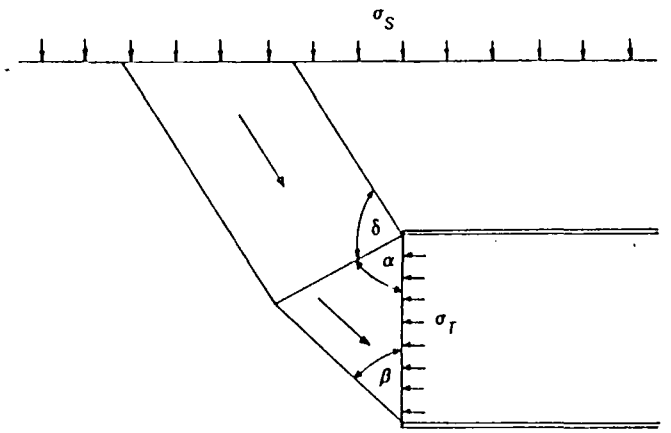

Figure 2.4 — Face stability - Upper bound mechanism

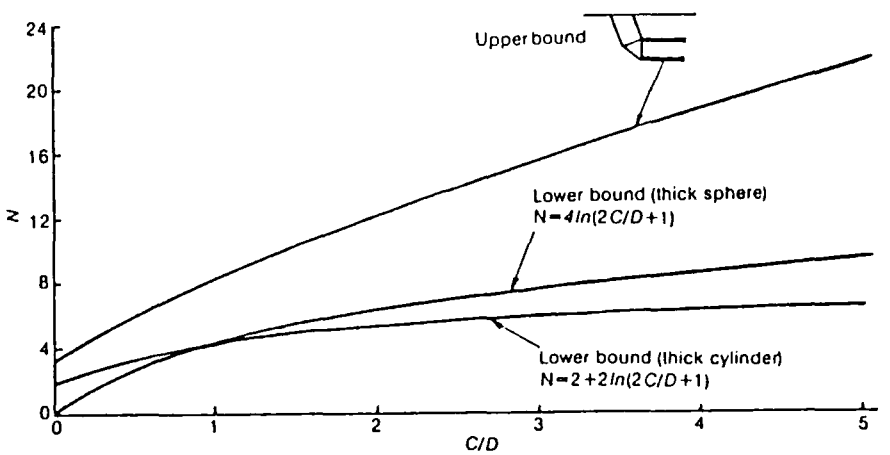

Figure 2.5 — Stability solutions using limit theorems

2.2.3 Coefficient factors

Atkinson and Mair (1981) present a method of analysing the stability of the face in terms of coefficient factors T_c, T_γ, and T_s which are analogous to the bearing capacity factors N_c, N_γ, and N_q derived from Prandtl's experiments in metal punching which are described in most soil mechanics and foundations text books (e.g. Craig 1987; Smith & Pole 1980).

For fine grained clayey soils, the stability analysis is carried out in terms of the

undrained shear strength, c_u. To achieve a factor of safety F_s against face collapse the required air pressure is given by

$$\sigma_T = \sigma_s - \frac{c_u}{F_s} T_c + \frac{1}{2}\gamma D \left(1 + \frac{2C}{D}\right) \tag{4}$$

where T_c is a dimensionless tunnel stability number for cohesive soils and the other terms are as defined in fig. 2.2. Values of T_c for circular tunnels were determined experimentally by Kimura & Mair (1981) using centrifuged models, which are plotted in fig. 2.6 for various ratios of P/D and C/D.

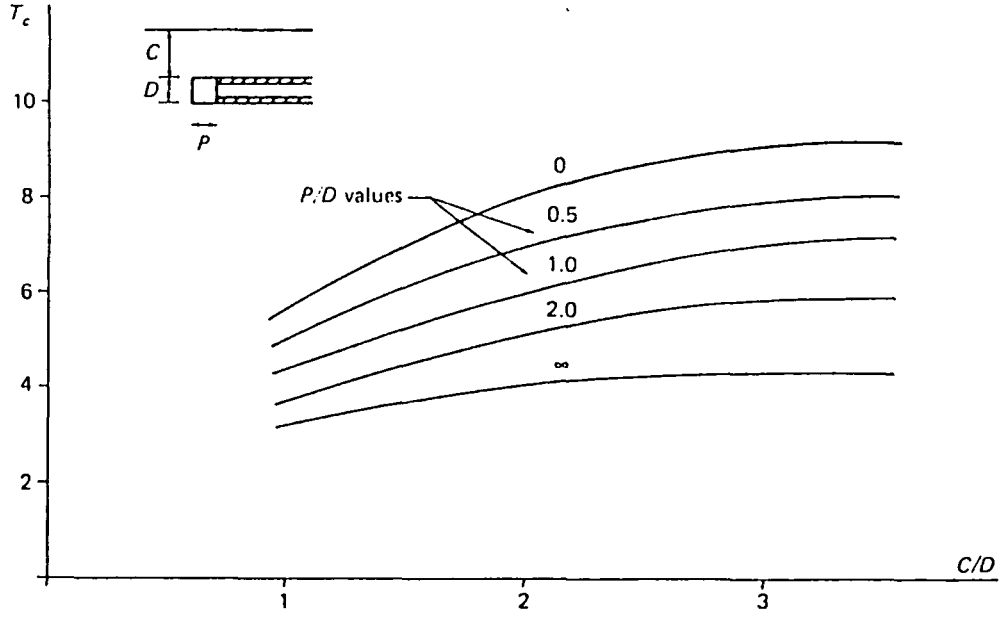

Figure 2.6 — Values of coefficient factor T_c

For coarse grained soils in drained conditions the analysis is presented in terms of either T_γ or T_s. T_γ is used in the case of dry soil with $\sigma_s = 0$ and depends only on the soil strength and is independent of tunnel depth. The required air pressure in this case is

$$\sigma_T = \gamma D T_\gamma. \tag{5}$$

T_s is used when there is a large surcharge on a shallow tunnel where the weight of the soil can be neglected, and is dependent on both soil strength and tunnel

depth. In this case the required air pressure is

$$\sigma_T = \sigma_s T_s. \tag{6}$$

Values of T_γ and T_s are given in fig.2.7. Note both T_γ and T_s are independent of span P, as a cohesionless material is incapable of supporting a span.

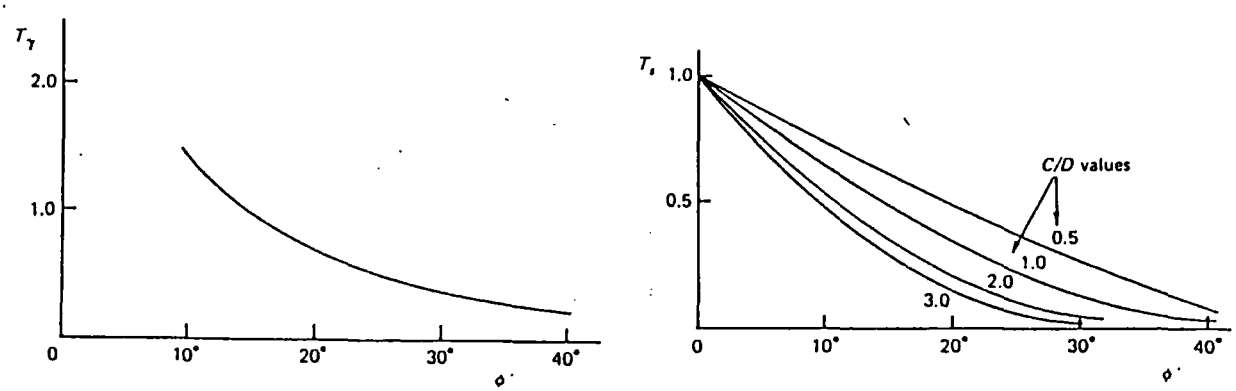

Figure 2.7 — Values of coeffecient factors T_γ and T_s

2.3 Face stability against blowouts

2.3.1 Nature of blowouts

There has been little research done to date on the stability of a face against blowouts. In fact it is not clear exactly what a blowout is or how they occur. A simple definition that would suit all descriptions of a blowout would be a sudden loss of air escaping from the tunnel face to the ground surface with a corresponding loss of face stability with the possibility of collapse and inundation of the excavation. The exact mechanism by which this occurs is not well understood. Pequignot (1963) describes a blowout as the result of piping caused by excessively high gradients of escaping air washing out a highly permeable channel or system of channels to the surface. Once a channel has been established the situation becomes increasingly worse as larger volumes of air flow through the channel until the air

the air pressure in the excavation is reduced to a point where the high flow gradients cannot be maintained and the channel collapses in on itself. Szechy (1973) describes a blowout in mechanical terms, where high air pressures in the crown of a tunnel with insufficient cover actually bursts out to the surface. Megaw and Bartlett (1981) attribute the forming of a channel to the expansion of the air escaping from the tunnel under high pressures, displacing water and fine material in the pore spaces.

2.3.2 Blowout occurrence

Blowouts are most frequent on river crossings, where often the tunnel is shallow and the cover soil is a permeable sand of various grades with high pore water pressures. Often the blowout will be associated with unforseen or unheeded ground conditions. Frequently along a river bottom ancient stream channels will cause sudden thinning of stable cover reducing the effective depth of the tunnel. In the case of the pilot tunnel for the first Dartford tunnel, a series of blowouts occured, apperently caused by piping through the vertical boreholes which were drilled for the site investigation along the tunnel line and never backfilled (Kell, 1963). In constructing the Clyde tunnel, a major blowout occurred when tunnelling beneath a ferry recess on the north side of the river which was constructed with timber piles, providing an ideal passage for escaping air. The blowout formed a large crater on the river bottom and inundated the works with 200 cu. yds. of silt and set progress back three and a half months (Haxton & Whyte, 1965).

2.3.3 Emergency measures

Often a blowout will provide some warning signs in which a short time is available to provide remedial measures. The most obvious will be a sudden loss of air pressure with a rushing breeze at the face. Often a whistling sound is heard, and a mist may form along with condensation. Immediate countermeasures include reducing the air pressure, advancing the shield, and covering the face, particularly the crown. This can be extremely dangerous as blowouts have been known to suck men and materials up into the void created. If the face collapses, it often does so suddenly and violently and can quickly inundate the excavation with soil and

water. For this reason an emergency air lock should be provided at a high level in the bulkhead where it is less vulnerable to being sealed in by debris.

2.3.4 Previous research

German engineers have made some effort to provide guidelines for safe cover for compressed air tunnels. Nussbaumer (1990) cites Scherle as recommending that compressed air tunnels lie at least one half a tunnel diameter beneath the water table. Szechy (1973) describes work done by Schenck and Wagner (1963) on the time delays involved in the drying out of the soil by compressed air in which some reference is made to stability against blowouts. They recommend a cover of twice the tunnel diameter in coarse grained permeable ground and one tunnel diameter in fine grained soil of low permeability. In the case of coarse soils, the amount of cover can be reduced to one tunnel diameter by provision of either a graded filter or impermeable clay blanket 1 m thick by 6 tunnel diameters wide on the surface (see fig 2.8). The graded filter is suggested to control the exit gradient at the surface, whereas the clay blanket forces the air to percolate a greater distance reducing its seepage velocity. Hewett and Johannesson (1922) made a similar recommendation suggesting the thickness of the impermeable clay blanket be one half the tunnel diameter.

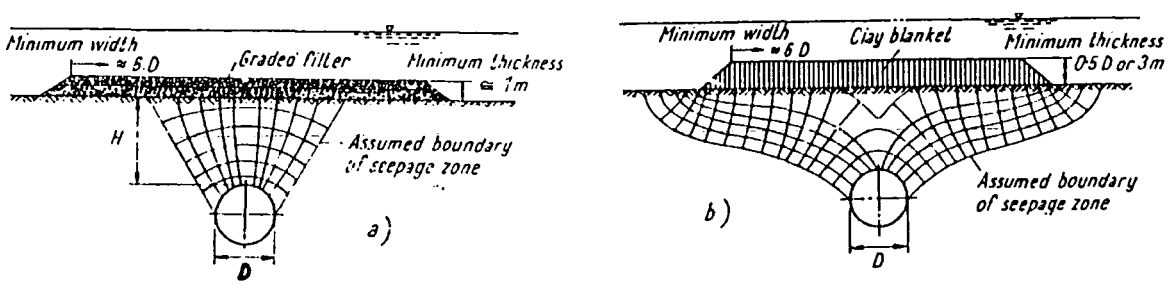

Figure 2.8 — Application of a safety blanket

2.3.5 Objectives of this research

It is the objective of the research described in this report to develop a method of predicting the occurrence of blowouts for subaqueous tunnels. The project

included the development of a plausible mechanical model of a blowout and the use of numerical methods to simulate blowouts with a computer. From the results obtained in computer simulation, quantitative estimates were made of the stability for various tunnelling conditions along with qualitative observations of the results as to the nature of blowouts.

Chapter III

Blowout modelling

3.1 General approach

As was previously mentioned, the actual mechanism wherby blowouts occur is poorly understood. In this chapter, a plausible mechanism is developed which is readily adaptable to numerical modelling. The method uses a combination of the likely mechanisms described in 2.3.1, namely piping due to gradients, mechanical force, and volumetric expansion of the escaping gasses. Standard principles of soil mechanics, hydrology, and fluid mechanics are used to approach the problem analytically in a manner suitable for computer modelling.

3.2 Principle of effective stress

A fundamental concept of soil mechanics is that of effective stress first recognized by Terzaghi. The principle applies only to fully saturated soils and recognizes three dependent stresses on a given plane in an element of soil. The total normal stress (σ) is the total force per unit area normal to the plane of interest imagining the soil to be a homogeneous solid. The pore water pressure (u) is the pressure of the water in the void spaces. Pore pressure is hydrostatic and if void spaces are continuous is equal to the weight of the water column, $\gamma_w z$, where γ_w is the unit weight of water and z is the depth below the water table. The effective normal stress (σ') is the stress transmitted through the skeleton of soil particles (see fig. 3.1). The stresses are related in Terzaghi's equation

$$\sigma = \sigma' + u \tag{7a}$$

or as is most common, to make effective stress the dependent variable

$$\sigma' = \sigma - u. \tag{7b}$$

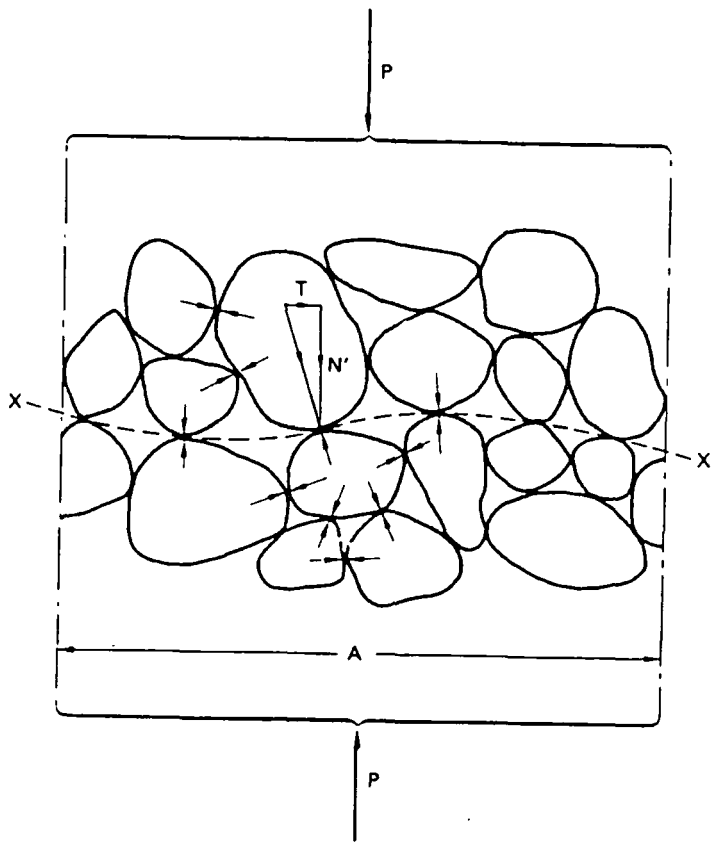

$$\sigma = \frac{P}{A}$$

$$\sigma' = \sum N'/A$$

$$u = \gamma_w z$$

Figure 3.1 — Illustration of effective stress

3.3 Soil strength

It is common practice in soil mechanics to represent the mechanical strength of a soil in terms of its shear strength (τ_f). If on any plane in a soil mass the shear stress equals the shear strength, failure occurs at that point. Shear strength is generally modelled as a linear relation of the normal stress (σ_f) to the plane in question

$$\tau_f = c + \sigma_f \tan \phi \tag{8}$$

where c and ϕ are shear strength parameters cohesion and angle of shear resistance, respectively. Since only the skeleton of solid particles offers resistance to shearing,

shear strength is commonly referred to in terms of effective stress

$$\tau_f = c' + \sigma'_f \tan \phi' \tag{9}$$

where c' and ϕ' are the effective strength parameters.

The effective shear stress and normal stress on any given plane is obtained from the equations of the Mohr circle representing the state of stress

$$\tau_f = \frac{1}{2}(\sigma'_1 - \sigma'_3) \sin 2\theta \tag{10}$$

$$\sigma'_f = \frac{1}{2}(\sigma'_1 + \sigma'_3) + \frac{1}{2}(\sigma'_1 - \sigma'_3) \cos 2\theta \tag{11}$$

with θ being the angle of the plane of interest from the direction of application of σ'_3, where $\theta = 45° + \phi/2$ at failure conditions.

If the maximum shear stress in a soil is less than the soil's cohesion, c', then the soil will be subjected to tensile stresses if the effective stress goes below zero. This occurs when pore pressures exceed the total stresses, and the failure criterion is normally defined by a tensile strength T_o, which is usually insignificant except for highly cohesive soils.

3.4 Unsaturated soil strength

When developing a mechanical model of a blowout, the soil cannot be treated as saturated since the air flow through the soil must take up some portion of the void space. Thus the plane shown in fig. 3.1 will pass through air as well as water and intergranular contacts, as shown in fig. 3.2. As air is compressible, this greatly influences the effective stress.

The first attempt to explain shear strength behaviour of unsaturated soils was done by Bishop (1959) who included a term for suction in the equation for effective stress

$$\sigma' = \sigma - u_a + \chi(u_a - u_w) \tag{12}$$

where u_a is the pore air pressure, u_w the pore water pressure, $u_a - u_w$ the suction in the soil, and χ a factor related to the degree of saturation. For a fully saturated

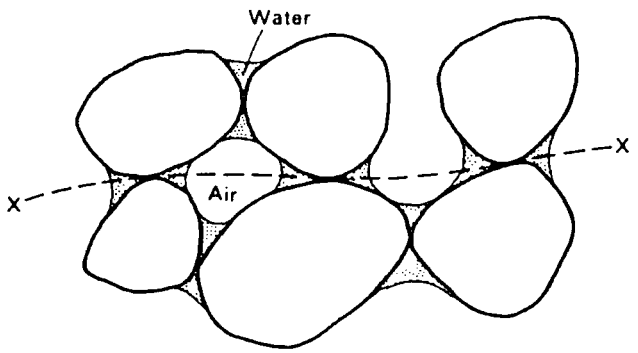

Figure 3.2 — Illustration of effective stress in a partially saturated soil

soil $\chi = 1$ and for a dry soil $\chi = 0$. Determining values of χ is difficult, and in practice χ is often assumed to be the average proportion of water for any cross section in the soil.

While Bishop's method of modifying the effective stress equation appears to satisfy unsaturated shear strength behavior, it has been criticized for not accounting for volume change behavior. Fredlund, Morgenstern and Widger (1978) modified the shear strength equation directly to

$$\tau = c' + (\sigma - u_a)\tan\phi' + (u_a - u_w)\tan\phi^b \tag{13}$$

where τ is the shear strength, c' the effective cohesion, ϕ' the angle of friction for changes in $\sigma - u_a$, and ϕ^b is the angle of friction for changes in $u_a - u_w$.

Toll (1990) presents a method of approach based on stress invariants p and q where

$$p = \frac{\sigma_1 + \sigma_2 + \sigma_3}{3} \tag{14}$$

$$q = \sigma_1 - \sigma_3 \tag{15}$$

from which he obtained the relation

$$q = m_a(p - u_a) + m_w(u_a - u_w) \tag{16}$$

where m_a is the total stress ratio and m_w is the suction stress ratio, both of which are dependent on the degree of saturation.

As can be seen from all these approaches, to develop a realistic strength criterion for a blowout, some means of estimating the excess air pressure in the soil as well as the amount of desaturation caused by escaping air is needed.

3.5 Desaturation

3.5.1 Processes of desaturation

Toll and Hight (1990) list four main processes by which an initially saturated soil can desaturate: gas entry, cavitation, gas ex solution, and gas generation. *Gas entry* involves the replacement of pore water by air resulting in a type of drainage. Gas entry is controlled by the difference between the pore water pressure and the pore air pressure. *Cavitation* involves the formation of vapour bubbles caused by negative pore water pressures in the soil. *Gas ex solution* results when the pore water pressure is reduced due to a drop in overpressure forming bubbles of gas which previously were dissolved in the higher pressure pore water. *Gas generation* is caused by chemical interactions between the pore water and various mineral constituents in the soil which often results in the formation of gases in the reaction products.

Of these four processes, gas entry is the most relevant to desaturation from compressed air workings and will form the theoretical basis used for modelling blowouts.

3.5.2 Capillarity and surface tension

The adhesive and cohesive properties of water result in the properties of capillarity and surface tension, two processes which, when combined, allow suction which is a pressure difference across the interface between pore air and pore water, $u_a - u_w$.

Capillarity results from the greater adhesive affinity water has for soil particles as opposed to air. This produces a characteristic contact angle, which defines the geometry of a junction of a soil particle with an air-water interface (see fig. 3.3).

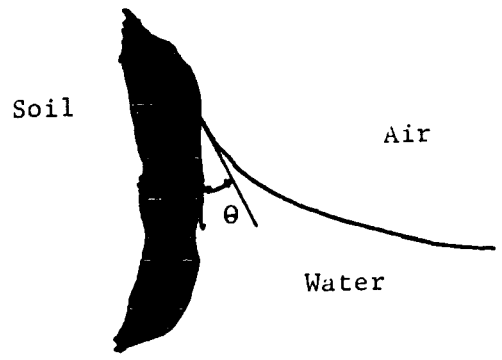

Figure 3.3 — Contact angle from capillary force

Surface tension is the result of an imbalance of molecular forces acting on the water molecules at the air-water interface. This results in a specific energy on the surface, and allows a pressure difference across the surface by the formation of a meniscus of radius r as is shown in the pressure balance diagram fig. 3.4.

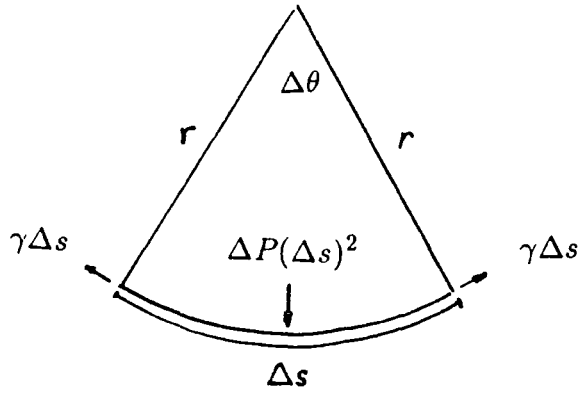

$$\Delta P(\Delta s^2) = 4\gamma \Delta s \sin \Delta\theta$$

$$u_i - u_w = \Delta P = 2\gamma / r$$

Figure 3.4 — Free body diagram illustrating surface tension

From fig 3.4 it can be seen that the maximum sustainable pressure difference is proportional to the surface tension and inversely proportional to the radius of curvature of the meniscus.

Hence, desaturation is dependent on the contact angle from capillary theory and the radius of curvature of the meniscus formed from surface tension. This suggests the size and shape of pores in the soil are major parameters affecting the process of desaturation. If the pressure difference requires a meniscus with a radius of curvature less than the minimum radius of curvature for the void, the water-air interface cannot be maintained and the pore will be drained (see fig. 3.5).

a.) At low suction, all entries to pore space able to maintain menisci of minimum radius of curvature.

b.) With increased suction, surface tension unable to mantain a meniscus across larges pore opening - pore drains.

Figure 3.5 — Air entry into pore spaces

Also influencing the process of desaturation is the tortuosity of the pore spaces. As the air flows through the soil displacing water, small pockets of water will be surrounded and trapped off by the advancing air. This results from capillary forces, which make water more difficult to displace from smaller pores than from larger

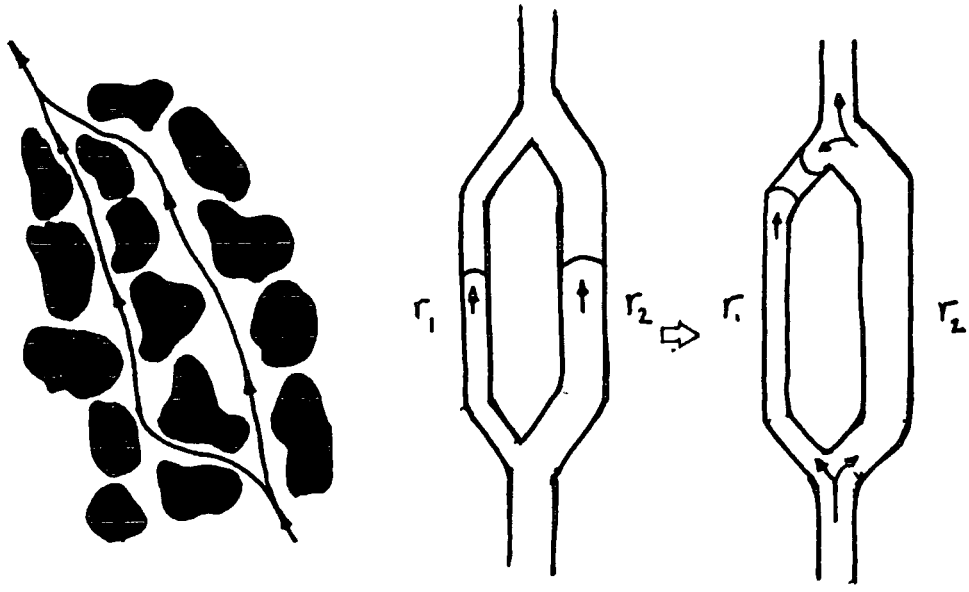

Figure 3.6 — Illustration of capillary resistance

ones. The principle is illustrated in fig. 3.6 which simplifies the pore structure as two capillary tubes of different diameter which diverge and come together again.

The capillary resistance encountered in the tubes is

$$\frac{2T\cos\theta}{r_1} \tag{17}$$

for the first tube and

$$\frac{2T\cos\theta}{r_2} \tag{18}$$

for the second tube, where T is the surface tension, θ is the contact angle, and r_1 and r_2 are the diameters of the first and second capillary tubes, respectively. As T and θ are constant for water, the smaller diameter tube will encounter more capillary resistance. If the suction is assumed to be the same in each tube, the air will reach the junction first in the larger diameter tube as it encounters less resistance. Thus a small amount of water will be trapped in the small diameter tube. This effect is influential only when the excess air pressures are very slight, since capillary forces are significant only for low suctions (Marle 1981).

3.5.3 Excess air pressure

As was previously discussed, some estimation of the excess air pressure in the soil is necessary in any stability analysis. The constraints of a system representing air flow from a pressurized tunnel are ideally suited for a potential flow analysis. For compressible fluids, potential flow problems use the general field equation (Screier, 1982)

$$\rho \nabla^2 \phi - \frac{\rho}{2c^2} \nabla \phi \cdot \nabla(\nabla\phi \cdot \nabla\phi) + Q = 0 \tag{19}$$

where ϕ is the fluid velocity potential ($\frac{L^2}{T}$), ρ is the fluid density ($\frac{M}{L^3}$), Q is the specific fluid flux applied at the system boundary ($\frac{M}{L^3T}$), c is the speed of sound ($\frac{L}{T}$), and ∇ is the differential operator $\left(\frac{\partial}{\partial x} + \frac{\partial}{\partial y}\right)$.

Boundary conditions are provided for at the tunnel face and at the ground surface. At the tunnel face, the excess air pressure is simply the difference between the air pressure in the tunnel and the hydrostatic water pressure at all points in the face. At the ground surface the excess air pressure reduces to 0, as the air is free to expand until its pressure equilibrates with the surrounding fluid pressure.

If the flow is steady state potential flow with no applied flux, equation 19 can be simplified to

$$\nabla^2\phi - \frac{1}{2c^2} \nabla \phi \cdot \nabla(\nabla\phi \cdot \nabla\phi) = 0. \tag{20}$$

If the fluid is incompressible, the sonic velocity is effectively infinite and the potential equation further reduces to the Laplace equation

$$\nabla^2\phi = 0 \tag{21}$$

which is readily determinant using standard numerical methods. However in the case of modelling air flow out of compressed air tunnels, the assumption that the flow is incompressible is invalid. Thus, any numerical solution must account for the highly non-linear term in equation 20. Suitable approaches to the problem are outlined in chapter 6 where finite element modelling is discussed in greater detail.

3.6 Seepage forces

In addition to total stresses in the soil skeleton and pore pressures from air and water in the void spaces, the flow of fluids through a soil exerts a frictional force in the direction of flow, transferring energy from the fluid's potential to the soil particles. These seepage forces are normally small enough to neglect, except in cases of high flow gradients in which case they can largely influence the stability of a soil mass. As high gradients can be expected for air excaping from compressed air works, seepage forces need to be accounted for in any effective stress relation for modelling blowouts.

The analysis for seepage force becomes straightforward if it is assumed to be a body force when acting on a small element of soil. The analysis presented by Craig (1987) uses a square element of unit thickness and dimension b oriented at angle θ from the horizontal so that the sides of the element are parallel and normal to the direction of flow (see fig 3.7a).

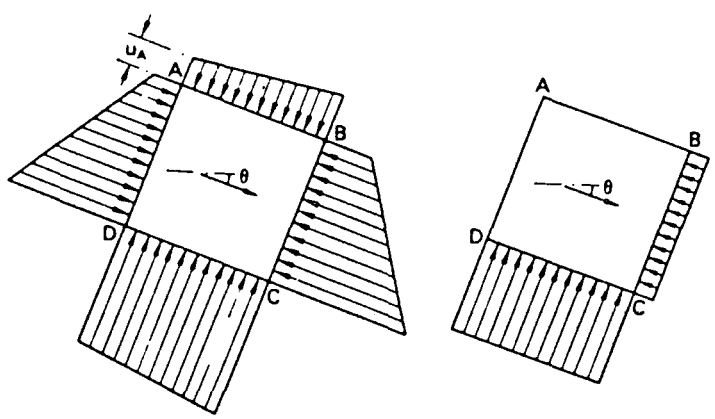

Figure 3.7 — Pore pressure forces acting on an element of soil

It is assumed that the sides of the element normal to the flow AD and BC are equipotentials in terms of total head, making the excess air pressure constant along these sides and the pore water pressure change only with change in elevation head. If the excess air pressure lost to seepage forces from AD to BC is ΔP_a, then

the following relations can be established for pore pressures:

$$u_A = u_{w_A} + u_{a_A} \tag{22}$$

$$u_B = u_{w_A} + u_{a_A} + \gamma_w(b\sin\theta) - \Delta P_a \tag{23}$$

$$u_C = u_{w_A} + u_{a_A} + \gamma_w(b\sin\theta + b\cos\theta) - \Delta P_a \tag{24}$$

$$u_D = u_{w_A} + u_{a_A} + \gamma_w(b\cos\theta) \tag{25}$$

and the following relations for pressure differences:

$$u_B - u_A = \gamma_w(b\sin\theta) - \Delta P_a \tag{26}$$

along BC and

$$u_D - u_A = \gamma_w(b\cos\theta) \tag{27}$$

along CD. These pore pressure distributions are shown acting on an element in fig 3.7b.

Thus, the net force acting along BC is $(\gamma_w b\sin\theta - \Delta P_a)b$ or $\gamma_w b^2\sin\theta - \Delta P_a b$ and $\gamma_w b^2\cos\theta$ along CD. The seepage force (J) is represented by the term $\Delta P_a b$ which is the only difference between the seepage force distribution and the static force distribution. The average hydraulic gradient i across the element is

$$i = \frac{\Delta h}{b} \tag{28}$$

where Δh is the head loss in total air pressure across the element. Since air pressure is represented as excess to the pore water pressure

$$\Delta h = \frac{\Delta P_a}{\gamma_w} \tag{29}$$

or

$$i = \frac{\Delta P_a}{b\gamma_w} \tag{30}$$

so

$$J = \Delta P_a b = b\gamma_w ib = b^2 i\gamma_w. \tag{31}$$

The seepage pressure (j) is defined as the seepage force per unit volume

$$j = \frac{J}{V} = \frac{J}{b^2} = i\gamma_w. \tag{32}$$

3.7 Blowout mechanism

For the purposes of this research an analytical definition of a blowout will be when a continuing line of points in a soil medium connecting the tunnel crown with the ground surface have mechanically failed due to excess pore pressures from the escaping air. For the sake of simplicity, the in-situ ground stresses will be assumed isotropic, which makes the failure criterion one dimensional and independent of soil strength parameters except for tensile strength, which will be assumed to be zero. Thus, failure will occur when the pore pressures exceed the total stresses, and a factor of safety can be defined as the ratio of the total stress to the pore pressure. Fig. 3.8 shows dimensions of factors influencing these stresses. Total stress is a combination of the bulk weight of the soil γz_s and any surcharge load which, since this research is concerned with subaqueous tunnels would be the weight of the water column in the channel or river, $\gamma_w z_r$. Likewise, pore pressures would be a combination of the hydrostatic water pressure $\gamma_w z_w$, the excess air pressure u_a, and the total seepage pressure $i\gamma_w$.

Thus

$$\sigma = \frac{G_s + S_r e}{1 + e}\gamma_w z_s + \gamma_w z_r \tag{33}$$

$$u = \gamma_w z_w + u_a + i\gamma_w \tag{34}$$

and the factor of safety ($f.o.s.$) at point P is

$$f.o.s. = \frac{\left\{\left(\frac{G_s+S_r e}{1+e} - 1\right)z_s + z_w\right\}\gamma_w}{\gamma_w z_w + u_a + i\gamma_w}. \tag{35}$$

If excess pore air pressure is measured in terms of head of water so that $u_a = h\gamma_w$,

$$f.o.s. = \frac{\left(\frac{G_s+S_r e}{1+e} - 1\right)z_s + z_w}{z_w + h + i}. \tag{36}$$

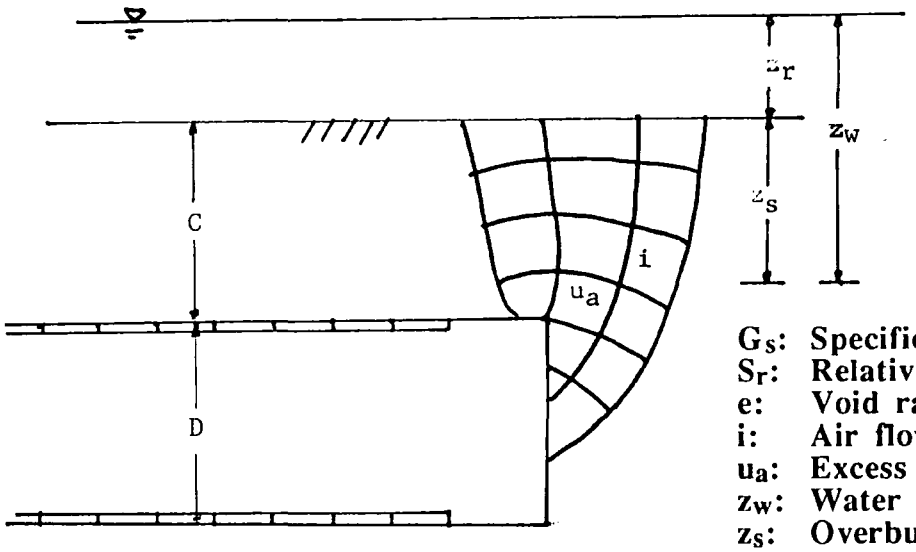

Figure 3.8 — Dimensions for stability calculations

The overall factor of safety against a blowout ($F.\mathcal{O}.S.$) will be defined as the maximum factor of safety along a line connecting points of minimum factor of safety ($f.o.s$) between the tunnel crown and the ground surface. A blowout will be defined to occur when $F.\mathcal{O}.S. \leq 1.0$.

Although this definition of factor of safety is suitable for modelling purposes, it does not convey much information for design. For this a factor of safety for design ($F.\mathcal{O}.S.D.$) will be definied as the tunnel depth over the critical depth at which a blowout will occur. For example, a tunnel 9 metres below the ground surface with a $F.\mathcal{O}.S. = 1.0$ at a depth of 6 metres will have a $F.\mathcal{O}.S.D.$ of 1.5.

Chapter IV

Permeability

4.1 Darcy's law

The potential loss for flow through porous media is dependent on the directional coefficients of permeability, which are material properties expressing the ease in which a fluid can flow through a given medium. The coefficient of permeability, k, is a proportionality constant used in an empirical relation developed in 1856 by Darcy, who measured head loss for various flows through samples of sand. By testing several samples of varying dimensions, Darcy made the observation that the total flow was proprtional to the area of the sample and the potential head drop for a given length, which he expressed in the equation

$$Q = kA\frac{h}{l} \tag{37}$$

where Q is the flow through the soil, A is the cross sectional area of the sample, h is the head loss, l is the length of the sample, and k is the coefficient of permeability.

The coefficient of permeability given in Darcy's equation is not an absolute property of the soil, but a property of the soil/fluid system. It is dependent on the fluid density and viscosity and hence cannot be used for different types of fluids. It is often referred to as the effective coefficient of permeability, and an absolute coefficient of permeability K, is used to define the permeability of a soil independently of the fluid characteristics. Effective and absolute permeability are related in the equation

$$k = \frac{\gamma_w}{\mu}K \tag{38}$$

where γ_w is the density of water and μ is the viscosity of water. Absolute permeability is usually expressed in units of Darcys, which is defined as the permeability of a soil given a fluid with a viscosity of 1 centipoise with a flow of 1 cm^3/s through a sample 1 cm^2 in cross sectional area with a pressure gradient of 1 atm/cm. The

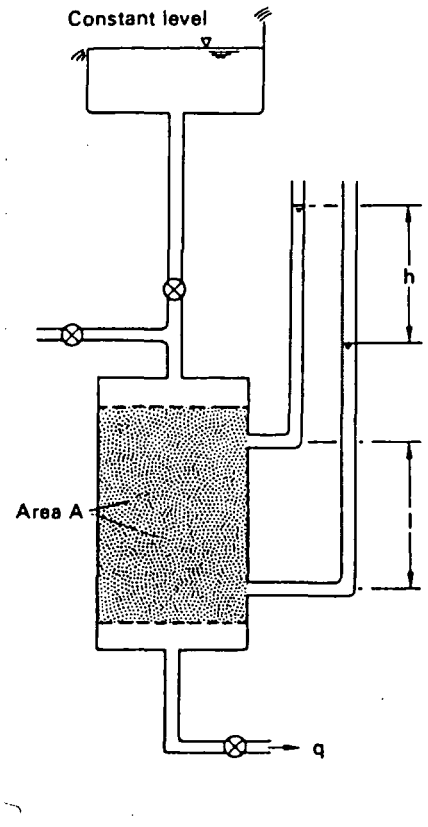

Figure 4.1 — Darcy's experiment

dimensions of a Darcy are L^2, and 1 Darcy is equivalent to 9.88×10^{-9} cm^2. This appears to be an extremely small number, but at 20° C and atmospheric pressure an absolute permeability of 1 Darcy would be an effective permeability 9.6×10^{-4} cm/s with respect to water and 6.42×10^{-5} cm/s with respect to air using equation 38.

4.2 Permeability with respect to compressible fluids

Past research has shown that the permeability of a porous medium to a compressible flow is not a constant but varies with fluid pressure. Compressible flows tend to yield higher permeabilities than liquid flows, and the permeability tends to increase with decreasing mean pressure.

Klinkenberg (1941) described this effect in terms of an additional parameter b which relates permeability values relative to the permeability at infinite pressure,

K_o. The expression used is

$$K_a = K_o(1 + \frac{b}{\bar{P}}) \tag{39}$$

where K_a is the permeability of the soil at mean pressure $\bar{P}$, K_o is the permeability at infinite pressure, and b is a constant of proportionality. Values of K_o and b are determined experimentally.

Blight (1971) accounted for compressibility by using a mass gradient instead of flow as the dependent variable. This is expressed in Fick's law which is generally applicable to mass transport problems, being used to describe thermal and osmotic migration of liquids as well as adsorption and molecular diffusion of gasses. In it general form, Ficks law is

$$\frac{\partial m}{\partial t} = -D\frac{\partial P}{\partial z} \tag{40}$$

where $\frac{\partial m}{\partial t}$ is the mass flow velocity, i.e. the mass of air flowing through a unit area of air filled pore space in unit time, D is a transmission constant, and $\frac{\partial P}{\partial z}$ is the pressure gradient through the soil. Fick's law can be compared with Darcy's law by employing the equation of state for air

$$PV = \frac{RT}{w}m \tag{41}$$

where P is the absolute pressure, V the volume, w the molecular weight of mass m of air, T the absolute temperature, and R the universal gas constant. If Qt is substituted for Vin equation 41 and solved for m, then equation 40 becomes

$$Q = -D\frac{RT}{w}\frac{1}{P}\frac{\partial P}{\partial z} \tag{42}$$

in which it can be seen that Fick's law varies from Darcy's law by the factor $\frac{1}{P}$. Blight compared the mass velocity vs. pressure gradients with the linear velocity vs. pressure gradients for several soils, and the results do seem to indicate slightly more linearity when using a mass gradient as shown in figure 4.2.

Sullivan and Hertel (1940) studied the permeability of spherical glass beads with respect to air flow, and based their analysis on the specific heat of the flow. They devised an empirical relation

$$Q = \frac{K\Delta PA}{\mu L}\frac{P_2^{1+m} - P_1^{1-m}}{(1+m)(P_2 - P_1)P_1^m} \tag{43}$$

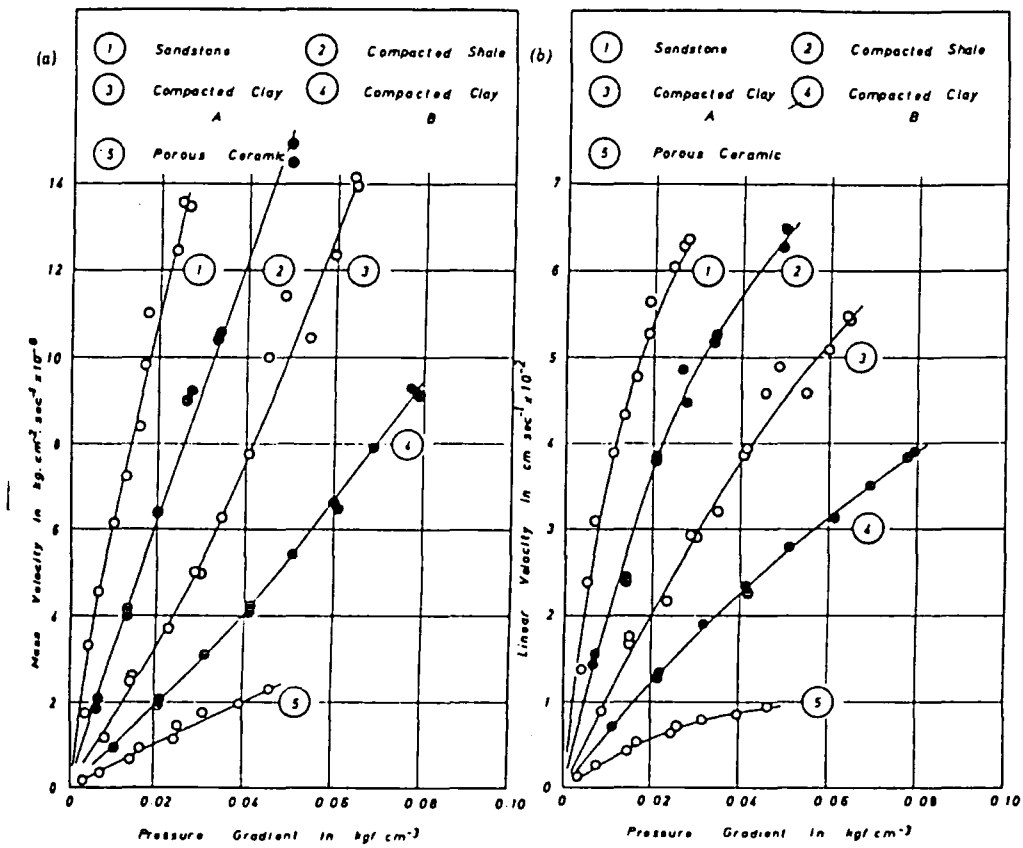

Figure 4.2 — Comparison of Fick's law with Darcy's law for air flow. (a) Mass velocity vs. pressure gradients (b) Linear velocity vs. pressure gradients

where Q is the rate of fluid flow, K is the permeability, μ is the fluid viscosity, ΔP is the pressure drop through a sample of length L and area A, P_2 is the entrance air pressure, P_1 is the exit air pressure, and m is a constant determined by the thermodynamic character of the flow. For isothermal flow, $m = 1$ so that

$$Q = \frac{K_a \Delta P A}{\mu L} \frac{P_2^2 - P_1^2}{2(P_2 - P_1)(P_1)} \tag{44}$$

or

$$K_a = \frac{2Q\mu L}{A\Delta P} \frac{P_1(P_2 - P_1)}{(P_2^2 - P_1^2)} = \frac{2Q\mu L P_1}{A\Delta P(P_1 + P_2)} = \frac{Q\mu L P_1}{A\Delta P \bar{P}} \tag{45}$$

where $\bar{P}$ is the mean pressure, $\frac{P_1+P_2}{2}$.

If we compare this equation with Darcy's law, an expression relating the permeabilities of compressible flow with incompressible flow can be found

$$K_i = \frac{Q\mu L}{A\Delta P} \tag{46}$$

$$\frac{K_i}{K_a} = \frac{\bar{P}}{P_1} \tag{47}$$

from which it can be said that for small pressure differences the permeability is not significantly altered by the compressible nature of the flow.

For this research, the relation by Sullivan and Hertel (eqn. 45) was used to account for the incompressible flow effects on permeability. The advantages of this relation are ease of use, steady state nature, and similarity to Darcy's law which makes it readily usable in numerical modelling procedures.

4.3 Degree of saturation - influence on permeability

The most important factor controlling the permeability of a soil is the degree of saturation (Olson & Daniels, 1981). Experiments performed by Topp and Miller (1966) on samples of glass beads showed the effective permeability with respect to water varied from 10^{-2} cm/s to 10^{-5} cm/s over a wide range of saturations (see fig. 4.3). The effect is intuitively obvious, as water in the pore spaces impede the flow of air just as pockets of air impede the flow of water.

It is common to approach unsaturated permeabilities as relative permeabilities, taking into account water and air permeabilities simultaneously. Relative permeabilities are defined as follows:

For water:

$$k_{rw_s} = \frac{k_{w_s}}{k_{w_{s=1}}} \tag{48}$$

For air:

$$k_{ra_s} = \frac{k_{a_s}}{k_{a_{s=0}}} \tag{49}$$

where k_{w_s} and k_{a_s} are the effective permeabilities at a degree of saturation s with respect to water and air respectively, and $k_{w_{s=1}}$ and $k_{a_{s=0}}$ are the effective permeabilities with respect to water and air at 100% saturation and 0% saturation,

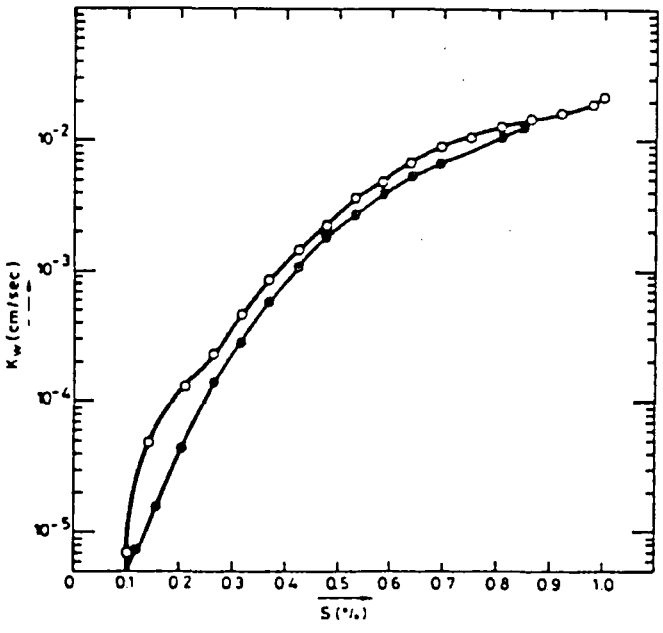

Figure 4.3 — Variation of water permeability in a glass bead sample

respectively. Thus relative permeabilities k_{rw} and k_{ra} are fractions ranging from 0.0 to 1.0. They are often shown in relation to each other, as in fig. 4.4. Due to capillary forces, there is a degree of saturation above which air will not flow, unless the soil is further desaturated by gas entry. This degree of saturation is known as the residual saturation, S_{ru}. Likewise, there is a degree of saturation below which water will not flow and where further reductions in saturation do not substantially increase the relative permeability with respect to air. This degree of saturation is known as the irreducable saturation S_i. Thus, relative permeability with respect to air is essentially confined to the range of saturations $S_i < S_r < S_{ru}$.

Extensive research has gone into developing empirical relations between permeability with respect to water and saturation, which has been summarized by Alonso, Gens, and Hight (Table 4.1). It should be noted they are characteristically power relations.

There has been comparatively little research done into relating air permeability with respect to degree of saturation. Yoshimi and Osterberg (1963) found an empirical relation

$$\log K_a = ae(1 - S_r) \tag{50}$$

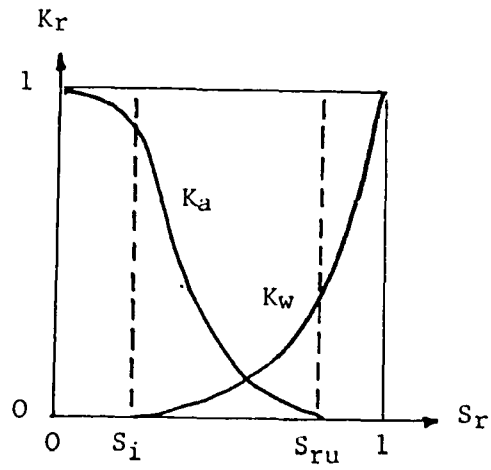

Figure 4.4 — Relative permeabilities of air and water

where e is the void ratio and a is constant. This they later revised as a power relation

$$K_a = b(e(1 - S_r)^a)\frac{\gamma}{\mu} \tag{51}$$

in which a and b are constants, γ is the specific weight of air and μ is the viscosity of air.

The approach adopted in this research used essentially the same procedure, however the effects of void ratio are neglected and assumed to contribute to the constant coefficient b. The effects of air density and viscosity are accounted for by measuring permeabilities with Sullivan and Hertels' relation (eqn. 45). A theoretical power curve was then fitted to permeabilities at different degrees of saturation so that

$$K_a = bS_r^{-a}. \tag{52}$$

This relation was used to account for the degree of saturation in the finite element model.

4.4 Permeability at failure conditions

There has been little previous research on the effects of mechanical failure on permeability, and there is no mention of the effects of failure in tension on permeability given in the available literature. Intuitively, the influence would be

Author(s)	Relation
Gardener (1958)	$K_w = \frac{K_o}{(1+a\|h\|^b)}$
Gardener (1958)	$K_w = K_o e^{-b\|h\|}$
Brooks &Corey (1966)	$K_w = K_o \; h \geq h_b$
	$K_w = K_o(h_b/h)^m \; h \leq h_b$
Richards & Chan (1969)	$K_w = \frac{E+DE}{(A+Bs^m+cs^n)}$
Irmay (1954)	$K_w = K_o(\frac{(S_r-S_{ru})}{(1-S_{ru})})^3$
Corey (1957)	$K_w = K_o(\frac{(S_r-S_{ru})}{(1-S_{ru})})^4$
Scott (1963)	$K_w = K_o(1 - n(1 - S_r))$
Brutsaert (1968)	$K_W = K_o S_r^n$
Kovacs (1981)	$K_w = K_o(\frac{(S_r-S_{ru})}{(1-S_{ru})})^{3.5}$
Nielson et. al. (1986)	$K_w = K_o S_e^n[1 - (1 - S_e^{1/m})^m]^2$

Symbols:

K_w	Permeability with respect to water
K_o	Permeability at full saturation
s	Matrix suction
h	Matrix suction head
S_r	Relative degree of saturation
S_{ru}	Irreducible degree of saturation
S_e	field saturation

Table 4.1 — Empirical expressions of permeability with respect to degree of saturation

immense as the soil volume would expand to create a large void space for fluid flow. For this research experimental results were used to determine an empirical permeability with respect to air at failure conditions.

Chapter V

Laboratory testing

5.1 Objectives of laboratory work

In order to use the finite element method to model blowouts, values of specific gravity and permeability with respect to air are needed for all soil types used in the analysis. As there is very little information on permeability with respect to air in the literature, Laboratory tests were performed to obtain representative values of all necessary parameters. Suitable tests were performed to obtain values of specific gravity, degree of saturation with respect to excess air pressure, permeability with respect to degree of saturation, and the permeability of soils at failure conditions. Soil types were restricted to silty sands as these are commonly encountered in subaqueous tunnels and are normally the most susceptible to blowouts.

5.2 Description of soil materials

The soils used for testing were made by mixing clean sand with silt to specific proportions of mass. Four soil types were used according to the divisions of the British Soil Classification System (BS 5930), a clean sand (S) with 0% silt, a slightly silty sand (S-W) with 5% silt, a silty sand (S-M) with 10% silt, and a very silty sand (SM) with 25% silt.

The sand used was a well graded coarse sand of rounded to subangular quartz grains. Specific gravity was measured at 2.65, and minimum bulk density was 1.53 g/cm^3 giving a void ratio of 0.74 and a porosity of 0.42.

The silt used was obtained from a highly organic mud dredged from the river Wear near Shincliffe, Durham. The mud was dried and sieved, with particles passing the 63 μm sieve retained and used in testing. Specific gravity of these particles averaged 2.66. The liquid limit of the soil was 0.73, and the plasticity index ranged from 0.20 to 0.23, which classifies as a very high plasticity silt (MV) by the British Classification System.

5.3 Testing equipment and procedures

5.3.1 Soil classification

Grain sizes were determined by the use of sieves for coarse grained particles according to BS1377:7 and the pipette method for fine grained materials according to BS1377:C. Five sieves were used, with mesh sizes 1.4 mm, 710 μm, 600 μm, 212 μm, and 63 μm. The pipette analysis used a 9.6752 ml pipette with a 500 ml beaker, along with twelve 10 ml test tubes. The results of these tests are given in appendix A on page A1 and grain size distribution plots for the four materials used are shown on pages A2 to A5.

Specific gravity of particles was measured according to BS1377:6. Four 50 ml pycnometers were used for the silt particles and two 100 ml pycnometers for the sand particles. Minimum bulk density was determined by dividing the weight of a sample of dry soil poured into a measured volume. The results of these tests are given in appendix A page A6.

Liquid limits were determined using a cone penetrometer which is described in BS4691 and the plastic limit was defined as the water content at which a thread of material will crumble when reduced to 3 mm in diameter as specified in BS1377:3. These results are given in appendix A page A7.

5.3.2 Desaturation and permeability

To determine degree of saturation at specified excess air pressures and permeabilities at different degrees of saturation, a gas permeameter manufactured by Ruska Instrument Corporation was used. The instrument measures pressure, temperature, and flow rate through a sample with which the permeability of a sample can be determined, assuming the viscosity and density of the gas is known.

First, a sample of soil is poured into a rubber thick walled cylinder with a length of 3.4 cm and inner diameter of 1.9 cm which is in turn encased in a thin walled steel cylnder. A wire screen mesh is placed on the downstream side of the sample to prevent excessive washing of material from the cylinder during testing. The sample is then loaded into the permeameter as illustrated in fig. 5.1.

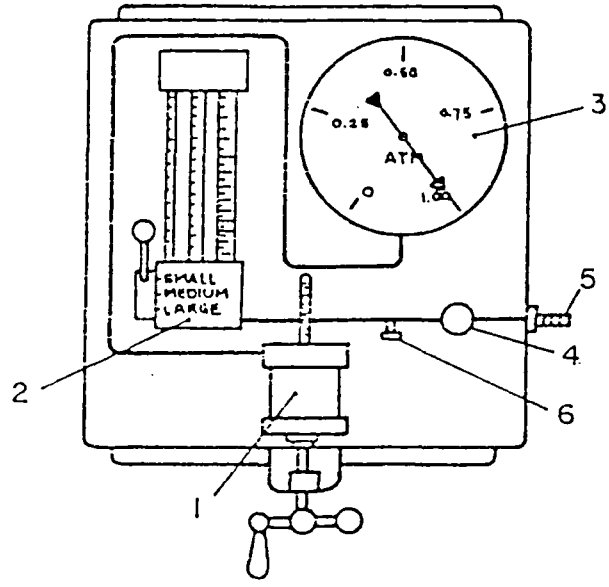

1. Sample
2. Flow meters
3. Pressure gauge
4. Pressure regulator
5. Gas inlet valve
6. Safety valve

Figure 5.1 — Ruska gas permeameter

For desaturation tests, each sample was initially saturated and a hydrostatic head equal to the height of the top of the sample was applied through the downstream exit at the base of the sample, thus ensuring pore water pressure was atmospheric. Gas was then forced through the sample for 5 minutes at a specific pressure to ensure a degree of saturation in equilibrium to the applied air pressure. The sample was then removed and the water content measured. Results from tests on the four soil types are given in appendix A on pages A8 to A12. The results show an inverse power relation of the form $S_r = a\Delta P^{-b}$ was suitable to characterize the desaturation process, and this type of relation was chosen for use in finite element modelling, with a cutoff at $S_r = 1$ to ensure saturation did not exceed 100%.

For permeability tests, samples were mixed with varying proportions of water to achieve varying degrees of saturation. The inside of the rubber thick walled cylinder was coated in vacuum grease to avoid excessive air flow along the sample edge. No back water pressure was applied to avoid increasing the degree of saturation. The applied pressure difference was kept within the range $0.1atm.$ to $0.2atm.$ for consistency and to prevent excessive drying of the sample. Readings

of airflow and pressure were taken as soon as possible to avoid desaturation, after which the moisture content of the sample was measured. The permeabilities and water contents for each of the materials are given in appendix A page A13 and A14, and plotted on pages A15 to A18. Again, the results showed a good inverse power correlation which was used in finite element modelling.

5.3.3 Permeability at failure

While suitable for measuring permeability under general conditions, the Ruska permeameter was unable to measure the permeability of samples with pore pressures exceeding the total stress, as the constraints of the apparatus ensured that the confining stress would always prevent the sample from reaching a tensile stress regime. In order to determine the influence of failure on permeability, a triaxial test machine was suitably re-outfitted with pressurized air connected to the back pressure inlet (see fig. 5.2). Samples were formed by pouring soil into cylindrical moulds 3 inches long by 1.5 inches in diameter, then saturating them with water and freezing. While freezing, a small dome of ice would form on the top of the sample which was chipped off with a small pick before removing the sample from the mould. The sample was inserted into a thin rubber membrane the inside of which was coated with vacuum grease. Once the rubber membrane was properly fitted, the sample was placed into the triaxial cell with small wire screens covering each end of the sample and a top platen with a 0.5 inch diameter hole bored through the centre to allow free passage of air to the cell chamber. The cell was immediately pressurized to $1.00atm.$ under which confining stress the sample was allowed to thaw for 2 hours to ensure no ice remained in the sample. No deviator stress was applied in order to keep effective stress isotropic. Air was then pumped into the sample at a pressure of $1.01atm.$ which gave a pressure difference of $0.01atm.$ across the sample and ensured the sample was in a state of tension with effective stress ranging from $-0.01atm.$ to $0.00atm.$

Air was allowed to exit the cell chamber at a controlled rate through the air release valve at the top of the cell. It was assumed that an equilibrium flow rate was established when the water level in the cell was kept at a constant level, at which time the air flow rate was measured using an inline flow meter upstream from the sample (see fig. 5.2). Thus, with known flow rate, pressure gradient, and

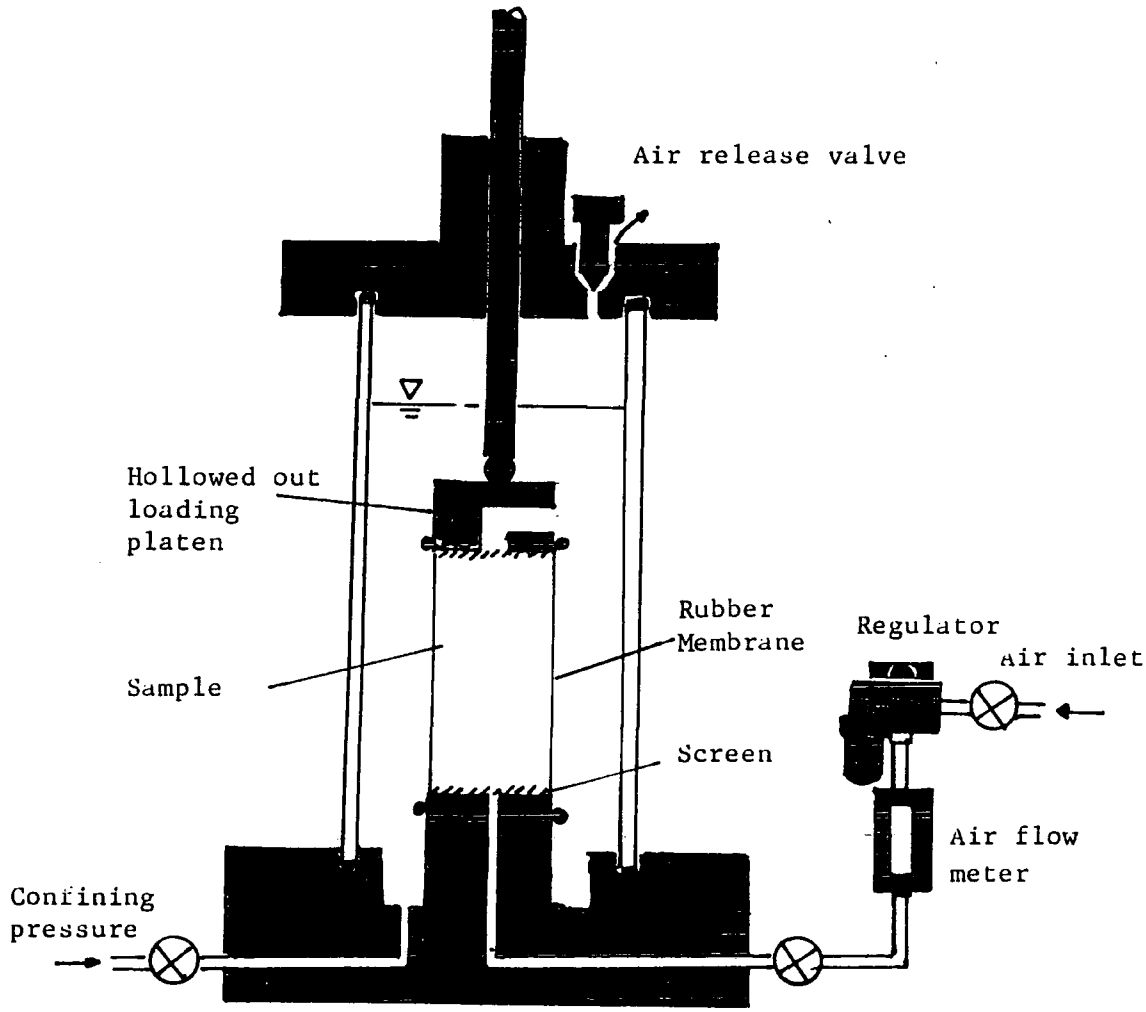

Figure 5.2 — Adapted triaxial cell

sample dimensions, the permeability of the failed sample was calculated with the Sullivan and Hertel relation (eqn. 45) for gases. Results from these tests are given in appendix A page A19.

Chapter VI

Finite element modelling

6.1 General principles of finite elements

The finite element method is a method originally developed by civil engineers to aid in the analysis of complex structures. The method does not provide exact solutions but approximates the exact solution by analysing the system in terms of smaller, simpler components or 'finite elements'. There are eight essential steps involved in any finite element formulation (Desai, 1979):

Step 1 - Discretize system into a configuration of finite elements. First the system or structure is divided up into a suitable number of elements. The intersections of the sides of the elements are referred to as nodes; and the interfaces between the elements are referred to as nodal lines or nodal planes. The number of elements used depends on the the complexity of the system and the degree of accuracy desired. The type of element used depends on the nature of the problem. For one dimensional problems such as column loading or fluid flow through a uniform pipe, line elements are used. For two dimensional bodies, triangular and/or quadrilateral elements are used. For three dimensional systems, hexahedron blocks of variable nodal geometry are used.

Step 2 - Select approximation functions. Next a relation for the distribution of the unknown quantity across an element is selected. This is normally done by using a polynomial interpolation function with the values at the nodes of the element as independant variables. Thus in a finite element formulation, the value of unknown u anywhere within a given element would be

$$u = N_1 u_1 + N_2 u_2 + \ldots + N_m u_m \tag{53}$$

where $u_1, u_2, \ldots, u_m$ are values of the unknown at the nodes of the element and $N_1, N_2, \ldots, N_m$ are interpolation functions dependent on the geometry of the element.

Step 3 - Define unknowns and constitutive relations. In this step, a relevant theoretical principle is used to derive suitable equations for the element in terms of the unknown. Principles such as strain and potential gradient are used for primary unknowns such as displacements and fluid potential. Secondary unknowns such as stress or flow velocity are likewise solved using constitutive laws such as Hooke's law or Darcy's law.

Step 4 - Derive Element equations. One of two basic approaches are used to determine the governing equation of an element in terms of fundamental principles. Energy methods determine governing equations from stationary values of energy or work. There is a variety of energy methods available, but the principle of minimum potential energy is the most common in finite elements. The method of weighted residuals minimizes the residual of a trial solution after substitution into a general governing differential equation. Use of either an energy method or the method of weighted residuals will lead to an equation governing the behaviour of an element. The element equation is expressed as a matrix function of the form

$$[K]\{q\} = \{Q\} \tag{54}$$

where $[K]$ is the element property matrix, $\{q\}$ is the vector of unknowns at the nodal points, and $\{Q\}$ is the vector of nodal forcing parameters.

Step 5 - Assemble Global FEM equation and introduce boundary conditions. In this step the equations of each of the elements are summed up into a global matrix equation which defines the behaviour of the whole system. The assembling process is based on the law of compatibility or continuity, which requires that the global solution of unknowns is continuous. Thus, the solution to a given node in one element will be the same as the solution for the same node in any other element. Once the global equation has been constructed, boundary conditions, which are values of the unknown specified by the physical constraints of the system, are entered into the global equation.

Step 6 - Solve for primary unknowns. Once boundary conditions have been entered into the global equation, the entire system becomes a set of simultaneous algebraic equations that can be solved by Gaussian elimination or any other method

of solution. Thus values of the primary unknown u are found at every node in the system.

Step 7 - Solve for secondary unknowns. Once primary unknowns are known, solutions to secondary unknowns are obtained through the use of simple constitutive relations as discussed under step 3.

Step 8 - Interpretation of results. Finally, solutions are reduced to a form suitable for analysis such as a table of nodal solutions or a plot contouring nodal solutions.

6.2 Finite elements and potential flow

In this section a finite element solution to incompressible potential is presented in two dimensions to illustrate the principle, but can easily be adapted to three dimensional flows.

The partial differential equation governing two dimensional potential flow is

$$P_x \frac{\partial^2 \Phi}{\partial x^2} + P_y \frac{\partial^2 \Phi}{\partial y^2} + q = 0 \tag{55}$$

where Φ is the potential, P_x and P_y are permeabilities in the x and y directions, and q is the inflow. The energy equation corresponding to eqn. 55 is

$$E = \int\int \left[\frac{P_x}{2} \left(\frac{\partial \Phi}{\partial x} \right)^2 + \frac{P_y}{2} \left(\frac{\partial \Phi}{\partial y} \right)^2 - q\Phi \right] dxdy. \tag{56}$$

The potential Φ for any point inside an element can be expressed in terms of the nodal potential vector $\{\phi\}$ and the interpolation function matrix $[N]$ so that

$$\{\Phi\} = [N]\{\phi\} \tag{57}$$

Therefore equation 56 can be expressed

$$E = \int\int \left[\frac{P_x}{2} \left(\frac{\partial [N]}{\partial x} \{\phi\} \right)^2 + \frac{P_y}{2} \left(\frac{\partial [N]}{\partial y} \{\phi\} \right)^2 - q[N]\{\phi\} \right] dxdy \tag{58}$$

If we assume a quadrilateral element with nodes i, j, k, and l, then the principle of minimum potential energy will produce a series of four simultaneous equations for $\{\phi\}$ by setting the partial derivative of equation 58 with respect to a given nodal potential equal to zero while keeping the other three nodal potentials constant (i.e. $\partial E/\partial\phi_i = 0$ for constant ϕ_j, ϕ_k, ϕ_l). In matrix form, these equations can be expressed as

$$[K]\{\phi\} = \{Q\} \tag{59}$$

which is the governing finite element equation where $[K]$ is the element stiffness matrix defined by

$$[K] = \int\int [D]^T [P][D] dx dy \tag{60}$$

in which $[D]$ is the matrix of first derivatives of the interpolation functions

$$[D] = \begin{bmatrix} \frac{\partial [N]}{\partial x} \\ \frac{\partial [N]}{\partial y} \end{bmatrix}, \tag{61}$$

$[P]$ is the permeability matrix

$$[P] = \begin{bmatrix} P_x & 0 \\ 0 & P_y \end{bmatrix}, \tag{62}$$

and $\{Q\}$ is the source vector

$$\{Q\} = \int\int q[N]^T dx dy. \tag{63}$$

6.3 Finite elements and compressible flow

6.3.1 Governing relations for compressible fluids

As was discussed in section 4.2, the potential of compressible fluids does not behave in a linear fashion which is required to satisfy the potential equation (eqn. 21) governing incompressible flow. The effect of compressibility is most pronounced for high gradients and with sudden volume changes as a compressible fluid will conserve head when expanding. As both these conditions are likely to occur for air escaping from a pressurized tunnel, some means of accounting for compressibility effects must be employed in the finite element method.

There are two methods commonly used for finite element modelling of compressible flow; adaptive remeshing and linearization of the potential equation. Adaptive remeshing is an iterative procedure which first computes a steady state solution then redraws the mesh changing element dimensions to account for compressibility. The procedure is repeated until a stable solution is found (Lohner et.al., 1985; Peraire et.al., 1987). The alternative is to simplify the compressible potential equation in a linear form suitable for use in the governing finite element equations. There are several methods available in the fluid mechanics literature to make these simplifying approximations.

It should be noted that these methods of simulating compressible flow were developed to model stream flow over air foils and are dependent on the Mach number in uniorm flow, M_∞. They are therefore not well suited to model the very low velocity flows of potential flow through porous media. It was decided, however, to use a method of linearizing the compressible potential to make some approximation to the effects of compressibility on the air flow potentials and to keep the model conservative in simulating blowouts.

6.3.2 Finite element formulation

For the purposes of this research the Rayleigh-Janzen method was used as developed by Carey (1975) for finite element modelling of compressible flows. The Raleigh-Janzen method linearizes compressible flow by considering perturbations in an otherwize uniform flow with velocity V_∞ and sound velocity c_∞. In such a flow, the continuity equation can be expressed as

$$\nabla^2\phi\left\{1 + M_\infty^2\left(\frac{\gamma-1}{2}\right)\left(1-(\nabla\cdot\phi)^2\right)\right\} - M_\infty^2\frac{\partial\phi}{\partial x}\frac{\partial\phi}{\partial y}\frac{\partial\phi}{\partial xy} = 0 \qquad (64)$$

where M_∞ is the Mach number in uniform flow, V_∞/c_∞, and $\frac{\partial\phi}{\partial x}$,$\frac{\partial\phi}{\partial y}$, and $\frac{\partial\phi}{\partial xy}$ are small perturbations in the flow velocity.

The Raleigh-Janzen method linearizes the potential function as an expansion

$$\phi = \phi^{(0)} + \varepsilon\phi^{(1)} + \varepsilon^2\phi^{(2)} + ... + \varepsilon^n\phi^{(n)} + O(\varepsilon^{n+1}) \qquad (65)$$

with $n+1$ terms and an error of the order $n+1$. In expanding equation 64, M_∞^2 can be used as the expansion coefficient ε as $\phi^{(0)}$ will then solve the Laplace

equation $\nabla^2\phi^{(0)} = 0$ making $\phi^{(0)}$ the solution for incompressible flow. In order to linearize the potential, the expansion is simplified to only one term representing the compressibility correction making the error of order ε^2 or M_∞^4. As only very low velocities are expected, this should be more than sufficient. Thus the expansion used is

$$\phi = \phi^{(0)} + \varepsilon\phi^{(1)} + O(\varepsilon^2) \tag{66}$$

which when substituted into equation 64 gives the following terms of expansion:

$$\nabla^2\phi^{(0)} = 0 \tag{67}$$

for ε^0, and

$$\nabla^2\phi^{(1)} - \frac{\partial\phi^{(0)}}{\partial x}\frac{\partial\phi^{(0)}}{\partial y}\frac{\partial\phi^{(0)}}{\partial xy} = 0 \tag{68}$$

for ε^1 where $\phi^{(0)}$ is the incompressible flow potential and $\phi^{(1)}$ is a correction for compressibility.

Using calculus of variations, the potential energy $\Pi^{(0)}$ of the zero order term $\phi^{(0)}$ over area A is expressed in the variational functional

$$\Pi^{(0)} = \frac{1}{2}\int_A \left(\frac{\partial\phi^{(0)}}{\partial x} + \frac{\partial\phi^{(0)}}{\partial y}\right)^2 dA. \tag{69}$$

Likewise the associated functional for $\Pi^{(1)}$ is

$$\Pi^{(1)} = \frac{1}{2}\int_A \left(\frac{\partial\phi^{(1)}}{\partial x} + \frac{\partial\phi^{(1)}}{\partial y}\right)^2 dA + \int_A \left(\frac{\partial\phi^{(0)}}{\partial x}\frac{\partial\phi^{(0)}}{\partial y}\frac{\partial\phi^{(0)}}{\partial xy}\right)\phi^{(1)}dA. \tag{70}$$

The term $\frac{\partial\phi^{(0)}}{\partial xy}$ in the second integral requires the incompressible solution $\phi^{(0)}$ to be twice differentiable. This term can be linearized by manipulating the integral into a form suitable for Gauss's divergence theorem. If we denote this integral Π^* and look at it seperately, it can be arranged into an appropriate format as follows:

$$\Pi^* = \int_A \frac{\partial}{\partial y}\left(\frac{\partial\phi^{(0)}}{\partial x}\frac{\partial\phi^{(0)}}{\partial y}\frac{\partial\phi^{(0)}}{\partial x}\phi^{(1)}\right)dA - \int_A \frac{\partial}{\partial y}\left(\frac{\partial\phi^{(0)}}{\partial x}\frac{\partial\phi^{(0)}}{\partial y}\phi^{(1)}\right)\frac{\partial\phi^{(0)}}{\partial x}dA \tag{71}$$

$$\Pi^* = \int_A \frac{\partial}{\partial y}\left(\frac{\partial\phi^{(0)}}{\partial x}\frac{\partial\phi^{(0)}}{\partial y}\frac{\partial\phi^{(0)}}{\partial x}\phi^{(1)}\right)dA - \int_A \left(\frac{\partial\phi^{(0)}}{\partial xy}\frac{\partial\phi^{(0)}}{\partial y}\frac{\partial\phi^{(0)}}{\partial x}\phi^{(1)}\right)dA$$

$$- \int_A \left(\frac{\partial\phi^{(0)}}{\partial x}\right)^2 \frac{\partial^2\phi^{(0)}}{\partial y^2}\phi^{(1)}dA - \int_A \left(\frac{\partial\phi^{(0)}}{\partial x}\frac{\partial\phi^{(0)}}{\partial y}\frac{\partial\phi^{(1)}}{\partial y}\frac{\partial\phi^{(0)}}{\partial x}\right)dA. \qquad (72)$$

Since the second integral is equivalent to Π^* and $\frac{\partial^2\phi^{(0)}}{\partial y^2} = 0$ in the third integral,

$$2\Pi^* = \int_A \frac{\partial}{\partial y}\left(\frac{\partial\phi^{(0)}}{\partial x}\frac{\partial\phi^{(0)}}{\partial y}\frac{\partial\phi^{(0)}}{\partial x}\phi^{(1)}\right)dA - \int_A \left(\frac{\partial\phi^{(0)}}{\partial x}\frac{\partial\phi^{(0)}}{\partial y}\frac{\partial\phi^{(1)}}{\partial y}\frac{\partial\phi^{(0)}}{\partial x}\right)dA. \qquad (73)$$

Applying Gauss's divergence theorem,

$$\Pi^* = \frac{1}{2}\int_S \left(\frac{\partial\phi^{(0)}}{\partial x}\right)^2 \frac{\partial\phi^{(0)}}{\partial\eta}\phi^{(1)}dS - \frac{1}{2}\int_A \left(\frac{\partial\phi^{(0)}}{\partial x}\right)^2 \frac{\partial\phi^{(0)}}{\partial y}\frac{\partial\phi^{(1)}}{\partial y}dA. \qquad (74)$$

The surface integral is zero from the prescribed boundary conditions of potential acting on an element, so that the potential energy associated with the functional for the compressibility correction can be expressed linearly as

$$\Pi^{(1)} = \frac{1}{2}\int_A \left(\frac{\partial\phi^{(1)}}{\partial x} + \frac{\partial\phi^{(1)}}{\partial y}\right)^2 dA + \frac{1}{2}\int_A \left(\frac{\partial\phi^{(0)}}{\partial x}\right)^2 \frac{\partial\phi^{(0)}}{\partial y}\frac{\partial\phi^{(1)}}{\partial y}dA. \qquad (75)$$

Applying the principle of minimum potential energy for the incompressible solution

$$\frac{\partial\Pi^{(0)}}{\partial\phi^{(0)}} = 0 = \sum_e \sum_n \frac{\partial\Pi_e^{(0)}}{\partial\phi_n^{(0)}} \qquad (76)$$

for elements e with nodes n.

Substituting equation 69 in for $\Pi_e^{(0)}$ and accumulating the contributions for each element, the finite element representation for $\phi^{(0)}$ is

$$\sum_e A\left(\frac{\partial[N]}{\partial x}\frac{\partial[N]^T}{\partial x} + \frac{\partial[N]}{\partial y}\frac{\partial[N]^T}{\partial y}\right)\{\phi^{(0)}\} = \sum_e A[M]\{\phi^{(0)}\} = 0. \qquad (77)$$

Using the same approach for the compressibility correction produces the finite element system

$$\sum_e \frac{A}{2}\left(2[M]\{\phi^{(1)}\} + [M]\{\phi^{(0)}\}\{\phi^{(0)}\}^T[M]\{\phi^{(0)}\}\right) = 0. \tag{78}$$

Thus once a solution to the incompressible potential $\phi^{(0)}$ has been found, the compressible flow correction can be modelled using a linear finite element equation of the form

$$[K]\{\phi^{(1)}\} = \{Q\} \tag{79}$$

and the compressible potential can be calculated

$$\{\phi\} = \{\phi^{(0)}\} + \varepsilon\{\phi^{(1)}\}. \tag{80}$$

The limitations of this formulation are that ε would tend to zero for low velocity flows such as potential flow through porous media. The model was run at $\varepsilon = 1$ neglecting the effects of fluid velocity and exaggerating the compressibility correction. This was justified to highlight the effects of compressibility on the flow and ensure that the model was conservative in calculating fluid potentials.

6.3.3 Boundary conditions

Boundary conditions for the incompressible potential $\phi^{(0)}$ are defined by natural constraints on the system. At the tunnel face, the incompressible potential can be specified as the difference between the air pressure in the tunnel and the hydrostatic water pressure for every point along the tunnel face. At the ground surface, the incompressible potential can be specified as zero, as the air pressure will equilibrate with the water pressure at that point.

Boundary conditions for the compressibility correction $\phi^{(1)}$ are not so straightforward. The compressibility correction can be assumed zero at the ground surface as there is no incompressible potential flow. To derive boundary conditions along the tunnel face, the head loss as flow passes from the excavation into the soil is first calculated for both a compressible and an incompressible fluid. The difference

between these values is taken as a boundary condition value for the compressibility correction $\phi^{(1)}$.

The head loss across the face can be considered using the fluid mechanics model of flow from a large reservoir through an orifice (fig. 6.1). The flow through the orifice is related to the head loss by a coefficient of discharge C_d

$$q = C_d b \sqrt{\frac{2\Delta P}{\rho}} \tag{81}$$

where q is the flow, C_d the coefficient of discharge, b the area of the orifice, ρ the density of the fluid, and ΔP the absolute pressure drop across the orifice.

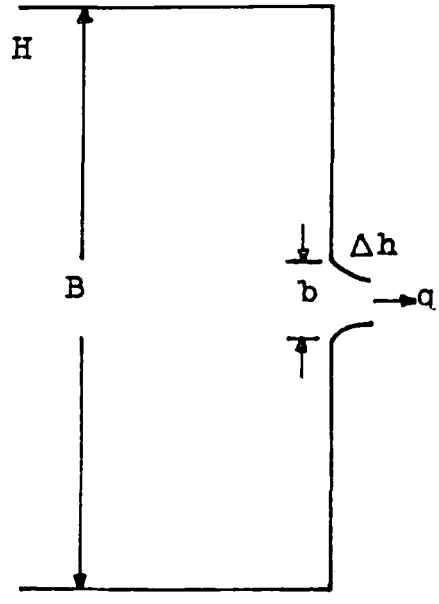

Figure 6.1 — Flow through an orifice

As the density of a compressible fluid changes with the loss of pressure, the average fluid density $\bar{\rho} = \frac{\rho_1+\rho_2}{2}$ should be used in equation 81. The coefficient of discharge for a compressible fluid relative to an incompressible fluid can then be specified assuming constant flow, pressure drop, and cross sectional area of the orifice

$$\frac{C_{dc}}{C_{di}} = \sqrt{\frac{\bar{\rho}}{\rho}} \tag{82}$$

which for an ideal gas

$$\frac{C_{dc}}{C_{di}} \approx \sqrt{\frac{P_1 + P_2}{2P_1}}. \tag{83}$$

The head loss across the orifice is related to C_d by

$$\Delta h = H(1 - C_d^2) \tag{84}$$

where H is the reservoir potential head and Δh the head loss.

Thus, the compressibility correction $\phi^{(1)}$ is

$$\phi^{(1)} = \Delta h_c - \Delta h_i = C_{di}^2 - C_{dc}^2 = \left(1 - \sqrt{\frac{P_1 + P_2}{2P_1}}\right) C_{di}^2 \tag{85}$$

where P_2 can be approximated by the pressure drop for incompressible flow.

The coefficient of discharge is dependent on the coefficient of contraction, C_c, which is in turn dependent on the relative dimensions of the orifice and the reservoir b/B. Rouse (1946) quotes values of C_c and C_d for various values of b/B from Von Mises. If we take the ratio b/B to be analagous to the soil's porosity, V_v/V_b, $C_d = 0.61$ to two significant digits for the range of porosities of interest in this study. Thus boundary conditions for the compressibility correction are proportional to the square root of the boundary conditions of the incompressible potential at the face.

6.4 Finite element model

In using the finite element method, a basic package of matrix algebra subroutines by NAg software was utilized and a host program developed to specifically model blowouts, which is listed in appendix F.

The program first reads in necessary information from an input file, such as nodal geometry, element topology, material type, tunnel size, depth, and the PBL. Boundary conditions are then generated, with values of the incompressible potential and the compressibility correction set to zero at the ground surface, the incompressible potential at the face set equal to the difference between air pressure

and water pressure, and the compressibility correction calculated from equation 85. Values of permeability are set at full saturation according to material type.

The program then enters an iteration loop for desaturation. The incompressible potential matrix and the compressibility correction matrix are constructed and the compressible nodal potentials calculated using the governing equation (eqn. 79).

At this point the gradient in each element is calculated, and excess air pressure in each element set at the average of the nodal potentials. From this a new degree of saturation is calculated for each element with which new permeabilities are calculated for each element. The total stresses in each element are set equal to the overburden plus the surcharge from the water column in the river, and the pore pressure is set equal to the initial water pressure plus the excess air presure. The factor of safety in each element is calculated, and a blowout defined to occur if a continuous chain of failed elements maps from the tunnel face to the ground surface. If not, the program loops back to the routine for incompressible potentials and the sequence of calculations repeated until either a blowout occurs or the critical elements between the tunnel face and the ground surface reach a stable pressurization.

Two meshes were used, one for a tunnel with a standard shield, and one for a tunnel with a hood equal to $\frac{1}{8}$ the tunnel diameter in length. Plots of the meshes are given in appendix B pages B1 and B2.

The meshes used consisted essentially of horizontal rows of linear quadrilateral elements numbered from bottom to top to make varying of the tunnel depth a simple matter of adding or removing rows of elements. An input parameter SCAFAC was used to scale the entire mesh according to tunnel diameter. Simulation runs were made for tunnels of $2m$, $4m$, $6m$, and $8m$ in diameter with the PBL at 0.0, 0.25, and 0.5. River depths of $2m$, $4m$, and $6m$ were used, and ground conditions included clean sand, slightly silty sand, silty sand, and very silty sand. Two meshes were used, one for a standard shield and one for a hooded shield. The basic meshes used are shown in appendix B along with illustrative plots of various parameters calculated in the finite element model.

Chapter VII

Results

7.1 Potential flow and desaturation

Example results from the FEM calculations of nodal excess air pressure parameters are plotted in appendix B pages B3 to B5. From these plots it can be seen that potential head rapidly decreases around the tunnel face in a series of concentric equipotentials tending towards smaller gradients with almost no horizontal component at great distances from the face. It should be noticed that the pore pressure distribution tends to bulge directly above the face, becoming less pronounced higher above the tunnel axis. The correction for compressibility is insignificant except for at the crown of the face, where potential is conserved by expansion around the top of the shield. The effect enhances the propagation of a blowout, but is of marginal significance, especially if measures are taken to stabilize this critical point by clay pocketting or the use of a hooded shield. The desaturation contours form a very pronounced series of concentric rings above and around the tunnel face in a fashion similar to the potential contours.

7.2 Distributions of f.o.s.

Example contours of local f.o.s. are given in appendix B pages B6 and B7. Note that the f.o.s. is greatly reduced around the crown of the face, as would be expected as there are high excess air pressures at that location.

It should also be noticed that the f.o.s. is noticeably lower at the surface directly above the tunnel than at the surface far away from the tunnel. This is a combination of two factors. The total stresses are very low at the ground surface, so excess air pressure has a larger effect on reducing the f.o.s. Also as the excess air pressure drops to zero at the immediate surface, there tends to be a high seepage gradient with larger seepage forces along the surface. It is an interesting observation, in that it implies that a blowout propagates from the surface down as

well as from the excavation up. This has been observed in practice, where often it is noticed that the ground tends to loosen on the surface above a compressed air tunnel (Kell, 63). It should also be noticed how large an effect a hood forepoling in front of the shield has on stabilizing the ground immediately above and in front of the crown of the face. A similar effect can be expected of clay pocketting this area.

7.3 F.O.S. vs tunnel depth graphs

Values of the total factor of safety (F.O.S.) for all tunnelling conditions tested are given in appendix C in table form on pages C1 to C8 and graphed on pages C9 to C56. It can be seen that F.O.S. is not linearly related to tunnel depth but gradually tends to a maximum value as the tunnel depth increases, which would correspond to the ratio of in-situ total stresses to pore pressures. The graphs shown on pages C9 to C56 show a power curve fitted to the data.

It should be noticed from these graphs that the F.O.S. becomes less sensitive to tunnel depth as the river depth increases, as the added surcharge of the river water to both the total stresses and pore pressures decreases the influence of the overburden on F.O.S. It is also evident that the river depth does not influence the critical depth, as the surcharge is redundant when the ratio of total stress to pore pressure is unity.

7.4 Blowout conditions

Appendix D provides data concerning the conditions at which blowouts occured, i.e. $F.O.S. \leq 1.0$. The tables on pages D1 and D2 were constructed by linearly interpolating the depth at which $F.O.S. = 1.0$ in the tables of factors of safety in appendix C. The graphs shown on pages D3 to D7 illustrate the influence of the various factors on stability.

7.4.1 Critical depth vs. tunnel diameter

These graphs are given on pages D3 through D5, showing a strong linear relation between critical depth and tunnel diameter. However, as there is a slight intercept on the graphs, it is not accurate to use C/D as a design parameter as

other methods discussed in 2.3.4 suggest, as C/D is not constant but contains a term inversely proportional to tunnel diameter. Thus, smaller diameter tunnels will require more cover relative to diameter than larger diameter tunnels. Critical depth is more sensitive to tunnel diameter for standard shields than for hooded shields as can be seen in the graphs on page D5. The critical depths for hooded shields range from 0.4 to 0.65 times the critical depth for standard shields. This factor tends to be higher for low values of PBL and lower for higher silt contents.

7.4.2 Percentage silt vs. critical depth

This data is shown plotted with a cubic spline on page D6, and the most pronounced effect is that the critical depth changes only marginally with increased silt content from a clean sand to a slightly silty sand, then drops significantly from a slightly silty sand to a silty sand, then hardly changes at all from a silty sand to a very silty sand. Thus it is important to recognize that there is a critical silt content between 5% and 10% at which sands can be divided into two basic stability groups. This effect seems independent of tunnel diameter and is less influential for higher PBL's.

7.4.3 Critical depth vs. pressure balance level (PBL)

These plots on page D7 show a good linear relation between critical depth and PBL. The effect is quite strong, as the critical depth decreases by up to 50% when the PBL is increased from 0.0 to 0.5. It should be noted that although the critical depth appears to be more sensitive for larger diameter tunnels, smaller diameter tunnels are in fact more susceptible to changes in PBL as the changes in critical depth are larger relative to tunnel diameter in smaller tunnels.

7.4.4 Design nomographs

The design nomographs in appendix E were constructed from the critical depth vs. tunnel diameter data. Five factors appear in the nomographs, the cover (C), tunnel diameter (D), material type, the pressure balance level (PBL), and the *F.O.S.D.*, where *F.O.S.D.* is the design factor of safety as defined in 3.7. River depth is not included in the nomograph parameters as *F.O.S.D.* is a function of tunnel depth and critical depth, both of which are independent of river depth.

Two seperate nomographs were constructed; one for a standard shield and one for a hooded shield.

7.5 Conclusions

The results from the finite element analysis indicated that for subaqueous tunnels under isotropic stress conditions, blowouts can occur at depths anywhere from one and a half tunnel diameters for a small highly pressurized tunnel in clean sand to less than a quarter the tunnel diameter for a large tunnel with low air pressures in a very silty sand. It is important to recognize that the stability of a tunnel against blowouts is a factor of many variables, not just the ground conditions. The design nomographs in appendix E can be used to provide guidelines for avoiding blowouts in subaqueous tunnels through silty sands, whether in designing tunnels and estimating safe tunnelling depths, or in constructing tunnels and estimating safe operating air pressures.

It is hoped that the findings of this study will prove valuable to those involved in the design or construction of tunnels using compressed air, and to any future research into the stability of compressed air tunnels.

Appendix A

Laboratory test results

Sieve Analysis
Coarse material

mass of tin 414.2
mass of tin + soil 1077.2
total mass of soil 663.0

sieve	Sieve wt (g)	soil+sieve wt	Soil wt	% pass
1.4 mm	---	---	0.0	100
710 um	425.9	837.6	411.7	38
600 um	423.5	555.9	132.4	18
212 um	378.0	495.0	117.0	0.3
63 um	299.2	301.3	2.1	0
Pan	425.1	425.2	0.1	0
			663.3	

Pipette analysis

Fine material

SG: 2.65
Volume of pipette: 9.6752
Wt. soil per sample: 12 g
Volume of suspension: 500 ml
Wt per ml of suspension (W1): 0.024 g/ml
Dispersing agent: 25 ml Na Hex

Time (min)	Temp C	F factor	Par size mm	sample	Cont. Wt	Wt cont+soil	Wt soil	% pass
0.5	25	0.0128	0.0572	1	10.0264	8.5318	1.4946	--
3.0	"	"	0.0234	2	20.2404	20.4131	0.1727	0.58
5.0	"	"	0.0181	3	19.1319	19.2629	0.1310	0.59
8.0	"	"	0.0143	4	18.6155	18.2078	---	--
10.0	"	"	0.0128	5	17.9096	18.0054	0.0958	0.43
15.0	"	"	0.0105	6	8.0064	8.4038	0.3974	--
30.0	"	"	0.0074	7	25.6552	25.7137	0.0586	0.26
60.0	"	"	0.0052	8	18.2333	18.6389	0.4058	--
120.0	"	"	0.0037	9	18.3877	18.4259	0.0382	0.17
240.0	"	"	0.0026	10	8.3608	8.3901	0.0293	0.13
480.0	"	"	0.0018	11	18.6493	18.6723	0.0230	0.10
1440.0	"	"	0.0011	12	16.7293	16.7196	0.0097	0.04

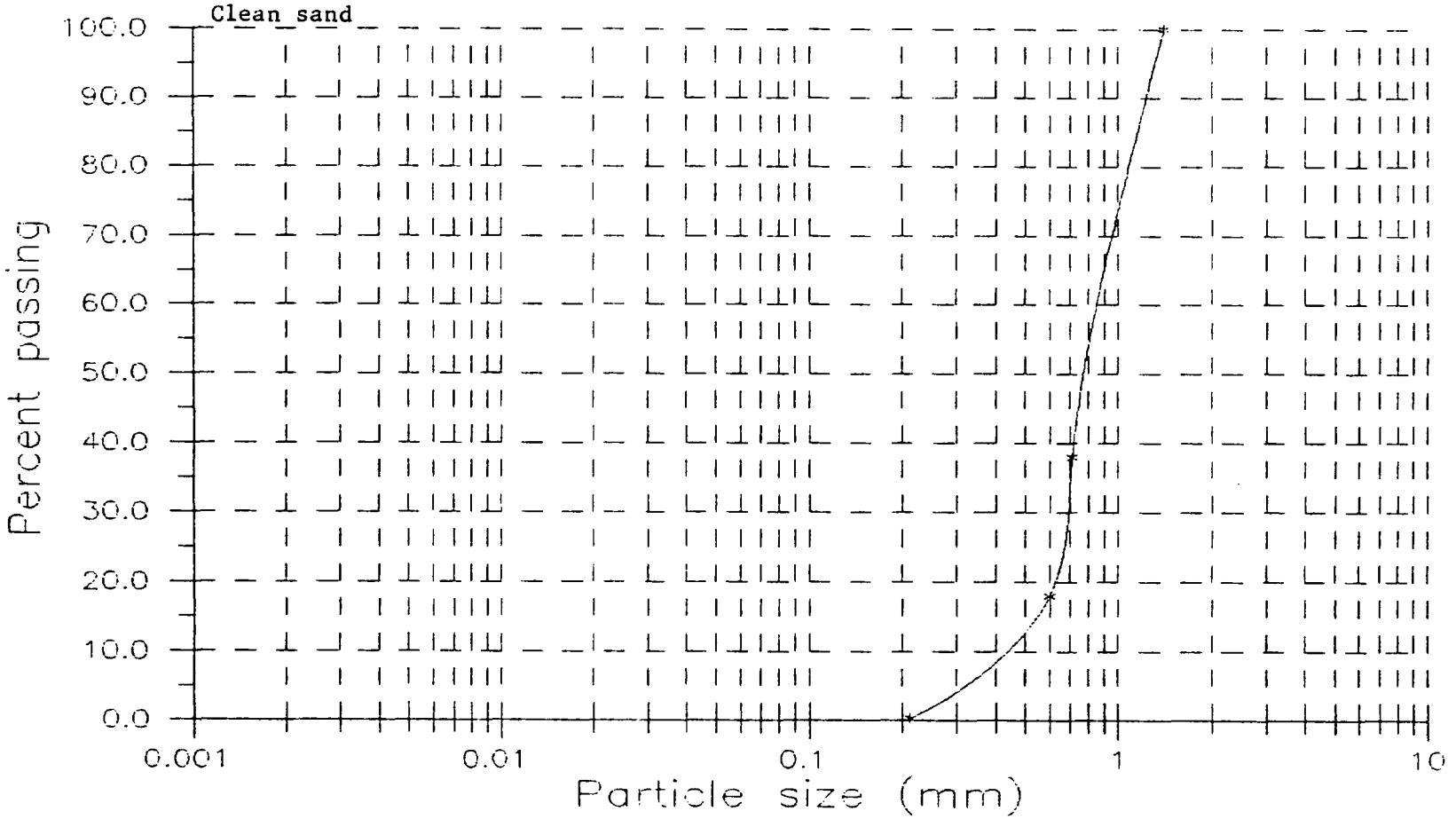
Clean sand
100.0
90.0
80.0
70.0
60.0
50.0
40.0
30.0
20.0
10.0
0.0
Percent passing
0.001
0.01
0.1
1
10
Particle size (mm)

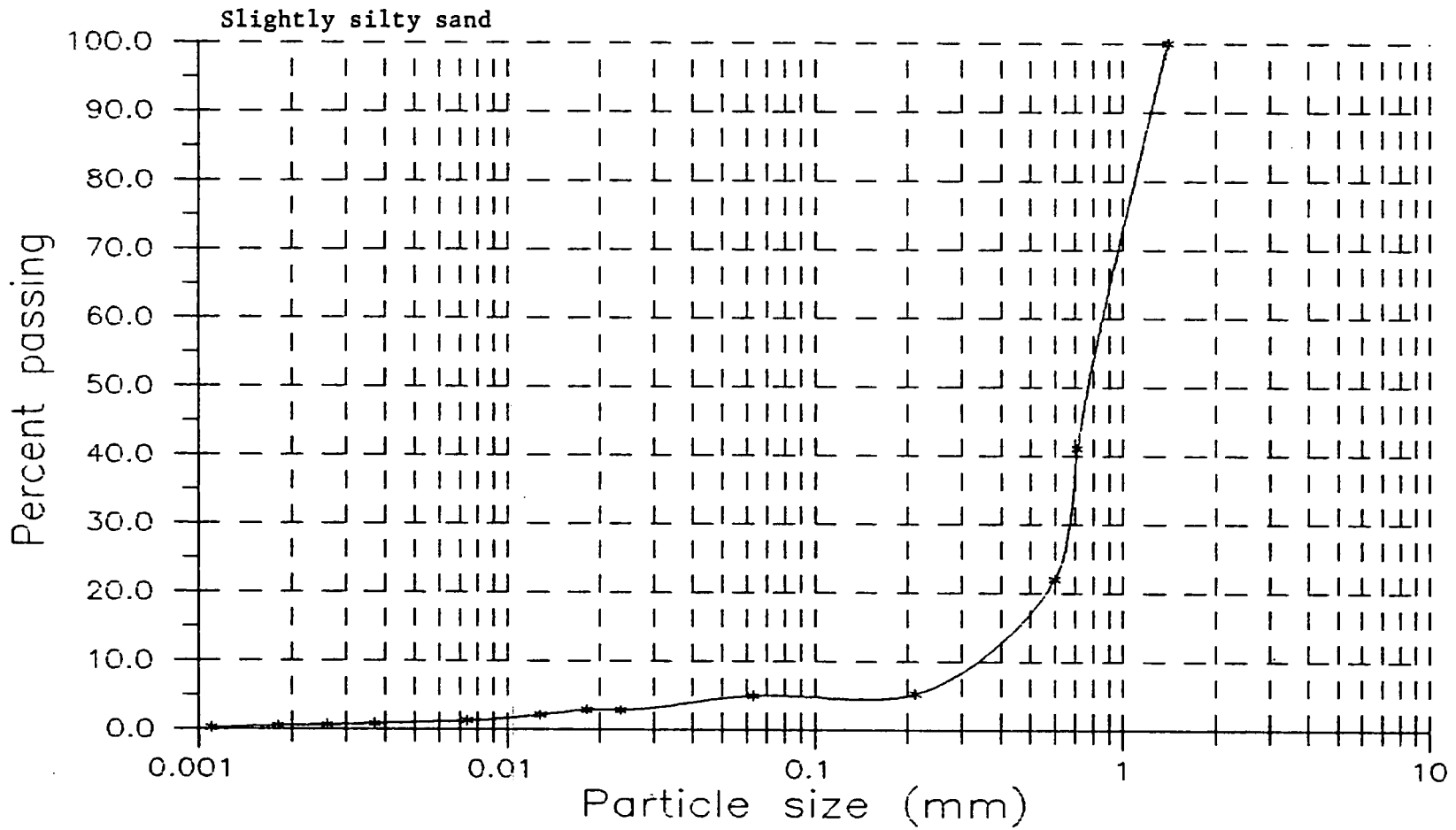
Slightly silty sand
100.0
90.0
80.0
70.0
60.0
50.0
40.0
30.0
20.0
10.0
0.0
Percent passing
0.001
0.01
0.1
1
10
Particle size (mm)

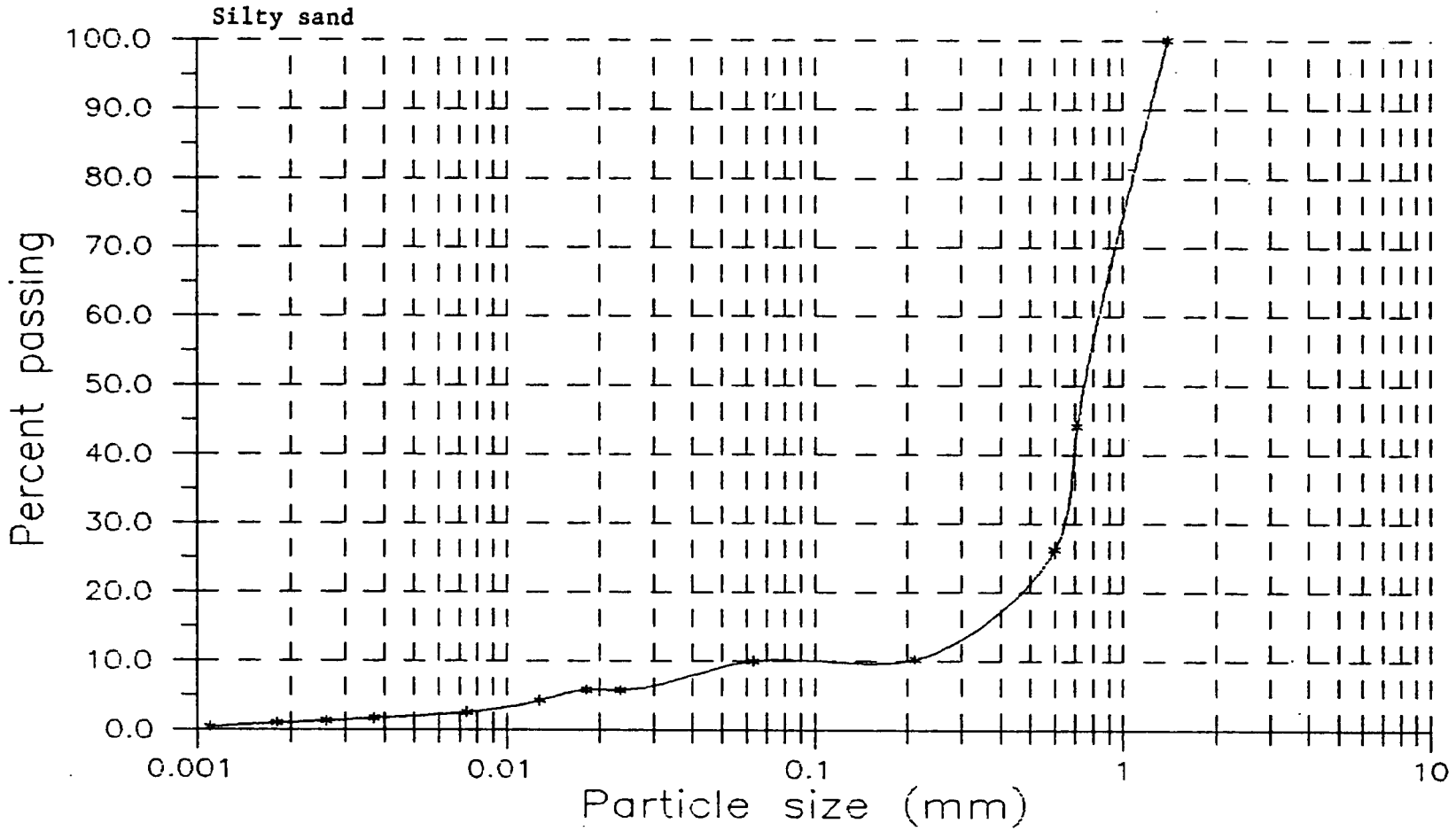
Silty sand
100.0
90.0
80.0
70.0
60.0
50.0
40.0
30.0
20.0
10.0
0.0
Percent passing
0.001
0.01
0.1
1
10
Particle size (mm)

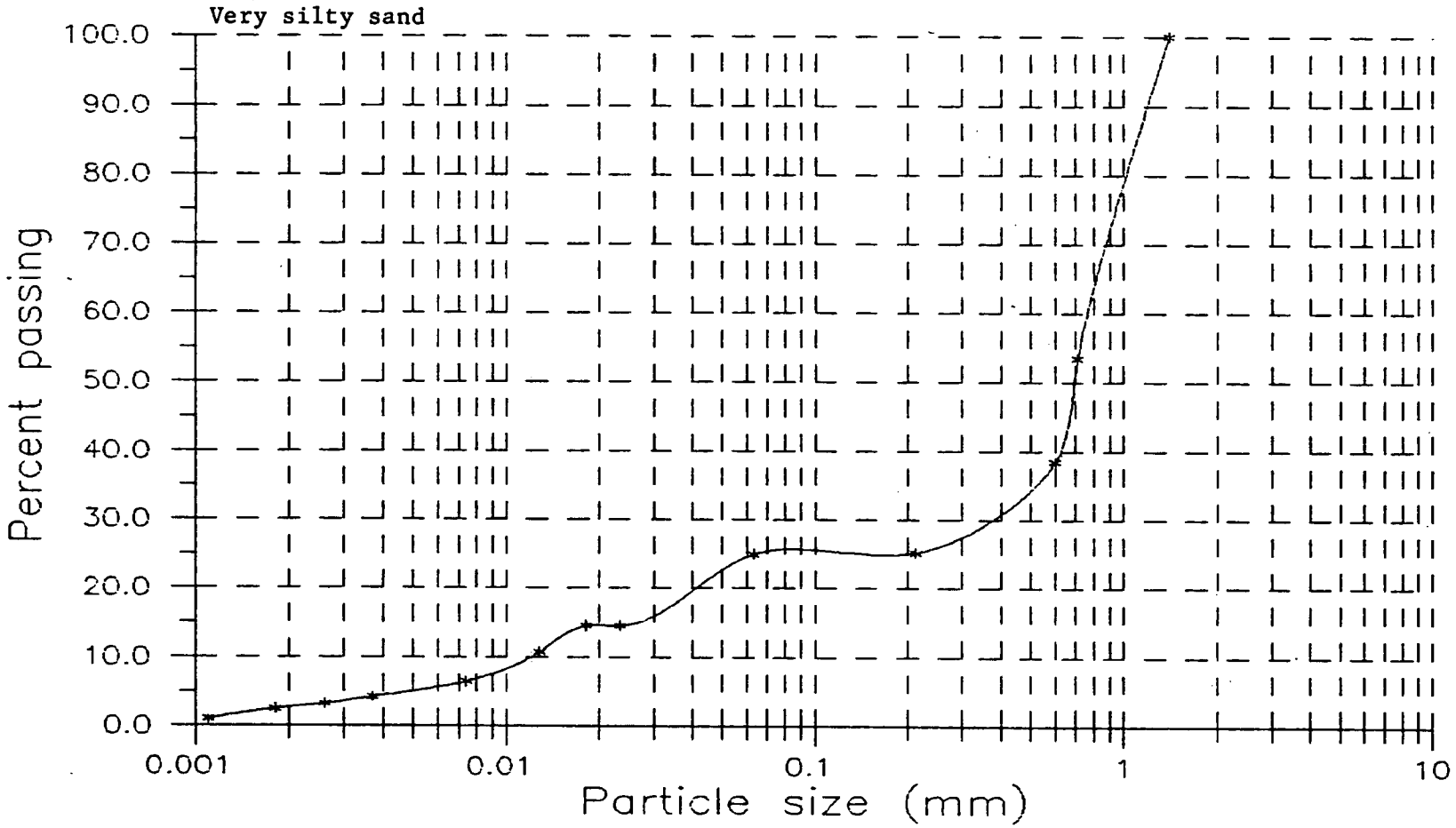
Very silty sand
100.0
90.0
80.0
70.0
60.0
50.0
40.0
30.0
20.0
10.0
0.0
Percent passing
0.001
0.01
0.1
1
10
Particle size (mm)

Specific Gravity

Coarse material

Sample no.	1	2	3	4
Bottle number	1473	1502	1515	1557
W3: bottle + soil + water	77.8	79.7	80.1	77.5
W2: bottle + soil	30.3	32.6	33.0	31.7
W4: bottle full of water	74.2	75.3	75.3	74.0
W1: bottle	24.4	25.6	25.4	25.7
W5: water used (W3-W2)	47.5	47.1	47.1	45.8
W6: soil used (W2-W1)	5.9	7.0	7.6	6.0
V: soil volume (W4-W1)-(W3-W2)	2.3	2.6	2.8	2.5
SG: specific gravity of soil	2.57	2.69	2.71	2.40
Average specific gravity	2.66			

Fine material

Sample no.	1	2
Bottle number	1	8
W3: bottle + soil + water	62.4	68.6
W2: bottle + soil	151.4	154.7
W4: bottle full of water	136.3	136.7
W1: bottle	24.2	29.4
W5: water used (W3-W2)	98.1	97.2
W6: soil used (W2-W1)	89.0	86.1
V: soil volume (W4-W1)-(W3-W2)	9.1	11.1
SG: specific gravity of soil	2.66	2.65
Average specific gravity	2.65	

Bulk Density

Soil type	Wt soil+beaker	Wt beaker	Wt soil	Bulk Dens	n	e
Clean sand	919.2	162.5	756.7	1.51	0.429	0.751
Slightly silty sand	920.0	162.5	757.5	1.52	0.428	0.748
Silty sand	929.4	162.5	766.9	1.53	0.421	0.727
Very silty sand	922.3	162.5	759.8	1.52	0.427	0.745

Atterberg Limits

Test no.	1	2	3	4	5	6	7	8
Test type	LL	LL	LL	LL	PL	PL	PL	PL
Initial reading (mm)	21.37	20.67	21.57	21.75	---	---	---	---
Final reading (mm)	45.02	35.99	42.01	41.94	---	---	---	---
Cone penetration	23.65	15.32	20.44	20.19	---	---	---	---
Tin no	PA4	5	10	A8	43	99	2	58
Mass wet soil+tin	13.6	16.4	29.6	43.7	5.4	5	5.7	6
mass of dried soi+tin	9.8	11.6	20.6	27.5	4.8	4.7	4.9	5.3
Mass of tin	5.0	4.6	8.5	5.3	3.6	4.1	3.4	3.9
mass of moisture	3.8	4.8	9.0	16.2	0.6	0.3	0.8	0.7
mass of dry soil	4.8	7.0	12.1	22.2	1.2	0.6	1.5	1.4
Moisture content	0.77	0.69	0.74	0.73	0.5	0.5	0.53	0.5

Liquid Limit (LL):	0.73
Plastic Limit (PL):	0.51
Plasticity index (PI):	0.23

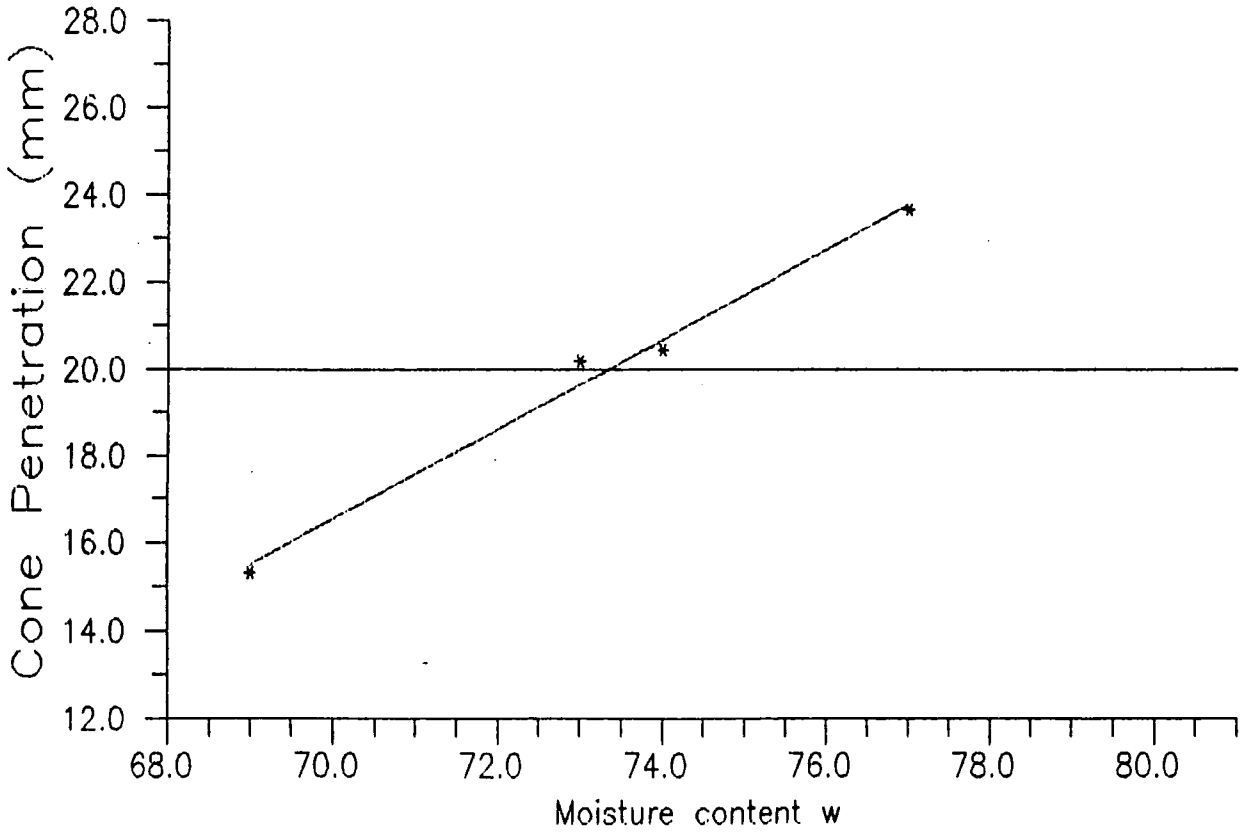

Desaturation tests
Ruska Permeameter

Clean sand

Sample no	1	2	3	4	5
Tin no	63	63	14	2	25
W2: Wt wet soil+tin	25.3	21.3	27.4	19.9	25.2
W3: Wt dry soil+tin	24.4	20.9	27.1	19.6	23.4
W1: Wt of tin	4.7	5.0	4.7	5.3	9.3
W4: Wt of moisture	0.9	0.4	0.3	0.3	1.8
W5: Wt dry soil	19.7	15.9	22.4	14.3	14.1
Moisture content W4/W5	0.05	0.03	0.01	0.02	0.13
Saturation wGs/e	0.18	0.11	0.04	0.07	0.47
Excess air press (atm)	0.04	0.05	0.10	0.08	0.02
Excess air press (m H2O)	0.41	0.52	1.03	0.82	0.21

Slightly silty sand

Sample no	1	2	3	4
Tin no	PA3	PA6	4	C
W2: Wt wet soil+tin	19.2	18.3	19.9	19.2
W3: Wt dry soil+tin	18.2	17.7	18.2	18.5
W1: Wt of tin	5.2	5.3	5.3	5.3
W4: Wt of moisture	1.0	0.6	1.7	0.7
W5: Wt dry soil	13.0	12.4	12.9	13.2
Moisture content W4/W5	0.08	0.05	0.13	0.05
Saturation wGs/e	0.30	0.19	0.49	0.20
Excess air press (atm)	0.04	0.05	0.02	0.07
Excess air press (m H2O)	0.41	0.52	0.21	0.72

Silty sand

Sample no	1	2	3	4	5
Tin no	25	2	PA6	63	PA3
W2: Wt wet soil+tin	25.4	18.9	19.0	20.2	18.6
W3: Wt dry soil+tin	24.5	16.8	16.9	17.7	16.9
W1: Wt of tin	9.3	5.3	5.1	4.8	5.2
W4: Wt of moisture	0.9	2.1	2.1	2.5	1.7
W5: Wt dry soil	15.2	11.5	11.8	12.9	11.7
Moisture content W4/W5	0.06	0.18	0.18	0.19	0.17
Saturation wGs/e	0.28	0.85	0.83	0.90	0.68
Excess air press (atm)	0.20	0.07	0.05	0.03	0.10
Excess air press (m H2O)	2.06	0.72	0.52	0.31	1.03

Very silty sand

Sample no	1	2	3	4	5
Tin no	C	PA2/A5	H3	PA7	PA2/A5
W2: Wt wet soil+tin	16.1	19.5	19.9	17.1	21.2
W3: Wt dry soil+tin	16.1	17.6	18.1	15.6	18.8
W1: Wt of tin	5.4	5.2	5.3	3.6	5.2
W4: Wt of moisture	0.0	1.9	1.8	1.5	2.4
W5: Wt dry soil	10.7	12.4	12.8	12.0	13.6
Moisture content W4/W5	0.00	0.15	0.14	0.13	0.18
Saturation wGs/e	0.00	0.67	0.64	0.56	0.80
Excess air press (atm)	0.10	0.08	0.05	0.12	0.03
Excess air press (m H2O)	1.03	0.82	0.52	1.24	0.31

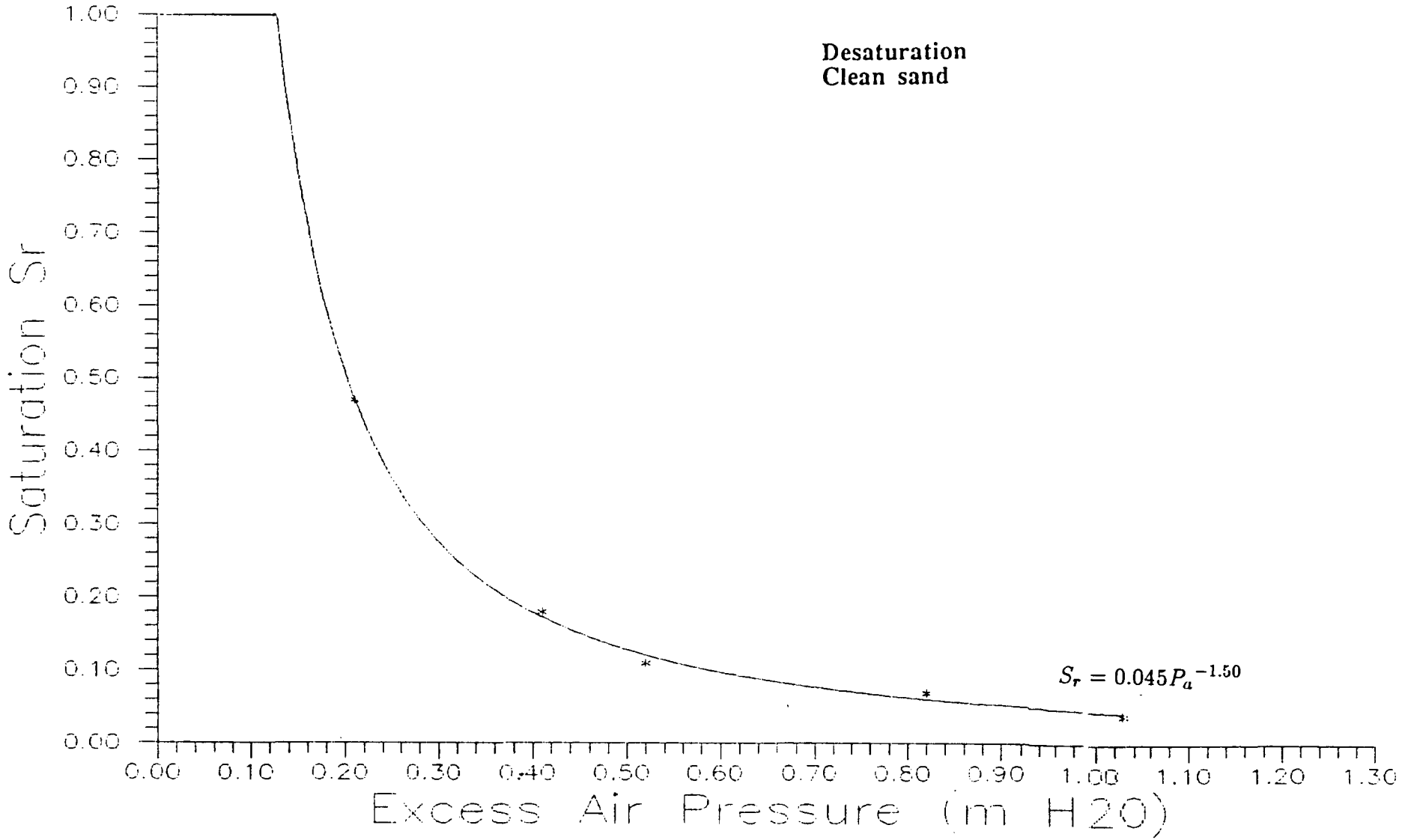
Desaturation
Clean sand
$S_r = 0.045 P_a^{-1.50}$
Saturation Sr
1.00
0.90
0.80
0.70
0.60
0.50
0.40
0.30
0.20
0.10
0.00
0.00 0.10 0.20 0.30 0.40 0.50 0.60 0.70 0.80 0.90 1.00 1.10 1.20 1.30
Excess Air Pressure (m H20)

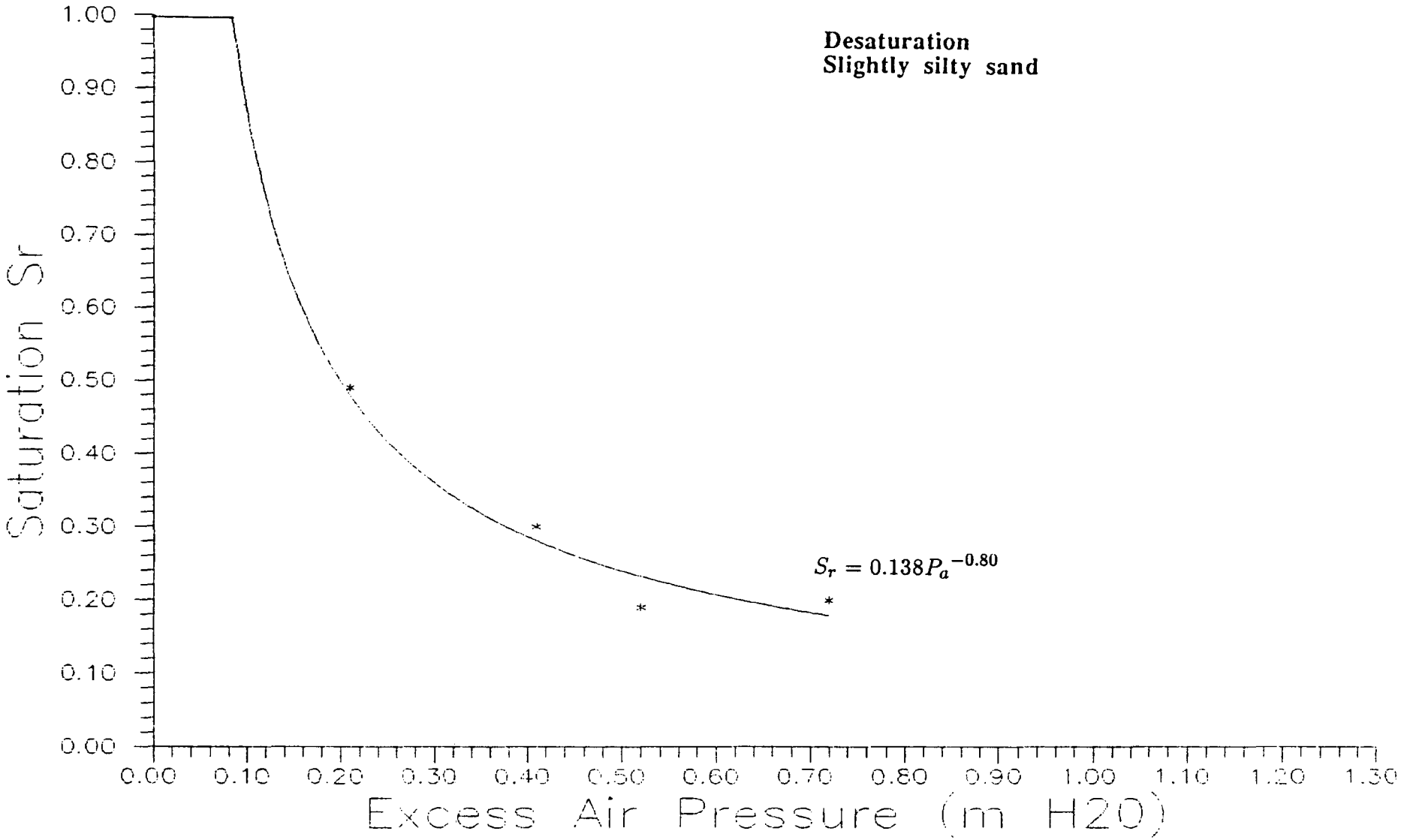
Desaturation
Slightly silty sand
$S_r = 0.138 P_a^{-0.80}$
Saturation Sr
1.00
0.90
0.80
0.70
0.60
0.50
0.40
0.30
0.20
0.10
0.00
0.00 0.10 0.20 0.30 0.40 0.50 0.60 0.70 0.80 0.90 1.00 1.10 1.20 1.30
Excess Air Pressure (m H20)

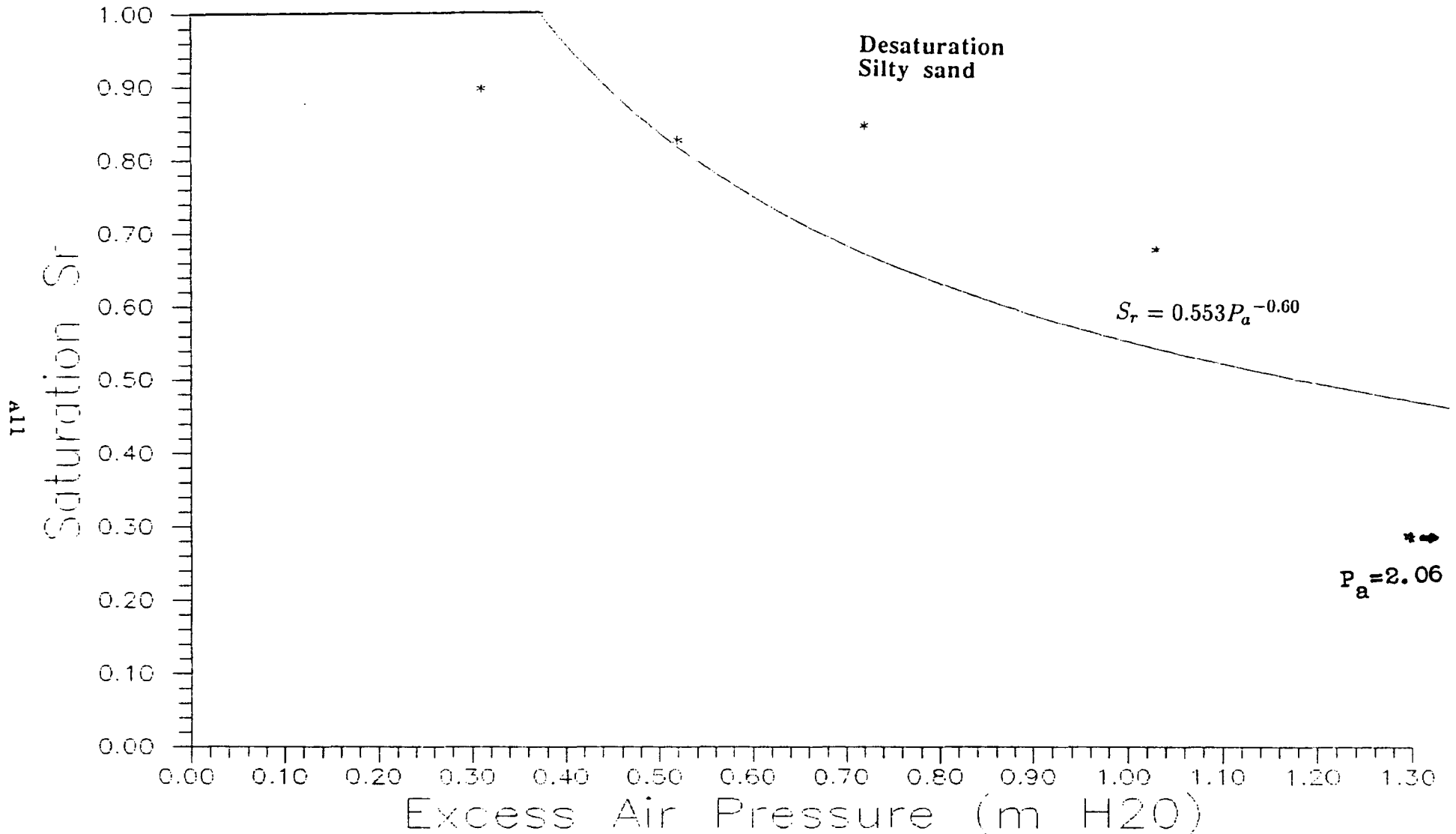
Desaturation
Silty sand
$S_r = 0.553 P_a^{-0.60}$
P_a=2.06
Saturation Sr
1.00
0.90
0.80
0.70
0.60
0.50
0.40
0.30
0.20
0.10
0.00
0.00 0.10 0.20 0.30 0.40 0.50 0.60 0.70 0.80 0.90 1.00 1.10 1.20 1.30
Excess Air Pressure (m H20)

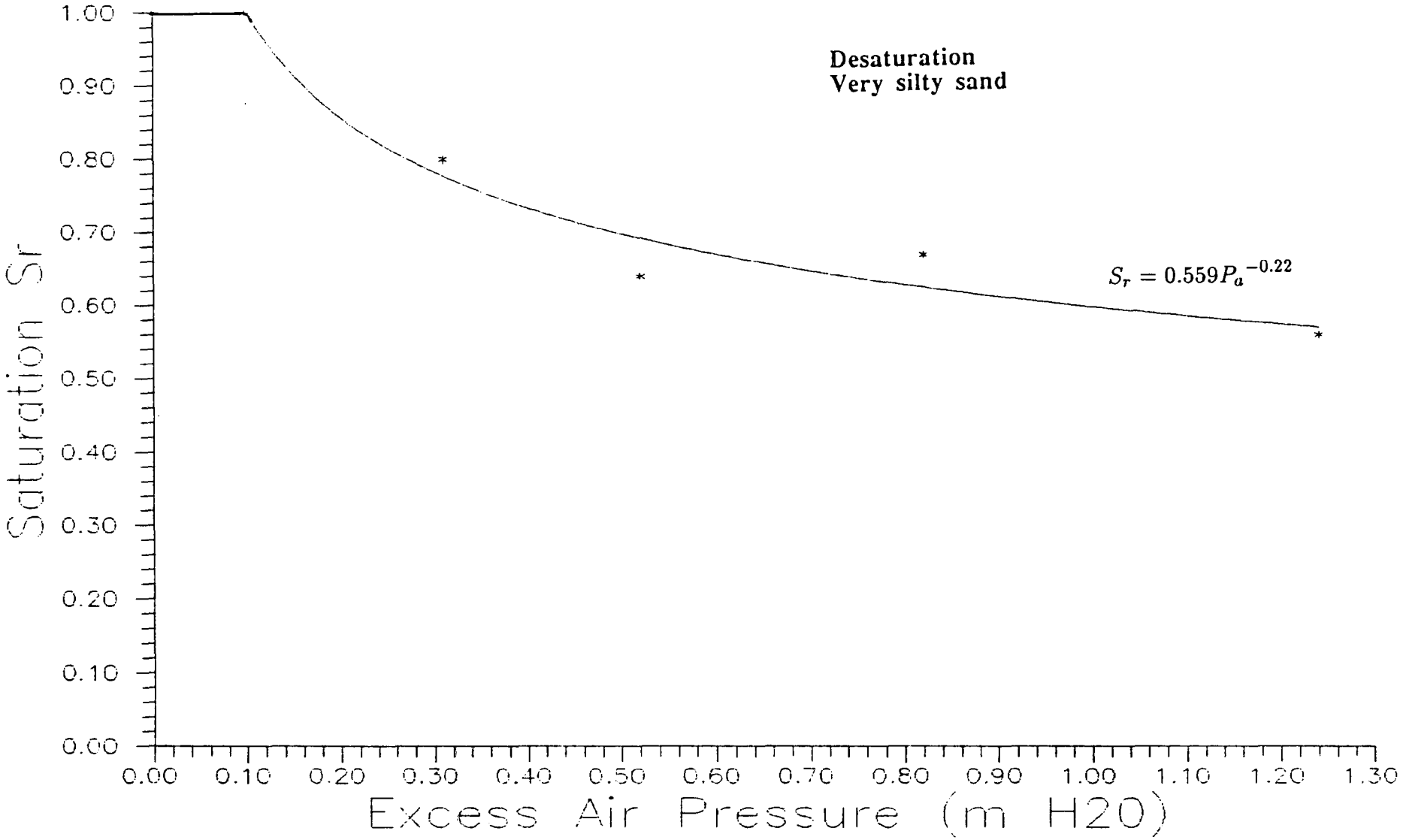
Desaturation
Very silty sand
$S_r = 0.559 P_a^{-0.22}$
Saturation Sr
1.00
0.90
0.80
0.70
0.60
0.50
0.40
0.30
0.20
0.10
0.00
0.00 0.10 0.20 0.30 0.40 0.50 0.60 0.70 0.80 0.90 1.00 1.10 1.20 1.30
Excess Air Pressure (m H20)

Permeability tests
Ruska Permeameter

Clean sand

Sample no	1	2	3	4	5	6	7
Tin no	63	63	H4	4	25	3	4
W2: Wt wet soil+tin	19.1	27.4	19.6	18.8	25.3	22.5	17.5
W3: Wt dry soil+tin	16.5	26.6	18.6	18.2	24.1	22.4	16.0
W1: Wt of tin	4.7	4.7	4.6	5.3	9.4	9.3	5.4
W4: Wt of moisture	2.6	0.8	1.0	0.6	1.2	0.1	1.5
W5: Wt dry soil	11.8	21.9	14.0	12.9	14.7	13.1	11.5
Moisture content W4/W5	0.22	0.04	0.07	0.05	0.08	0.01	0.13
Saturation wGs/e	0.79	0.13	0.26	0.17	0.29	0.04	0.47
Flow rate (cc/s)	14.0	37.0	57.0	55.0	41.0	73.0	34.5
P1 (atm)	1.02	1.01	1.02	1.02	1.02	1.02	1.03
Pav (atm)	1.01	1.005	1.01	1.01	1.01	1.01	1.015
P1-P2 (atm)	0.02	0.01	0.02	0.02	0.02	0.02	0.03
K (Darcy's)	14.9	78.1	33.8	32.6	43.5	77.5	24.5
k (x10-5 cm/s)	5.7	30.0	13.0	12.6	16.7	29.8	9.4

Slightly silty sand

Sample no	1	2	3	4	5	6
Tin no	25	CBDA5	PA6	4	63	PA6
W2: Wt wet soil+tin	22.1	20.6	21.2	21.2	19.1	18.7
W3: Wt dry soil+tin	20.4	17.7	18.6	18.8	17.7	16.9
W1: Wt of tin	9.4	4.9	5.3	5.3	4.8	5.3
W4: Wt of moisture	1.7	2.9	2.6	2.4	1.4	1.8
W5: Wt dry soil	11.0	12.8	13.3	13.5	12.9	11.6
Moisture content W4/W5	0.15	0.23	0.20	0.18	0.11	0.16
Saturation wGs/e	0.55	0.86	0.74	0.66	0.40	0.58
Flow rate (cc/s)	58.0	49.0	44.0	46.0	52.0	21.0
P1 (atm)	1.05	1.10	1.10	1.05	1.04	1.10
Pav (atm)	1.025	1.05	1.05	1.025	1.02	1.05
P1-P2 (atm)	0.05	0.1	0.1	0.05	0.04	0.10
K (Darcy's)	25.0	10.8	9.7	19.8	27.8	4.6
k (x10-5 cm/s)	9.6	4.2	3.7	7.6	10.7	1.8

Permeability tests
Ruska permeameter

Silty sand

Sample no	1	2	3	4	5
Tin no	PA3	4	25	2	PA6
W2: Wt wet soil+tin	20.8	19.4	19.6	18.3	19.2
W3: Wt dry soil+tin	18.6	17.2	18.6	17.6	17.5
W1: Wt of tin	5.2	5.4	4.6	5.2	5.3
W4: Wt of moisture	2.2	2.2	1.0	0.7	1.7
W5: Wt dry soil	13.4	11.8	14.0	12.4	12.2
Moisture content W4/W5	0.16	0.19	0.07	0.06	0.14
Saturation wGs/e	0.74	0.87	0.26	0.26	0.65
Flow rate (cc/s)	58.0	39.0	57.0	21.0	25.0
P1 (atm)	1.15	1.15	1.02	1.01	1.05
Pav (atm)	1.075	1.075	1.01	1.005	1.025
P1-P2 (atm)	0.15	0.15	0.02	0.01	0.05
K (Darcy's)	8.7	5.8	12.5	44.3	10.8

Very silty sand

Sample no	1	2	3	4	5	6
Tin no	PA6	25	2	63	CBDA5	PA2
W2: Wt wet soil+tin	19.6	22.8	18.8	18.1	19.0	21.2
W3: Wt dry soil+tin	17.3	20.8	16.8	16.7	17.8	18.8
W1: Wt of tin	5.2	9.3	5.3	4.7	5.1	5.2
W4: Wt of moisture	2.3	2.0	2.0	1.4	1.2	2.4
W5: Wt dry soil	12.1	11.5	11.5	12.0	12.7	13.6
Moisture content W4/W5	0.19	0.17	0.17	0.12	0.09	0.18
Saturation wGs/e	0.97	0.87	0.87	0.61	0.46	0.80
Flow rate (cc/s)	62.0	24.0	56.0	52.0	44.0	19.5
P1 (atm)	1.20	1.20	1.10	1.04	1.25	1.03
Pav (atm)	1.1	1.1	1.05	1.02	1.125	1.015
P1-P2 (atm)	0.2	0.2	0.1	0.04	0.25	0.03
K (Darcy's)	7.1	2.7	12.3	19.8	27.8	4.6

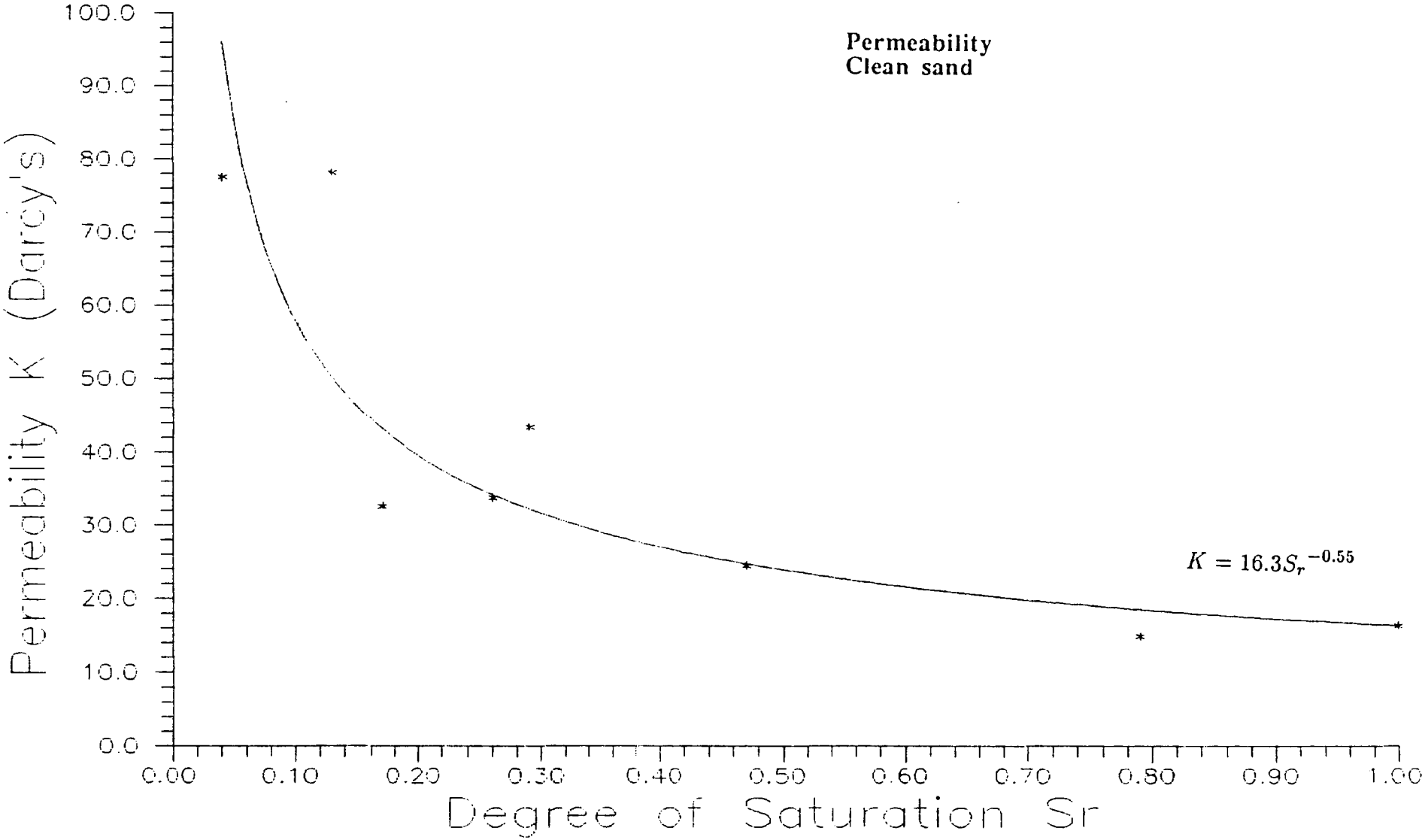
Permeability
Clean sand
$K = 16.3S_r^{-0.55}$
Permeability K (Darcy's)
100.0
90.0
80.0
70.0
60.0
50.0
40.0
30.0
20.0
10.0
0.0
0.00
0.10
0.20
0.30
0.40
0.50
0.60
0.70
0.80
0.90
1.00
Degree of Saturation Sr

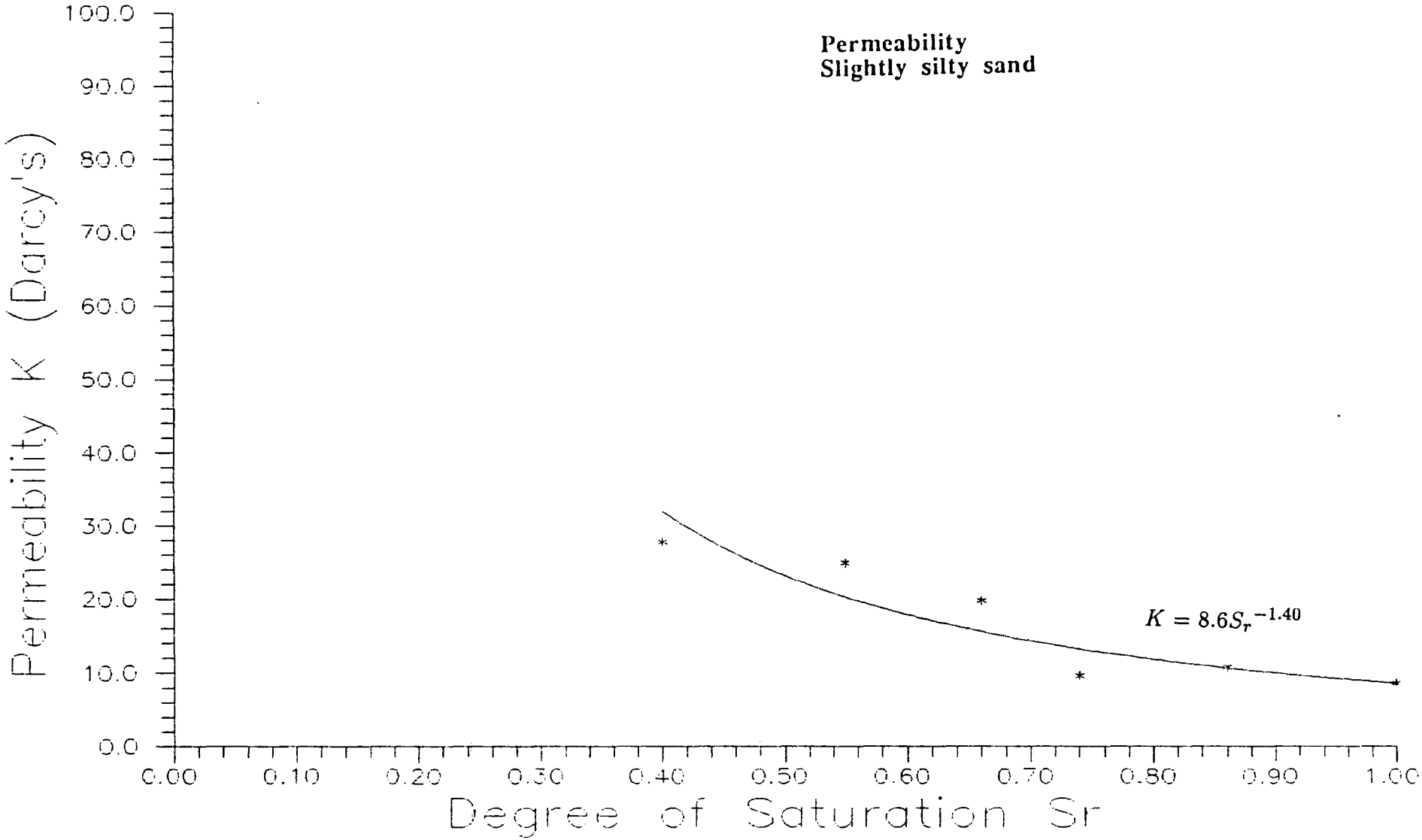
Permeability
Slightly silty sand
$K = 8.6S_r^{-1.40}$
Permeability K (Darcy's)
100.0
90.0
80.0
70.0
60.0
50.0
40.0
30.0
20.0
10.0
0.0
0.00
0.10
0.20
0.30
0.40
0.50
0.60
0.70
0.80
0.90
1.00
Degree of Saturation Sr

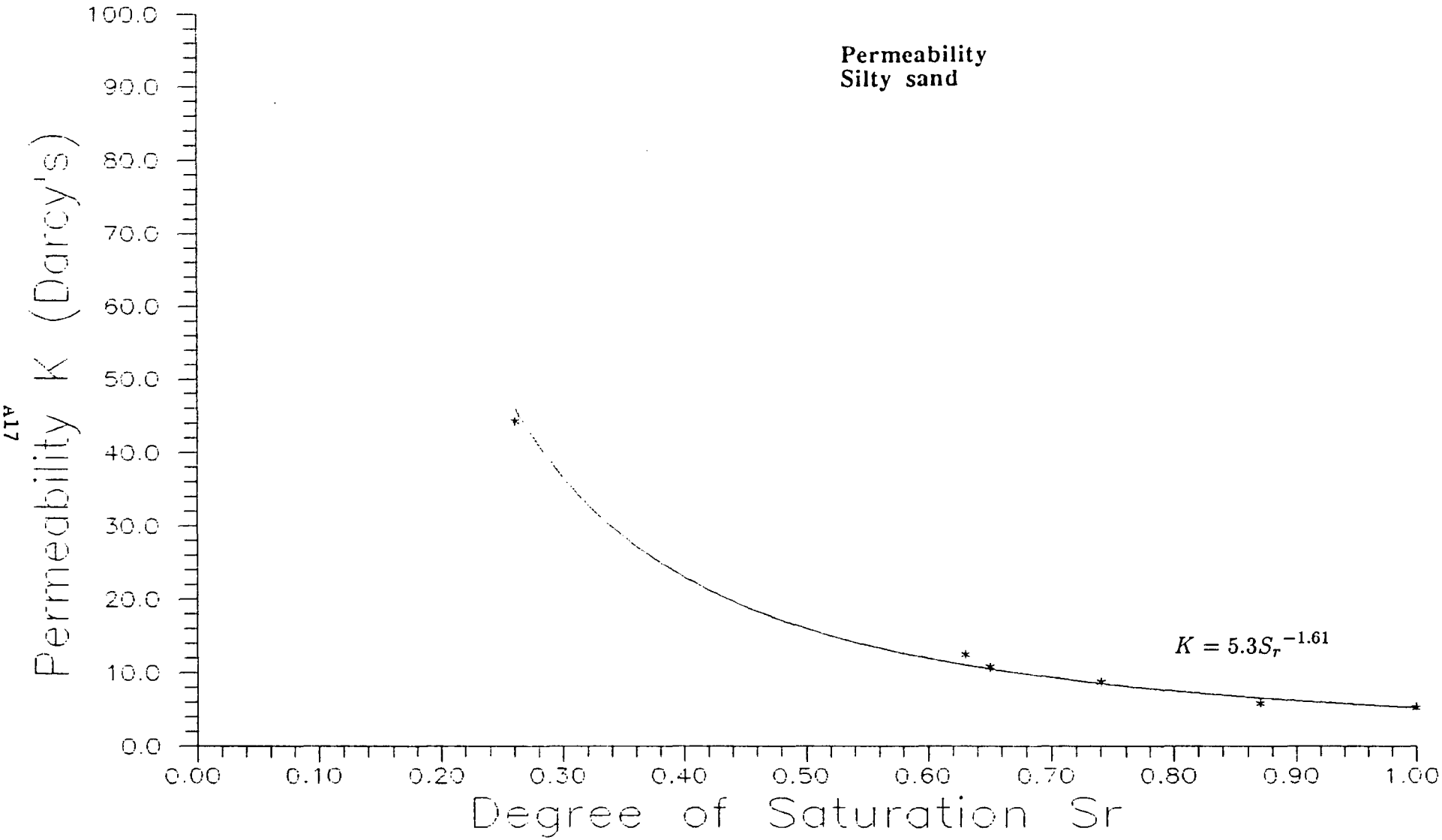
Permeability
Silty sand
$K = 5.3S_r^{-1.61}$
Permeability K (Darcy's)
100.0
90.0
80.0
70.0
60.0
50.0
40.0
30.0
20.0
10.0
0.0
0.00
0.10
0.20
0.30
0.40
0.50
0.60
0.70
0.80
0.90
1.00
Degree of Saturation Sr

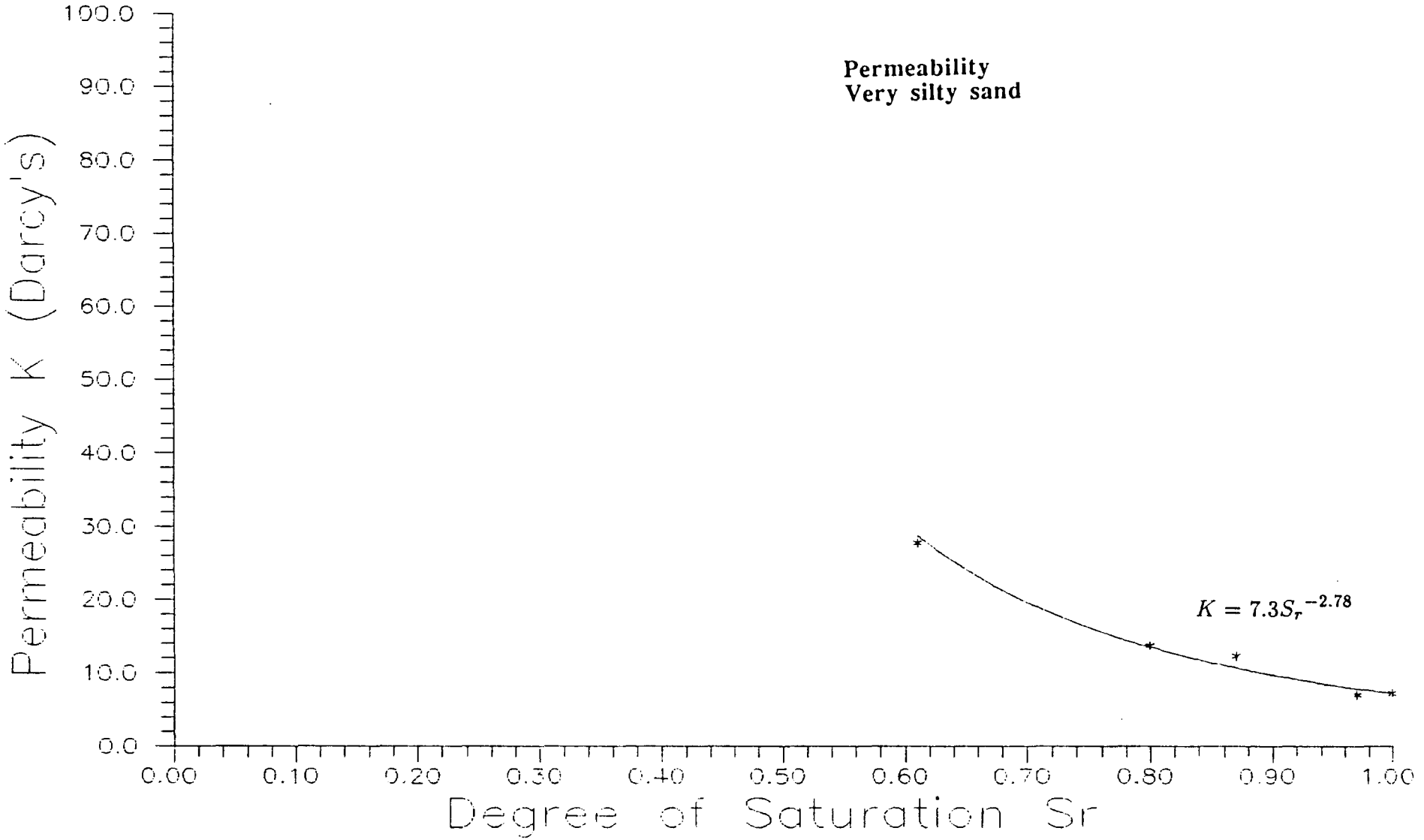
Permeability
Very silty sand
$K = 7.3S_r^{-2.78}$
Permeability K (Darcy's)
100.0
90.0
80.0
70.0
60.0
50.0
40.0
30.0
20.0
10.0
0.0
0.00
0.10
0.20
0.30
0.40
0.50
0.60
0.70
0.80
0.90
1.00
Degree of Saturation Sr

Permeability tests
Modified triaxial cell

P1=1.01 bar (1.03 atm)
P2=1.00 bar (1.02 atm)
P1-P2=0.01 atm
Pav=1.02 atm
A=11.34 sq cm
u=0.0175 cp

Sample	Material	L (cm)	Q (L/min)	Q (cc/s)	K (Darcy's)	Kavg (Darcy's)
1	Clean sand	7.4	12.0	200	225	214
2	Clean sand	7.2	11.5	191	209	
3	Clean sand	7.2	11.5	191	209	
4	Slightly silty sand	7.4	10.9	182	205	200
5	Slightly silty sand	7.3	11.5	191	212	
6	Slightly silty sand	7.2	10.0	167	183	
7	Silty sand	7.1	7.0	117	126	155
8	Silty sand	7.4	7.7	128	144	
9	Silty sand	7.3	10.6	177	196	
10	Very silty sand	7.3	5.8	97	108	132
11	Very silty sand	7.4	9.5	158	178	
12	Very silty sand	7.2	6.0	100	109	

Appendix B

FEM mesh plots

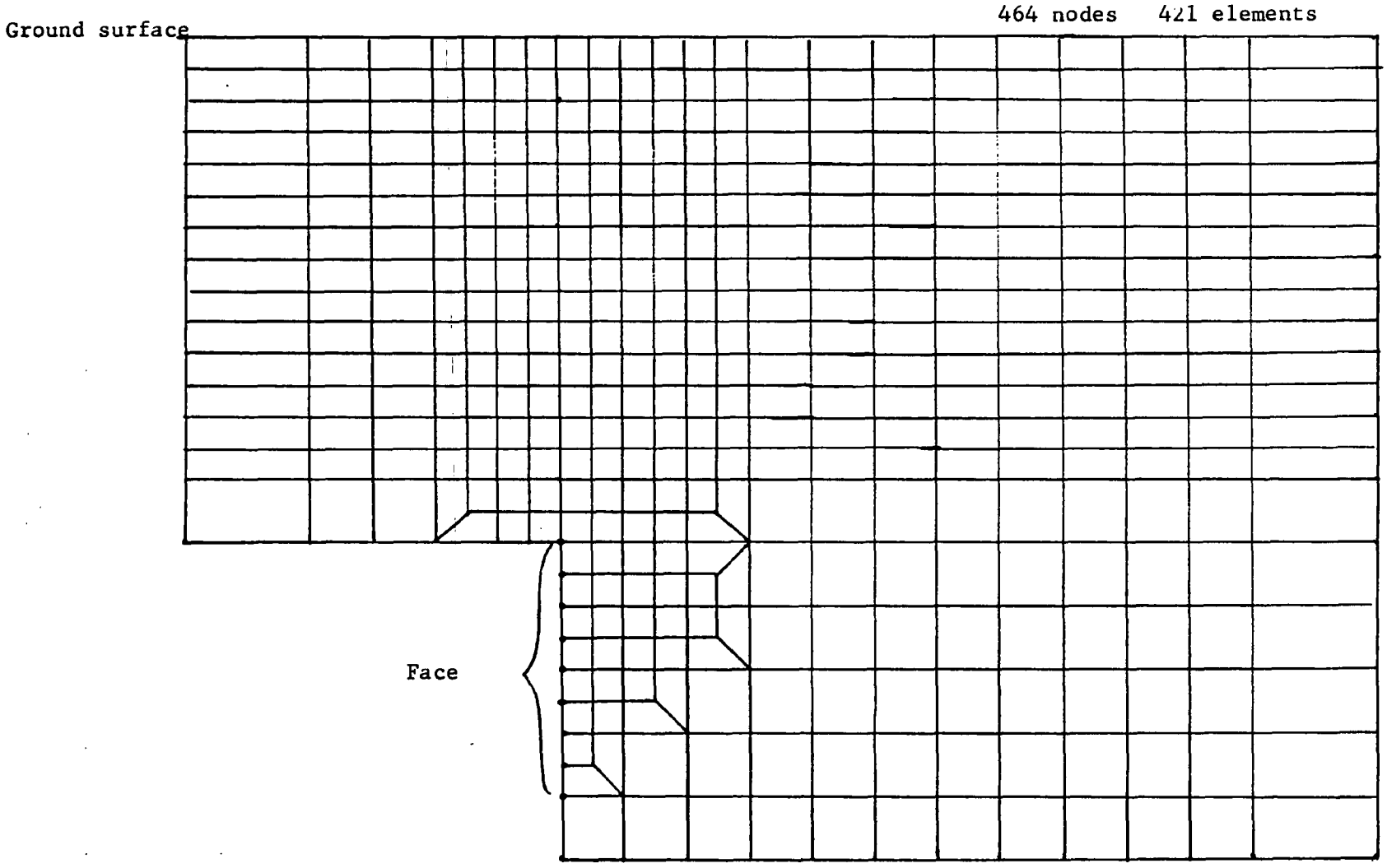

FEM mesh - Standard Shield

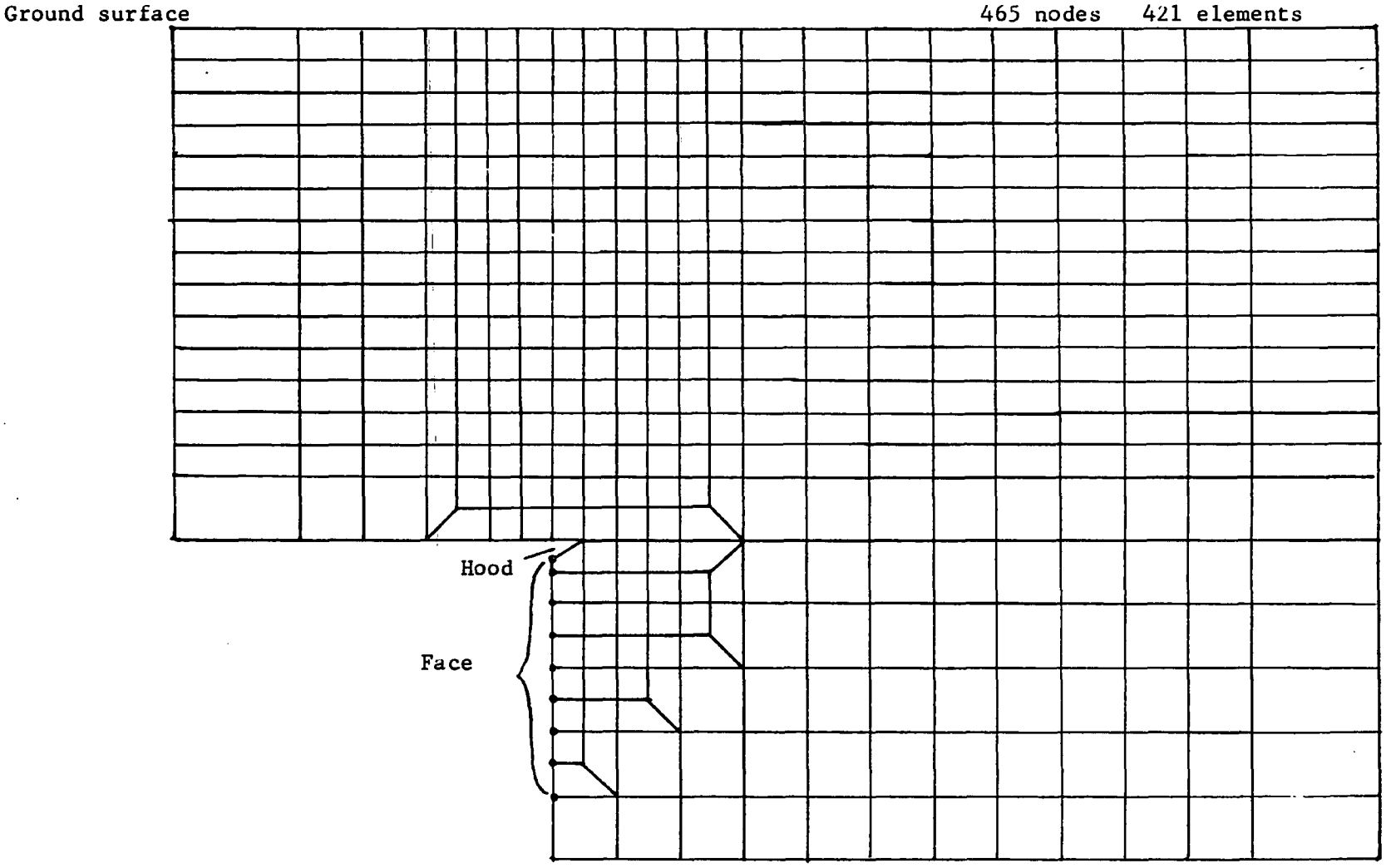

FEM mesh - Hooded Shield

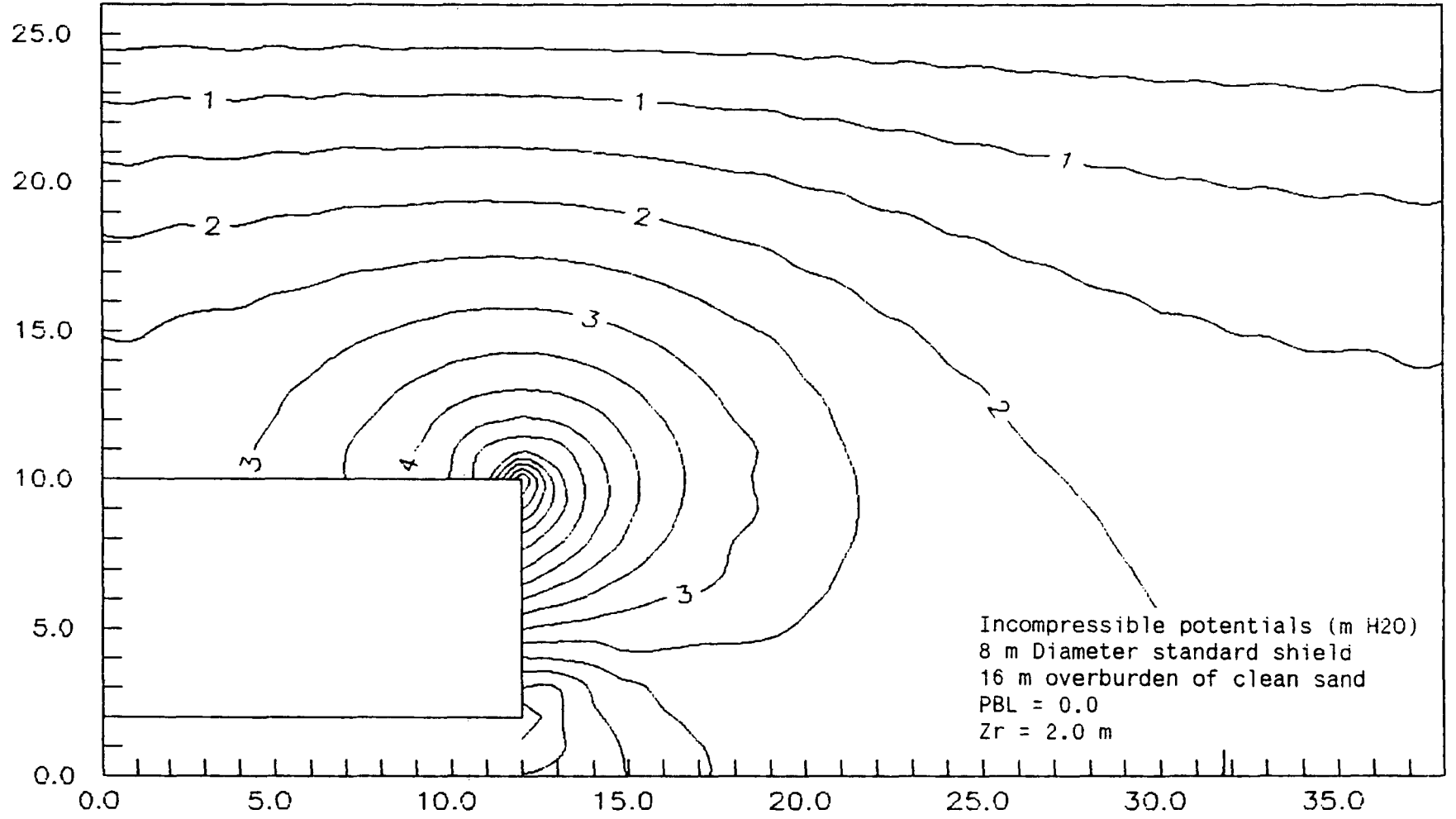
25.0
20.0
15.0
10.0
5.0
0.0
0.0
5.0
10.0
15.0
20.0
25.0
30.0
35.0
1
1
1
2
2
2
3
3
3
4
Incompressible potentials (m H2O)
8 m Diameter standard shield
16 m overburden of clean sand
PBL = 0.0
Zr = 2.0 m

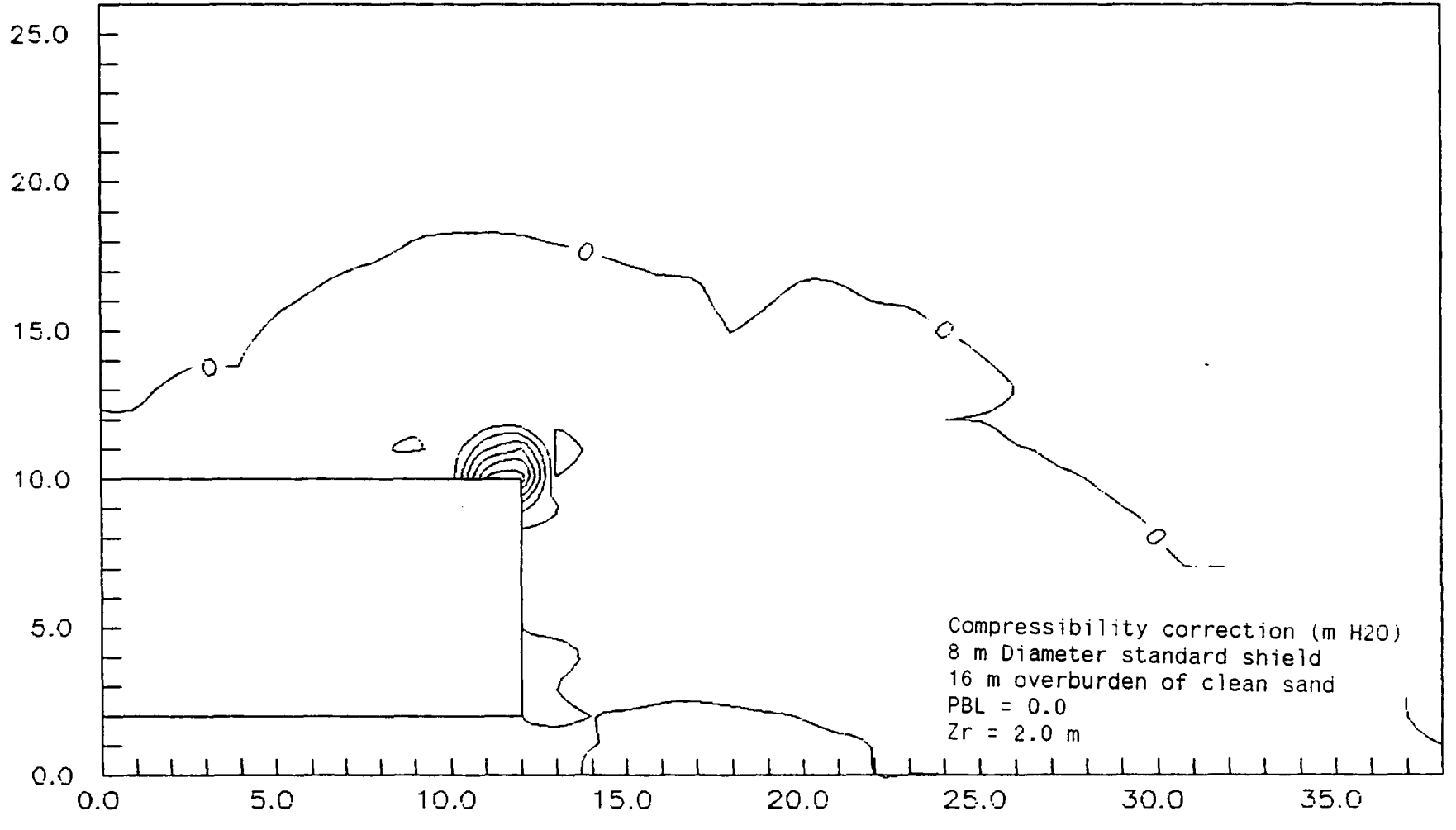
25.0
20.0
15.0
10.0
5.0
0.0
0.0
5.0
10.0
15.0
20.0
25.0
30.0
35.0
0
0
0
0
Compressibility correction (m H20)
8 m Diameter standard shield
16 m overburden of clean sand
PBL = 0.0
Zr = 2.0 m

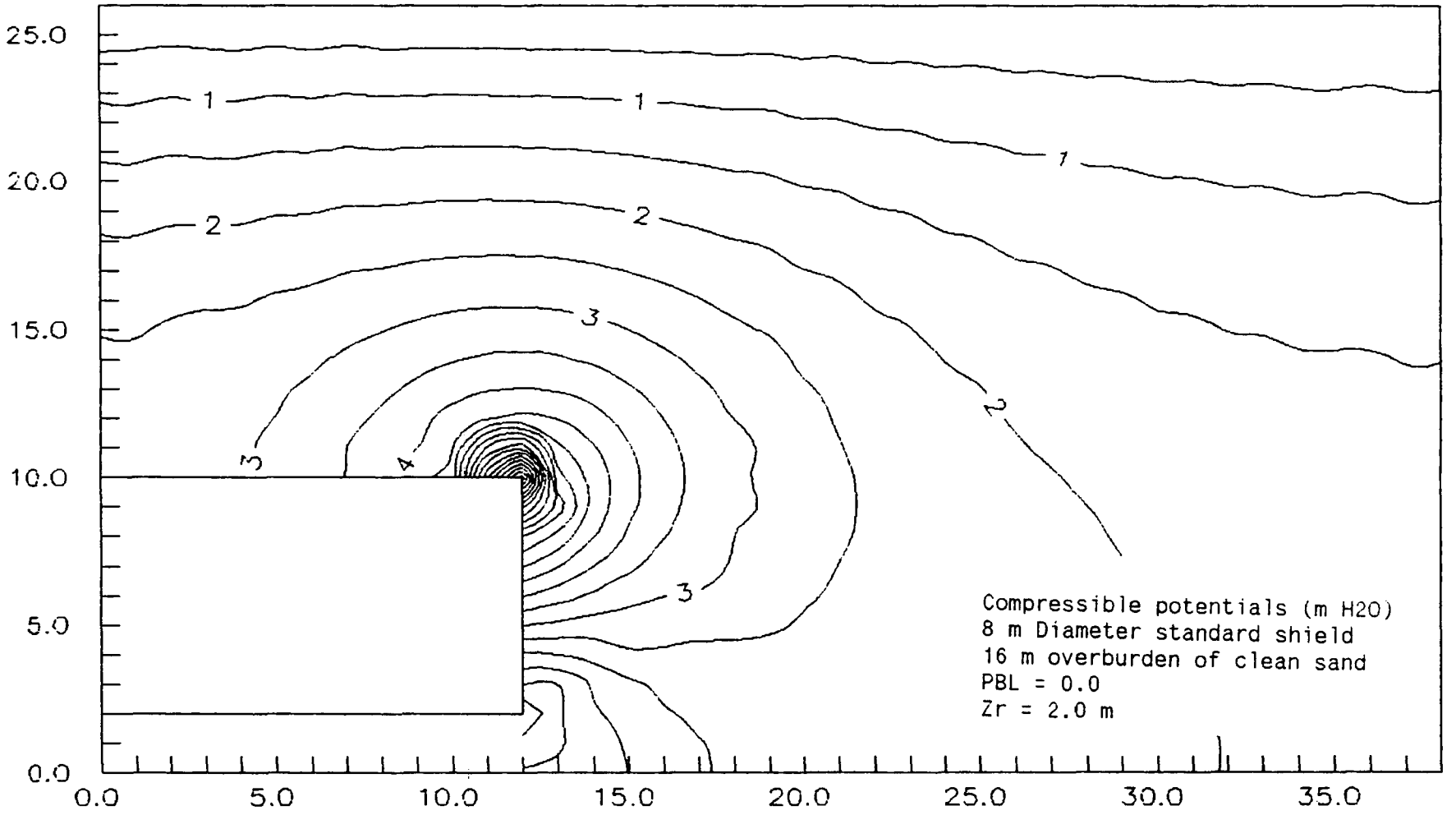
25.0
20.0
15.0
10.0
5.0
0.0
0.0
5.0
10.0
15.0
20.0
25.0
30.0
35.0
1
1
1
2
2
2
3
3
3
4
Compressible potentials (m H2O)
8 m Diameter standard shield
16 m overburden of clean sand
PBL = 0.0
Zr = 2.0 m

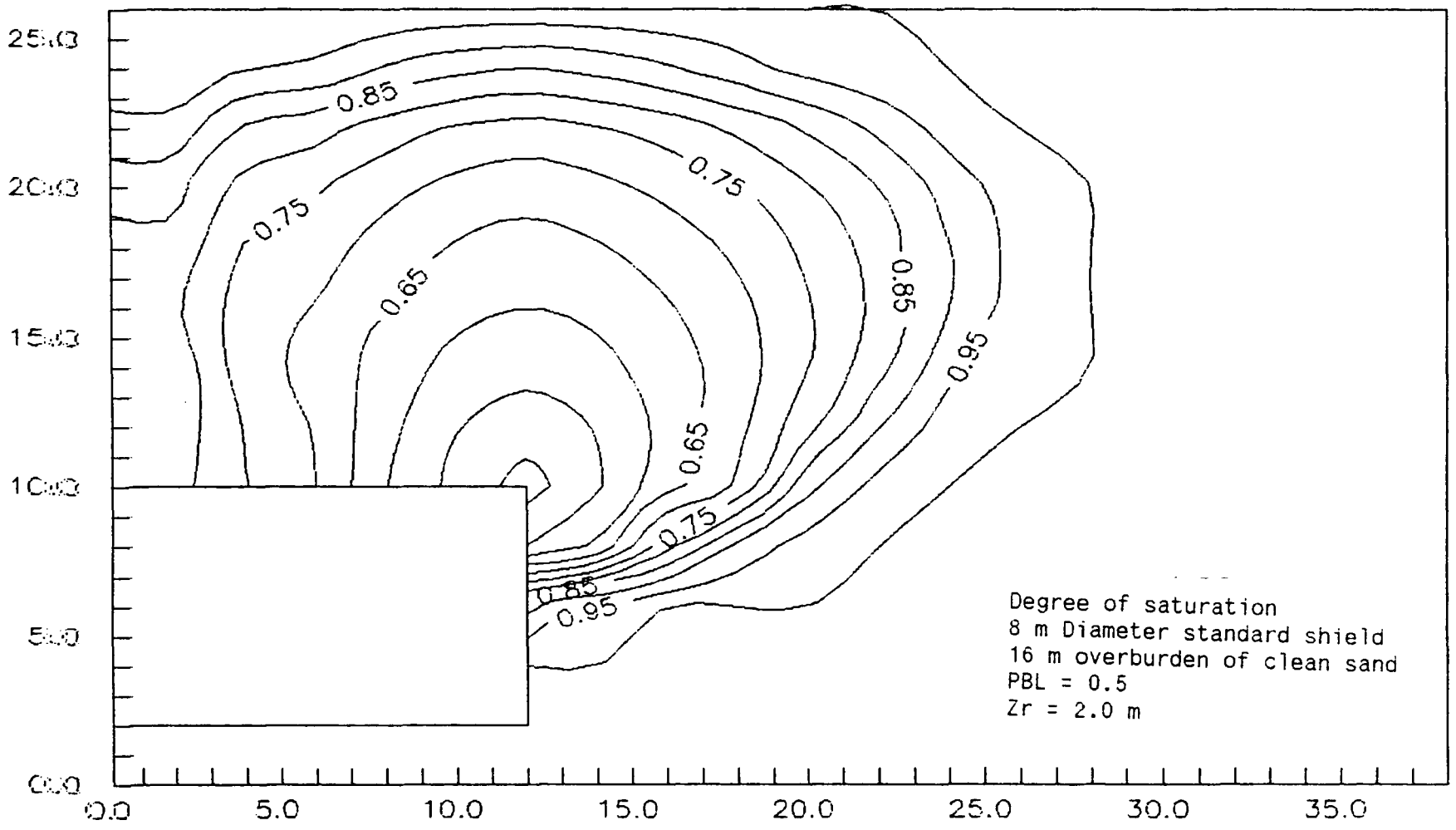
0.85
0.75
0.75
0.65
0.85
0.95
0.65
0.75
0.85
0.95
0.0
5.0
10.0
15.0
20.0
25.0
30.0
35.0
Degree of saturation
8 m Diameter standard shield
16 m overburden of clean sand
PBL = 0.5
Zr = 2.0 m

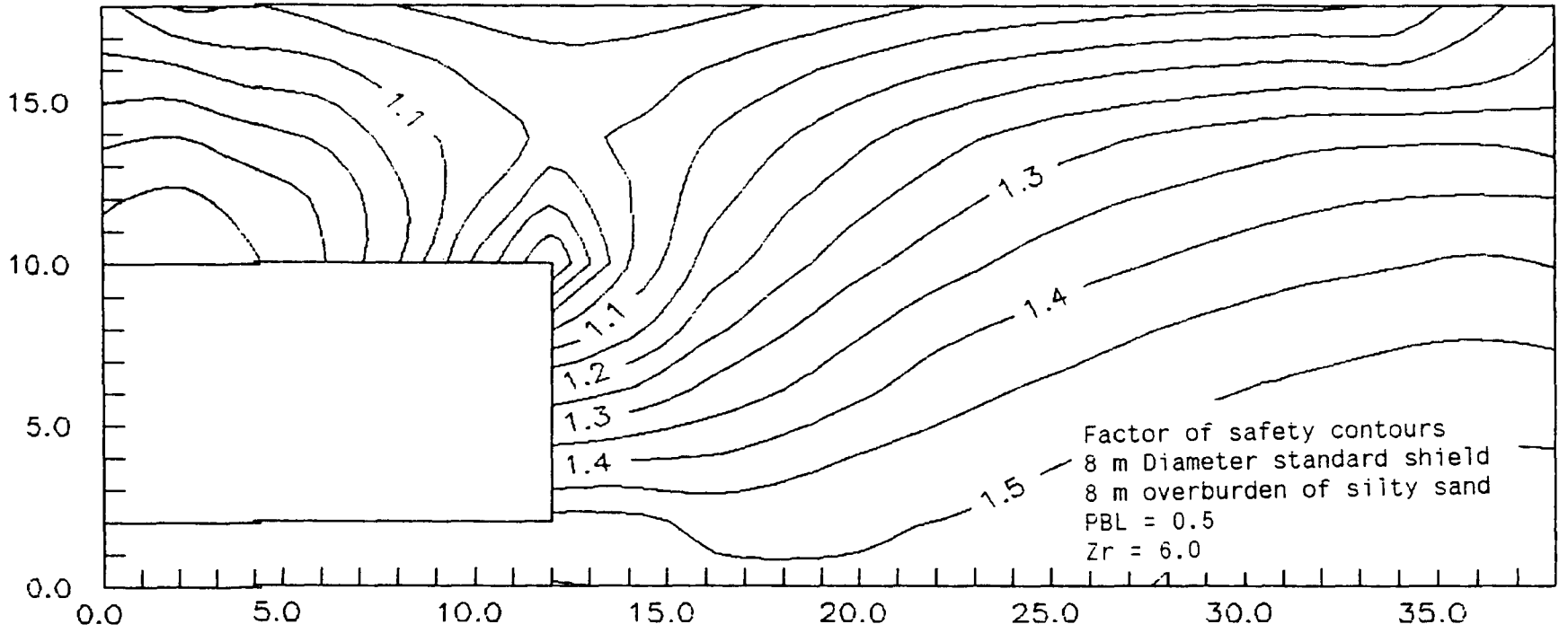
15.0
10.0
5.0
0.0
0.0
5.0
10.0
15.0
20.0
25.0
30.0
35.0
1.1
1.1
1.2
1.3
1.4
1.3
1.4
1.5
Factor of safety contours
8 m Diameter standard shield
8 m overburden of silty sand
PBL = 0.5
Zr = 6.0

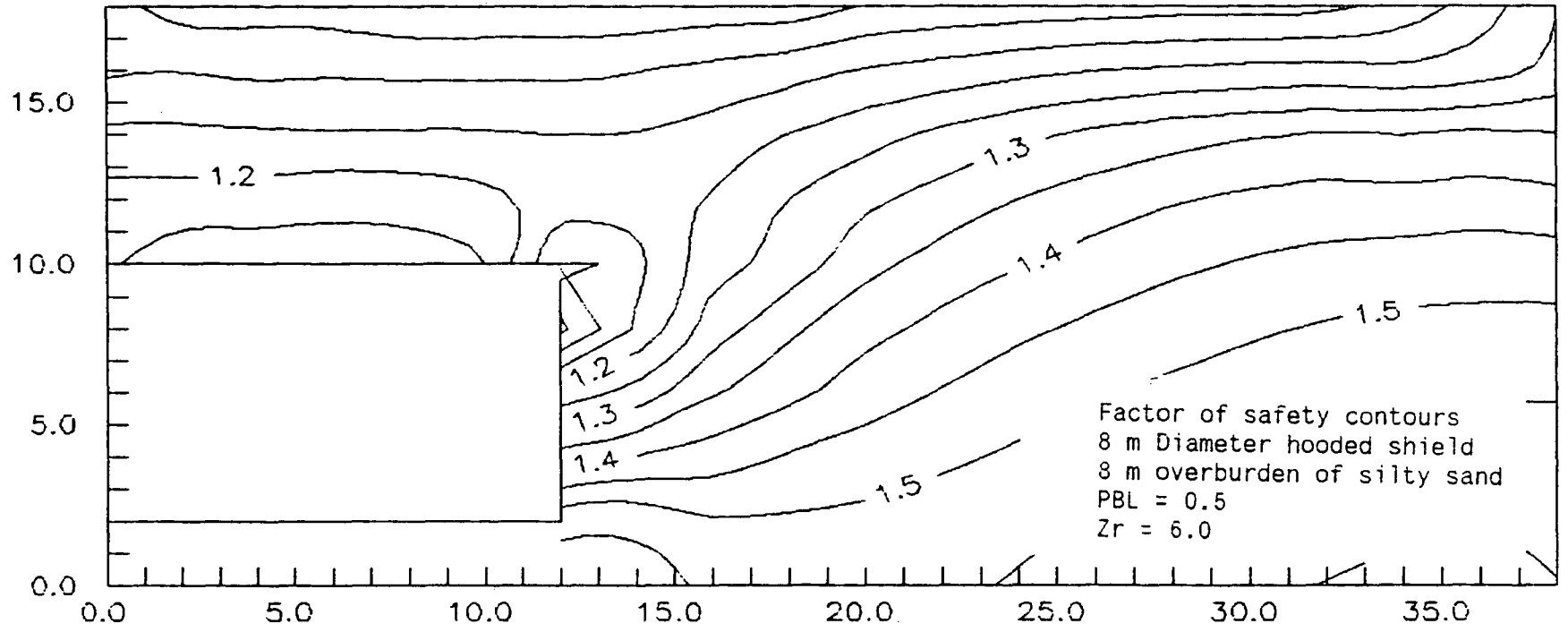
15.0
10.0
5.0
0.0
0.0
5.0
10.0
15.0
20.0
25.0
30.0
35.0
1.2
1.3
1.4
1.5
1.2
1.3
1.4
1.5
Factor of safety contours
8 m Diameter hooded shield
8 m overburden of silty sand
PBL = 0.5
Zr = 6.0

Appendix C

Factor of saftey results

Factors of Safety
Standard Shield
Clean sand

Dia.	Depth	PBL=0.0 Zr=2	Zr=4	Zr=6	PBL=0.25 Zr=2	Zr=4	Zr=6	PBL=0.50 Zr=2	Zr=4	Zr=6
8.0	5	--	--	--	--	--	--	0.99	0.99	1.00
	6	--	--	--	--	--	--	1.05	1.04	1.03
	7	--	--	--	0.98	0.99	0.99	1.11	1.08	1.07
	8	--	--	--	1.02	1.02	1.02	1.15	1.03	1.02
	9	--	--	--	1.06	1.05	1.05	1.19	1.15	1.13
	10	1.00	1.00	1.00	1.09	1.08	1.07	1.21	1.18	1.15
	11	1.03	1.03	1.03	--	--	--	--	--	--
	12	1.06	1.05	1.05	--	--	--	--	--	--
	13	1.08	1.07	1.07	--	--	--	--	--	--
	14	1.10	1.09	1.08	--	--	--	--	--	--
	15	1.12	1.11	1.10	--	--	--	--	--	--
	16	1.13	1.12	1.11	1.22	1.19	1.18	1.32	1.28	1.25

Dia.	Depth	PBL=0.0 Zr=2	Zr=4	Zr=6	PBL=0.25 Zr=2	Zr=4	Zr=6	PBL=0.50 Zr=2	Zr=4	Zr=6
6.0	3.75	--	--	--	--	--	--	0.98	0.98	0.99
	4.50	--	--	--	--	--	--	1.04	1.03	1.02
	5.25	--	--	--	0.97	0.98	0.98	--	--	--
	6.00	--	--	--	1.01	1.01	1.01	1.13	1.10	1.08
	6.75	0.96	0.97	0.98	1.05	1.04	1.04	--	--	--
	7.50	0.99	1.00	1.00	1.08	1.07	1.06	1.20	1.16	1.13
	8.25	1.02	1.02	1.02	--	--	--	--	--	--
	9.00	1.05	1.04	1.04	1.14	1.12	1.10	1.25	1.20	1.17
	9.75	1.07	1.06	1.06	--	--	--	--	--	--
	10.50	1.09	1.08	1.07	1.18	1.15	1.13	1.28	1.23	1.20
	12.00	1.13	1.11	1.10	1.21	1.18	1.16	1.31	1.26	1.23

Dia.	Depth	PBL=0.0 Zr=2	Zr=4	Zr=6	PBL=0.25 Zr=2	Zr=4	Zr=6	PBL=0.50 Zr=2	Zr=4	Zr=6
4.0	2.5	--	--	--	--	--	--	0.96	0.98	0.98
	3.0	--	--	--	--	--	--	1.02	1.01	1.01
	3.5	--	--	--	0.95	0.97	0.98	1.07	1.05	1.04
	4.0	--	--	--	0.99	1.00	1.00	1.11	1.08	1.06
	4.5	0.95	0.96	0.97	1.03	1.03	1.02	1.15	1.11	1.08
	5.0	0.98	0.99	0.99	1.07	1.05	1.04	1.18	1.13	1.10
	5.5	1.01	1.01	1.01	1.09	1.07	1.06	--	--	--
	6.0	1.04	1.03	1.03	1.12	1.09	1.08	1.23	1.17	1.14
	8.0	1.12	1.10	1.08	1.19	1.16	1.13	1.30	1.24	1.20

Dia.	Depth	PBL=0.0 Zr=2	Zr=4	Zr=6	PBL=0.25 Zr=2	Zr=4	Zr=6	PBL=0.50 Zr=2	Zr=4	Zr=6
2.0	1.25	--	--	--	--	--	--	0.95	0.97	0.98
	1.50	--	--	--	--	--	--	1.00	1.00	1.00
	1.75	--	--	--	--	--	--	1.05	1.03	1.02
	2.00	--	--	--	0.97	0.98	0.99	1.07	1.05	1.04
	2.25	--	--	--	1.00	1.00	1.00	1.13	1.08	1.06
	2.50	0.95	0.97	0.98	1.03	1.02	1.02	1.17	1.10	1.08
	2.75	1.00	1.00	1.00	--	--	--	--	--	--
	3.00	1.03	1.02	1.02	1.08	1.06	1.04	--	--	--
	3.25	1.02	1.02	1.02	1.13	1.09	1.07	--	--	--
	3.50	1.05	1.04	1.03	--	--	--	--	--	--
	4.00	1.09	1.06	1.05	1.16	1.12	1.09	1.30	1.20	1.15

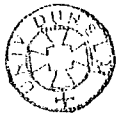

Factors of Safety
Standard Shield
Slightly silty sand

Dia.	Depth	PBL=0.0 Zr=2	Zr=4	Zr=6	PBL=0.25 Zr=2	Zr=4	Zr=6	PBL=0.50 Zr=2	Zr=4	Zr=6
8.0	4.0	--	--	--	--	--	--	0.93	0.95	0.96
	5.0	--	--	--	--	--	--	1.02	1.01	1.01
	6.0	--	--	--	0.94	0.96	0.97	1.08	1.07	1.05
	7.0	--	--	--	1.01	1.01	1.01	--	--	--
	8.0	0.94	0.96	0.97	1.05	1.04	1.04	--	--	--
	9.0	0.99	0.99	1.00	--	--	--	1.22	1.18	1.15
	10.0	1.02	1.02	1.02	1.13	1.11	1.09	--	--	--
	11.0	1.06	1.05	1.05	--	--	--			
	12.0	1.08	1.07	1.07	1.18	1.16	1.14	1.30	1.26	1.22
	14.0	1.13	1.12	1.11	1.22	1.19	1.18			
	16.0	1.17	1.15	1.14	1.25	1.23	1.21	1.32	1.28	1.25

Dia.	Depth	PBL=0.0 Zr=2	Zr=4	Zr=6	PBL=0.25 Zr=2	Zr=4	Zr=6	PBL=0.50 Zr=2	Zr=4	Zr=6
6.0	3.00	--	--	--	--	--	--	0.92	0.95	0.96
	3.75	--	--	--	--	--	--	1.00	1.00	1.00
	4.50	--	--	--	0.93	0.95	0.97	1.07	1.05	1.04
	5.25	--	--	--	0.99	1.00	1.00	--	--	--
	6.00	0.94	0.96	0.97	1.04	1.03	1.03	1.17	1.13	1.11
	6.75	0.98	0.99	0.99	--	--	--	--	--	--
	7.50	1.02	1.02	1.02	1.12	1.10	1.08	1.24	1.19	1.16
	8.25	1.05	1.04	1.04	--	--	--	--	--	--
	9.00	1.08	1.07	1.06	1.17	1.14	1.12	--	--	--
	9.75	1.10	1.09	1.08	--	--	--	--	--	--
	10.50	1.13	1.11	1.10	1.22	1.18	1.16	--	--	--
	12.00	1.16	1.14	1.13	1.25	1.22	1.19	1.36	1.31	1.27

Dia.	Depth	PBL=0.0 Zr=2	Zr=4	Zr=6	PBL=0.25 Zr=2	Zr=4	Zr=6	PBL=0.50 Zr=2	Zr=4	Zr=6
4.0	2.0	--	--	--	--	--	--	0.90	0.94	0.95
	2.5	--	--	--	--	--	--	0.98	0.99	0.99
	3.0	--	--	--	--	--	--	1.04	1.03	1.02
	3.5	--	--	--	0.97	0.98	0.99	--	--	--
	4.0	--	--	--	1.02	1.02	1.01	1.14	1.10	1.08
	4.5	0.97	0.98	0.99	1.06	1.05	1.04	--	--	--
	5.0	1.01	1.01	1.01	1.10	1.08	1.06	1.22	1.16	1.13
	5.5	1.04	1.03	1.03	--	--	--	--	--	--
	6.0	1.07	1.05	1.05	1.16	1.12	1.10	--	--	--
	6.5	1.09	1.07	1.06	--	--	--	--	--	--
	7.0	1.11	1.09	1.08	1.20	1.16	1.13	--	--	--
	8.0	1.15	1.25	1.21	1.24	1.19	1.16	1.35	1.28	1.23

Dia.	Depth	PBL=0.0 Zr=2	Zr=4	Zr=6	PBL=0.25 Zr=2	Zr=4	Zr=6	PBL=0.50 Zr=2	Zr=4	Zr=6
2.0	1.25	--	--	--	--	--	--	0.94	0.98	0.98
	1.50	--	--	--	--	--	--	1.00	1.00	1.00
	1.75	--	--	--	--	--	--	1.05	1.03	1.02
	2.00	--	--	--	0.98	0.99	0.99	1.09	1.06	1.04
	2.25	--	--	--	1.02	1.01	1.01	--	--	--
	2.50	0.97	0.98	0.99	1.05	1.04	1.03	--	--	--
	2.75	1.00	1.00	1.00	1.08	1.06	1.04	--	--	--
	3.00	1.03	1.02	1.02	1.11	1.08	1.06	1.22	1.15	1.11
	3.25	1.06	1.04	1.03	1.14	1.09	1.07	--	--	--
	3.50	1.08	1.06	1.04	1.16	1.11	1.09	--	--	--
	3.75	1.10	1.07	1.06	--	--	--	--	--	--
	4.00	1.12	1.09	1.07	1.19	1.14	1.11	1.30	1.21	1.17

Factors of Safety
Standard Shield
Silty sand

Dia.	Depth	PBL=0.0 Zr=2	Zr=4	Zr=6	PBL=0.25 Zr=2	Zr=4	Zr=6	PBL=0.50 Zr=2	Zr=4	Zr=6
8.0	3.0	--	--	--	--	--	--	0.86	0.91	0.94
	4.0	--	--	--	--	--	--	1.03	1.02	1.02
	5.0	--	--	--	0.96	0.97	0.98	--	--	--
	6.0	0.92	0.94	0.95	1.05	1.04	1.03	1.22	1.17	1.14
	7.0	0.99	1.00	1.00	--	--	--	--	--	--
	8.0	1.05	1.04	1.04	1.18	1.15	1.13	1.35	1.28	1.23
	10.0	1.14	1.13	1.11	--	--	--	--	--	--
	16.0	1.31	1.28	1.25	1.42	1.38	1.34	1.58	1.51	1.45

Dia.	Depth	PBL=0.0 Zr=2	Zr=4	Zr=6	PBL=0.25 Zr=2	Zr=4	Zr=6	PBL=0.50 Zr=2	Zr=4	Zr=6
6.0	2.25	--	--	--	--	--	--	0.84	0.90	0.93
	3.00	--	--	--	--	--	--	1.01	1.01	1.01
	3.75	--	--	--	0.92	0.95	0.96	--	--	--
	4.50	0.91	0.94	0.95	1.04	1.03	1.02	1.20	1.15	1.12
	5.25	0.98	0.99	0.99	--	--	--	--	--	--
	6.00	1.04	1.04	1.03	1.17	1.13	1.11	1.33	1.25	1.21
	7.50	1.14	1.12	1.10	--	--	--	--	--	--
	12.00	1.31	1.27	1.24	1.42	1.36	1.32	1.58	1.49	1.43

Dia.	Depth	PBL=0.0 Zr=2	Zr=4	Zr=6	PBL=0.25 Zr=2	Zr=4	Zr=6	PBL=0.50 Zr=2	Zr=4	Zr=6
4.0	1.5	--	--	--	--	--	--	0.82	0.89	0.92
	2.0	--	--	--	--	--	--	0.98	0.99	0.99
	2.5	--	--	--	0.88	0.92	0.94	1.08	1.06	1.04
	3.0	0.90	0.93	0.95	1.01	1.01	1.01	1.16	1.12	1.09
	3.5	0.97	0.98	0.98	--	--	--	--	--	--
	4.0	1.03	1.02	1.02	1.14	1.11	1.08	1.30	1.22	1.17
	5.0	1.12	1.10	1.08	1.24	1.18	1.15	--	--	--
	8.0	1.30	1.25	1.21	1.41	1.34	1.28	1.57	1.46	1.38

Dia.	Depth	PBL=0.0 Zr=2	Zr=4	Zr=6	PBL=0.25 Zr=2	Zr=4	Zr=6	PBL=0.50 Zr=2	Zr=4	Zr=6
2.0	1.00	--	--	--	--	--	--	0.91	0.94	0.96
	1.25	--	--	--	--	--	--	1.00	1.00	1.00
	1.50	--	--	--	0.95	0.97	0.98	1.07	1.05	1.03
	1.75	0.92	0.95	0.96	1.02	1.02	1.01	--	--	--
	2.00	0.98	0.99	0.99	1.08	1.06	1.04	1.19	1.13	1.10
	2.25	1.03	1.02	1.02	--	--	--	--	--	--
	2.50	1.08	1.05	1.04	1.18	1.12	1.09	1.29	1.20	1.15
	3.00	1.15	1.11	1.08	--	--	--	--	--	--
	4.00	1.27	1.20	1.16	1.37	1.27	1.21	1.48	1.36	1.28

Factors of Safety
Standard Shield
Very silty sand

Dia.	Depth	PBL=0.0 Zr=2	Zr=4	Zr=6	PBL=0.25 Zr=2	Zr=4	Zr=6	PBL=0.50 Zr=2	Zr=4	Zr=6
8.0	3.0	--	--	--	--	--	--	0.87	0.91	0.93
	4.0	--	--	--	0.87	0.91	0.93	1.04	1.03	1.02
	5.0	--	--	--	0.99	1.00	1.00	1.16	1.12	1.10
	6.0	0.95	0.97	0.98	1.08	1.07	1.06	1.25	1.20	1.16
	7.0	1.03	1.03	1.03	--	--	--	1.32	1.26	1.22
	8.0	1.10	1.09	1.08	1.23	1.19	1.16	1.38	1.31	1.27
	9.0	--	--	--	--	--	--	1.43	1.36	1.31
	10.0	1.20	1.17	1.15	1.32	1.28	1.24	1.47	1.40	1.34
	16.0	1.38	1.35	1.32	1.42	1.38	1.34	1.63	1.55	1.50

Dia.	Depth	PBL=0.0 Zr=2	Zr=4	Zr=6	PBL=0.25 Zr=2	Zr=4	Zr=6	PBL=0.50 Zr=2	Zr=4	Zr=6
6.0	2.25	--	--	--	--	--	--	0.88	0.91	0.93
	3.00	--	--	--	0.86	0.90	0.93	1.01	1.01	1.01
	3.75	--	--	--	0.97	0.98	0.98	1.13	1.09	1.07
	4.50	0.94	0.96	0.97	1.06	1.05	1.04	1.22	1.16	1.13
	5.25	1.02	1.02	1.02	--	--	--	--	--	--
	6.00	1.08	1.07	1.05	1.20	1.16	1.13	1.35	1.27	1.23
	6.75	1.14	1.11	1.10	--	--	--	--	--	--
	9.00	1.26	1.22	1.19	1.38	1.32	1.27	1.51	1.42	1.36
	12.00	1.37	1.32	1.29	1.48	1.41	1.37	1.61	1.52	1.46

Dia.	Depth	PBL=0.0 Zr=2	Zr=4	Zr=6	PBL=0.25 Zr=2	Zr=4	Zr=6	PBL=0.50 Zr=2	Zr=4	Zr=6
4.0	1.5	--	--	--	--	--	--	0.90	0.92	0.93
	2.0	--	--	--	0.83	0.89	0.91	0.97	0.98	0.99
	2.5	--	--	--	0.94	0.96	0.97	1.08	1.05	1.04
	3.0	0.91	0.94	0.95	1.02	1.02	1.01	1.16	1.12	1.09
	3.5	0.99	0.99	1.00	--	--	--	--	--	--
	4.0	1.05	1.04	1.03	1.15	1.12	1.09	1.29	1.22	1.17
	4.5	1.10	1.08	1.07	--	--	--	--	--	--
	5.0	1.15	1.12	1.10	--	--	--	--	--	--
	6.0	1.24	1.19	1.16	1.34	1.27	1.22	1.46	1.36	1.30
	8.0	1.35	1.29	1.25	1.45	1.37	1.31	1.57	1.46	1.39

Dia.	Depth	PBL=0.0 Zr=2	Zr=4	Zr=6	PBL=0.25 Zr=2	Zr=4	Zr=6	PBL=0.50 Zr=2	Zr=4	Zr=6
2.0	1.00	--	--	--	--	--	--	0.91	0.94	0.96
	1.25	--	--	--	0.87	0.92	0.94	0.99	1.00	1.00
	1.50	0.86	0.91	0.93	0.95	0.97	0.98	0.99	1.00	1.00
	2.00	0.98	0.99	0.99	1.07	1.05	1.04	1.18	1.12	1.09
	2.25	1.03	1.02	1.02	1.12	1.08	1.06	--	--	--
	2.50	1.08	1.05	1.04	1.16	1.11	1.09	--	--	--
	2.75	1.12	1.08	1.06	--	--	--	--	--	--
	3.00	1.15	1.11	1.09	1.24	1.17	1.13	--	--	--
	4.00	1.27	1.21	1.16	1.36	1.27	1.21	1.46	1.34	1.27

Factors of Safety
Hooded shield
Clean sand

Dia.	Depth	PBL=0.0 Zr=2	Zr=4	Zr=6	PBL=0.25 Zr=2	Zr=4	Zr=6	PBL=0.50 Zr=2	Zr=4	Zr=6
8.0	2.0	--	--	--	--	--	--	0.97	0.98	0.99
	3.0	--	--	--	0.90	0.93	0.95	1.09	1.06	1.04
	4.0	--	--	--	0.98	0.99	0.99	1.17	1.12	1.09
	5.0	0.94	0.96	0.97	1.05	1.04	1.03	--	--	--
	6.0	0.99	1.00	1.00	1.11	1.08	1.07	--	--	--
	7.0	1.04	1.03	1.03	--	--	--	--	--	--
	8.0	1.08	1.06	1.06	1.18	1.15	1.13	1.39	1.28	1.23
	10.0	1.14	1.12	1.10	1.24	1.20	1.17	--	--	--
	16.0	1.24	1.22	1.20	1.33	1.29	1.26	1.62	1.49	1.41

Dia.	Depth	PBL=0.0 Zr=2	Zr=4	Zr=6	PBL=0.25 Zr=2	Zr=4	Zr=6	PBL=0.50 Zr=2	Zr=4	Zr=6
6.0	1.50	--	--	--	--	--	--	0.97	0.98	0.99
	2.25	--	--	--	0.89	0.93	0.95	1.07	1.05	1.04
	3.00	--	--	--	0.97	0.98	0.99	1.17	1.11	1.08
	3.75	0.93	0.95	0.96	1.04	1.03	1.02	--	--	--
	4.50	0.98	0.99	0.99	1.09	1.07	1.06	--	--	--
	5.25	1.03	1.02	1.02	--	--	--	--	--	--
	6.00	1.07	1.05	1.05	1.17	1.13	1.11	1.40	1.28	1.22
	7.50	1.13	1.10	1.09	1.22	1.18	1.15	--	--	--
	9.00	1.18	1.15	1.13	--	--	--	--	--	--
	12.00	1.23	1.20	1.18	1.32	1.27	1.24	1.64	1.50	1.41

Dia.	Depth	PBL=0.0 Zr=2	Zr=4	Zr=6	PBL=0.25 Zr=2	Zr=4	Zr=6	PBL=0.50 Zr=2	Zr=4	Zr=6
4.0	1.0	--	--	--	--	--	--	0.94	0.97	0.98
	1.5	--	--	--	0.89	0.93	0.95	1.06	1.04	1.03
	2.0	--	--	--	0.96	0.98	0.98	1.15	1.09	1.06
	2.5	0.92	0.95	0.96	1.02	1.02	1.01	--	--	--
	3.0	0.97	0.98	0.99	1.07	1.05	1.04	--	--	--
	3.5	1.01	1.01	1.01	--	--	--	--	--	--
	4.0	1.05	1.04	1.03	1.15	1.11	1.09	1.38	1.26	1.20
	4.5	1.08	1.06	1.05	--	--	--	--	--	--
	5.0	--	--	--	1.21	1.15	1.12	--	--	--
	5.5	1.14	1.01	1.01	--	--	--	--	--	--
	8.0	1.22	1.10	1.08	1.31	1.25	1.21	1.63	1.49	1.40

Dia.	Depth	PBL=0.0 Zr=2	Zr=4	Zr=6	PBL=0.25 Zr=2	Zr=4	Zr=6	PBL=0.50 Zr=2	Zr=4	Zr=6
2.0	0.50	--	--	--	--	--	--	0.91	0.95	0.96
	0.75	--	--	--	--	--	--	1.01	1.01	1.00
	1.00	--	--	--	0.96	0.97	0.98	1.09	1.06	1.04
	1.25	--	--	--	1.00	1.00	1.00	--	--	--
	1.50	0.95	0.97	0.98	--	--	--	--	--	--
	1.75	0.99	0.99	1.00	1.10	1.06	1.04	--	--	--
	2.00	1.02	1.01	1.01	--	--	--	1.30	1.19	1.14
	2.25	1.05	1.03	1.03	1.17	1.11	1.08	--	--	--
	2.50	1.08	1.05	1.04	--	--	--	--	--	--
	2.75	1.10	1.07	1.05	--	--	--	--	--	--
	3.00	--	--	--	1.26	1.17	1.12	--	--	--
	3.25	1.15	1.10	1.08	--	--	--	--	--	--
	4.00	1.19	1.14	1.11	1.33	1.22	1.17	1.53	1.39	1.31

Factors of Safety
Hooded shield
Slightly silty sand

Dia.	Depth	PBL=0.0 Zr=2	Zr=4	Zr=6	PBL=0.25 Zr=2	Zr=4	Zr=6	PBL=0.50 Zr=2	Zr=4	Zr=6
8.0	2.0	--	--	--	--	--	--	0.97	0.98	0.99
	3.0	--	--	--	0.92	0.95	0.96	1.11	1.08	1.06
	4.0	--	--	--	1.01	1.01	1.01	--	--	--
	5.0	0.96	0.97	0.98	--	--	--	1.27	1.20	1.16
	6.0	1.02	1.02	1.02	1.14	1.11	1.09	--	--	--
	7.0	1.07	1.06	1.05	--	--	--	--	--	--
	9.0	1.14	1.12	1.10	--	--	--	--	--	--
	10.0	--	--	--	1.28	1.23	1.20	1.46	1.37	1.32
	12.0	1.22	1.19	1.17	--	--	--	--	--	--
	16.0	1.28	1.22	1.20	1.38	1.33	1.30	1.57	1.47	1.42

Dia.	Depth	PBL=0.0 Zr=2	Zr=4	Zr=6	PBL=0.25 Zr=2	Zr=4	Zr=6	PBL=0.50 Zr=2	Zr=4	Zr=6
6.0	1.50	--	--	--	--	--	--	0.96	0.98	0.98
	2.25	--	--	--	0.91	0.94	0.96	1.09	1.06	1.04
	3.00	--	--	--	1.00	1.00	1.00	1.18	1.12	1.09
	3.75	--	--	--	--	--	--	--	--	--
	4.50	0.95	0.97	0.98	1.13	1.10	1.08	1.30	1.22	1.17
	5.25	1.01	1.01	1.01	--	--	--	--	--	--
	6.00	1.06	1.05	1.04	1.21	1.16	1.14	1.30	1.22	1.17
	6.75	1.13	1.11	1.09	--	--	--	--	--	--
	7.50	--	--	--	--	--	--	1.45	1.35	1.29
	9.00	1.22	1.18	1.16	1.32	1.26	1.22	--	--	--
	12.00	1.28	1.24	1.21	1.37	1.32	1.28	1.58	1.46	1.40

Dia.	Depth	PBL=0.0 Zr=2	Zr=4	Zr=6	PBL=0.25 Zr=2	Zr=4	Zr=6	PBL=0.50 Zr=2	Zr=4	Zr=6
4.0	1.0	--	--	--	--	--	--	0.94	0.97	0.98
	1.5	--	--	--	0.89	0.93	0.95	1.06	1.04	1.03
	2.0	--	--	--	0.98	0.99	0.99	1.14	1.09	1.07
	2.5	0.94	0.96	0.97	1.05	1.03	1.02	--	--	--
	3.0	0.99	1.00	1.00	1.10	1.07	1.05	--	--	--
	3.5	1.04	1.03	1.02	--	--	--	--	--	--
	4.0	1.08	1.06	1.05	1.18	1.13	1.11	--	--	--
	5.0	1.14	1.11	1.09	--	--	--	1.43	1.31	1.25
	6.0	--	--	--	1.30	1.23	1.19	--	--	--
	6.5	1.22	1.17	1.14	--	--	--	--	--	--
	8.0	1.26	1.22	1.18	1.36	1.29	1.24	1.58	1.44	1.36

Dia.	Depth	PBL=0.0 Zr=2	Zr=4	Zr=6	PBL=0.25 Zr=2	Zr=4	Zr=6	PBL=0.50 Zr=2	Zr=4	Zr=6
2.0	0.50	--	--	--	--	--	--	0.91	0.95	0.96
	0.75	--	--	--	--	--	--	1.01	1.01	1.01
	1.00	--	--	--	0.94	0.97	0.98	1.08	1.05	1.04
	1.25	--	--	--	1.00	1.00	1.00	--	--	--
	1.50	0.96	0.97	0.98	1.05	1.03	1.02	--	--	--
	1.75	1.00	1.00	1.00	1.09	1.06	1.04	--	--	--
	2.00	1.04	1.02	1.02	--	--	--	1.29	1.19	1.14
	2.25	--	--	--	1.16	1.11	1.08	--	--	--
	2.50	1.10	1.07	1.05	--	--	--	--	--	--
	3.00	--	--	--	--	--	--	1.43	1.30	1.22
	3.25	1.17	1.12	1.09	1.27	1.19	1.14	--	--	--
	4.00	1.22	1.16	1.13	1.32	1.23	1.18	1.53	1.38	1.29

Factors of Safety
Hooded shield
Silty sand

Dia.	Depth	PBL=0.0 Zr=2	Zr=4	Zr=6	PBL=0.25 Zr=2	Zr=4	Zr=6	PBL=0.50 Zr=2	Zr=4	Zr=6
8.0	2.0	--	--	--	0.85	0.90	0.93	1.05	1.04	1.03
	3.0	0.86	0.90	0.93	1.02	1.01	1.01	--	--	--
	4.0	0.98	0.99	0.99	1.13	1.10	1.08	1.38	1.27	1.21
	5.0	1.07	1.06	1.05	--	--	--	--	--	--
	6.0	1.14	1.11	1.10	1.30	1.23	1.19	--	--	--
	8.0	1.25	1.20	1.18	1.40	1.32	1.27	1.65	1.52	1.43
	10.0	1.32	1.27	1.24	--	--	--	--	--	--
	16.0	1.45	1.40	1.36	1.59	1.51	1.46	1.84	1.73	1.66

Dia.	Depth	PBL=0.0 Zr=2	Zr=4	Zr=6	PBL=0.25 Zr=2	Zr=4	Zr=6	PBL=0.50 Zr=2	Zr=4	Zr=6
6.0	1.50	--	--	--	0.83	0.90	0.92	1.02	1.02	1.01
	2.25	0.85	0.89	0.92	1.00	1.00	1.00	--	--	--
	3.00	0.96	0.98	0.99	1.11	1.08	1.06	1.33	1.23	1.17
	3.75	1.06	1.04	1.04	--	--	--	--	--	--
	4.50	1.13	1.10	1.08	1.28	1.21	1.16	--	--	--
	6.00	1.24	1.19	1.16	1.39	1.30	1.25	1.60	1.47	1.39
	7.50	--	--	--	--	--	--	--	--	--
	12.00	1.45	1.39	1.34	1.59	1.50	1.44	1.81	1.70	1.61

Dia.	Depth	PBL=0.0 Zr=2	Zr=4	Zr=6	PBL=0.25 Zr=2	Zr=4	Zr=6	PBL=0.50 Zr=2	Zr=4	Zr=6
4.0	1.0	--	--	--	0.81	0.89	0.92	0.98	0.99	0.99
	1.5	0.83	0.89	0.92	0.97	0.98	0.99	1.12	1.08	1.05
	2.0	0.94	0.97	0.98	1.07	1.05	1.04	1.24	1.16	1.12
	2.5	1.03	1.02	1.02	1.16	1.11	1.09	--	--	--
	3.0	1.10	1.08	1.06	--	--	--	--	--	--
	4.0	1.22	1.16	1.13	--	--	--	1.52	1.38	1.31
	5.0	1.30	1.23	1.19	1.44	1.33	1.27	--	--	--
	8.0	1.44	1.36	1.31	1.48	1.47	1.40	1.74	1.61	1.52

Dia.	Depth	PBL=0.0 Zr=2	Zr=4	Zr=6	PBL=0.25 Zr=2	Zr=4	Zr=6	PBL=0.50 Zr=2	Zr=4	Zr=6
2.0	0.50	--	--	--	--	--	--	0.91	0.95	0.97
	0.75	--	--	--	0.90	0.94	0.96	1.03	1.02	1.01
	1.00	0.89	0.93	0.95	0.99	0.99	1.00	1.12	1.07	1.05
	1.25	0.97	0.98	0.99	1.06	1.04	1.03	--	--	--
	1.50	1.04	1.03	1.02	1.13	1.08	1.06	1.25	1.16	1.12
	1.75	1.10	1.07	1.05	--	--	--	--	--	--
	2.00	1.15	1.10	1.08	1.24	1.16	1.12	1.35	1.23	1.17
	2.50	1.24	1.16	1.12	1.33	1.23	1.17	1.43	1.30	1.23
	3.00	1.30	1.21	1.17	--	--	--	--	--	--
	4.00	1.41	1.30	1.24	1.50	1.38	1.30	1.59	1.44	1.35

Factors of Safety
Hooded shield
Very silty sand

Dia.	Depth	PBL=0.0 Zr=2	Zr=4	Zr=6	PBL=0.25 Zr=2	Zr=4	Zr=6	PBL=0.50 Zr=2	Zr=4	Zr=6
8.0	2.0	--	--	--	0.84	0.90	0.93	1.06	1.04	1.03
	3.0	0.88	0.91	0.93	1.03	1.02	1.02	--	--	--
	4.0	1.00	1.00	1.00	1.15	1.12	1.09	1.36	1.26	1.20
	5.0	1.10	1.08	1.07	1.24	1.19	1.16	--	--	--
	6.0	1.18	1.15	1.12	--	--	--	--	--	--
	8.0	1.30	1.25	1.21	1.43	1.36	1.30	1.62	1.50	1.43
	16.0	1.52	1.47	1.42	1.64	1.57	1.51	1.80	1.70	1.63

Dia.	Depth	PBL=0.0 Zr=2	Zr=4	Zr=6	PBL=0.25 Zr=2	Zr=4	Zr=6	PBL=0.50 Zr=2	Zr=4	Zr=6
6.0	1.50	--	--	--	0.83	0.89	0.92	1.02	1.01	1.01
	2.25	0.86	0.90	0.93	1.00	1.00	1.00	1.18	1.12	1.09
	3.00	0.98	0.98	0.99	1.12	1.09	1.07	1.31	1.21	1.16
	3.75	1.08	1.06	1.05	--	--	--	--	--	--
	4.50	1.16	1.12	1.10	1.29	1.22	1.18	--	--	--
	6.00	1.27	1.22	1.18	1.40	1.32	1.26	1.58	1.45	1.37
	7.50	1.36	1.29	1.25	--	--	--	--	--	--
	12.00	1.51	1.44	1.39	1.62	1.53	1.47	1.78	1.66	1.58

Dia.	Depth	PBL=0.0 Zr=2	Zr=4	Zr=6	PBL=0.25 Zr=2	Zr=4	Zr=6	PBL=0.50 Zr=2	Zr=4	Zr=6
4.0	1.0	--	--	--	0.81	0.89	0.92	0.97	0.98	0.98
	1.5	--	--	--	0.96	0.98	0.98	1.12	1.07	1.05
	2.0	0.94	0.96	0.97	1.07	1.05	1.04	1.24	1.15	1.11
	2.5	1.03	1.03	1.02	1.16	1.11	1.09	--	--	--
	3.0	1.11	1.08	1.06	1.23	1.16	1.13	1.40	1.28	1.21
	3.5	1.18	1.13	1.10	--	--	--	--	--	--
	4.0	1.23	1.17	1.14	1.35	1.26	1.20	1.50	1.37	1.29
	6.0	1.38	1.30	1.26	--	--	--	--	--	--
	8.0	1.48	1.40	1.34	1.58	1.48	1.41	1.73	1.59	1.50

Dia.	Depth	PBL=0.0 Zr=2	Zr=4	Zr=6	PBL=0.25 Zr=2	Zr=4	Zr=6	PBL=0.50 Zr=2	Zr=4	Zr=6
2.0	0.50	--	--	--	--	--	--	0.91	0.95	0.97
	0.75	--	--	--	0.90	0.94	0.96	1.03	1.02	1.01
	1.00	0.88	0.93	0.95	0.99	0.99	0.99	1.12	1.07	1.05
	1.25	0.96	0.98	0.98	1.06	1.04	1.03	--	--	--
	1.50	1.03	1.02	1.01	1.12	1.08	1.06	1.26	1.16	1.12
	1.75	1.08	1.06	1.04	1.18	1.12	1.09	--	--	--
	2.00	1.13	1.09	1.07	--	--	--	1.36	1.24	1.18
	2.25	--	--	--	1.27	1.19	1.14	--	--	--
	2.50	1.22	1.15	1.12	--	--	--	--	--	--
	3.00	1.29	1.20	1.16	1.38	1.27	1.21	1.51	1.35	1.27
	4.00	1.39	1.29	1.23	1.48	1.36	1.28	1.61	1.45	1.35

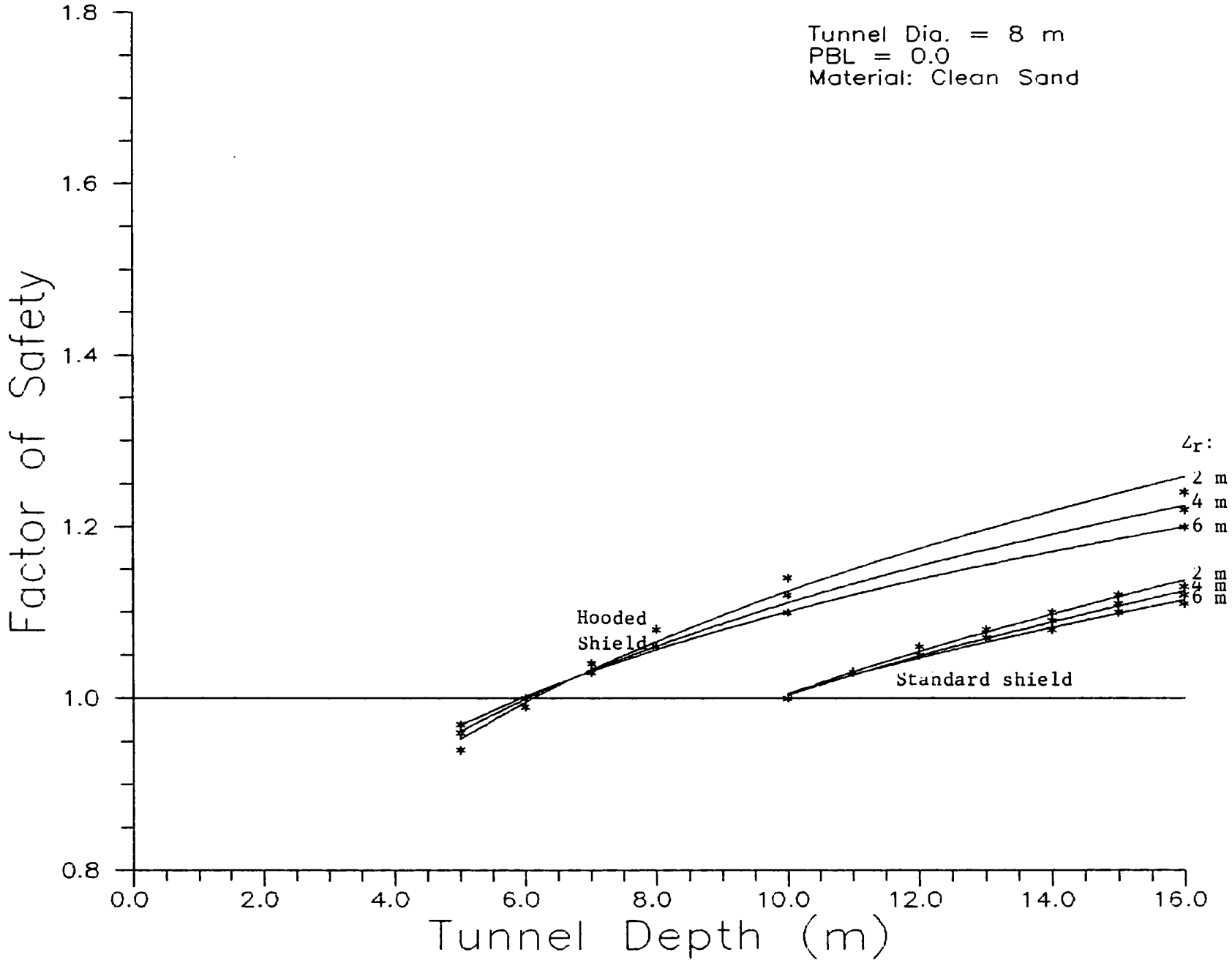
Tunnel Dia. = 8 m
PBL = 0.0
Material: Clean Sand
Factor of Safety
Tunnel Depth (m)
1.8
1.6
1.4
1.2
1.0
0.8
0.0
2.0
4.0
6.0
8.0
10.0
12.0
14.0
16.0
λ_r:
2 m
4 m
6 m
2 m
4 m
6 m
Hooded Shield
Standard shield

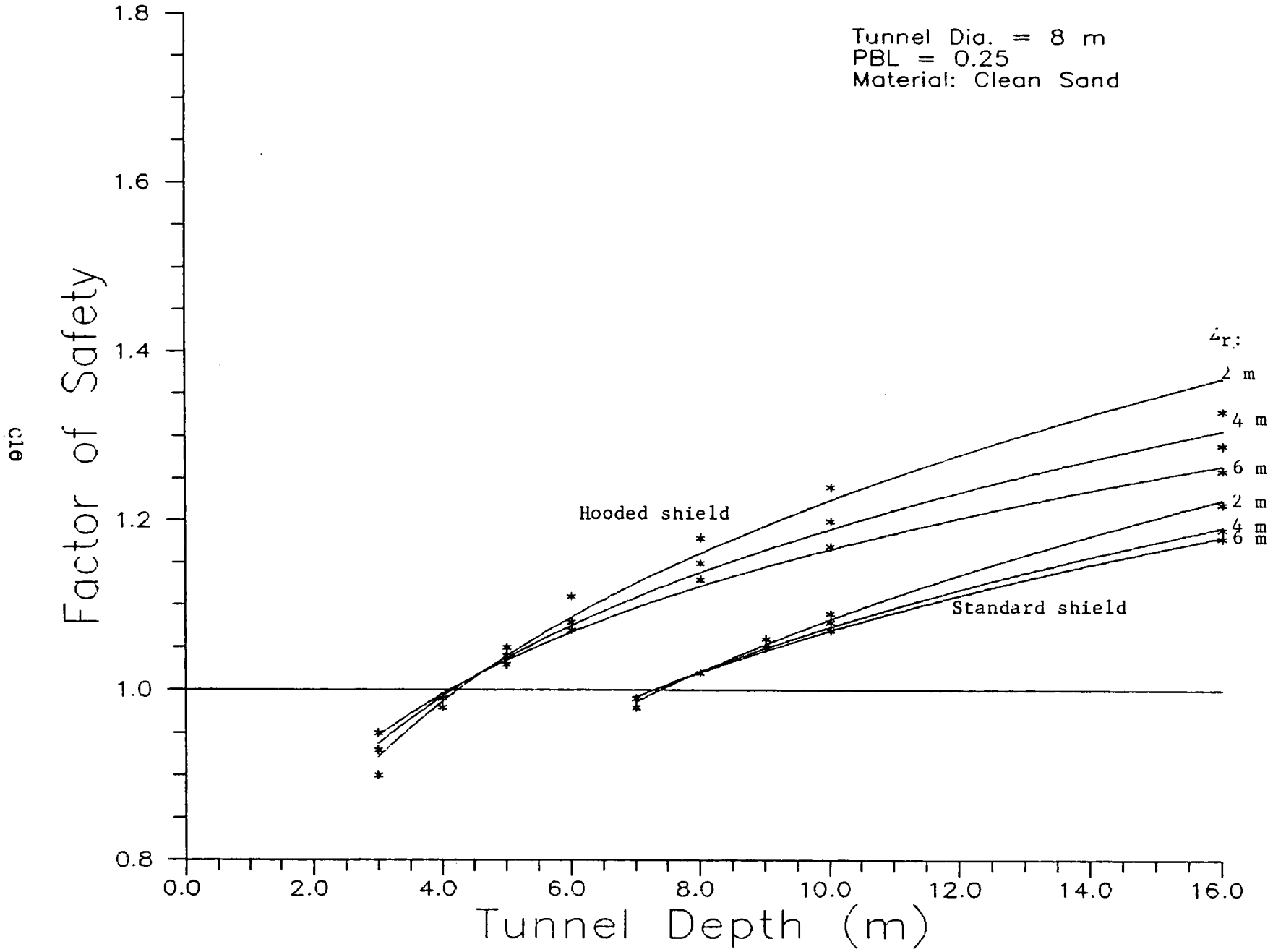
Tunnel Dia. = 8 m
PBL = 0.25
Material: Clean Sand
Factor of Safety
Tunnel Depth (m)
Hooded shield
Standard shield
2 m
4 m
6 m
2 m
4 m
6 m
1.8
1.6
1.4
1.2
1.0
0.8
0.0
2.0
4.0
6.0
8.0
10.0
12.0
14.0
16.0

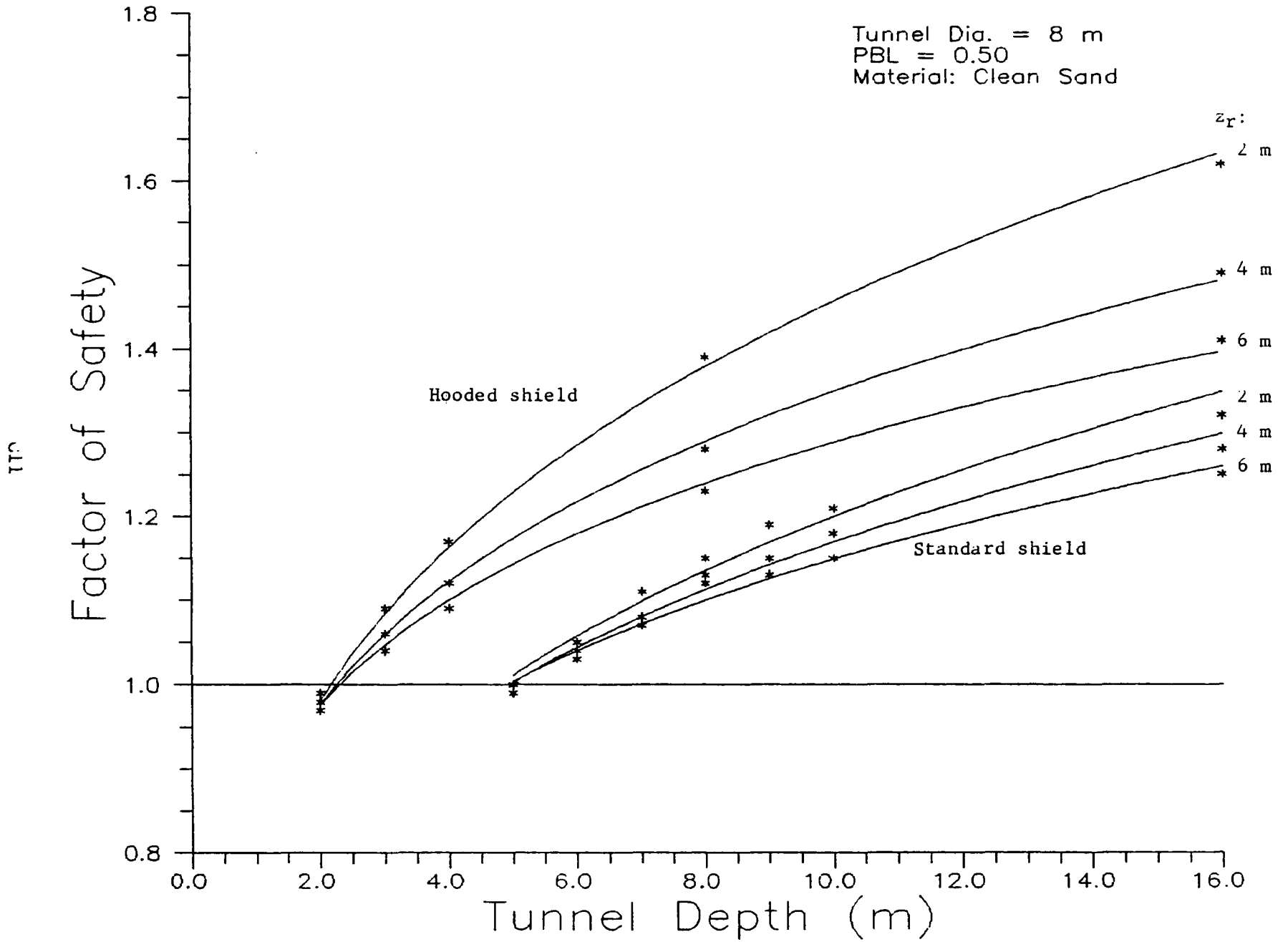
Tunnel Dia. = 8 m
PBL = 0.50
Material: Clean Sand
z_r:
2 m
4 m
6 m
2 m
4 m
6 m
Hooded shield
Standard shield
Factor of Safety
Tunnel Depth (m)
1.8
1.6
1.4
1.2
1.0
0.8
0.0
2.0
4.0
6.0
8.0
10.0
12.0
14.0
16.0

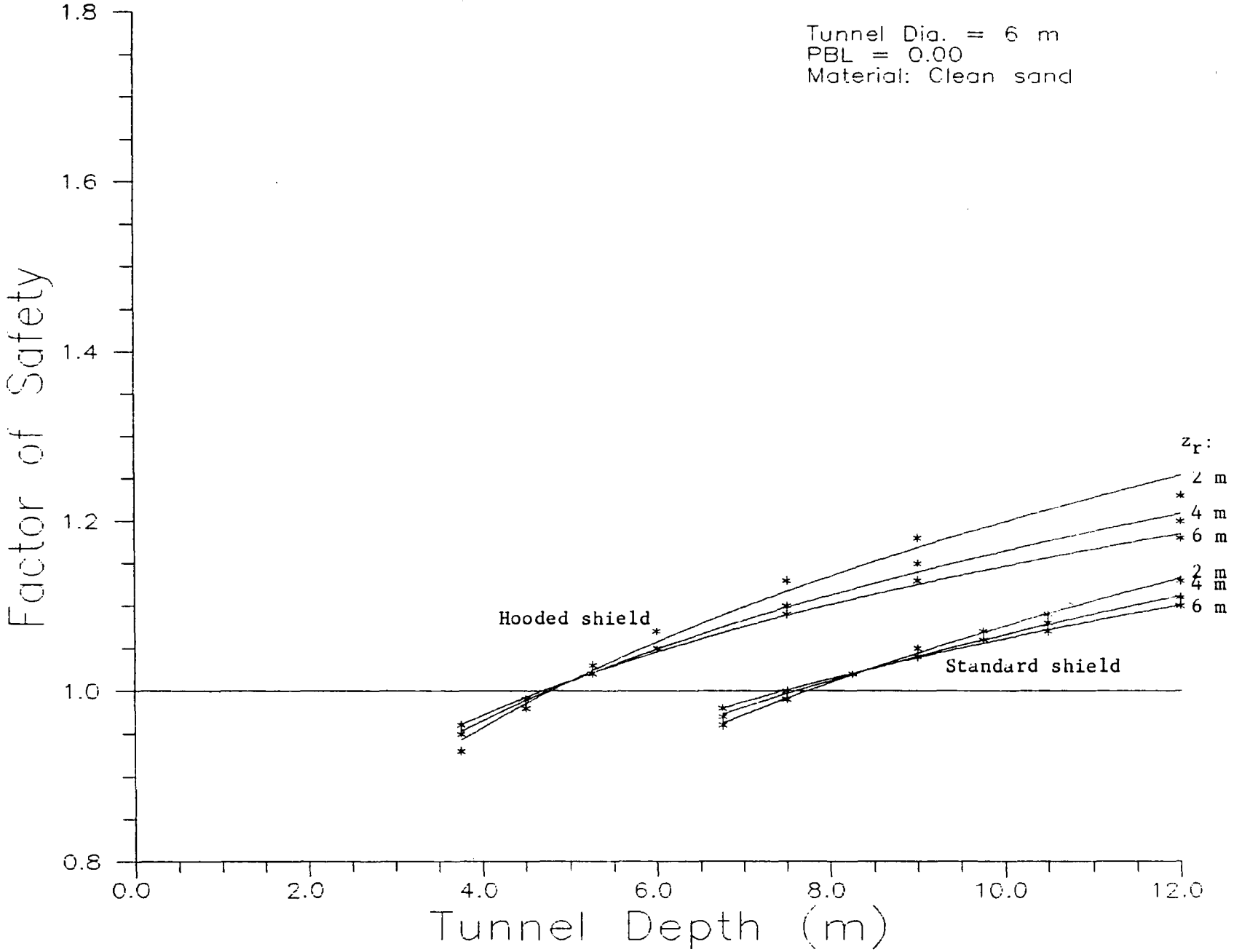
Tunnel Dia. = 6 m
PBL = 0.00
Material: Clean sand
Factor of Safety
Tunnel Depth (m)
1.8
1.6
1.4
1.2
1.0
0.8
0.0
2.0
4.0
6.0
8.0
10.0
12.0
z_r:
2 m
4 m
6 m
2 m
4 m
6 m
Hooded shield
Standard shield

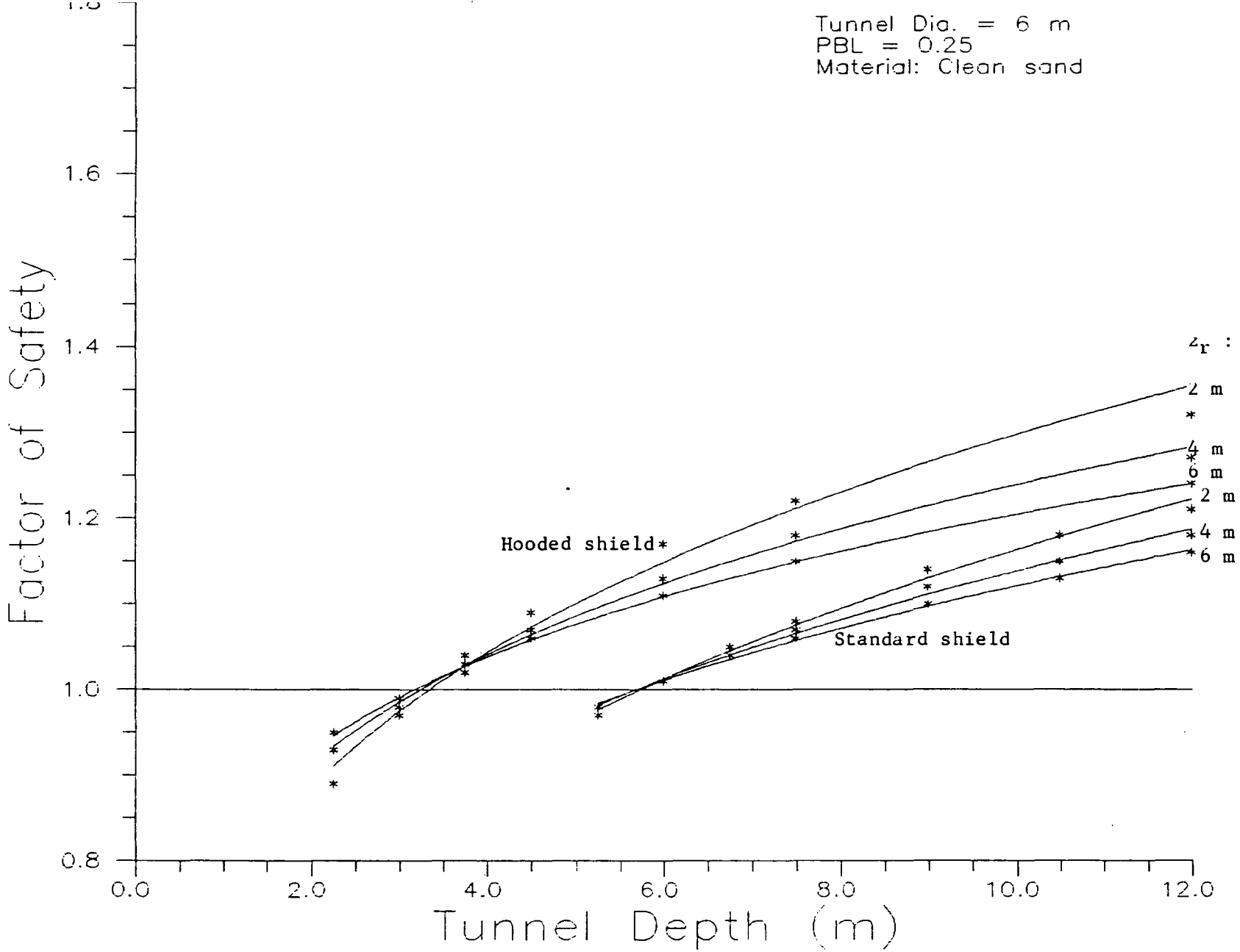
Tunnel Dia. = 6 m
PBL = 0.25
Material: Clean sand
Factor of Safety
1.6
1.4
1.2
1.0
0.8
z_r :
2 m
4 m
6 m
2 m
4 m
6 m
Hooded shield
Standard shield
0.0
2.0
4.0
6.0
8.0
10.0
12.0
Tunnel Depth (m)

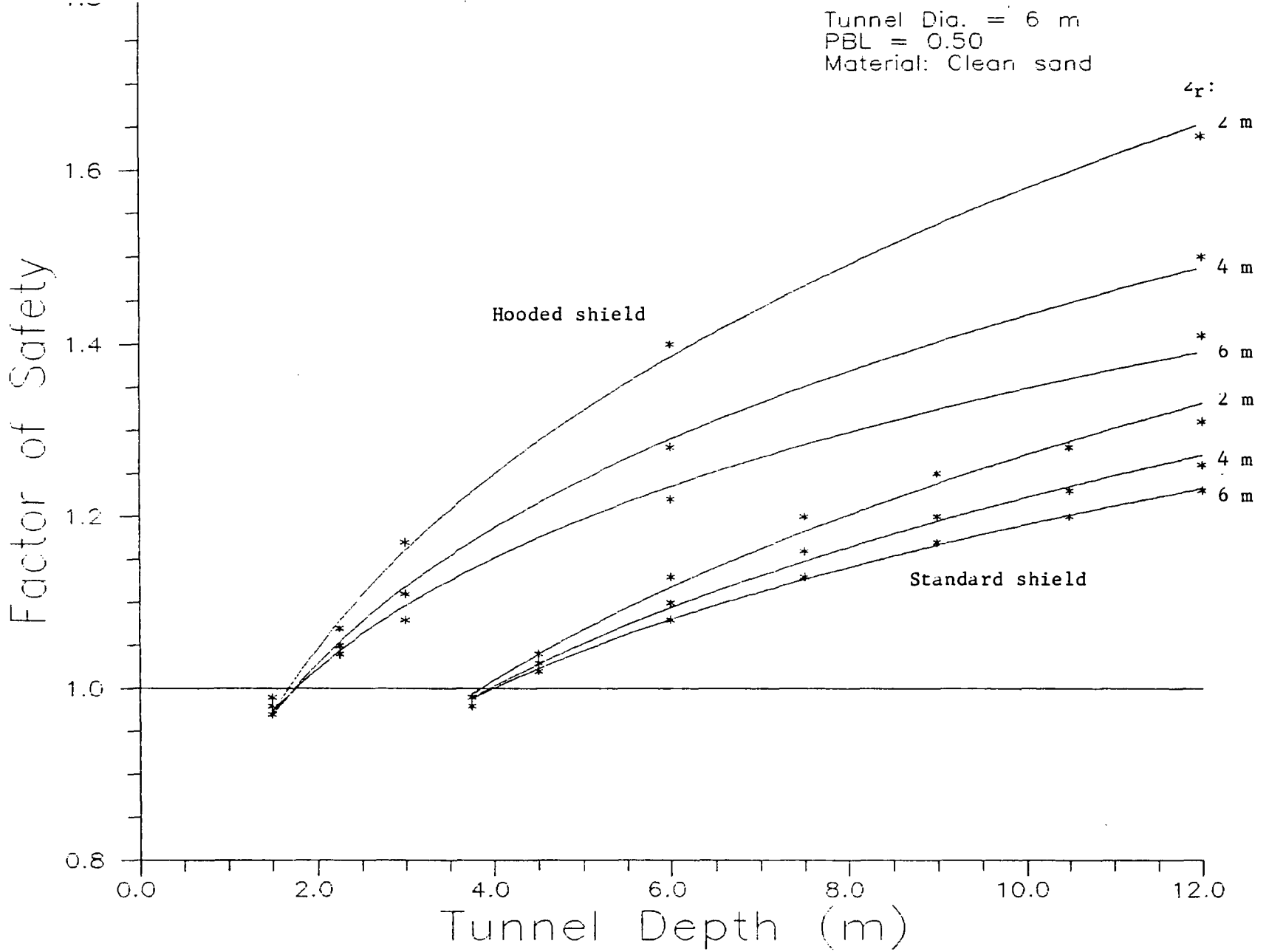
Tunnel Dia. = 6 m
PBL = 0.50
Material: Clean sand
z_r:
2 m
4 m
6 m
2 m
4 m
6 m
Hooded shield
Standard shield
Factor of Safety
Tunnel Depth (m)
0.8
1.0
1.2
1.4
1.6
0.0
2.0
4.0
6.0
8.0
10.0
12.0

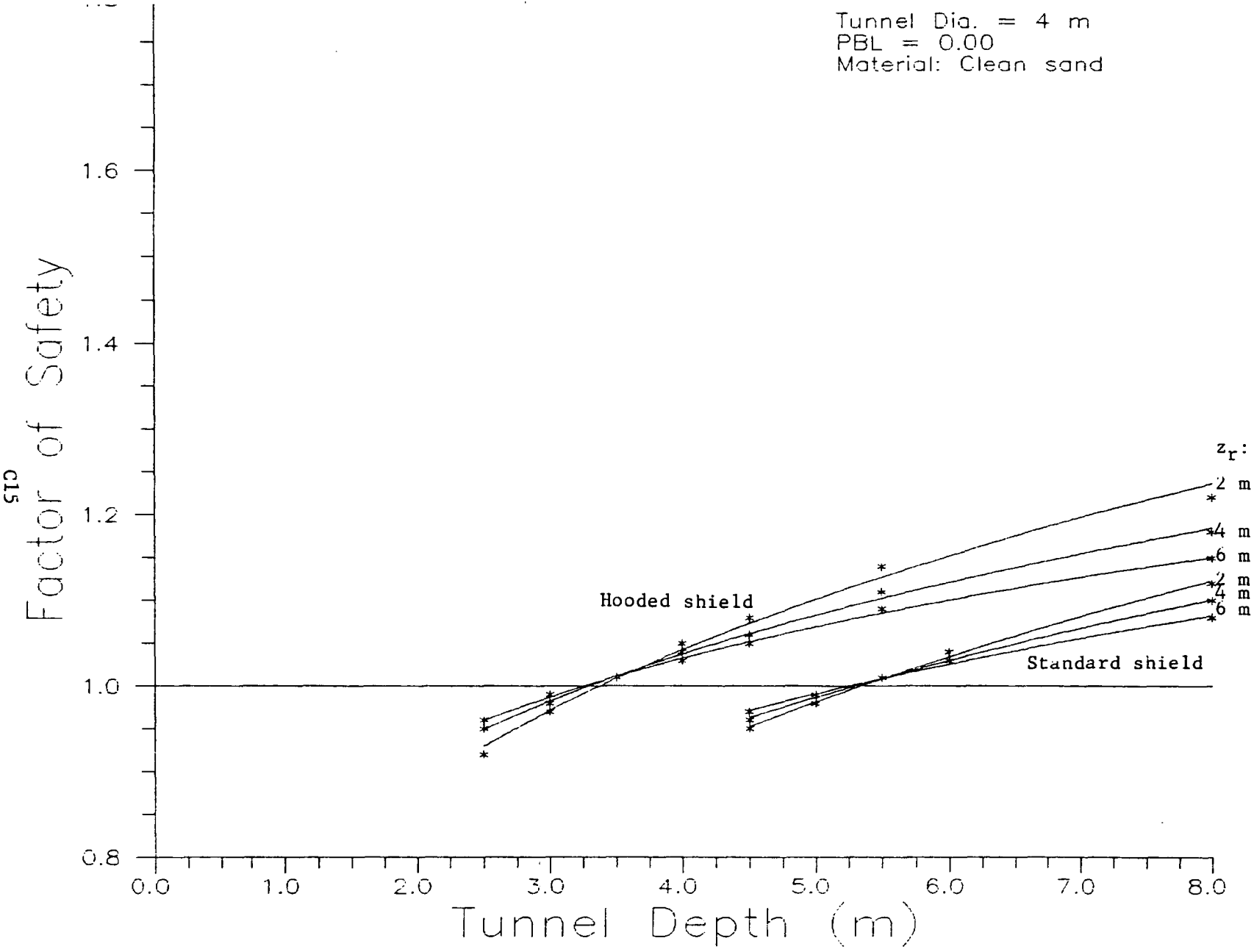
Tunnel Dia. = 4 m
PBL = 0.00
Material: Clean sand
Factor of Safety
c_{15}
1.6
1.4
1.2
1.0
0.8
z_r:
2 m
4 m
6 m
2 m
4 m
6 m
Hooded shield
Standard shield
0.0
1.0
2.0
3.0
4.0
5.0
6.0
7.0
8.0
Tunnel Depth (m)

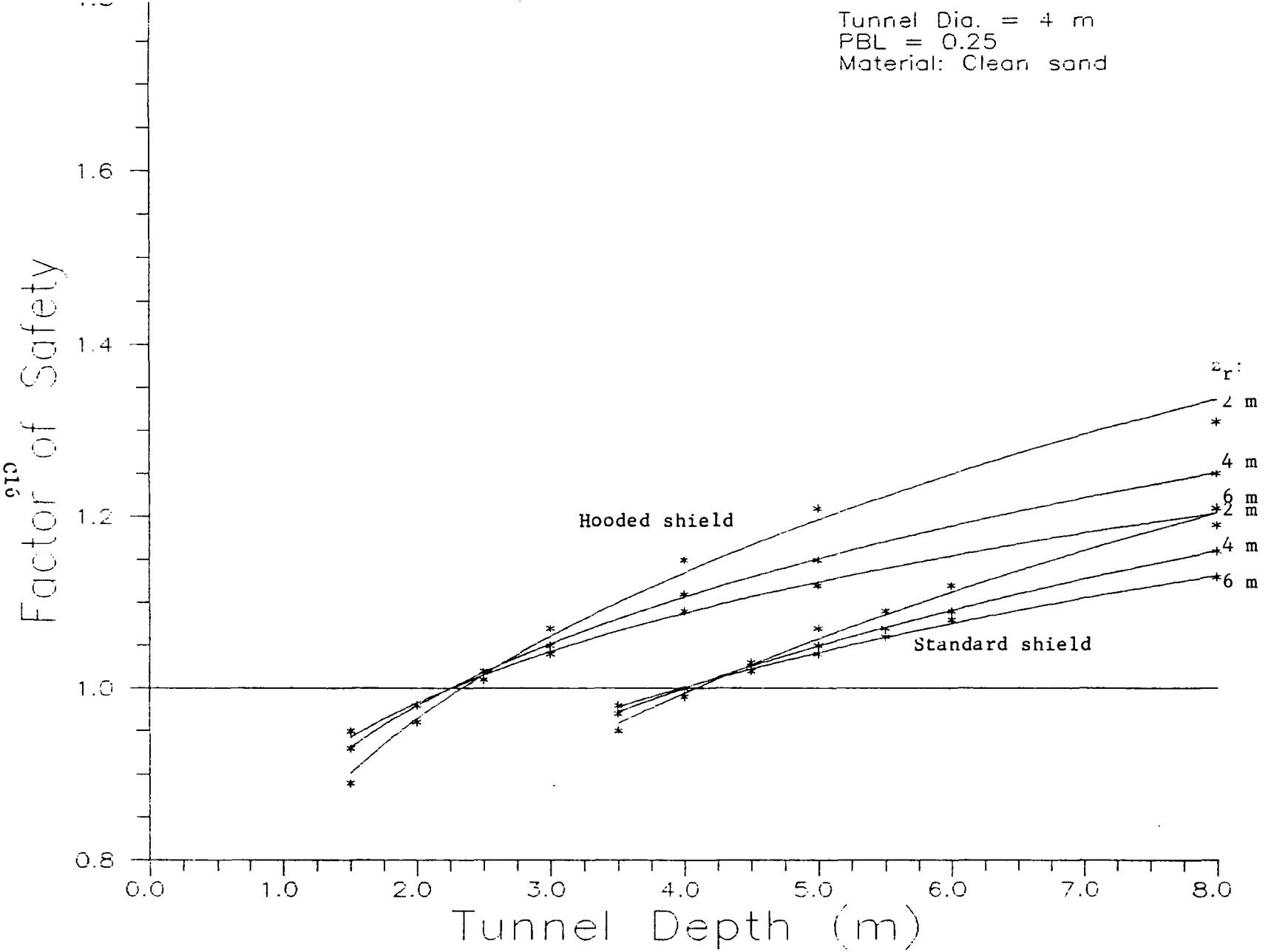
Tunnel Dia. = 4 m
PBL = 0.25
Material: Clean sand
Factor of Safety
c_{16}
1.6
1.4
1.2
1.0
0.8
z_r:
2 m
4 m
6 m
2 m
4 m
6 m
Hooded shield
Standard shield
0.0
1.0
2.0
3.0
4.0
5.0
6.0
7.0
8.0
Tunnel Depth (m)

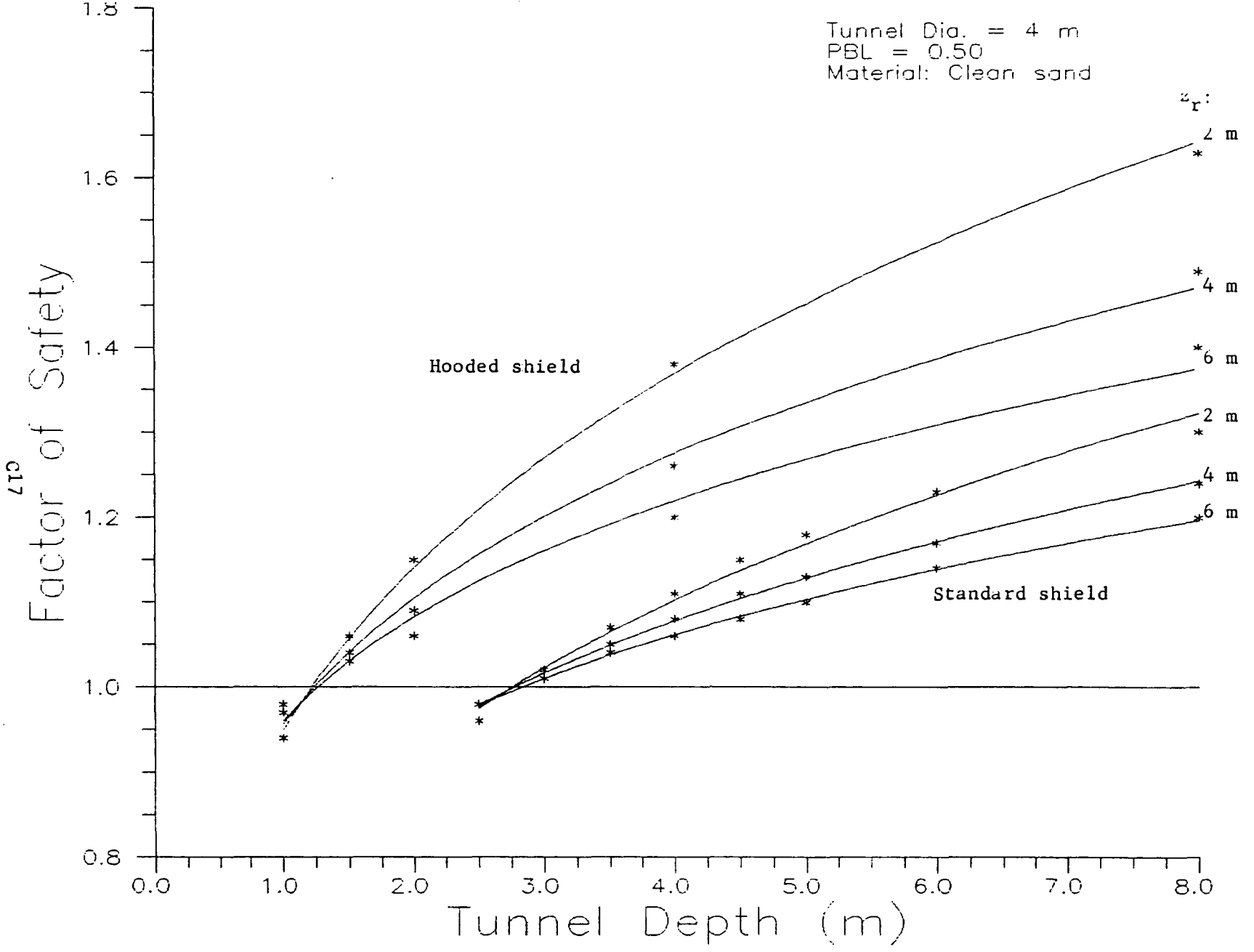
Tunnel Dia. = 4 m
PBL = 0.50
Material: Clean sand
z_r:
2 m
4 m
6 m
2 m
4 m
6 m
Hooded shield
Standard shield
Factor of Safety
c_{17}
1.8
1.6
1.4
1.2
1.0
0.8
0.0
1.0
2.0
3.0
4.0
5.0
6.0
7.0
8.0
Tunnel Depth (m)

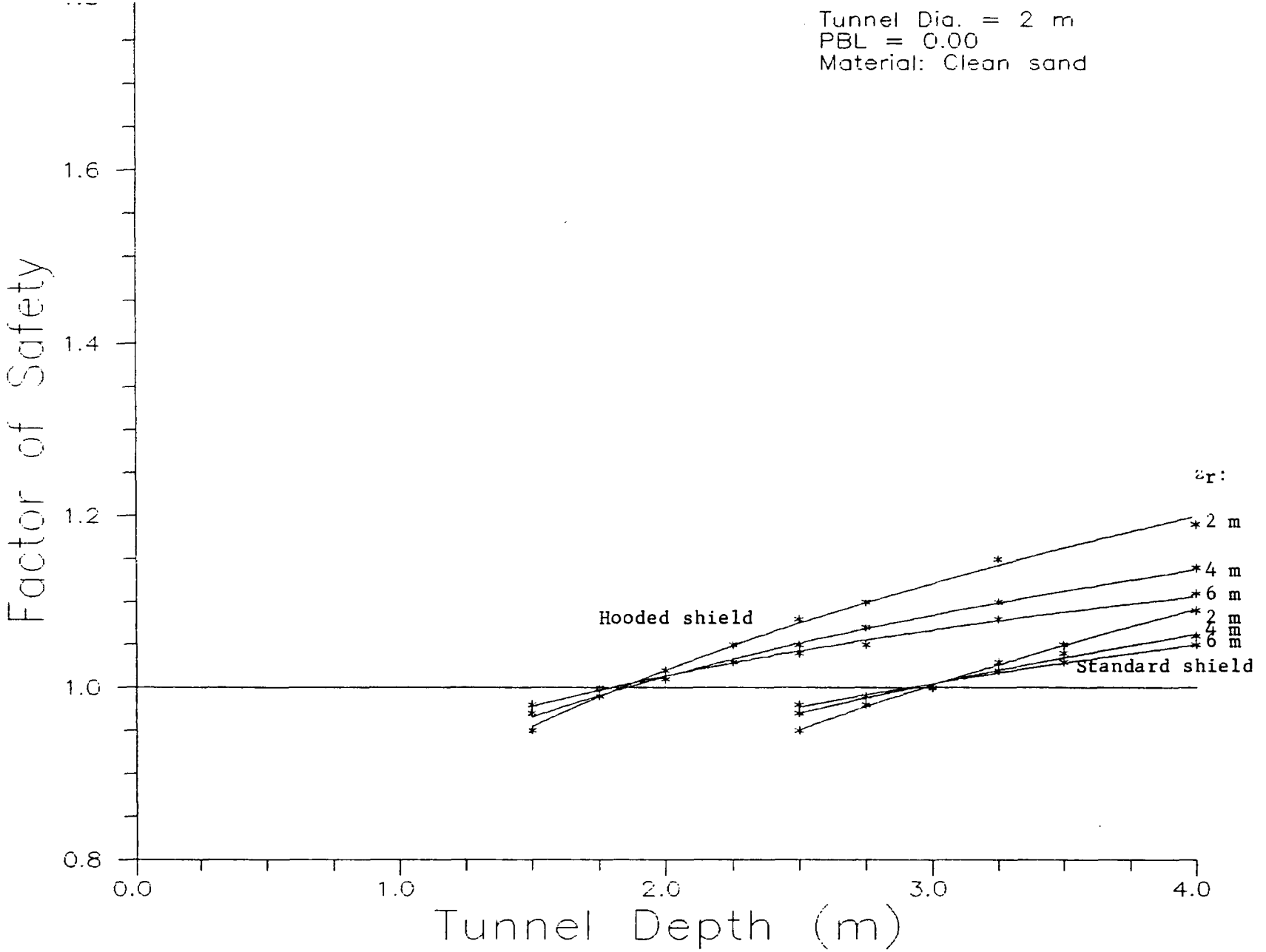
Tunnel Dia. = 2 m
PBL = 0.00
Material: Clean sand
Factor of Safety
1.6
1.4
1.2
1.0
0.8
0.0
1.0
2.0
3.0
4.0
Tunnel Depth (m)
Hooded shield
Standard shield
2 m
4 m
6 m
2 m
4 m
6 m

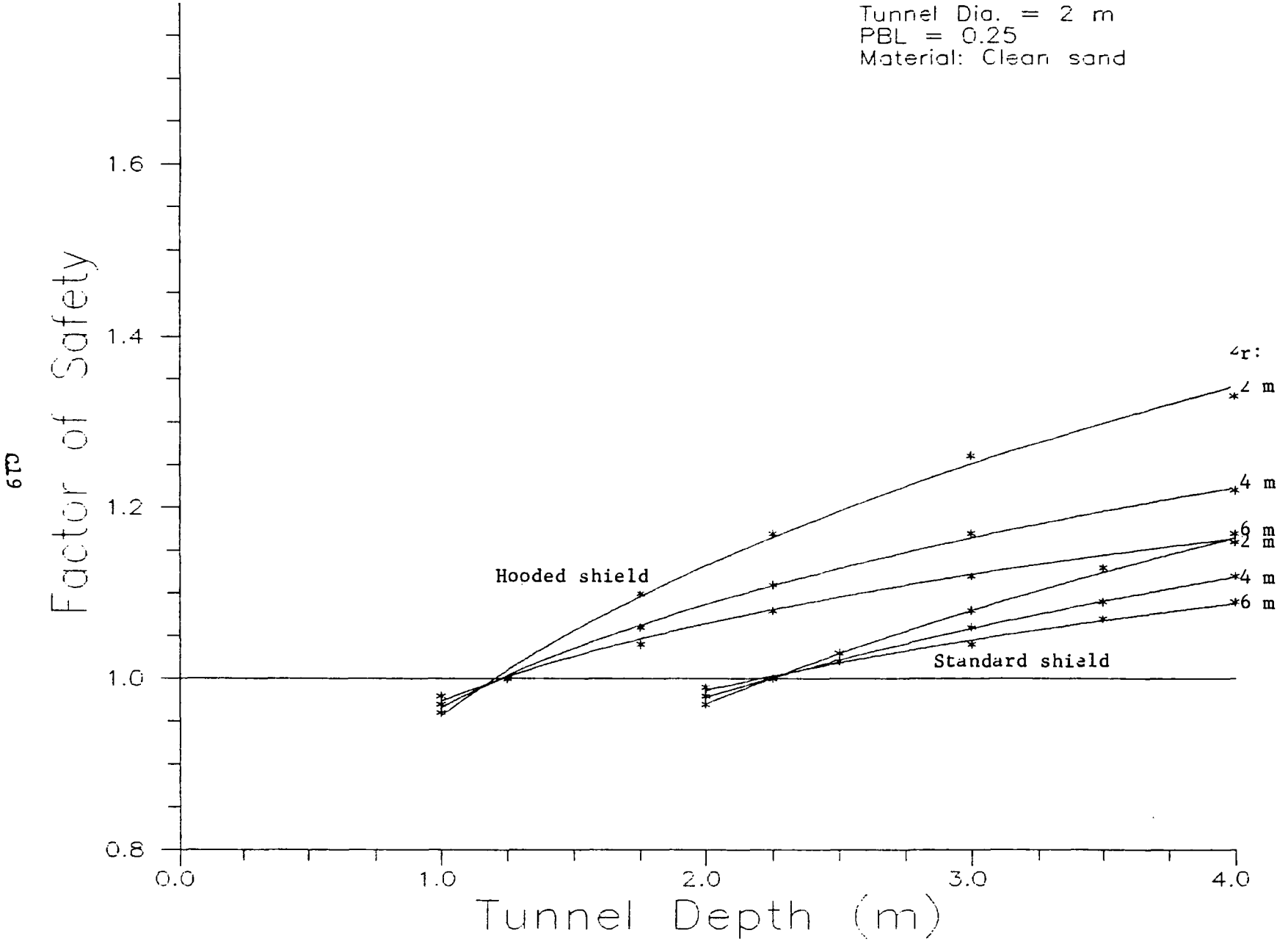
Tunnel Dia. = 2 m
PBL = 0.25
Material: Clean sand
Factor of Safety
1.6
1.4
1.2
1.0
0.8
0.0
1.0
2.0
3.0
4.0
Tunnel Depth (m)
Hooded shield
Standard shield
4 m
6 m
2 m
4 m
6 m

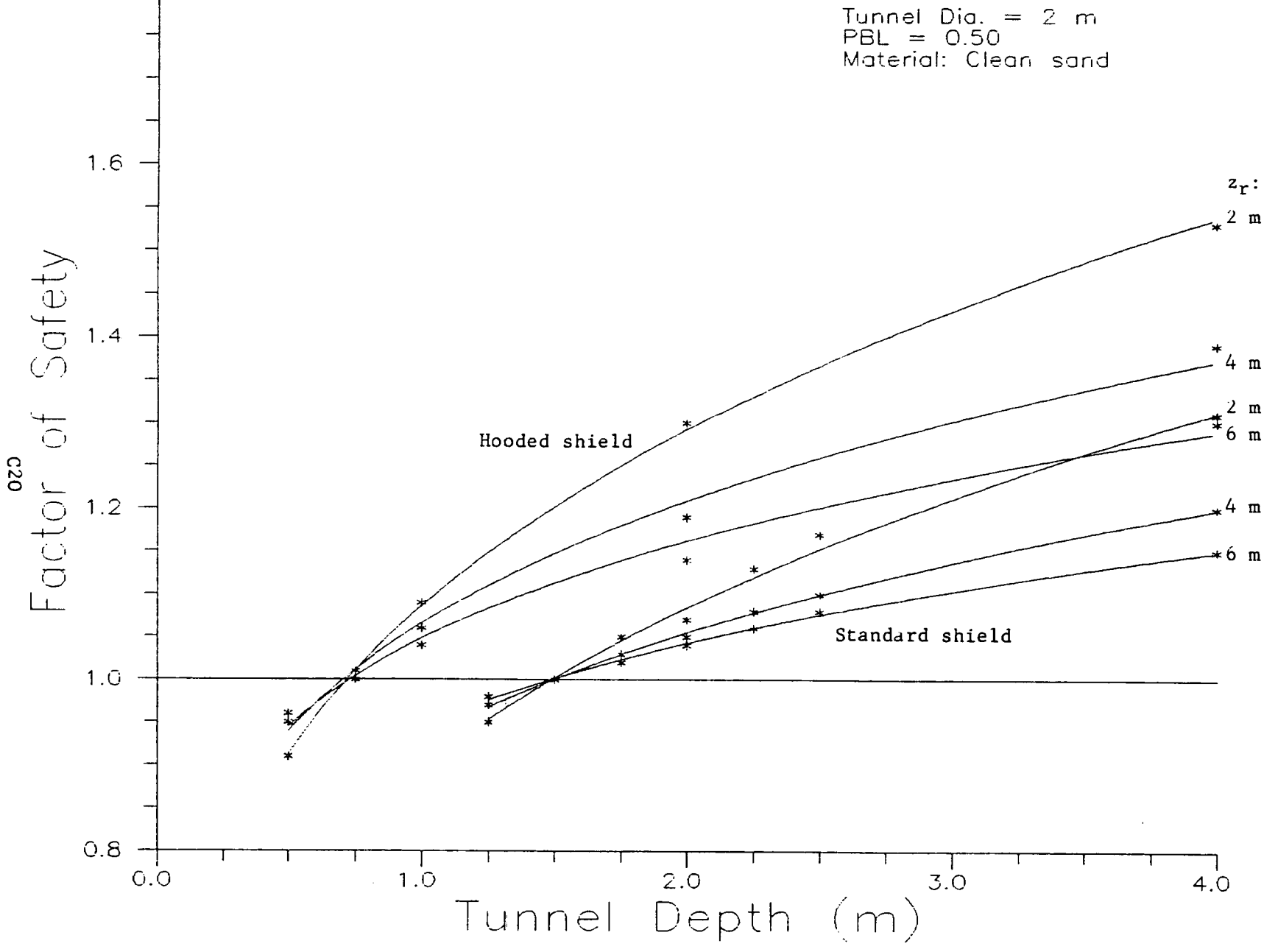
Tunnel Dia. = 2 m
PBL = 0.50
Material: Clean sand
z_r:
2 m
4 m
2 m
6 m
4 m
6 m
Hooded shield
Standard shield
Factor of Safety
c_{20}
1.6
1.4
1.2
1.0
0.8
0.0
1.0
2.0
3.0
4.0
Tunnel Depth (m)

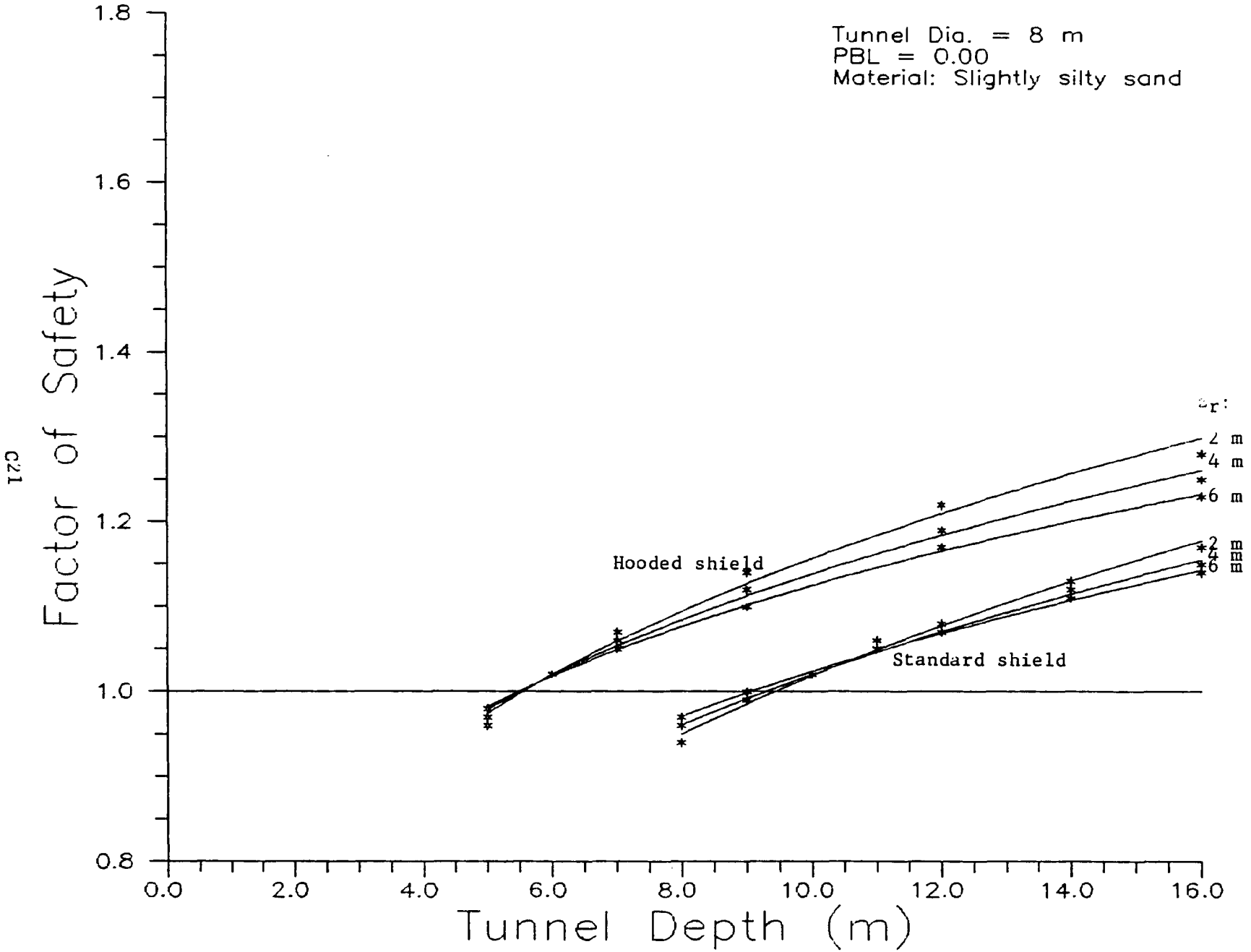
Tunnel Dia. = 8 m
PBL = 0.00
Material: Slightly silty sand
Factor of Safety
c_{z1}
1.8
1.6
1.4
1.2
1.0
0.8
0.0
2.0
4.0
6.0
8.0
10.0
12.0
14.0
16.0
Tunnel Depth (m)
c_r:
2 m
4 m
6 m
2 mm
4 mm
6 mm
Hooded shield
Standard shield

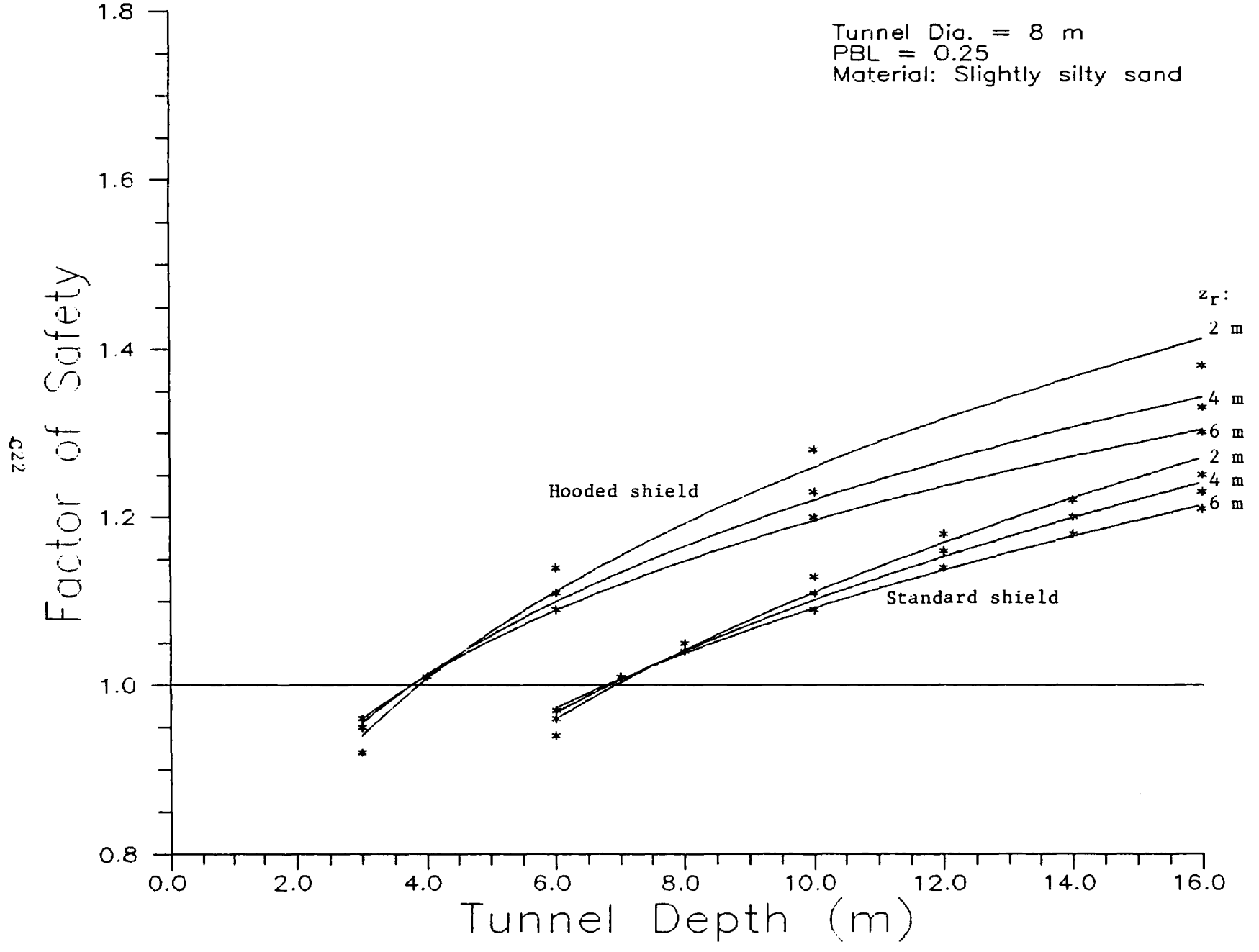
Tunnel Dia. = 8 m
PBL = 0.25
Material: Slightly silty sand
Factor of Safety
ε_{zz}
1.8
1.6
1.4
1.2
1.0
0.8
0.0
2.0
4.0
6.0
8.0
10.0
12.0
14.0
16.0
Tunnel Depth (m)
z_r:
2 m
4 m
6 m
2 m
4 m
6 m
Hooded shield
Standard shield

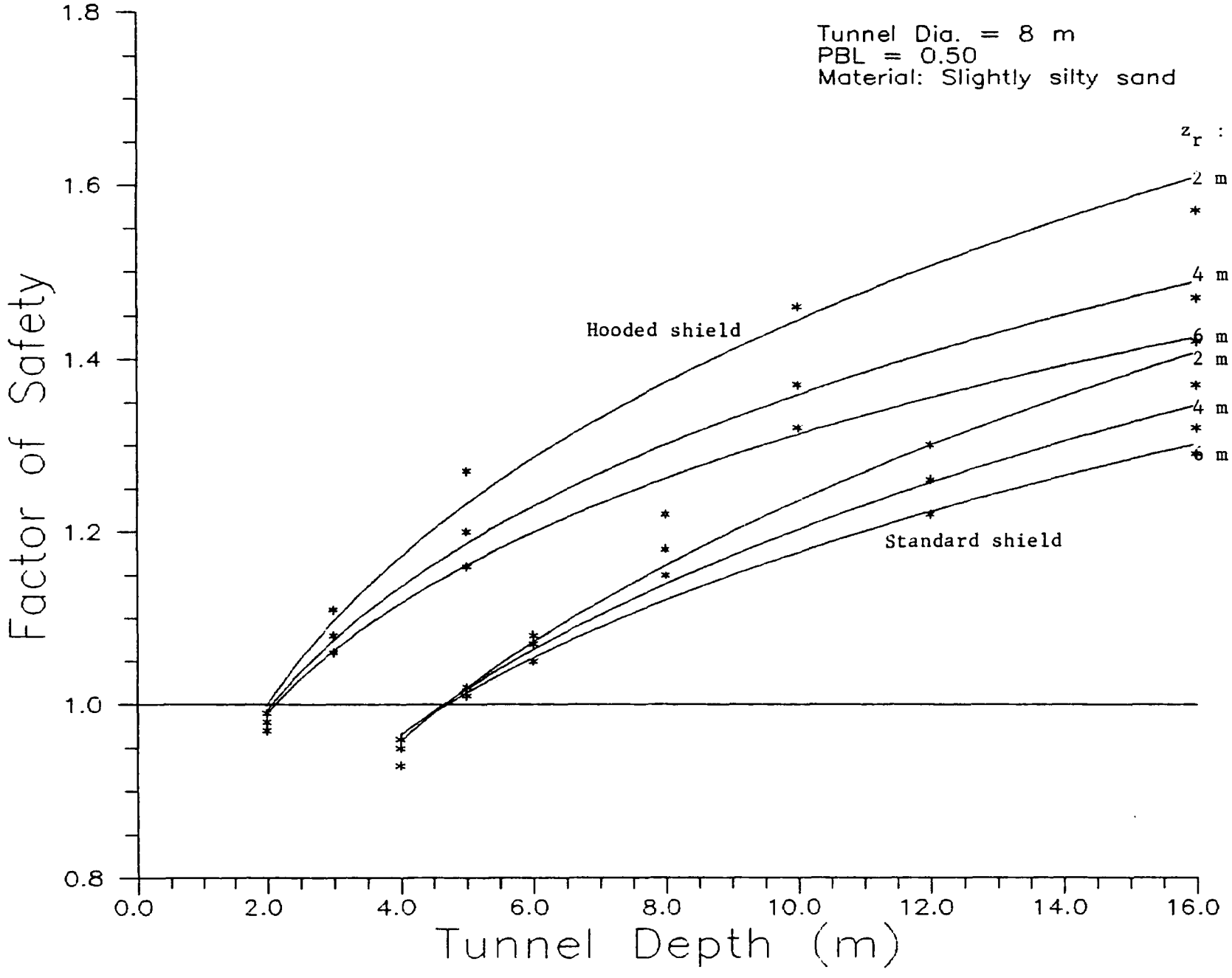
Tunnel Dia. = 8 m
PBL = 0.50
Material: Slightly silty sand
z_r :
2 m
4 m
6 m
2 m
4 m
6 m
Hooded shield
Standard shield
Factor of Safety
Tunnel Depth (m)
1.8
1.6
1.4
1.2
1.0
0.8
0.0
2.0
4.0
6.0
8.0
10.0
12.0
14.0
16.0

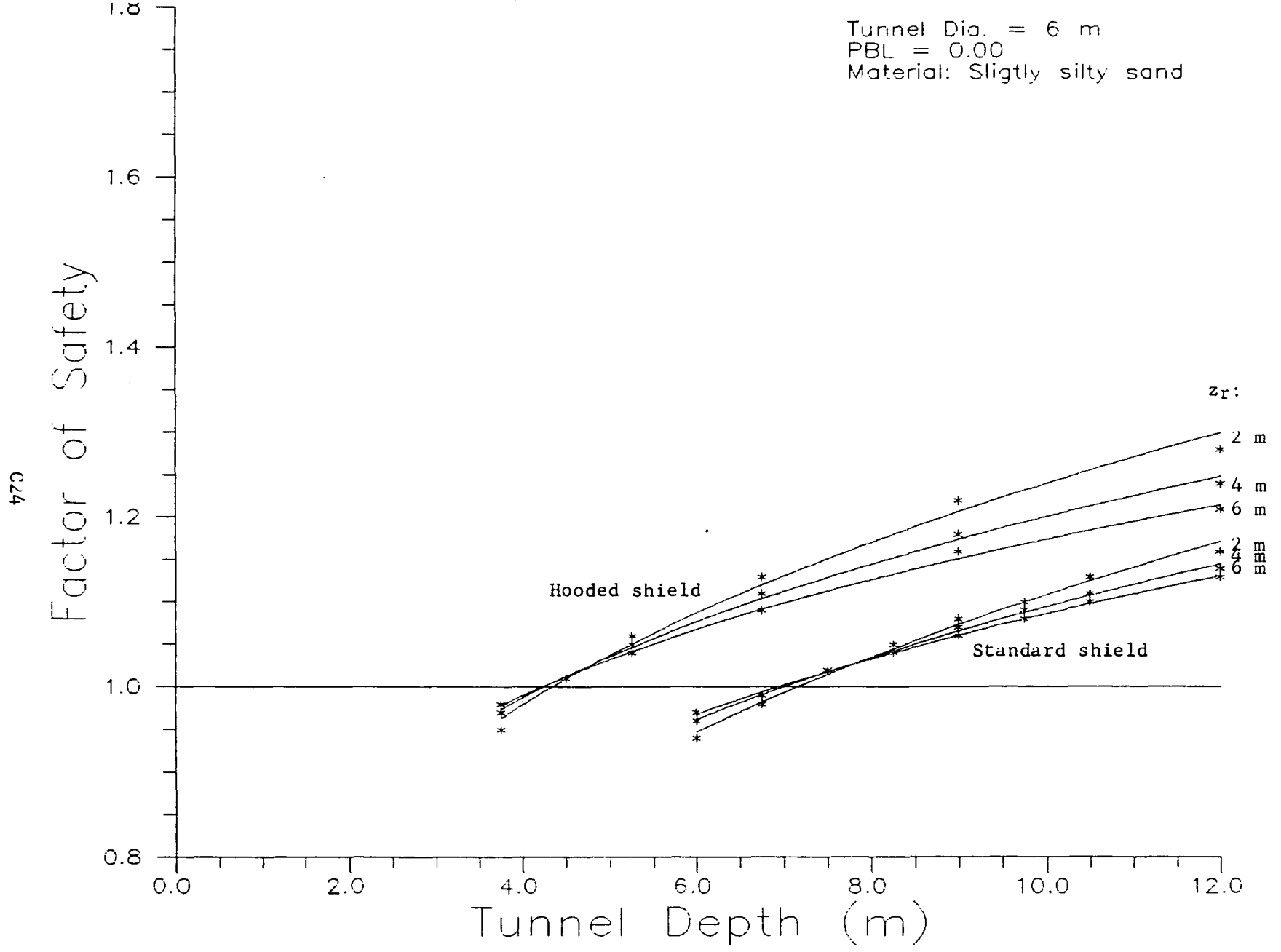
Tunnel Dia. = 6 m
PBL = 0.00
Material: Sligtly silty sand
Factor of Safety
Tunnel Depth (m)
0.8
1.0
1.2
1.4
1.6
1.8
0.0
2.0
4.0
6.0
8.0
10.0
12.0
Hooded shield
Standard shield
z_r:
2 m
4 m
6 m
2 mm
4 mm
6 mm

c24

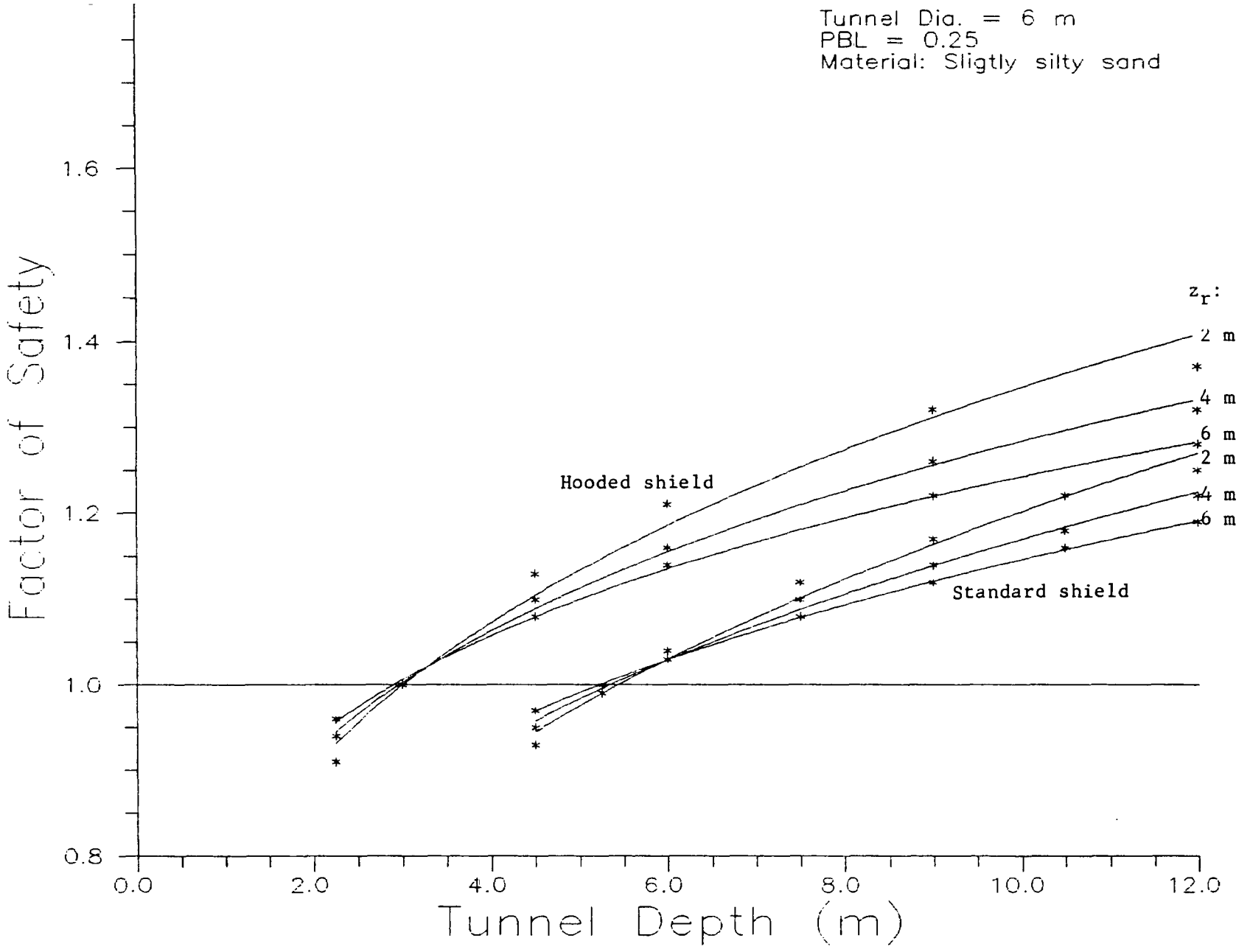
Tunnel Dia. = 6 m
PBL = 0.25
Material: Sligtly silty sand
Factor of Safety
1.6
1.4
1.2
1.0
0.8
0.0
2.0
4.0
6.0
8.0
10.0
12.0
Tunnel Depth (m)
z_r:
2 m
4 m
6 m
2 m
4 m
6 m
Hooded shield
Standard shield

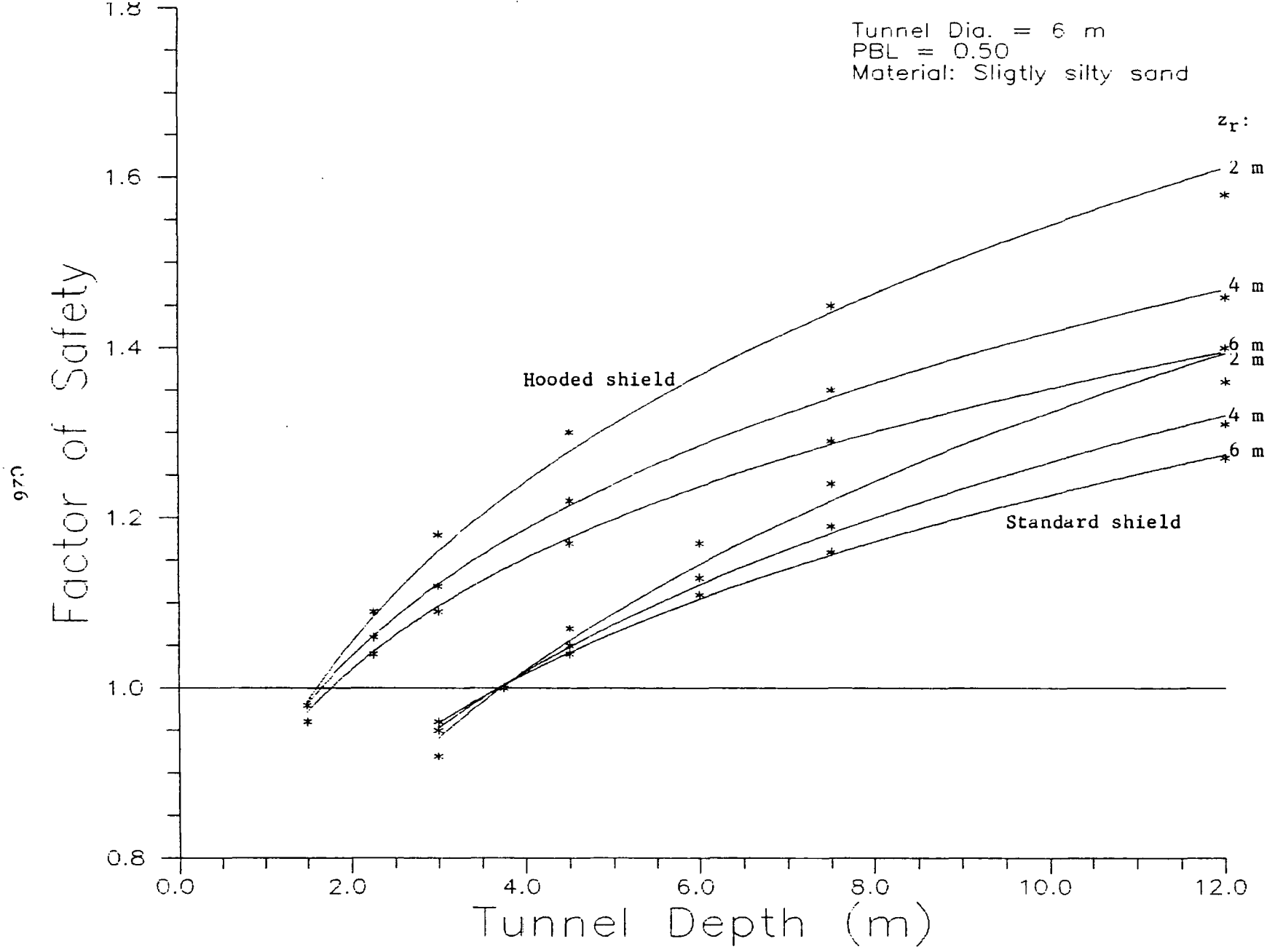
Tunnel Dia. = 6 m
PBL = 0.50
Material: Sligtly silty sand
z_r:
2 m
4 m
6 m
2 m
4 m
6 m
Hooded shield
Standard shield
Factor of Safety
Tunnel Depth (m)
1.8
1.6
1.4
1.2
1.0
0.8
0.0
2.0
4.0
6.0
8.0
10.0
12.0

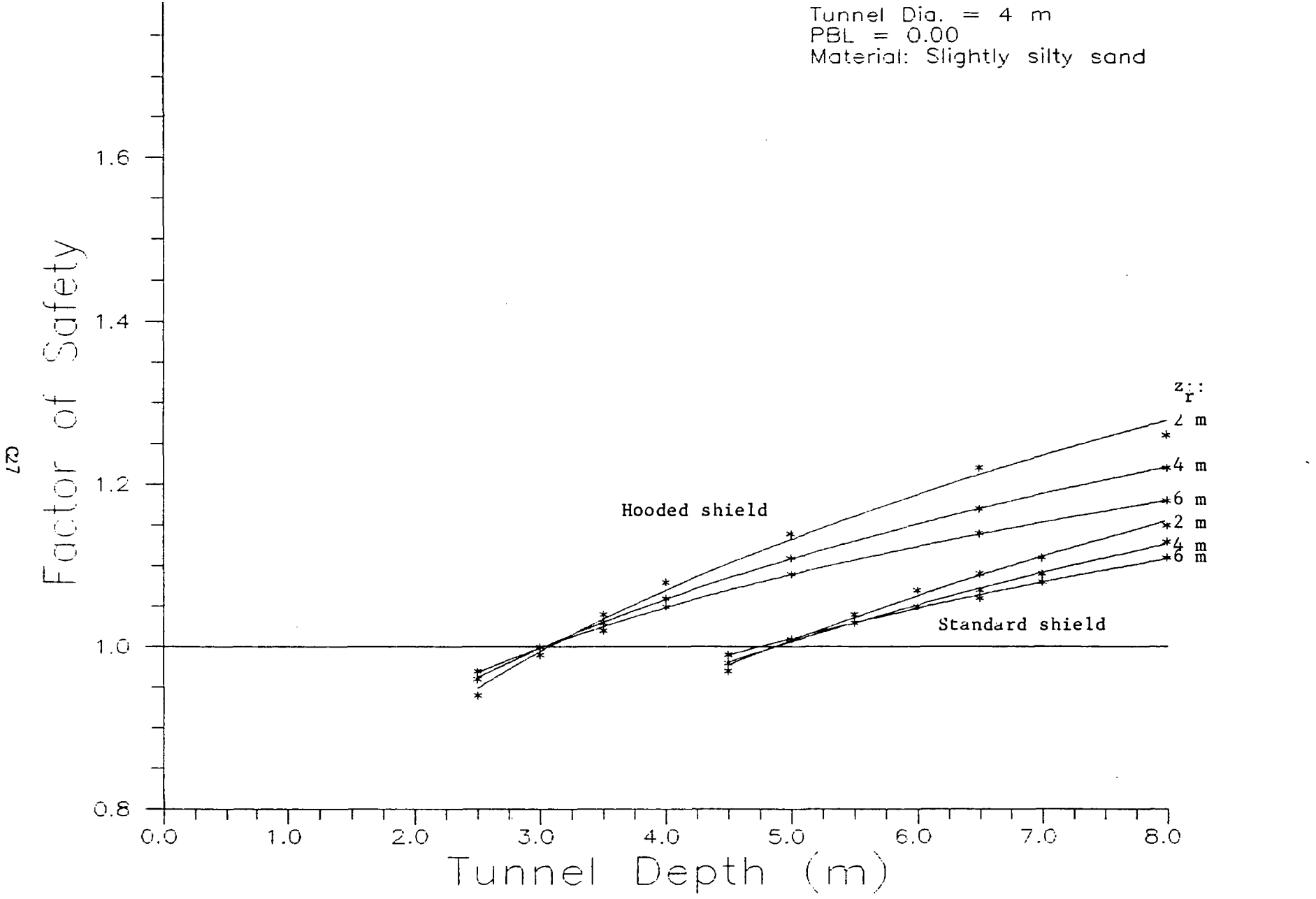
Tunnel Dia. = 4 m
PBL = 0.00
Material: Slightly silty sand
Factor of Safety
1.6
1.4
1.2
1.0
0.8
0.0
1.0
2.0
3.0
4.0
5.0
6.0
7.0
8.0
Tunnel Depth (m)
Hooded shield
Standard shield
z_r:
2 m
4 m
6 m
2 m
4 m
6 m

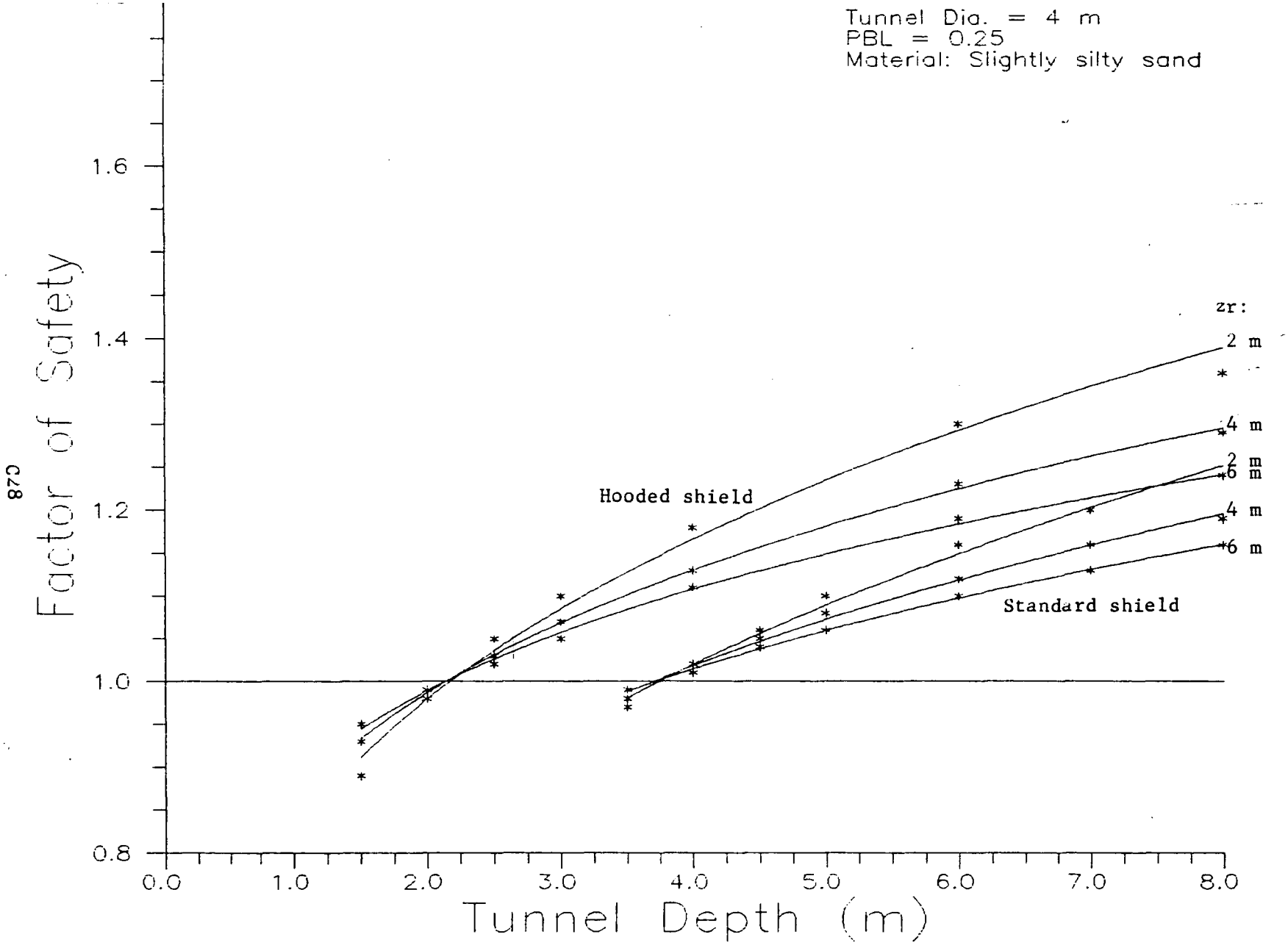
Tunnel Dia. = 4 m
PBL = 0.25
Material: Slightly silty sand
Factor of Safety
Tunnel Depth (m)
zr:
2 m
4 m
2 m
6 m
4 m
6 m
Hooded shield
Standard shield
0.8
1.0
1.2
1.4
1.6
0.0
1.0
2.0
3.0
4.0
5.0
6.0
7.0
8.0

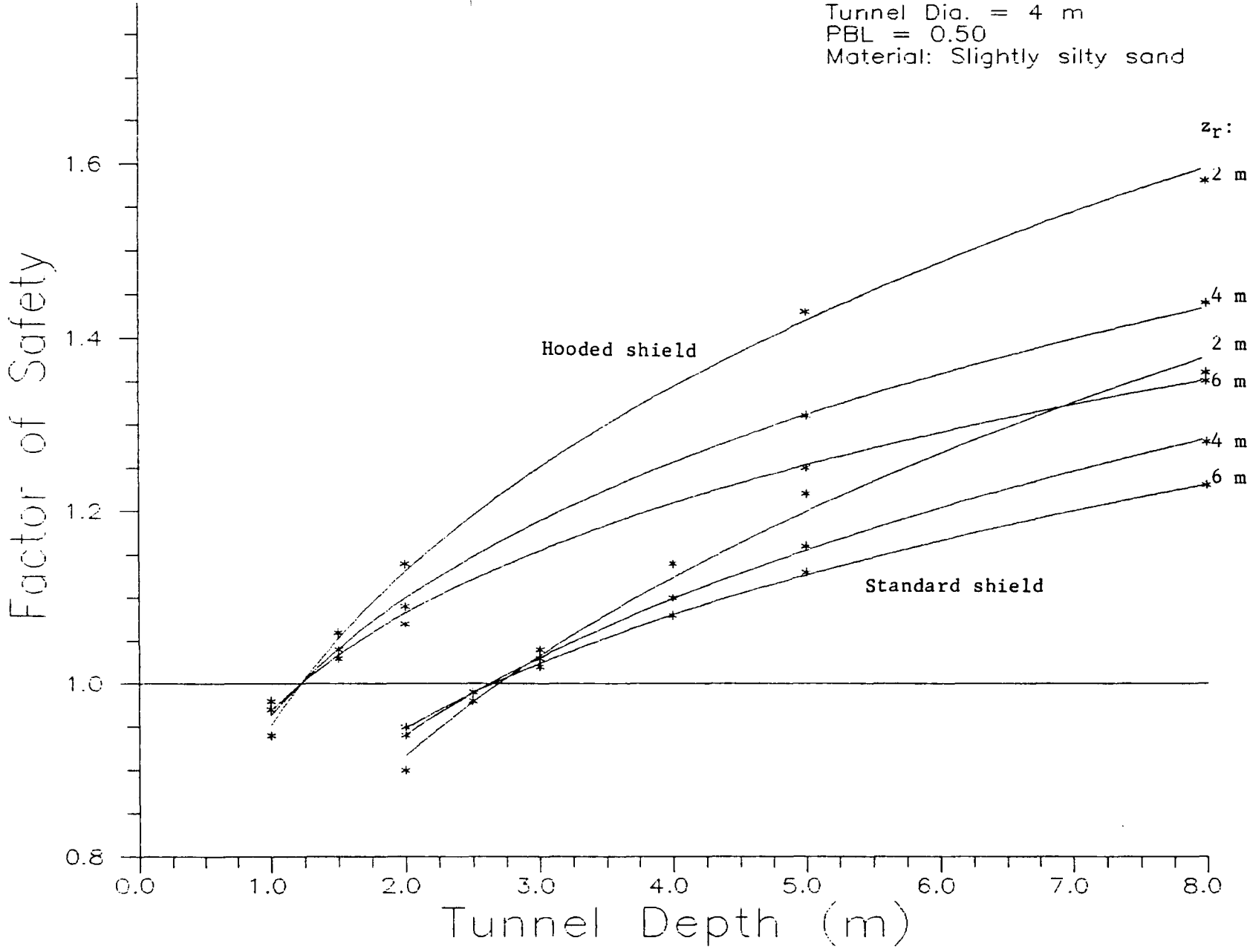
Tunnel Dia. = 4 m
PBL = 0.50
Material: Slightly silty sand
z_r:
2 m
4 m
2 m
6 m
4 m
6 m
Hooded shield
Standard shield
Factor of Safety
1.6
1.4
1.2
1.0
0.8
0.0
1.0
2.0
3.0
4.0
5.0
6.0
7.0
8.0
Tunnel Depth (m)

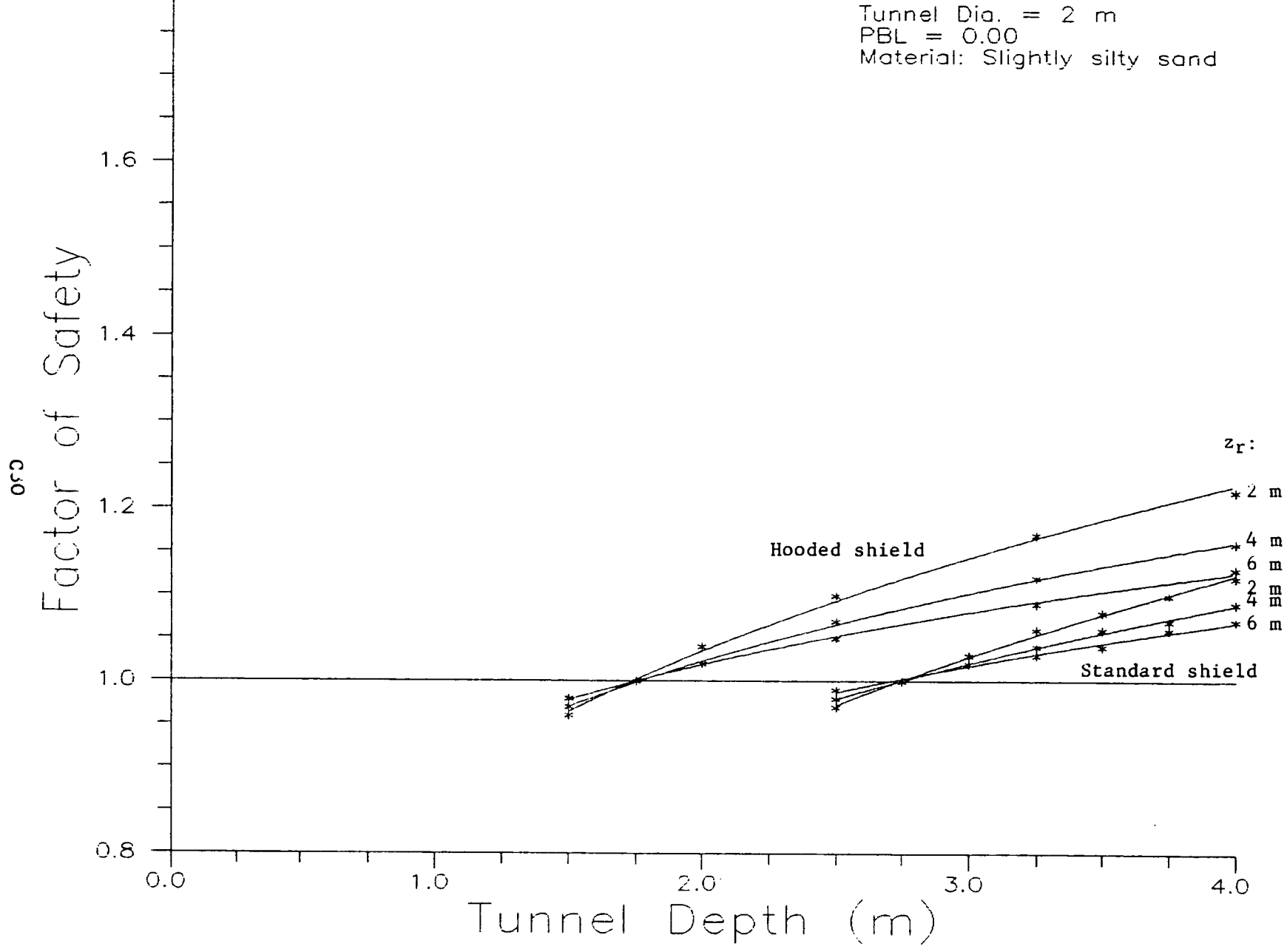
Tunnel Dia. = 2 m
PBL = 0.00
Material: Slightly silty sand
Factor of Safety
csσ
1.6
1.4
1.2
1.0
0.8
0.0
1.0
2.0
3.0
4.0
Tunnel Depth (m)
z_r:
2 m
4 m
6 m
2 m
4 m
6 m
Hooded shield
Standard shield

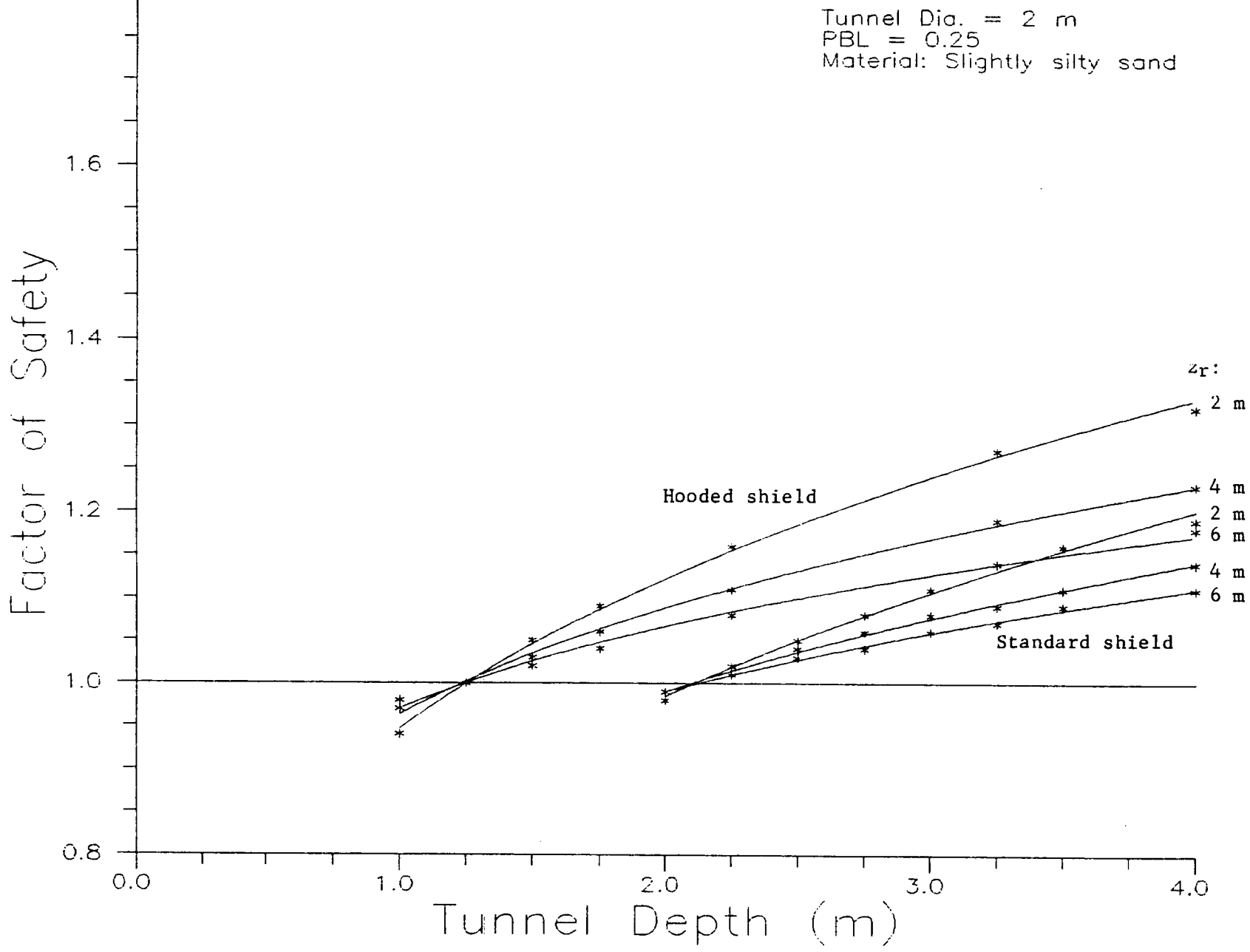
Tunnel Dia. = 2 m
PBL = 0.25
Material: Slightly silty sand
Factor of Safety
1.6
1.4
1.2
1.0
0.8
0.0
1.0
2.0
3.0
4.0
Tunnel Depth (m)
Hooded shield
Standard shield
z_r:
2 m
4 m
2 m
6 m
4 m
6 m

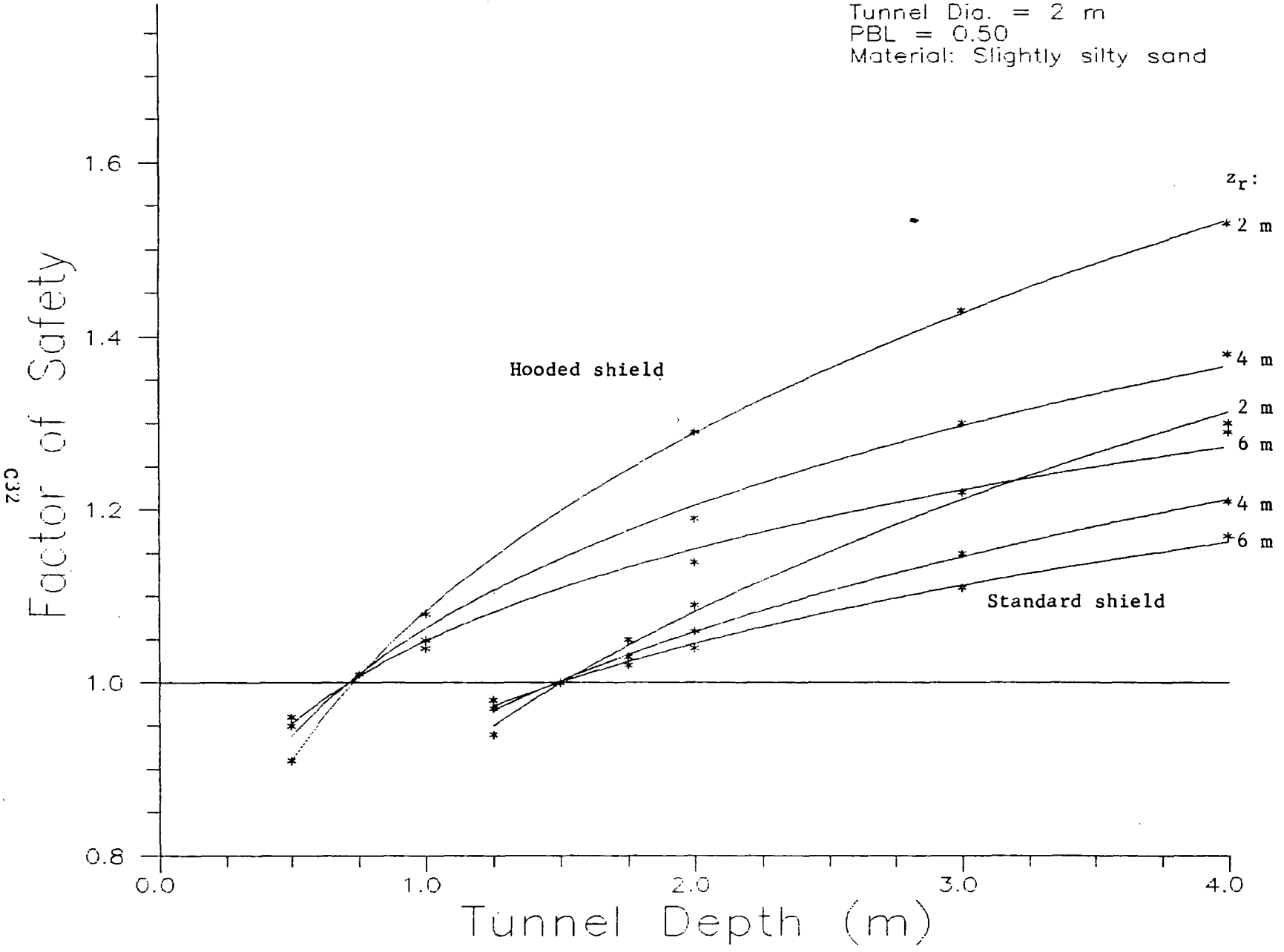
Tunnel Dia. = 2 m
PBL = 0.50
Material: Slightly silty sand
z_r:
2 m
4 m
2 m
6 m
4 m
6 m
Hooded shield
Standard shield
Factor of Safety
c/z
1.6
1.4
1.2
1.0
0.8
0.0
1.0
2.0
3.0
4.0
Tunnel Depth (m)

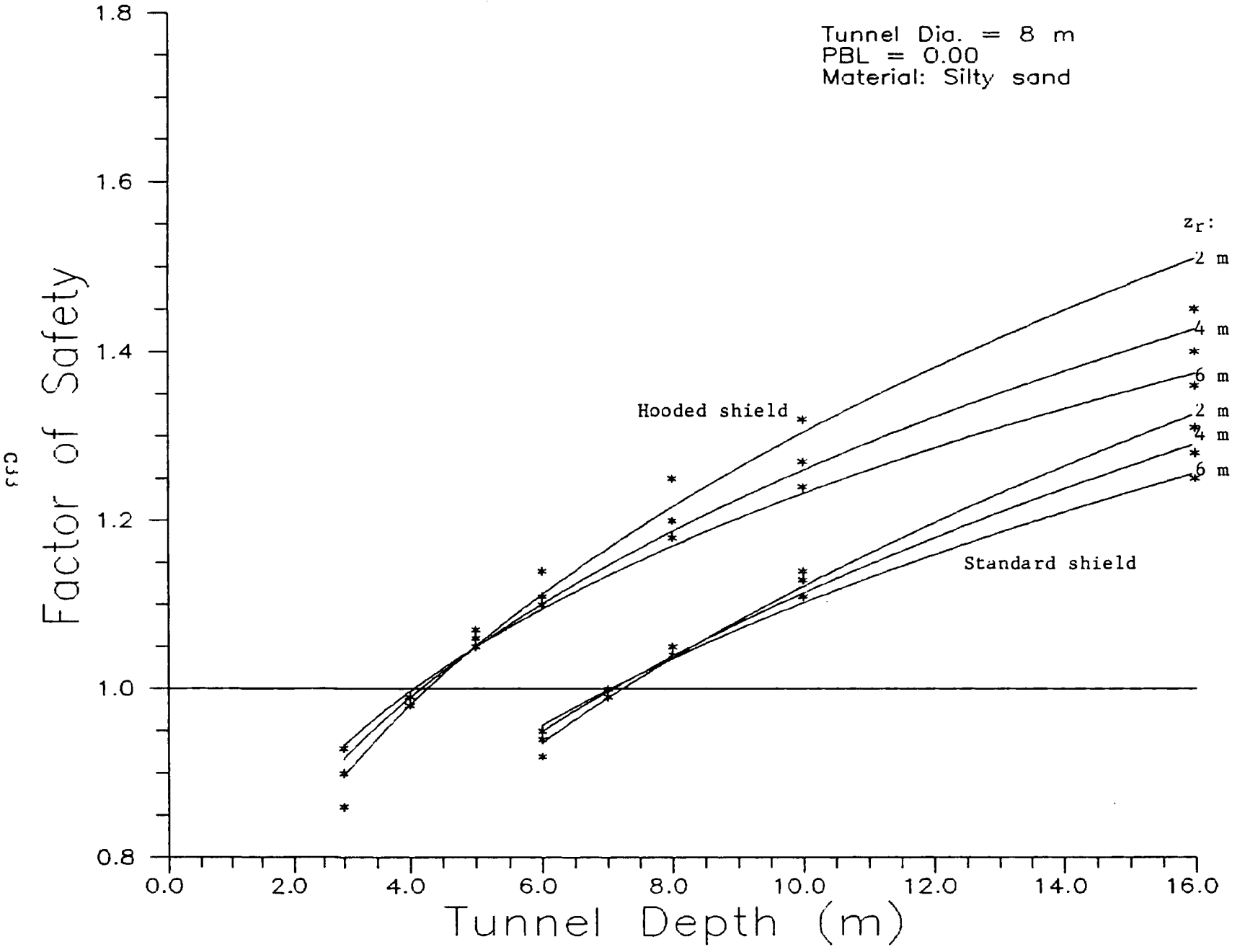
Tunnel Dia. = 8 m
PBL = 0.00
Material: Silty sand
z_r:
2 m
4 m
6 m
2 m
4 m
6 m
Hooded shield
Standard shield
Factor of Safety
c_{rs}
1.8
1.6
1.4
1.2
1.0
0.8
0.0
2.0
4.0
6.0
8.0
10.0
12.0
14.0
16.0
Tunnel Depth (m)

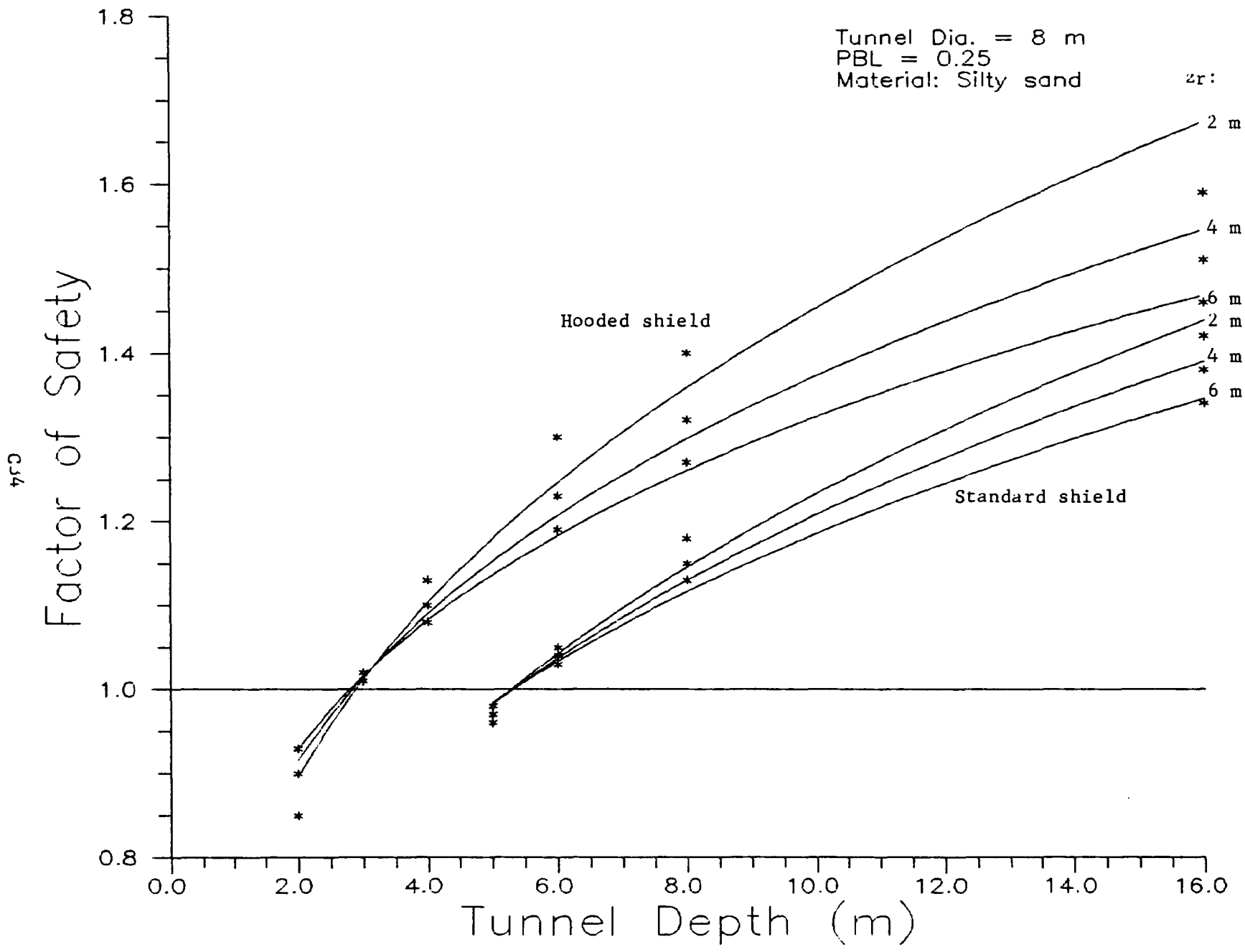
Tunnel Dia. = 8 m
PBL = 0.25
Material: Silty sand
zr:
2 m
4 m
6 m
2 m
4 m
6 m
Hooded shield
Standard shield
Factor of Safety
Tunnel Depth (m)
1.8
1.6
1.4
1.2
1.0
0.8
0.0
2.0
4.0
6.0
8.0
10.0
12.0
14.0
16.0

cr4

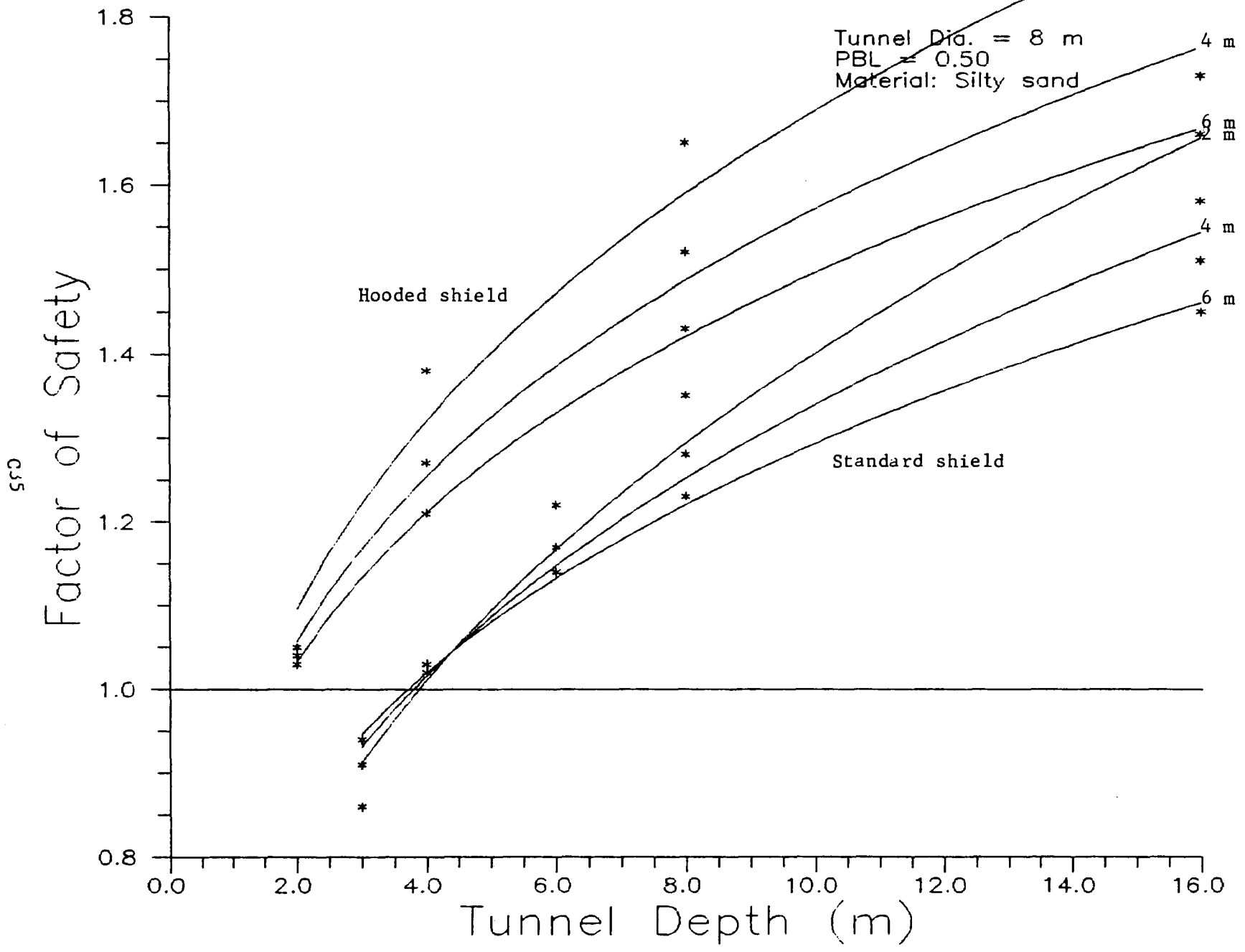
Tunnel Dia. = 8 m
PBL = 0.50
Material: Silty sand
4 m
6 m
4 m
6 m
Hooded shield
Standard shield
Factor of Safety
Tunnel Depth (m)
1.8
1.6
1.4
1.2
1.0
0.8
0.0
2.0
4.0
6.0
8.0
10.0
12.0
14.0
16.0

c55

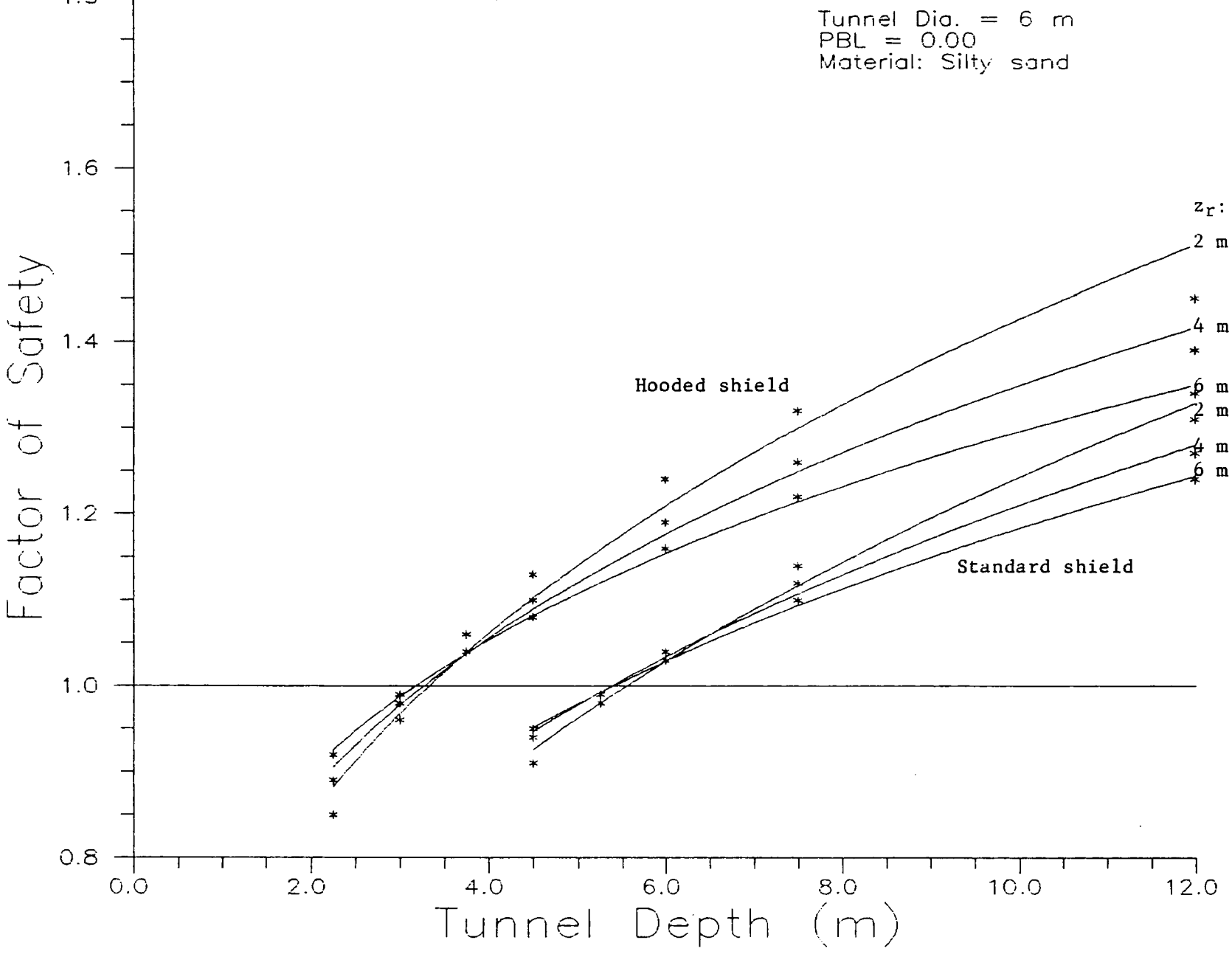
Tunnel Dia. = 6 m
PBL = 0.00
Material: Silty sand
z_r:
2 m
4 m
6 m
2 m
4 m
6 m
Hooded shield
Standard shield
Factor of Safety
Tunnel Depth (m)
0.8
1.0
1.2
1.4
1.6
0.0
2.0
4.0
6.0
8.0
10.0
12.0

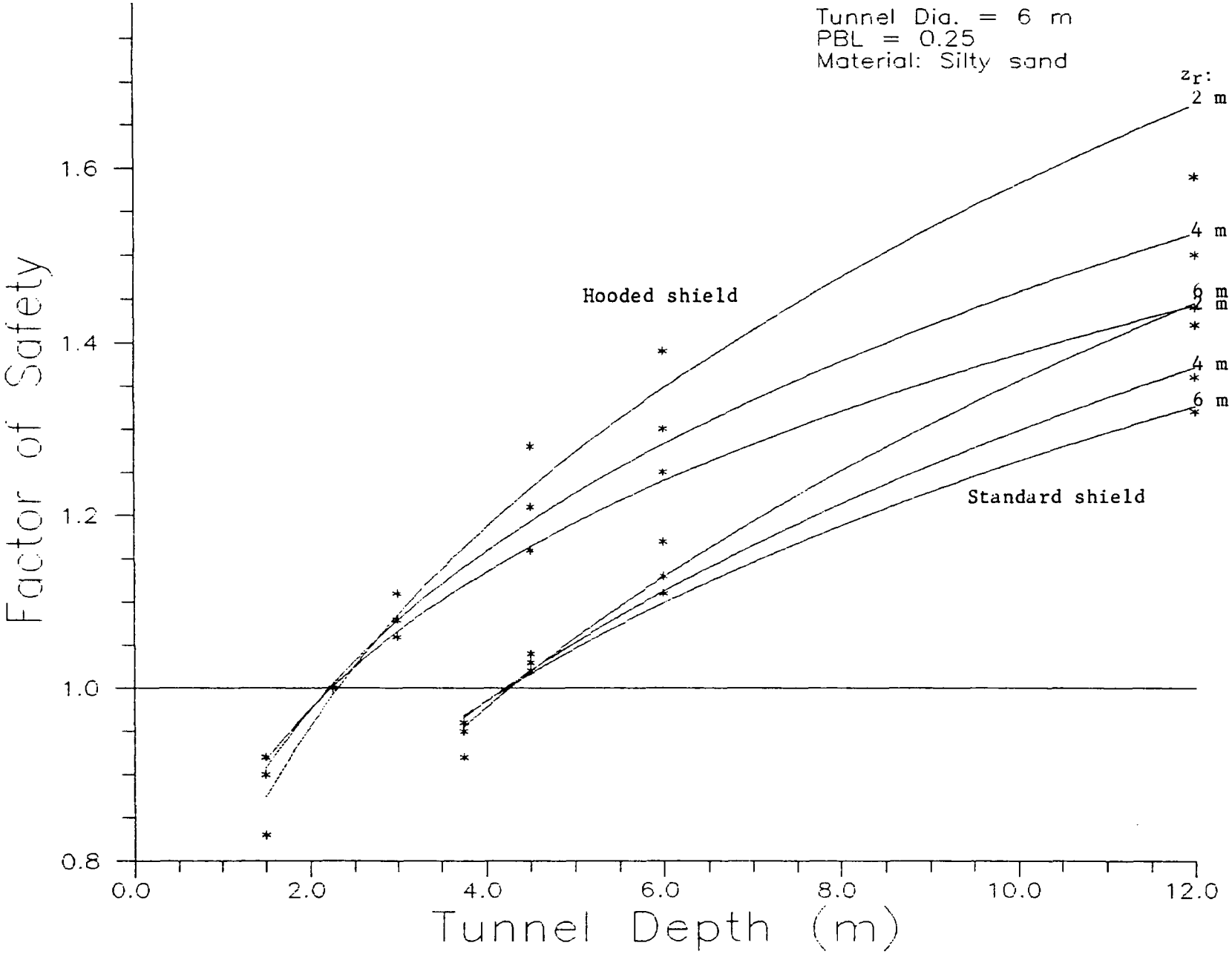
Tunnel Dia. = 6 m
PBL = 0.25
Material: Silty sand
z_r:
2 m
4 m
6 m
2 m
4 m
6 m
Hooded shield
Standard shield
Factor of Safety
1.6
1.4
1.2
1.0
0.8
0.0
2.0
4.0
6.0
8.0
10.0
12.0
Tunnel Depth (m)

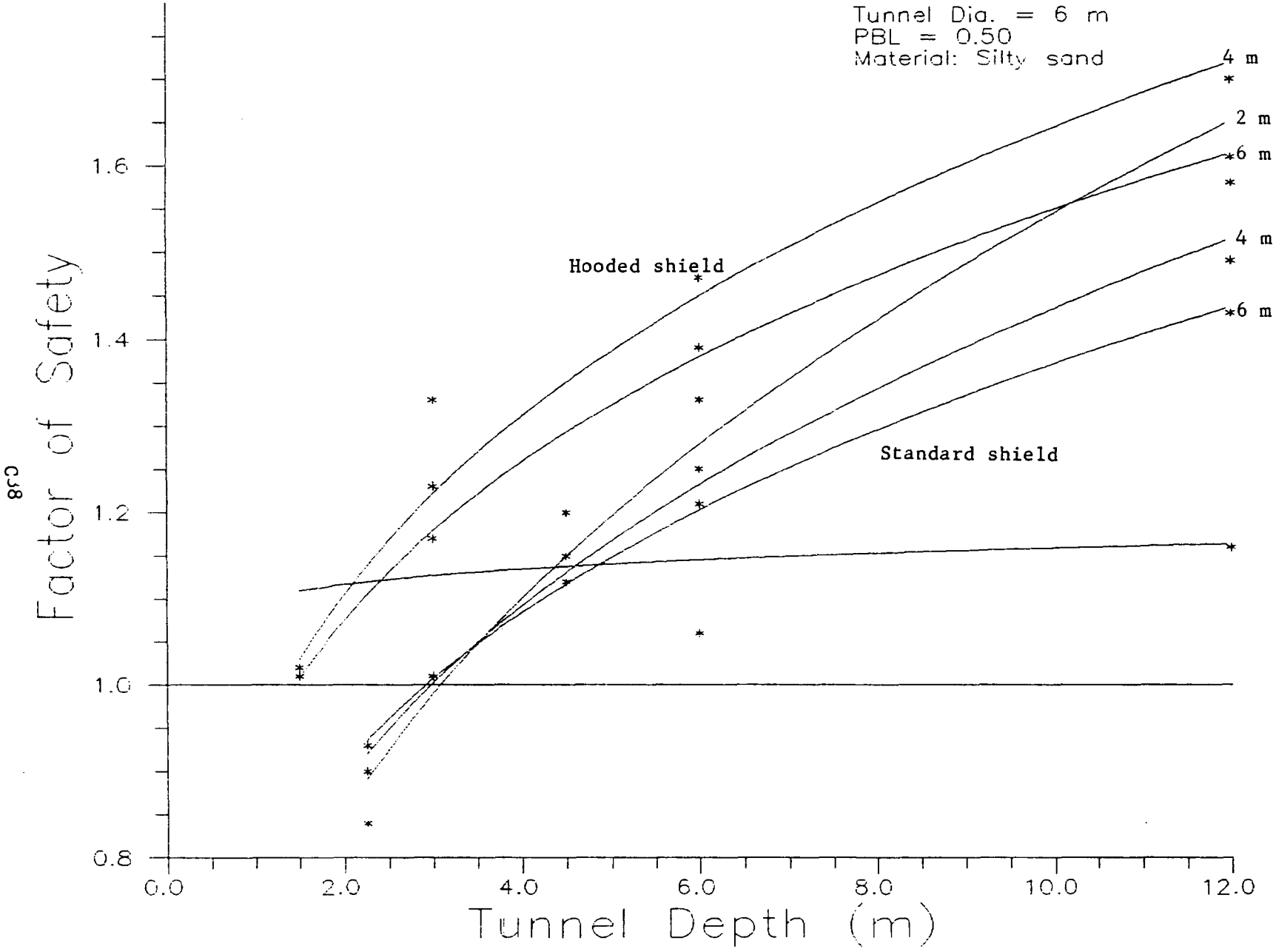
Tunnel Dia. = 6 m
PBL = 0.50
Material: Silty sand
4 m
2 m
6 m
4 m
6 m
Hooded shield
Standard shield
Factor of Safety
1.6
1.4
1.2
1.0
0.8
0.0
2.0
4.0
6.0
8.0
10.0
12.0
Tunnel Depth (m)

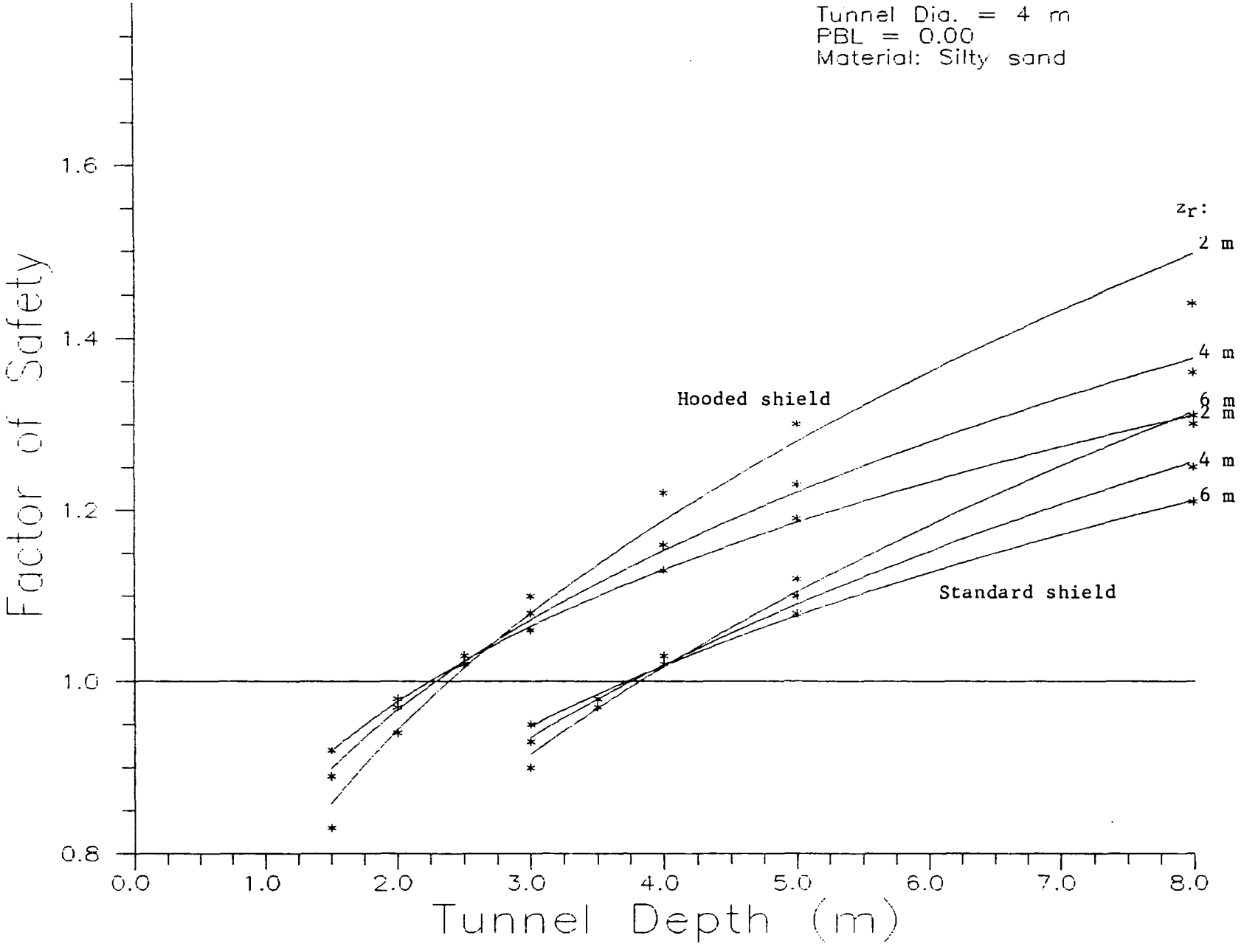
Tunnel Dia. = 4 m
PBL = 0.00
Material: Silty sand
Factor of Safety
1.6
1.4
1.2
1.0
0.8
0.0
1.0
2.0
3.0
4.0
5.0
6.0
7.0
8.0
Tunnel Depth (m)
z_r:
2 m
4 m
6 m
Hooded shield
2 m
4 m
6 m
Standard shield

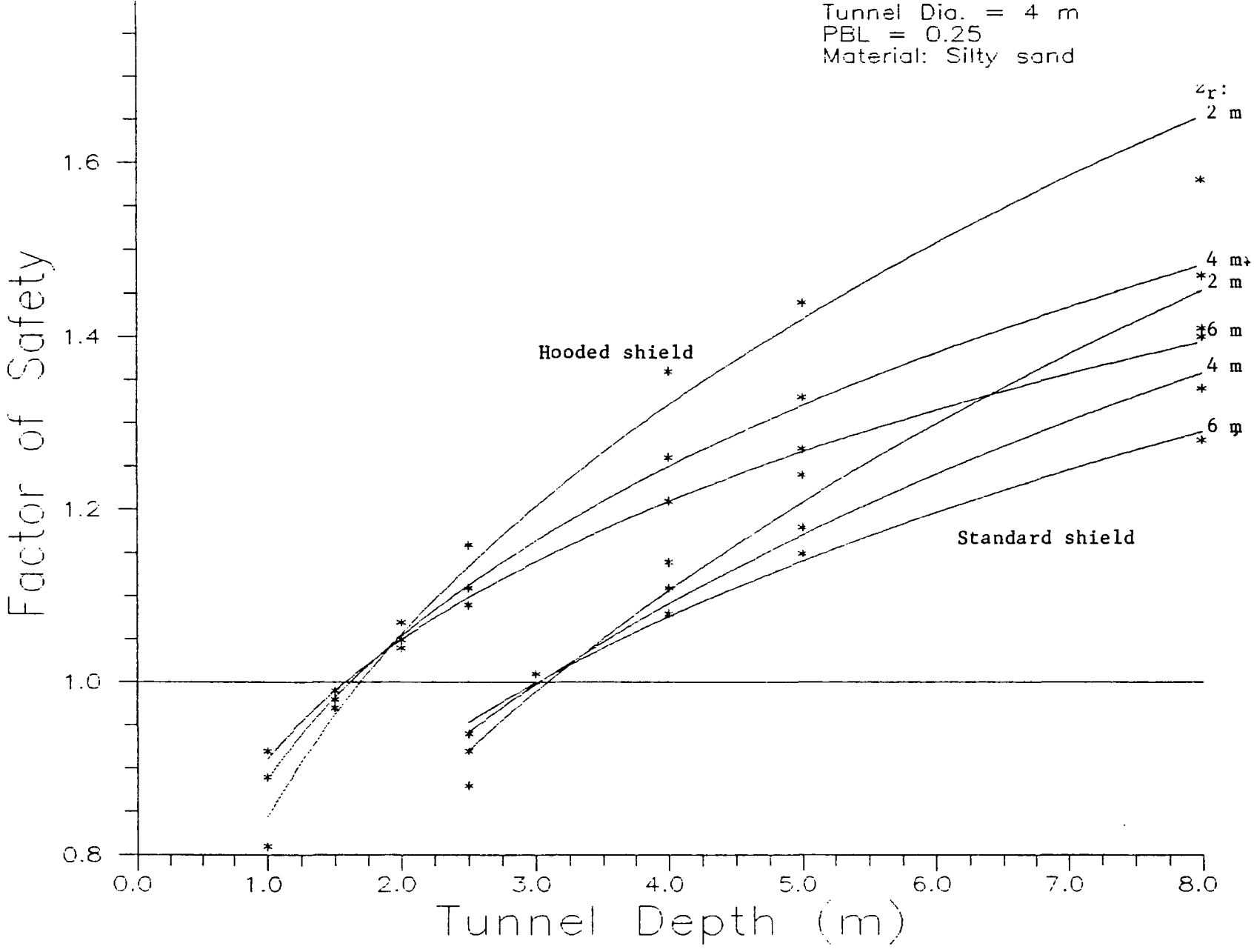
Tunnel Dia. = 4 m
PBL = 0.25
Material: Silty sand
z_r:
2 m
4 m
2 m
6 m
4 m
6 m
Hooded shield
Standard shield
Factor of Safety
Tunnel Depth (m)
0.8
1.0
1.2
1.4
1.6
0.0
1.0
2.0
3.0
4.0
5.0
6.0
7.0
8.0

c40

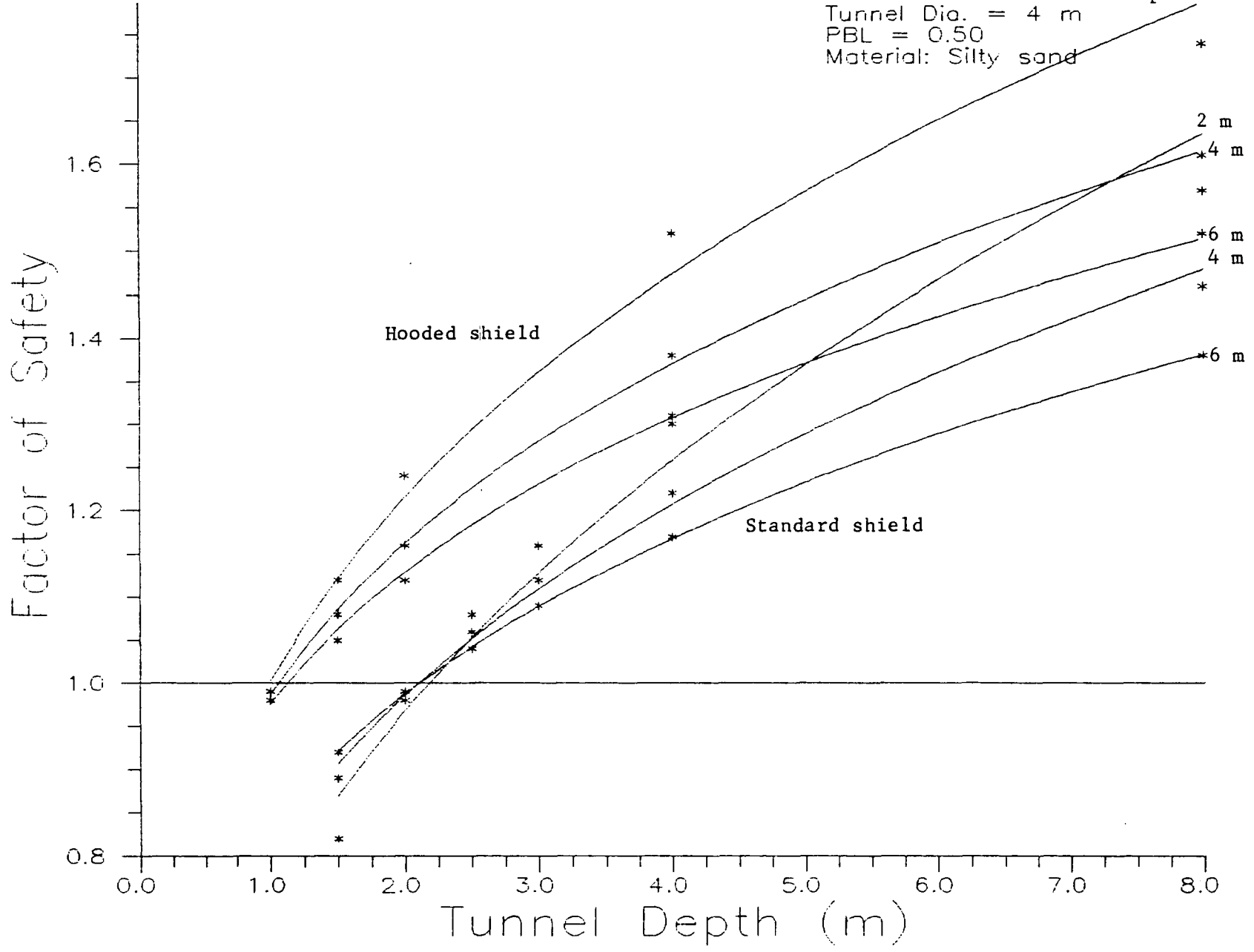
Tunnel Dia. = 4 m
PBL = 0.50
Material: Silty sand
2 m
4 m
6 m
4 m
6 m
Hooded shield
Standard shield
Factor of Safety
Tunnel Depth (m)
0.8
1.0
1.2
1.4
1.6
0.0
1.0
2.0
3.0
4.0
5.0
6.0
7.0
8.0

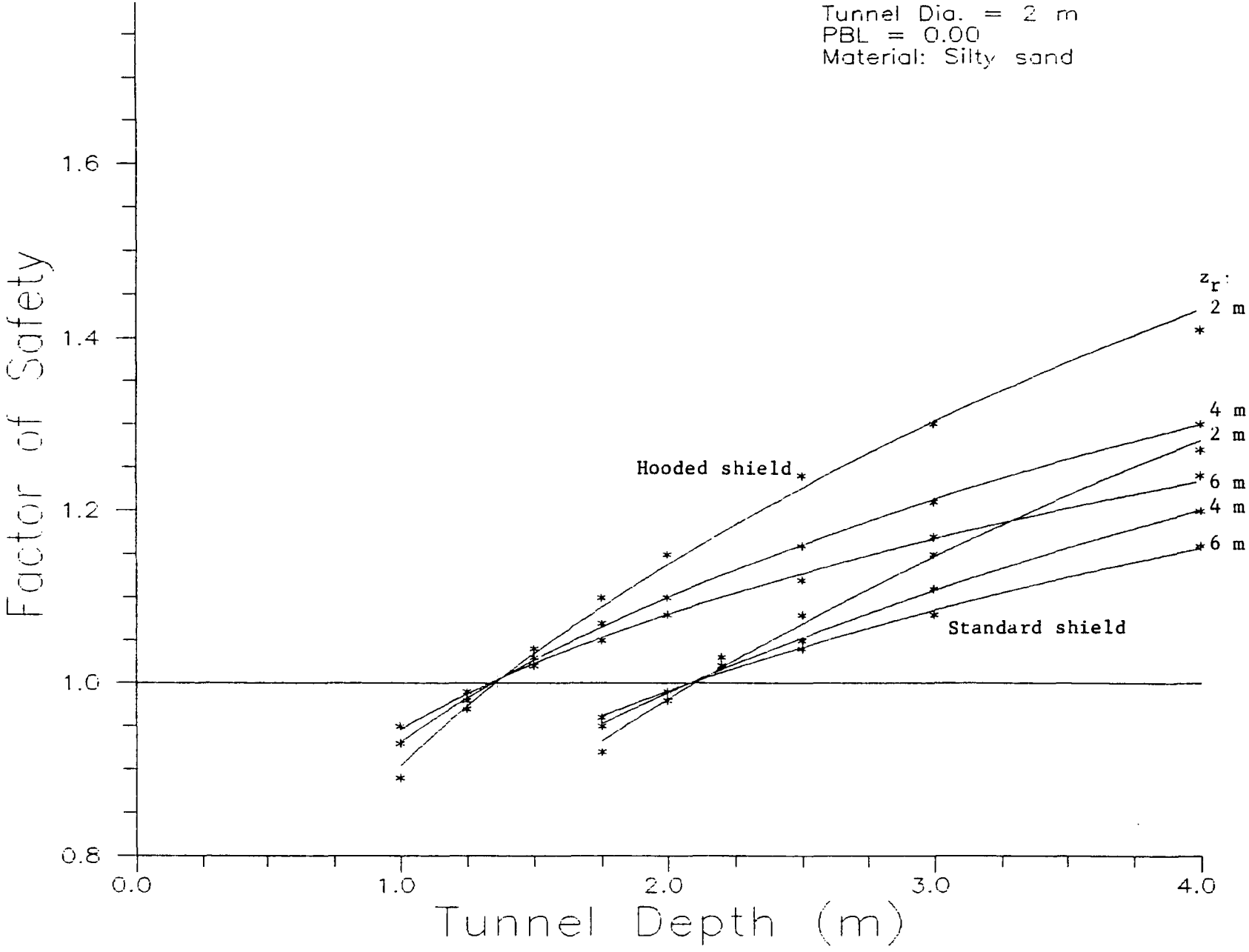
Tunnel Dia. = 2 m
PBL = 0.00
Material: Silty sand
Factor of Safety
1.6
1.4
1.2
1.0
0.8
0.0
1.0
2.0
3.0
4.0
Tunnel Depth (m)
z_r:
2 m
4 m
2 m
6 m
4 m
6 m
Hooded shield
Standard shield

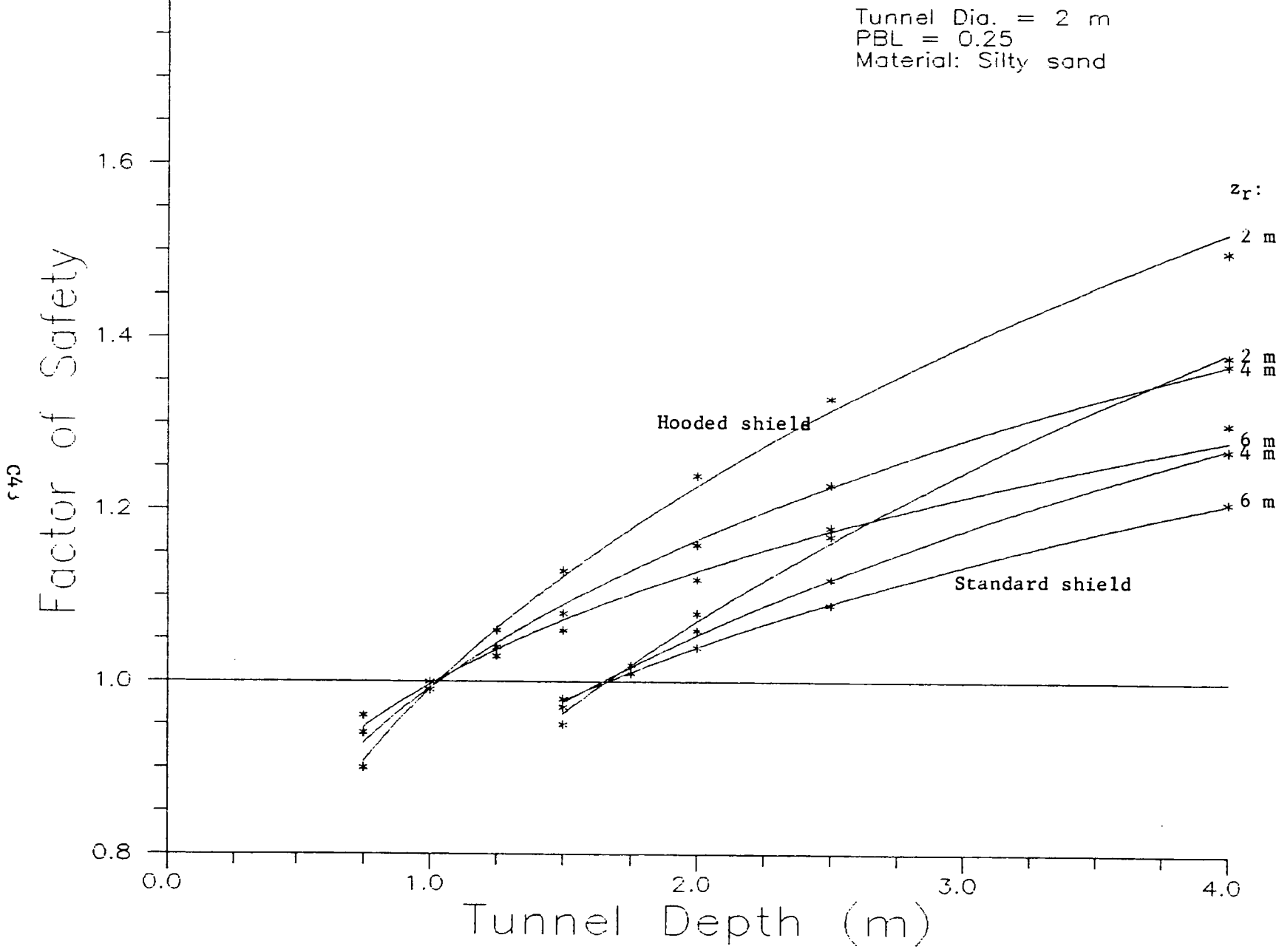
Tunnel Dia. = 2 m
PBL = 0.25
Material: Silty sand
z_r:
2 m
2 m
4 m
6 m
4 m
6 m
Hooded shield
Standard shield
Factor of Safety
$C_{4,5}$
1.6
1.4
1.2
1.0
0.8
0.0
1.0
2.0
3.0
4.0
Tunnel Depth (m)

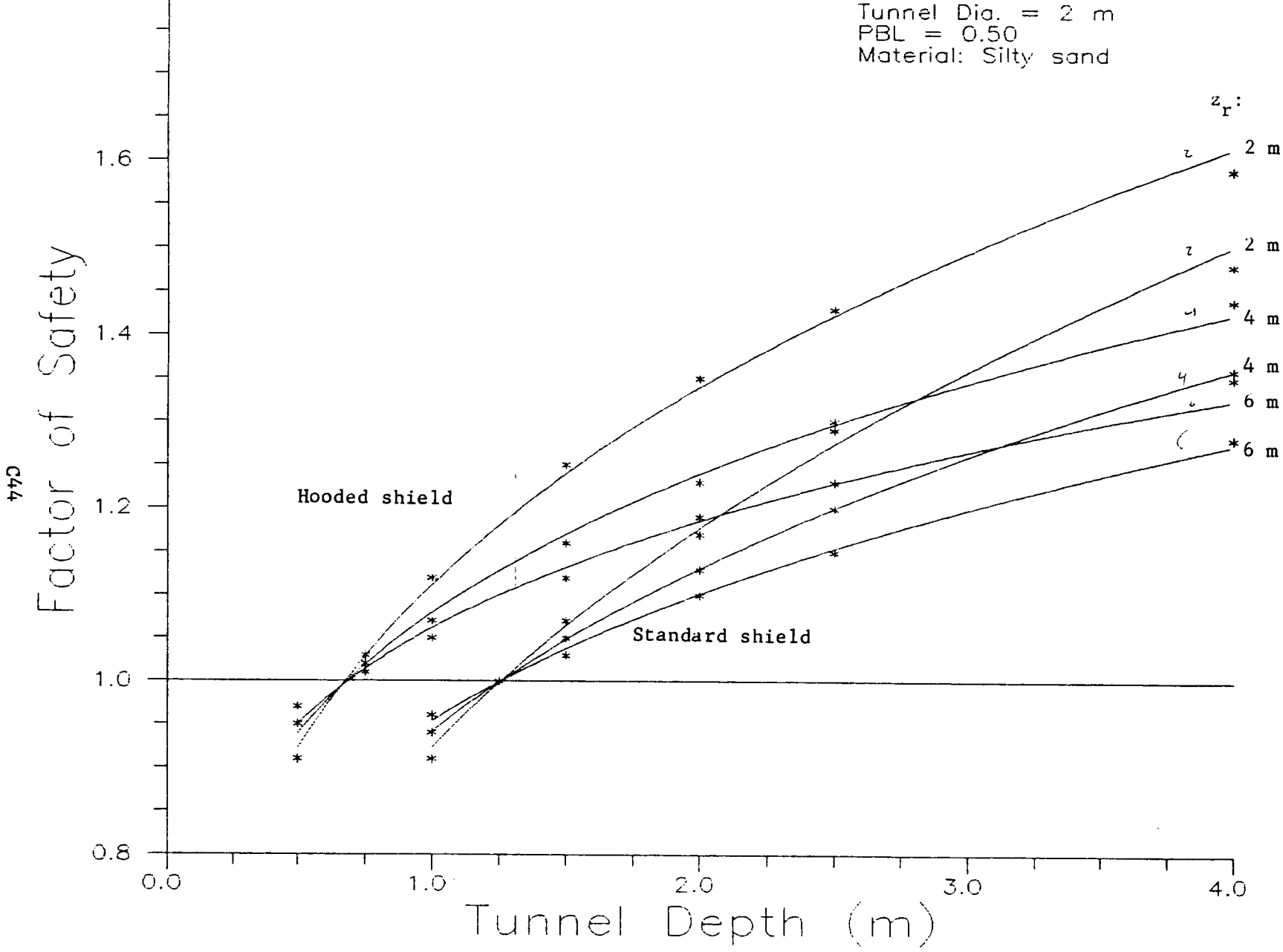
Tunnel Dia. = 2 m
PBL = 0.50
Material: Silty sand
z_r:
2 m
2 m
4 m
4 m
6 m
6 m
Hooded shield
Standard shield
Factor of Safety
C44
1.6
1.4
1.2
1.0
0.8
0.0
1.0
2.0
3.0
4.0
Tunnel Depth (m)

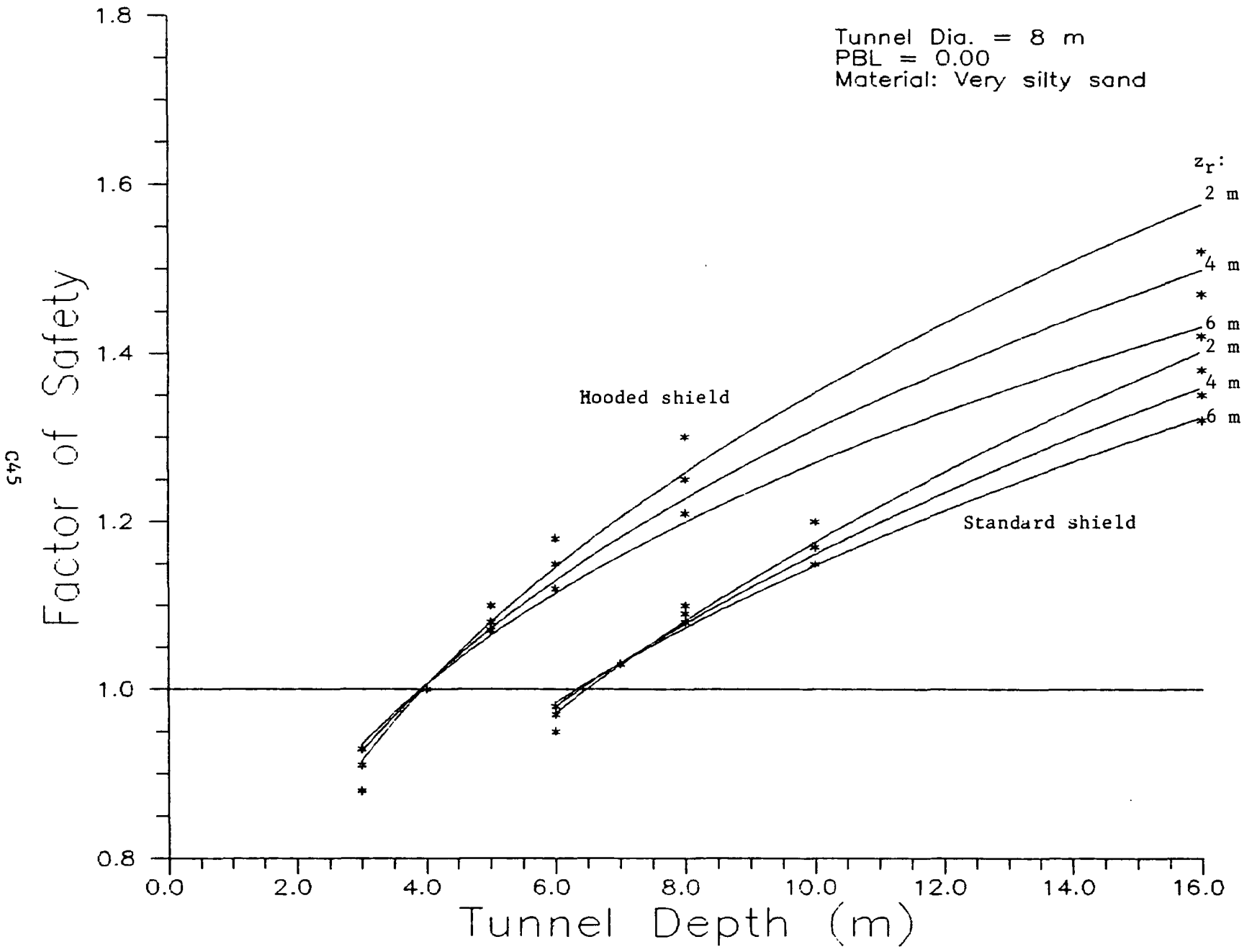
Tunnel Dia. = 8 m
PBL = 0.00
Material: Very silty sand
z_r:
2 m
4 m
6 m
2 m
4 m
6 m
Hooded shield
Standard shield
Factor of Safety
Tunnel Depth (m)
1.8
1.6
1.4
1.2
1.0
0.8
0.0
2.0
4.0
6.0
8.0
10.0
12.0
14.0
16.0

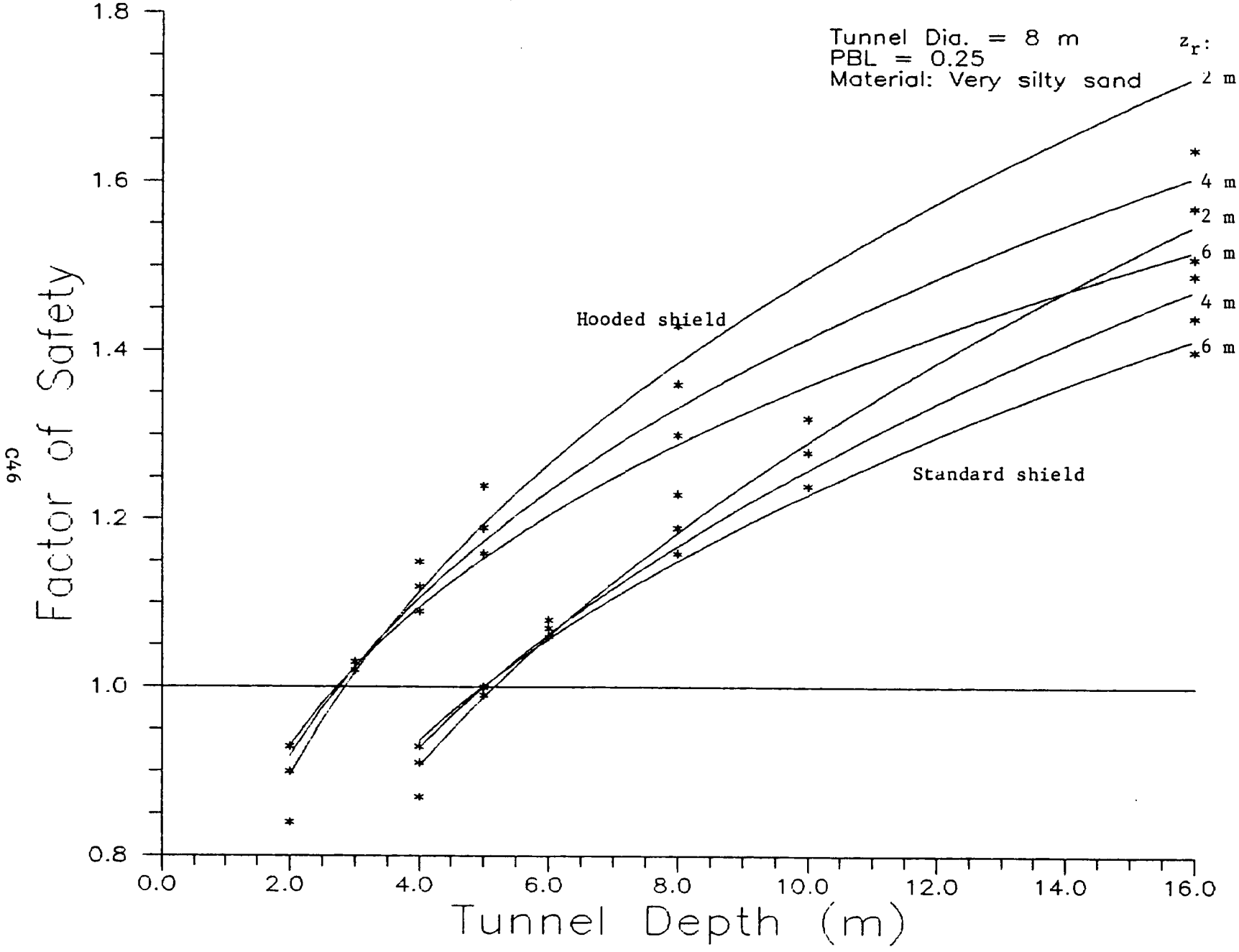
Tunnel Dia. = 8 m
PBL = 0.25
Material: Very silty sand
z_r:
2 m
4 m
2 m
6 m
4 m
6 m
Hooded shield
Standard shield
Factor of Safety
Tunnel Depth (m)
1.8
1.6
1.4
1.2
1.0
0.8
0.0
2.0
4.0
6.0
8.0
10.0
12.0
14.0
16.0

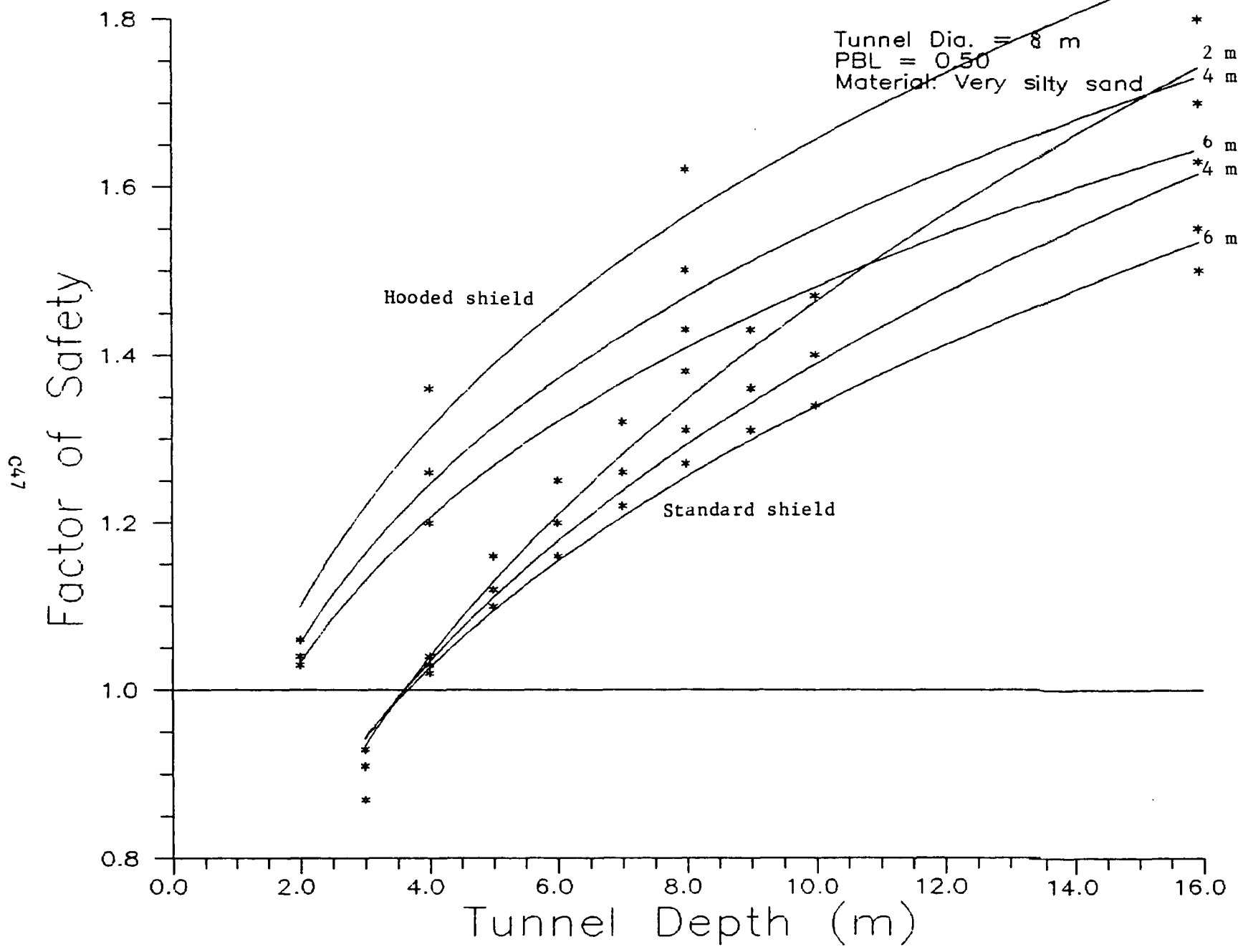
Tunnel Dia. = 8 m
PBL = 0.50
Material: Very silty sand
2 m
4 m
6 m
4 m
6 m
Hooded shield
Standard shield
Factor of Safety
Tunnel Depth (m)
1.8
1.6
1.4
1.2
1.0
0.8
0.0
2.0
4.0
6.0
8.0
10.0
12.0
14.0
16.0

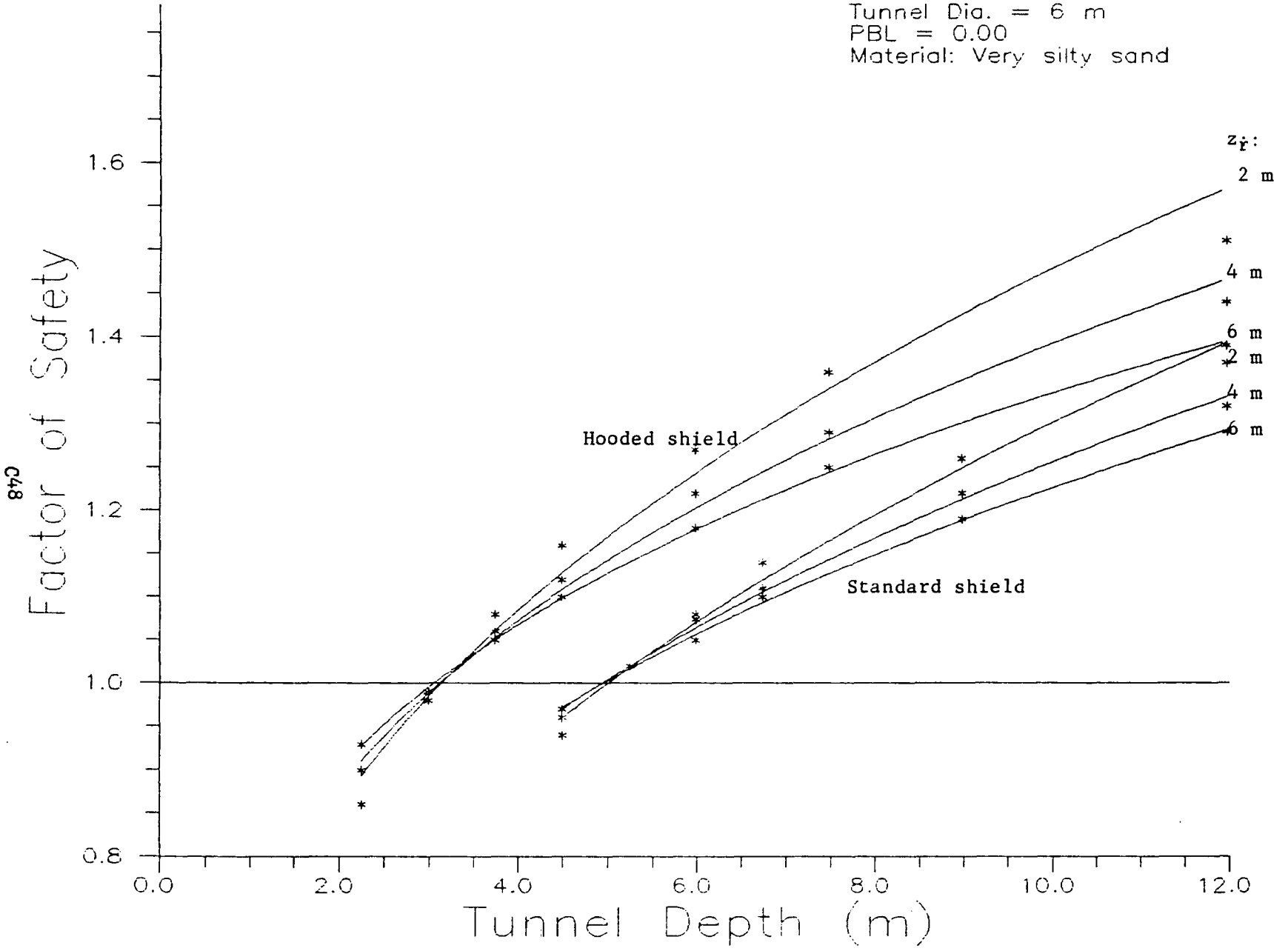
Tunnel Dia. = 6 m
PBL = 0.00
Material: Very silty sand
z_r:
2 m
4 m
6 m
2 m
4 m
6 m
Hooded shield
Standard shield
Factor of Safety
1.6
1.4
1.2
1.0
0.8
0.0
2.0
4.0
6.0
8.0
10.0
12.0
Tunnel Depth (m)

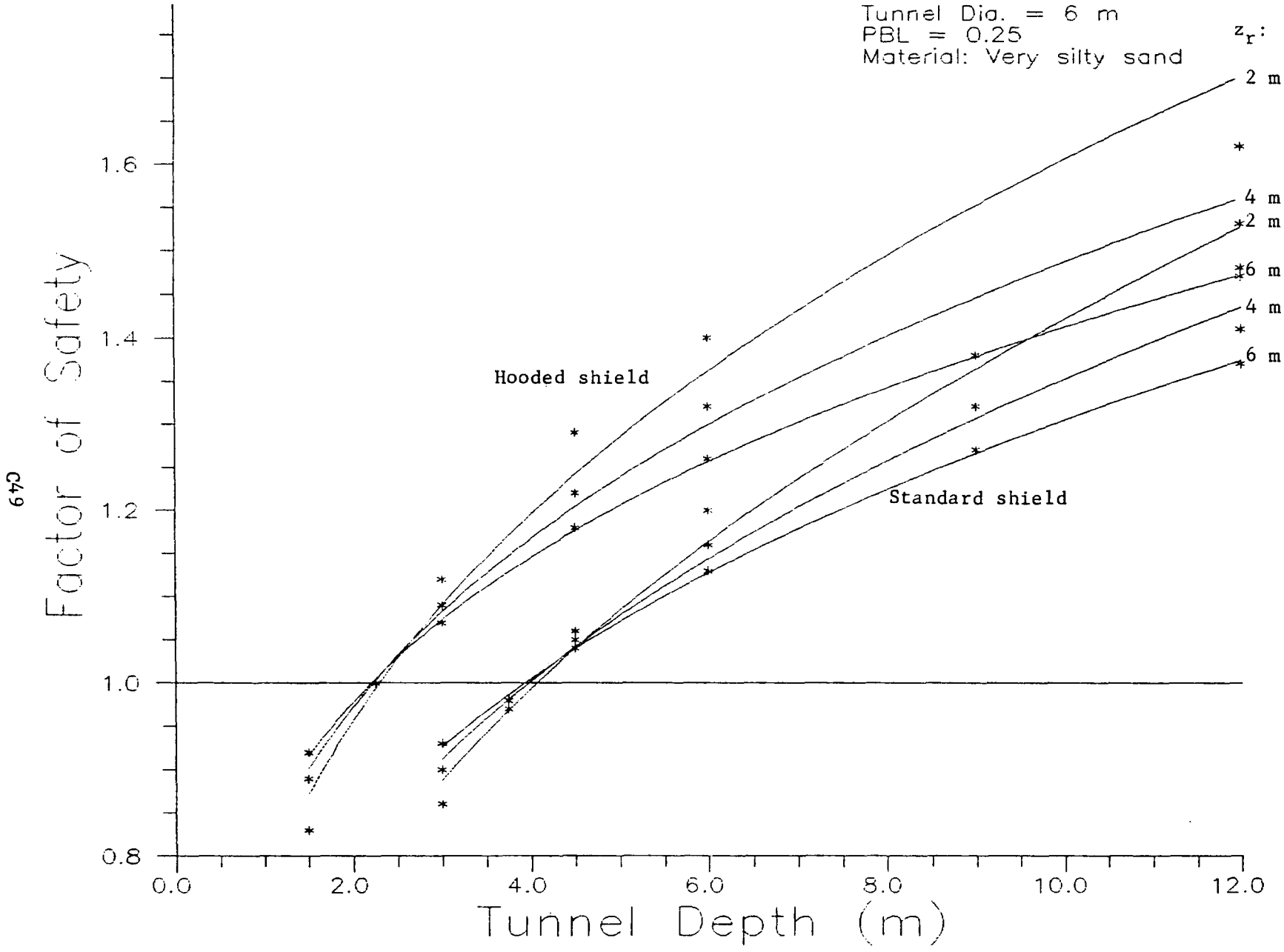
Tunnel Dia. = 6 m
PBL = 0.25
Material: Very silty sand
z_r:
2 m
4 m
2 m
6 m
4 m
6 m
Hooded shield
Standard shield
Factor of Safety
1.6
1.4
1.2
1.0
0.8
0.0
2.0
4.0
6.0
8.0
10.0
12.0
Tunnel Depth (m)

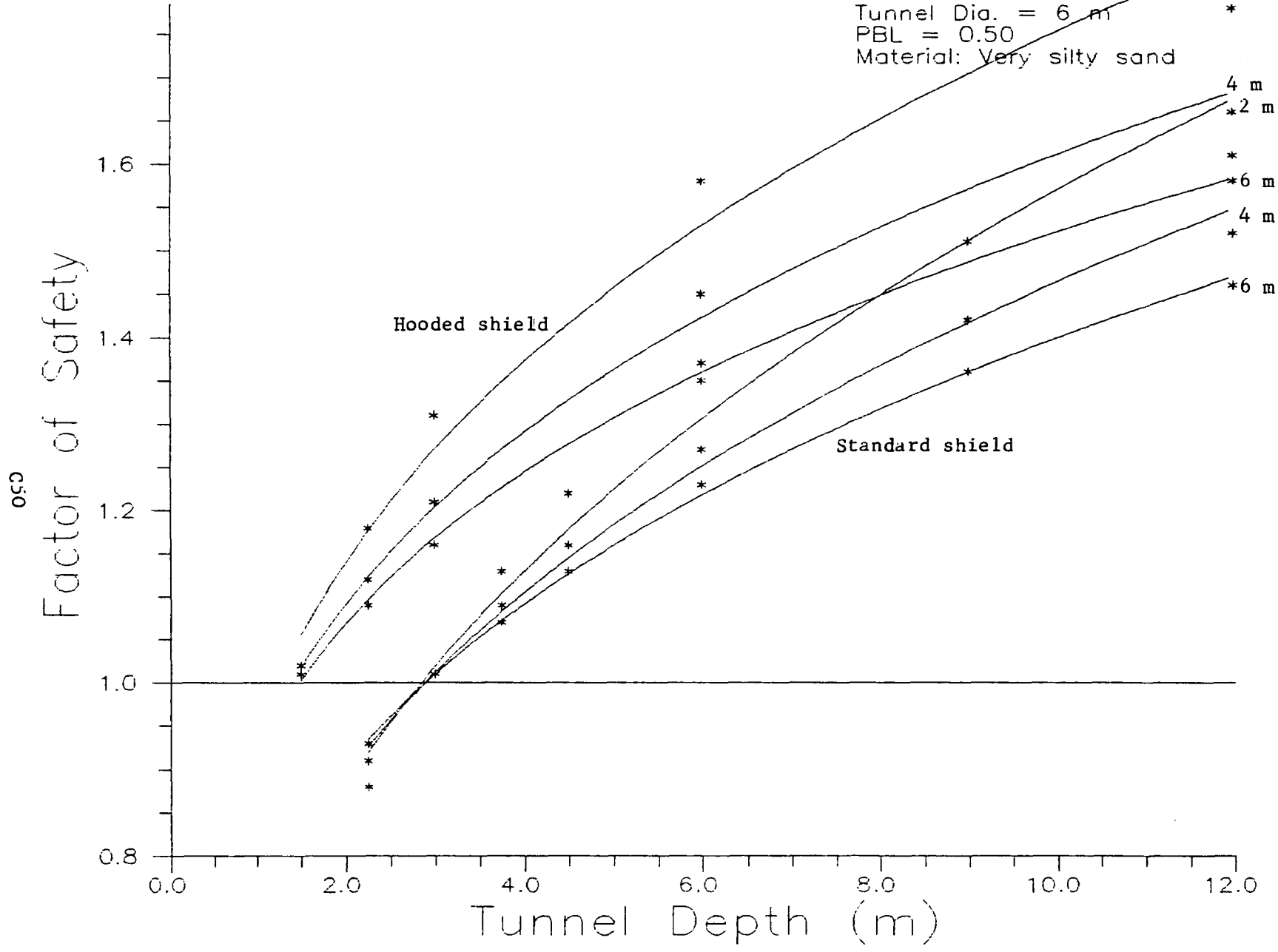
Tunnel Dia. = 6 m
PBL = 0.50
Material: Very silty sand
4 m
2 m
6 m
4 m
6 m
Hooded shield
Standard shield
Factor of Safety
c50
1.6
1.4
1.2
1.0
0.8
0.0
2.0
4.0
6.0
8.0
10.0
12.0
Tunnel Depth (m)

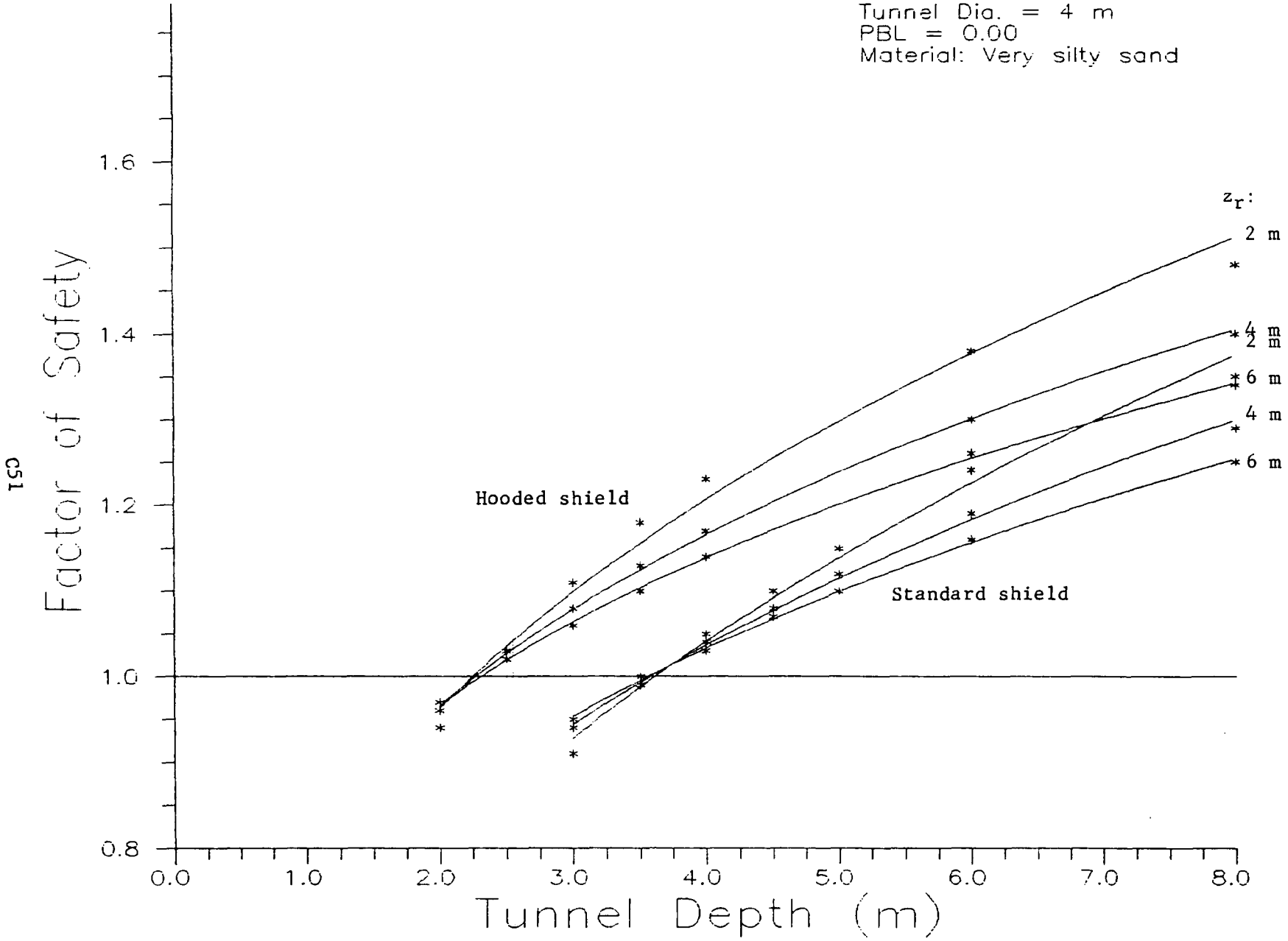
Tunnel Dia. = 4 m
PBL = 0.00
Material: Very silty sand
Factor of Safety
1.6
1.4
1.2
1.0
0.8
0.0
1.0
2.0
3.0
4.0
5.0
6.0
7.0
8.0
Tunnel Depth (m)
z_r:
2 m
4 m
2 m
6 m
4 m
6 m
Hooded shield
Standard shield

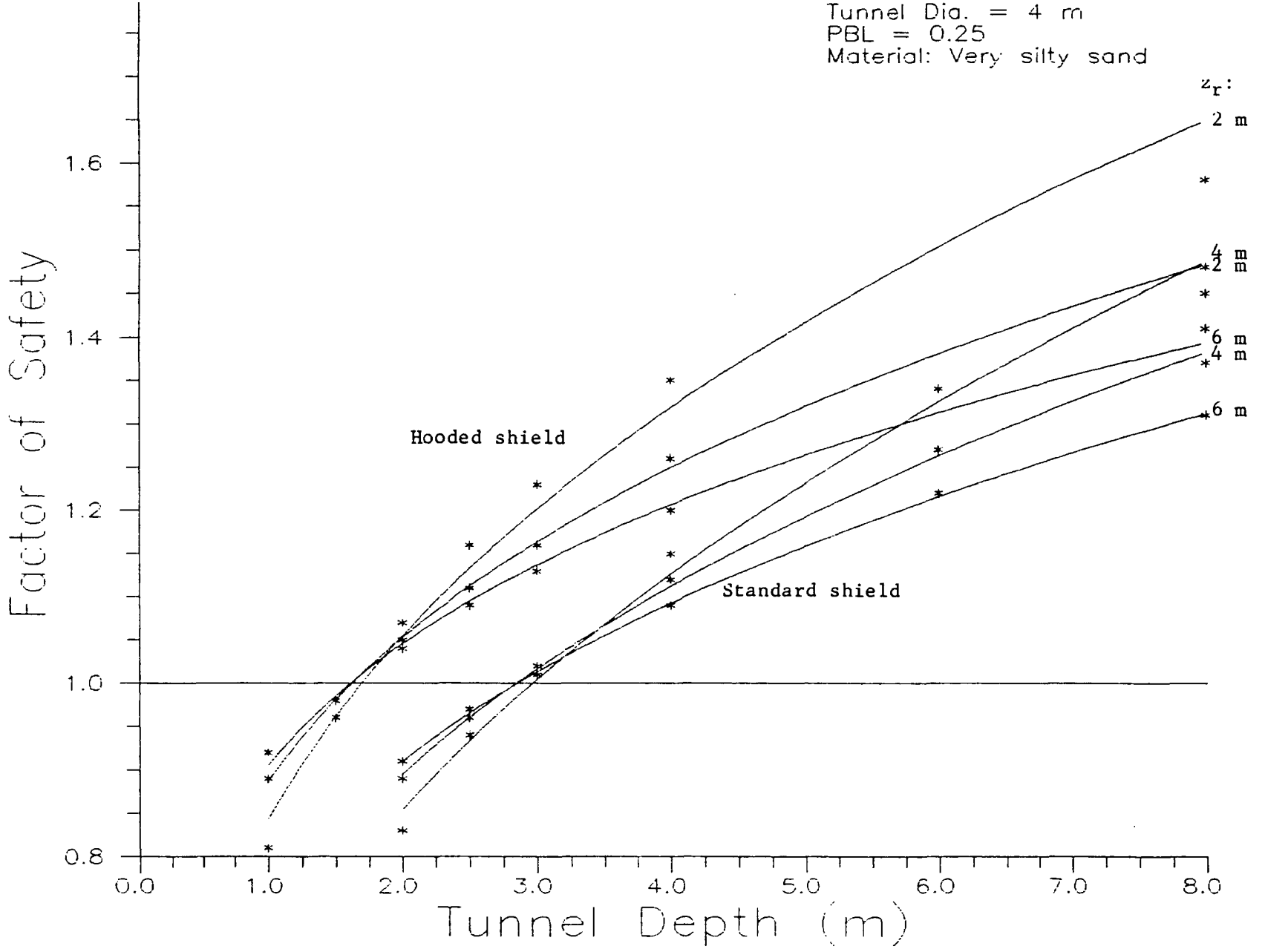
Tunnel Dia. = 4 m
PBL = 0.25
Material: Very silty sand
z_r:
2 m
4 m
2 m
6 m
4 m
6 m
Hooded shield
Standard shield
Factor of Safety
1.6
1.4
1.2
1.0
0.8
0.0
1.0
2.0
3.0
4.0
5.0
6.0
7.0
8.0
Tunnel Depth (m)

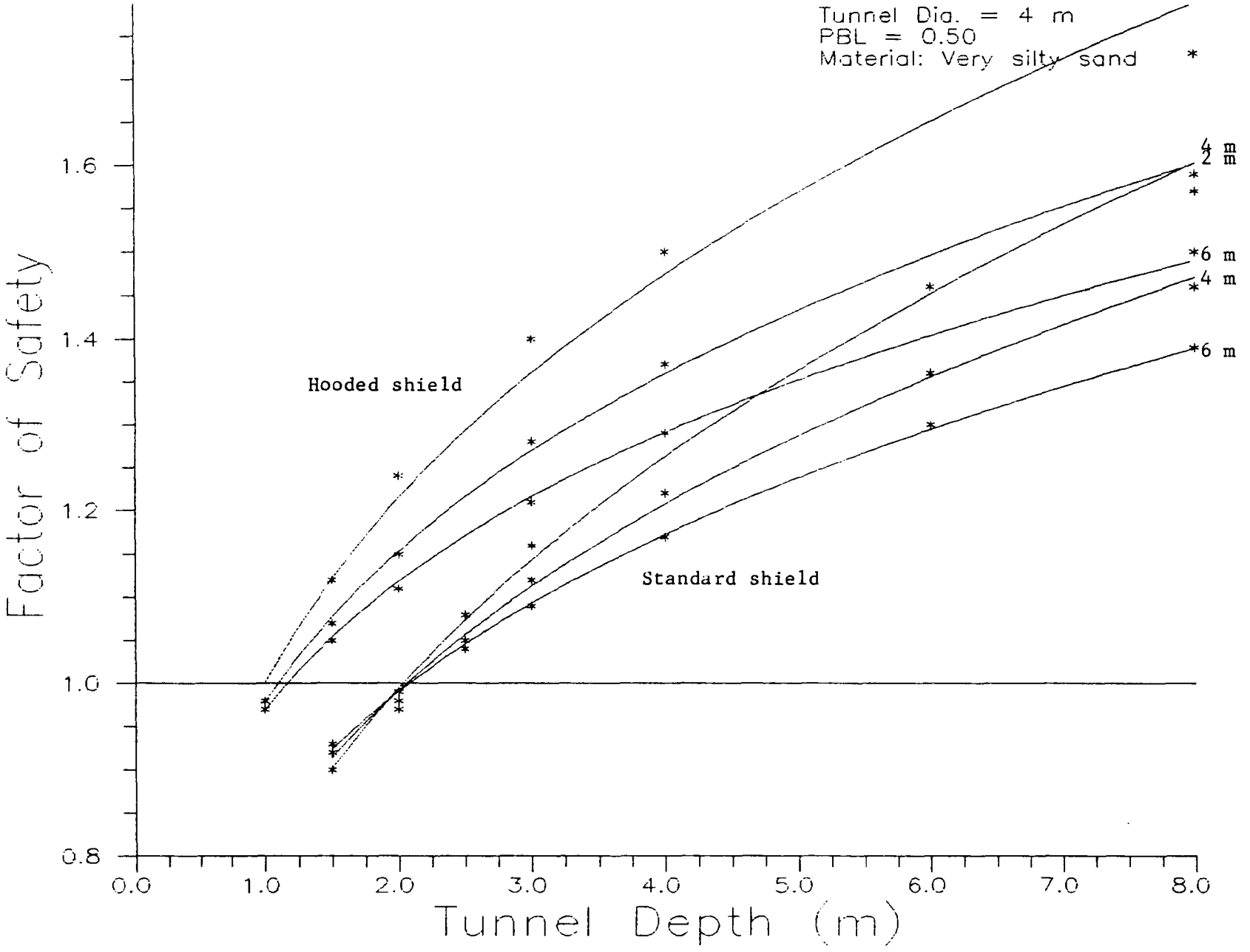
Tunnel Dia. = 4 m
PBL = 0.50
Material: Very silty sand
4 m
2 m
6 m
4 m
6 m
Hooded shield
Standard shield
Factor of Safety
1.6
1.4
1.2
1.0
0.8
0.0
1.0
2.0
3.0
4.0
5.0
6.0
7.0
8.0
Tunnel Depth (m)

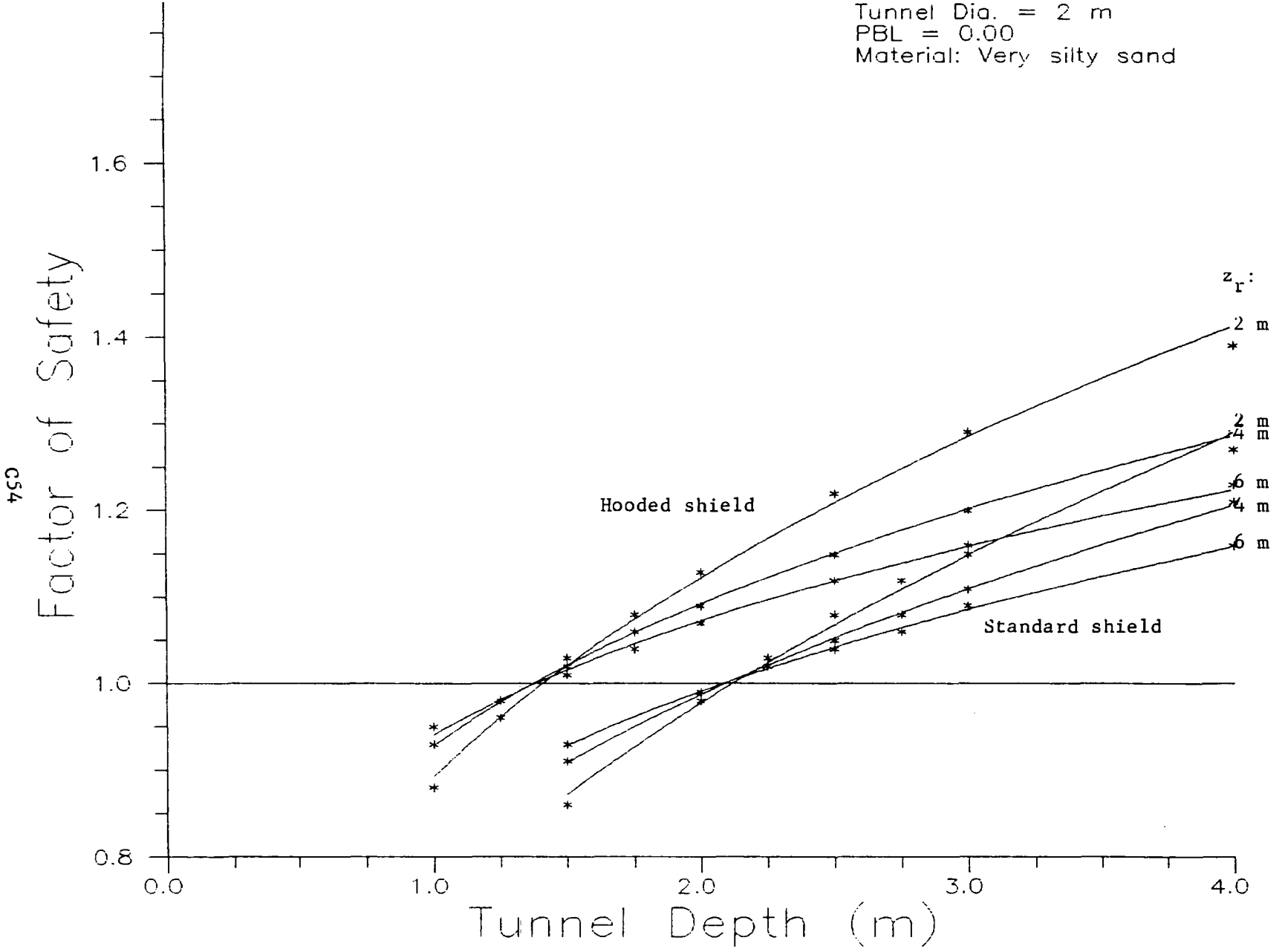
Tunnel Dia. = 2 m
PBL = 0.00
Material: Very silty sand
Factor of Safety
1.6
1.4
1.2
1.0
0.8
0.0
1.0
2.0
3.0
4.0
Tunnel Depth (m)
z_r:
2 m
2 m
4 m
6 m
4 m
6 m
Hooded shield
Standard shield

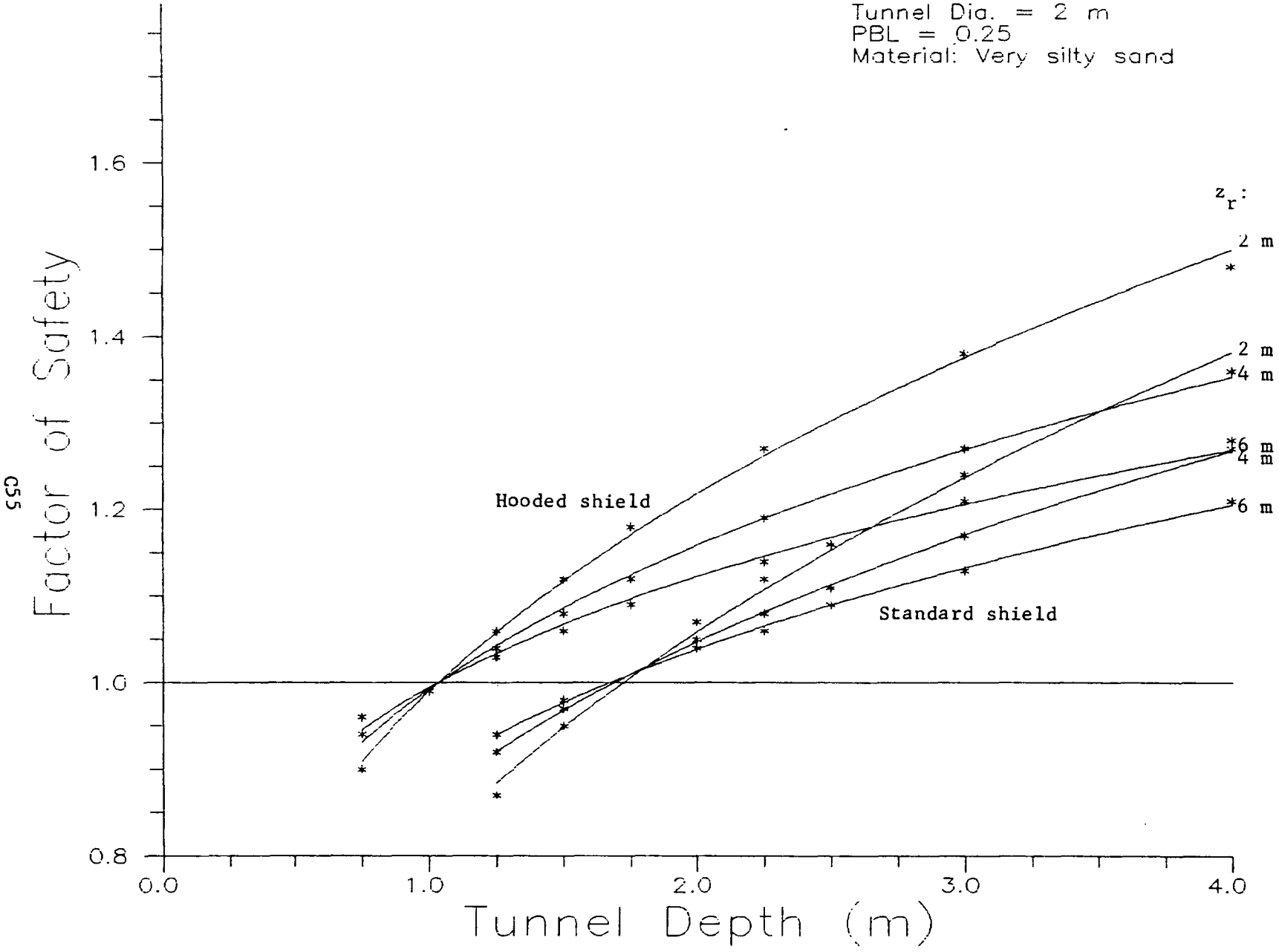
Tunnel Dia. = 2 m
PBL = 0.25
Material: Very silty sand
z_r:
2 m
2 m
4 m
6 m
4 m
6 m
Hooded shield
Standard shield
Factor of Safety
CSS
1.6
1.4
1.2
1.0
0.8
0.0
1.0
2.0
3.0
4.0
Tunnel Depth (m)

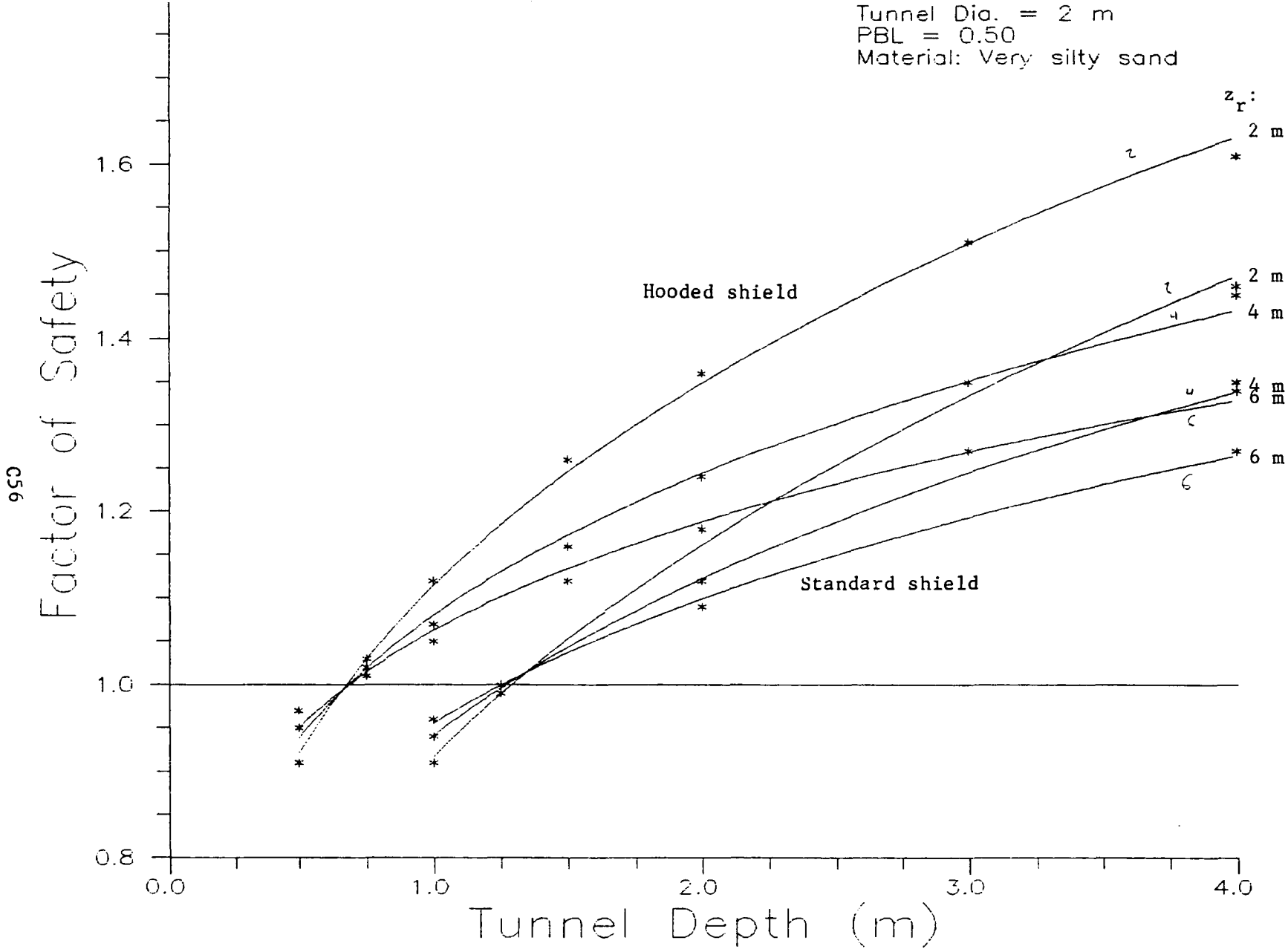
Tunnel Dia. = 2 m
PBL = 0.50
Material: Very silty sand
z_r:
2 m
2 m
4 m
4 m
6 m
6 m
Hooded shield
Standard shield
Factor of Safety
Tunnel Depth (m)
0.8
1.0
1.2
1.4
1.6
0.0
1.0
2.0
3.0
4.0

Appendix D

Critical depth results

Critical Depths (F.O.S. = 1.0)

Standard Shield

Clean Sand

Dia (m)	PBL	Zr=2	Zr=4	Zr=6	Avg
8.0	0.0	10.00	10.00	10.00	10.00
	0.25	7.50	7.33	7.33	7.39
	0.50	5.17	5.20	5.00	5.12
6.0	0.0	7.75	7.50	7.50	7.58
	0.25	5.81	5.75	5.75	5.77
	0.50	4.00	4.05	4.00	4.02
4.0	0.0	5.33	5.25	5.25	5.28
	0.25	4.13	4.00	4.00	4.04
	0.50	2.83	2.83	2.83	2.83
2.0	0.0	3.00	3.00	3.00	3.00
	0.25	2.25	2.25	2.25	2.25
	0.50	1.50	1.50	1.50	1.50

Slightly silty sand

Dia (m)	PBL	Zr=2	Zr=4	Zr=6	Avg
8.0	0.0	9.33	9.33	9.00	9.22
	0.25	6.86	6.80	6.75	6.80
	0.50	4.78	4.83	4.80	4.80
6.0	0.0	7.13	7.00	7.00	7.04
	0.25	5.40	5.25	5.25	5.30
	0.50	3.75	3.75	3.75	3.75
4.0	0.0	4.88	4.83	4.75	4.82
	0.25	3.80	3.75	3.75	3.77
	0.50	2.83	2.75	2.83	2.80
2.0	0.0	2.75	2.75	2.75	2.75
	0.25	2.13	2.13	2.13	2.13
	0.50	1.50	1.50	1.50	1.50

Silty sand

Dia (m)	PBL	Zr=2	Zr=4	Zr=6	Avg
8.0	0.0	7.17	7.00	7.00	7.06
	0.25	5.44	5.43	5.40	5.42
	0.50	3.82	3.82	3.75	3.80
6.0	0.0	5.44	5.40	5.44	5.43
	0.25	4.25	4.38	4.31	4.31
	0.50	2.96	2.93	2.91	2.93
4.0	0.0	3.75	3.75	3.75	3.75
	0.25	2.96	2.86	2.93	2.92
	0.50	2.10	2.07	2.10	2.09
2.0	0.0	2.10	2.08	2.08	2.09
	0.25	1.68	1.65	1.67	1.67
	0.50	1.25	1.25	1.25	1.25

Very silty sand

Dia (m)	PBL	Zr=2	Zr=4	Zr=6	Avg
8.0	0.0	6.63	6.50	6.40	6.51
	0.25	5.11	5.00	5.00	5.04
	0.50	3.76	3.75	3.78	3.76
6.0	0.0	5.00	5.00	4.95	4.98
	0.25	4.08	3.96	4.00	4.01
	0.50	2.94	2.93	2.91	2.93
4.0	0.0	3.63	3.60	3.50	3.58
	0.25	2.88	2.88	2.88	2.88
	0.50	2.17	2.14	2.10	2.14
2.0	0.0	2.10	2.08	2.08	2.09
	0.25	1.59	1.58	1.57	1.58
	0.50	1.27	1.25	1.25	1.26

All depths in metres

Critical Depths (F.O.S. = 1.0)

Hooded Shield

Clean Sand

Dia (m)	PBL	Zr=2	Zr=4	Zr=6	Avg
8.0	0.0	6.20	6.00	6.00	6.07
	0.25	4.29	4.20	4.25	4.25
	0.50	2.25	2.25	2.25	2.25
6.0	0.0	4.80	4.75	4.75	4.77
	0.25	3.32	3.30	3.25	3.29
	0.50	1.73	1.71	1.65	1.70
4.0	0.0	3.38	3.33	3.25	3.32
	0.25	2.33	2.25	2.33	2.30
	0.50	1.20	1.21	1.20	1.20
2.0	0.0	1.83	1.88	1.75	1.82
	0.25	1.25	1.25	1.25	1.25
	0.50	0.73	0.71	0.75	0.73

Slightly silty sand

Dia (m)	PBL	Zr=2	Zr=4	Zr=6	Avg
8.0	0.0	5.66	5.60	5.50	5.59
	0.25	3.89	3.83	3.80	3.84
	0.50	2.21	2.20	2.17	2.19
6.0	0.0	4.38	4.31	4.25	4.31
	0.25	3.00	3.00	3.00	3.00
	0.50	1.73	1.69	1.75	1.72
4.0	0.0	3.10	3.00	3.00	3.03
	0.25	2.14	2.13	2.17	2.15
	0.50	1.20	1.21	1.20	1.20
2.0	0.0	1.75	1.75	1.75	1.75
	0.25	1.25	1.25	1.25	1.25
	0.50	0.73	0.71	0.70	0.71

Silty sand

Dia (m)	PBL	Zr=2	Zr=4	Zr=6	Avg
8.0	0.0	4.22	4.14	4.17	4.18
	0.25	2.71	2.91	2.88	2.83
	0.50	****	****	****	****
6.0	0.0	3.30	3.25	3.15	3.23
	0.25	2.25	2.25	2.25	2.25
	0.50	****	****	****	****
4.0	0.0	2.33	2.30	2.50	2.38
	0.25	1.65	1.79	1.70	1.71
	0.50	1.07	1.06	1.08	1.07
2.0	0.0	1.36	1.35	1.33	1.35
	0.25	1.04	1.05	1.00	1.03
	0.50	0.69	0.68	0.69	0.69

Very silty sand

Dia (m)	PBL	Zr=2	Zr=4	Zr=6	Avg
8.0	0.0	4.00	4.00	4.00	4.00
	0.25	2.84	2.83	2.78	2.82
	0.50	****	****	****	****
6.0	0.0	3.15	3.19	3.13	3.16
	0.25	2.84	2.83	2.78	2.82
	0.50	****	****	****	****
4.0	0.0	2.33	2.22	2.25	2.27
	0.25	1.68	1.64	1.67	1.66
	0.50	1.10	1.11	1.14	1.12
2.0	0.0	1.39	1.38	1.42	1.40
	0.25	1.04	1.05	1.06	1.05
	0.50	0.69	0.68	0.69	0.69

All depths in metres

**** indicates blowout did not occur at depths greater than 0.25D

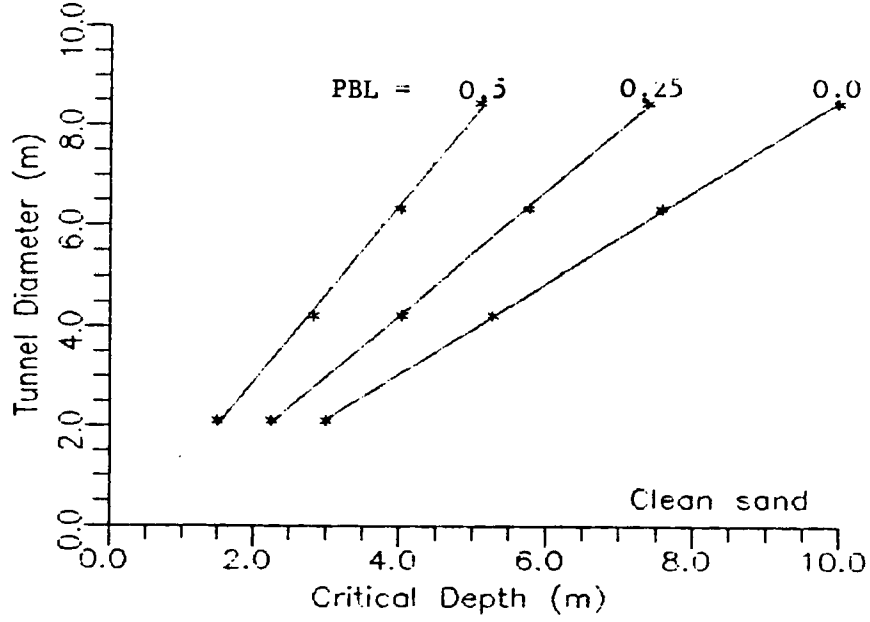

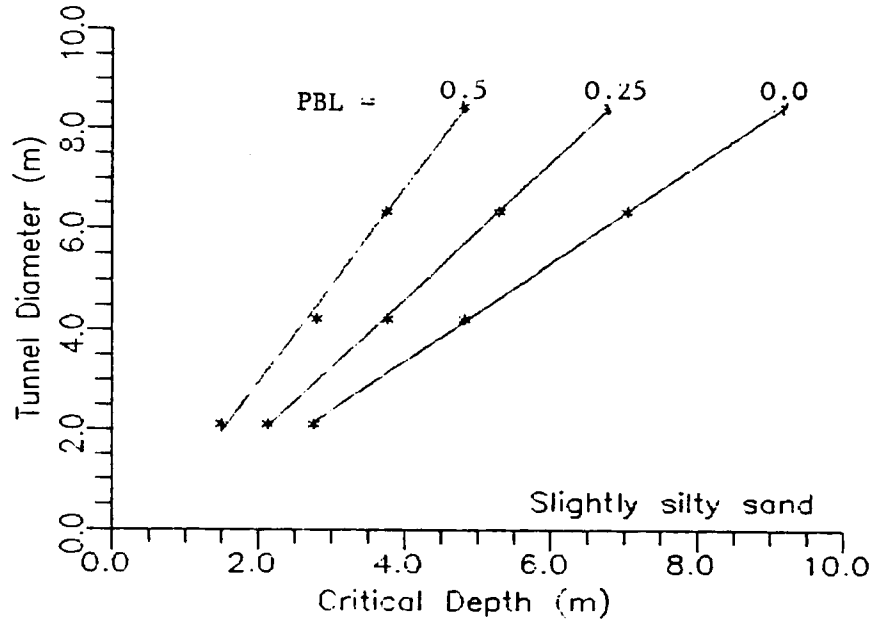

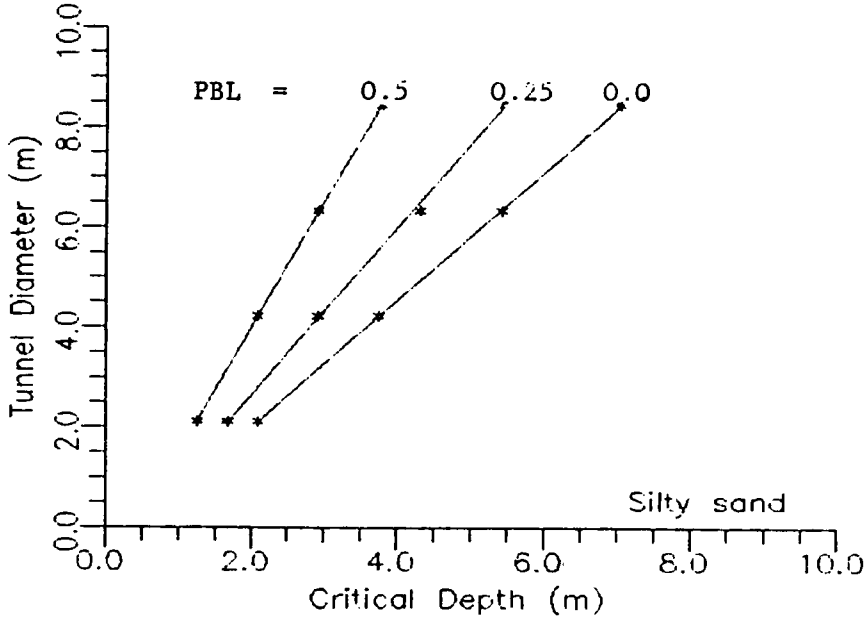

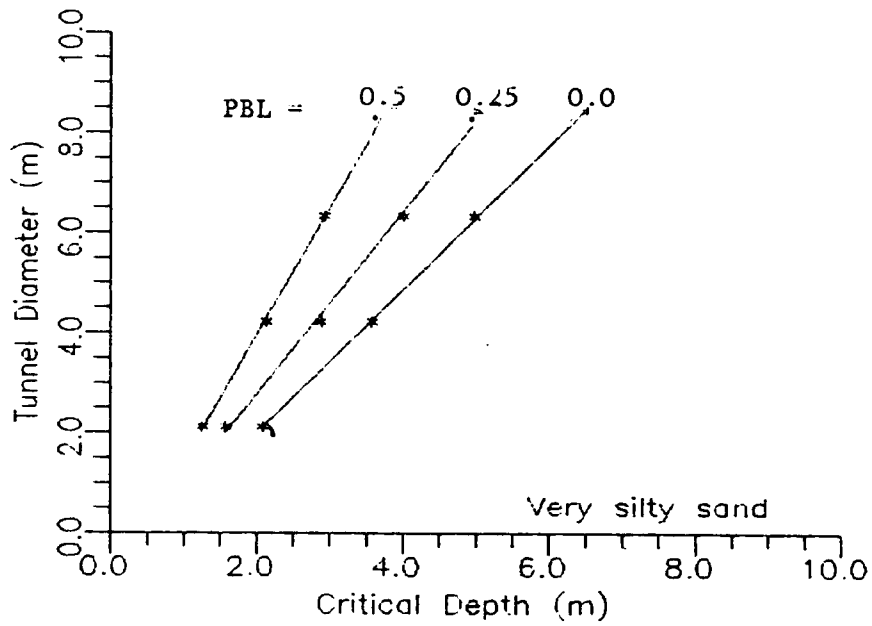

All plots standard shield

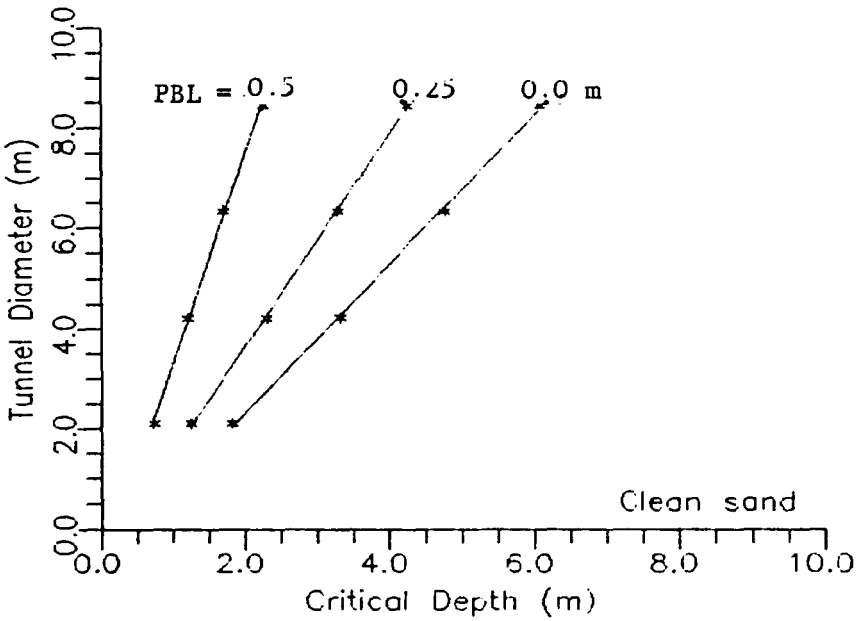

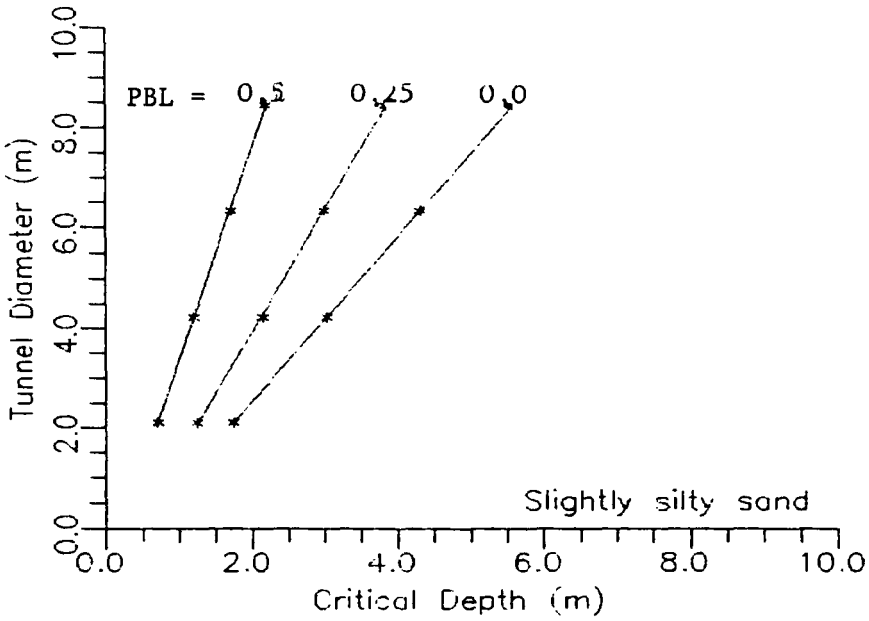

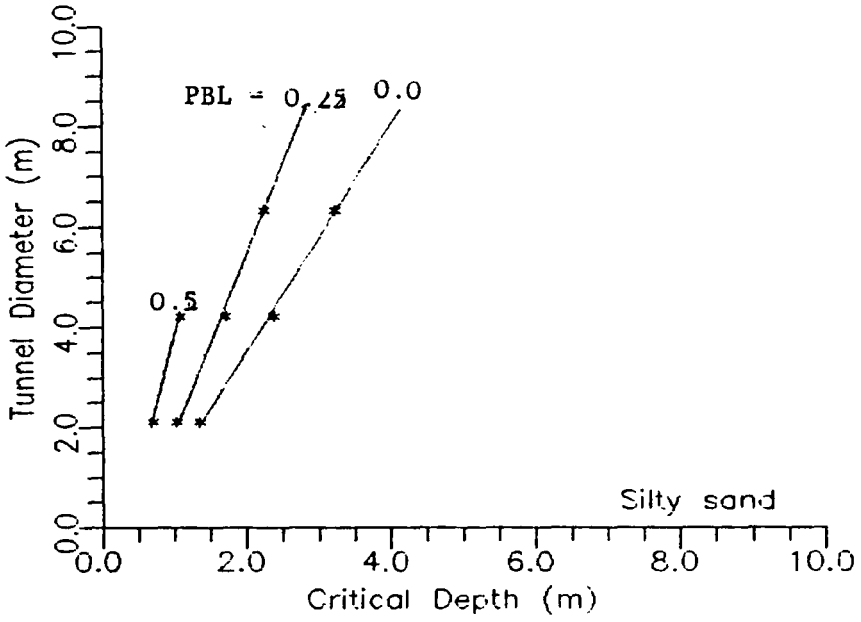

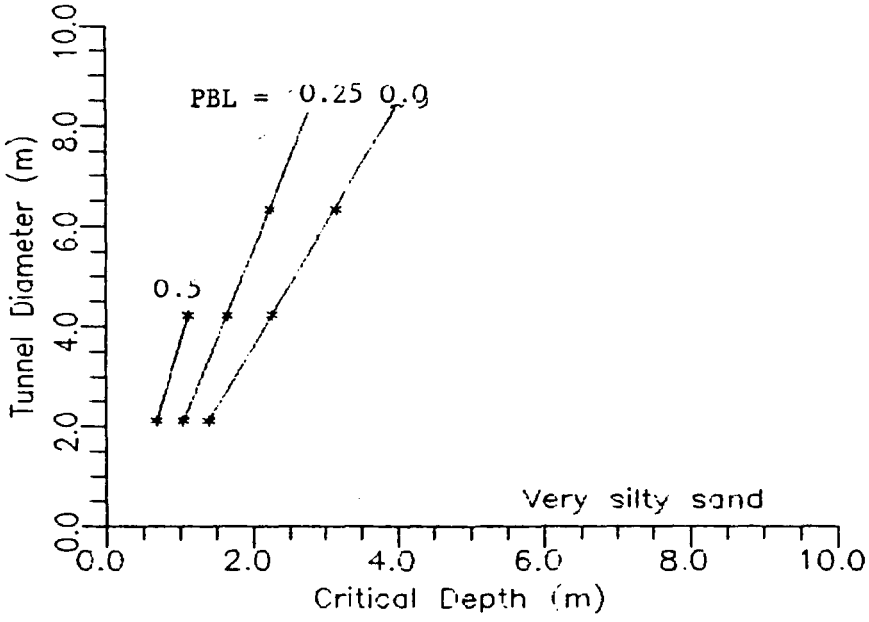

All plots hooded shield

All plots PBL=0.45

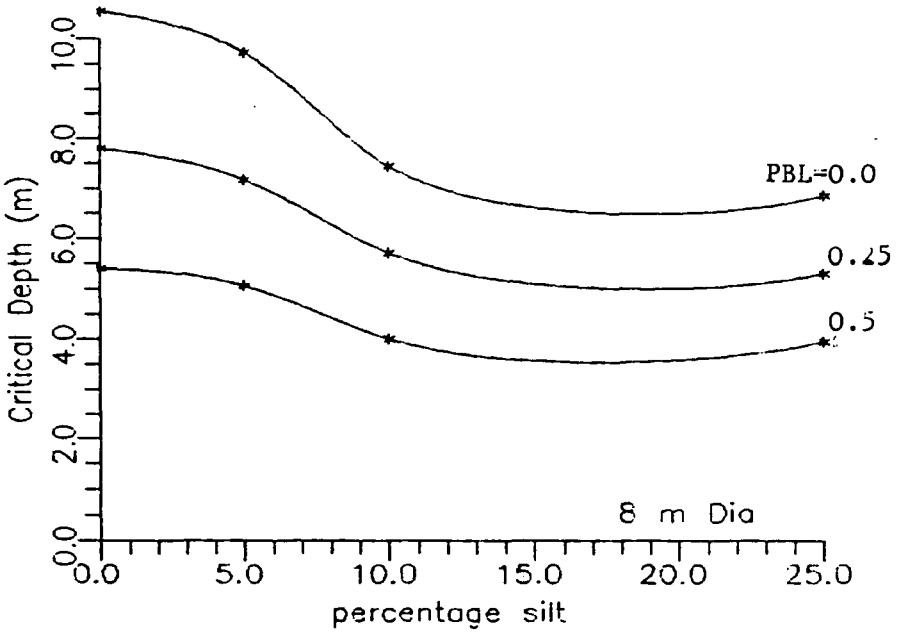
Critical Depth (m)
0.0
2.0
4.0
6.0
8.0
10.0
PBL=0.0
0.25
0.5
8 m Dia
0.0
5.0
10.0
15.0
20.0
25.0
percentage silt

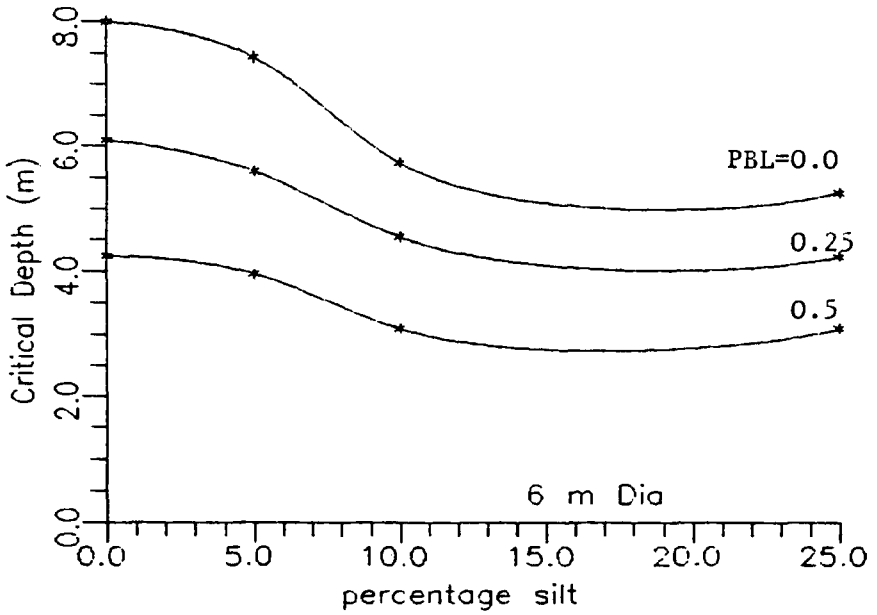
Critical Depth (m)
0.0
2.0
4.0
6.0
8.0
PBL=0.0
0.25
0.5
6 m Dia
0.0
5.0
10.0
15.0
20.0
25.0
percentage silt

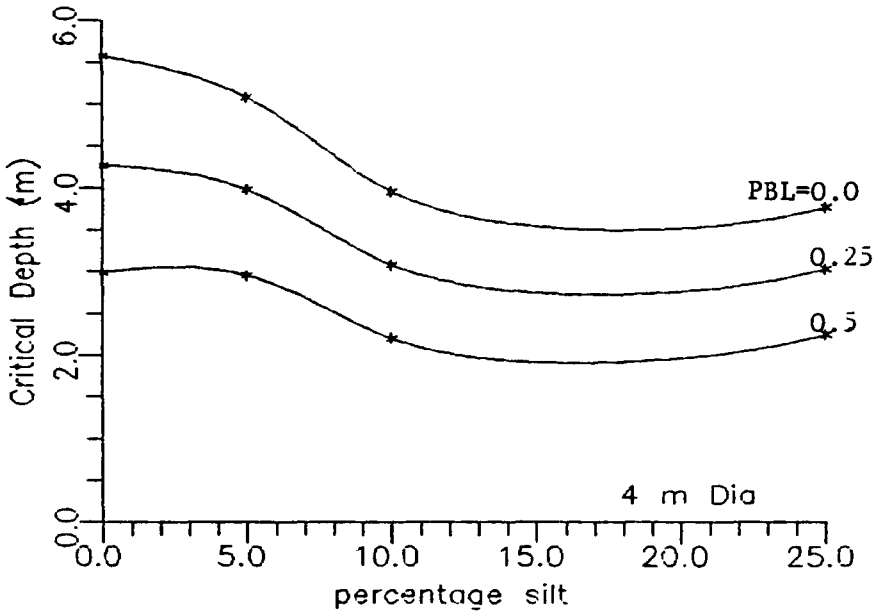
Critical Depth (m)
0.0
2.0
4.0
6.0
PBL=0.0
0.25
0.5
4 m Dia
0.0
5.0
10.0
15.0
20.0
25.0
percentage silt

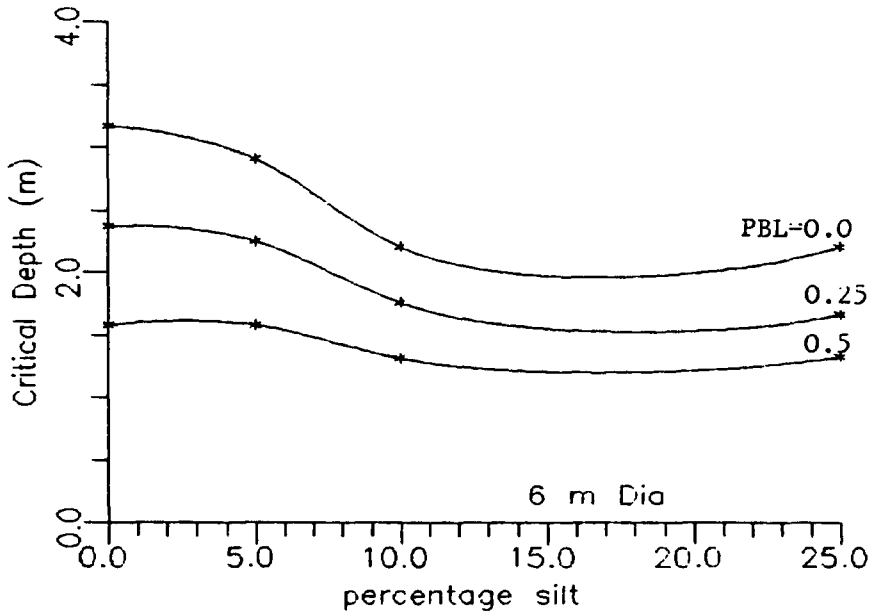
Critical Depth (m)
0.0
2.0
4.0
PBL=0.0
0.25
0.5
6 m Dia
0.0
5.0
10.0
15.0
20.0
25.0
percentage silt

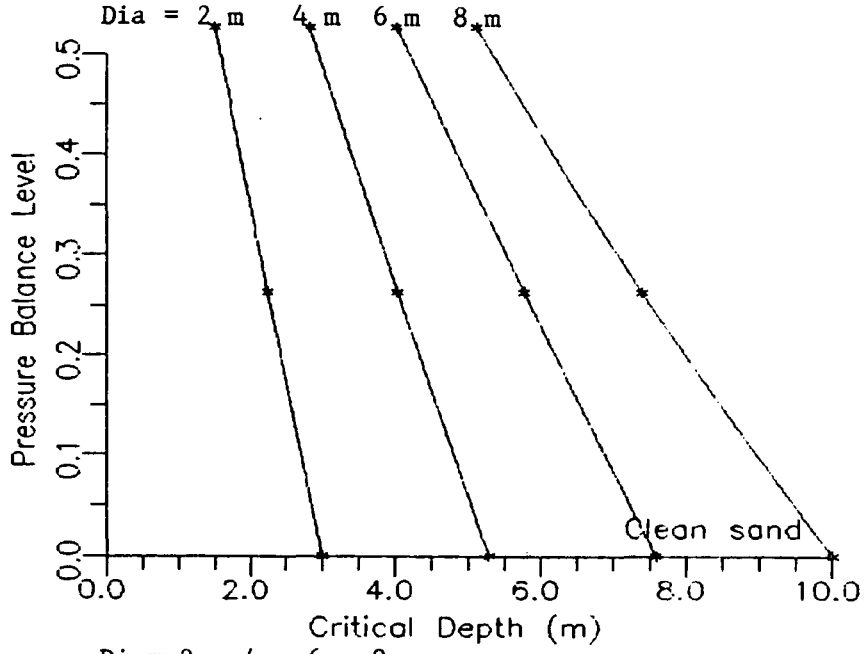
Dia = 2 m 4 m 6 m 8 m
Pressure Balance Level
0.0
0.1
0.2
0.3
0.4
0.5
0.0
2.0
4.0
6.0
8.0
10.0
Critical Depth (m)
Clean sand

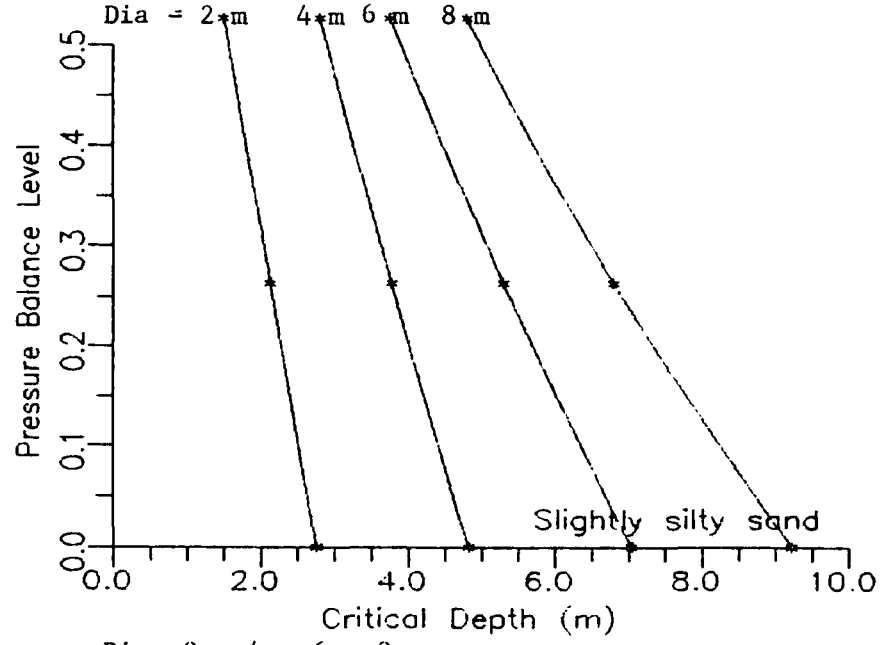
Dia = 2 m 4 m 6 m 8 m
Pressure Balance Level
0.0
0.1
0.2
0.3
0.4
0.5
0.0
2.0
4.0
6.0
8.0
10.0
Critical Depth (m)
Slightly silty sand

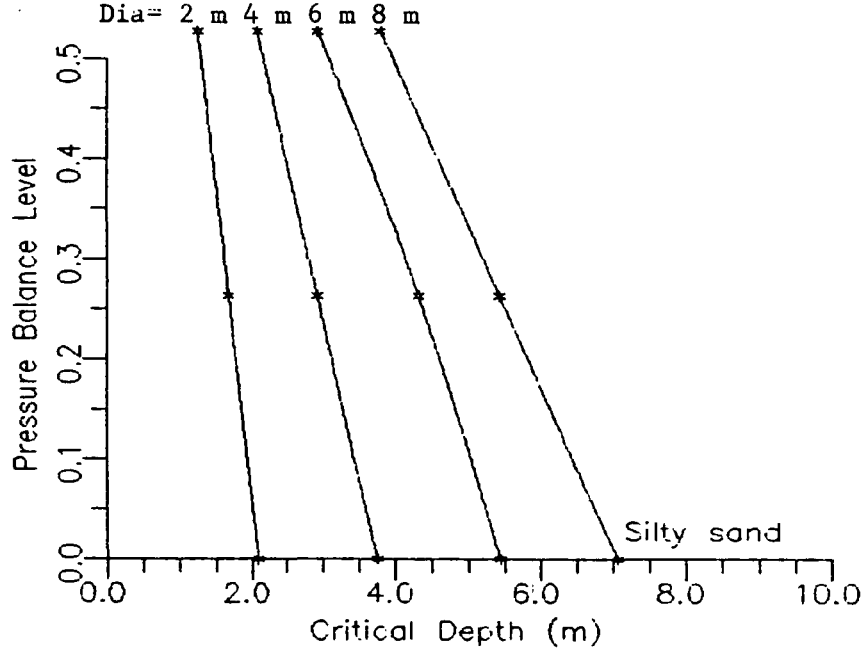
Dia= 2 m 4 m 6 m 8 m
Pressure Balance Level
0.0
0.1
0.2
0.3
0.4
0.5
0.0
2.0
4.0
6.0
8.0
10.0
Critical Depth (m)
Silty sand

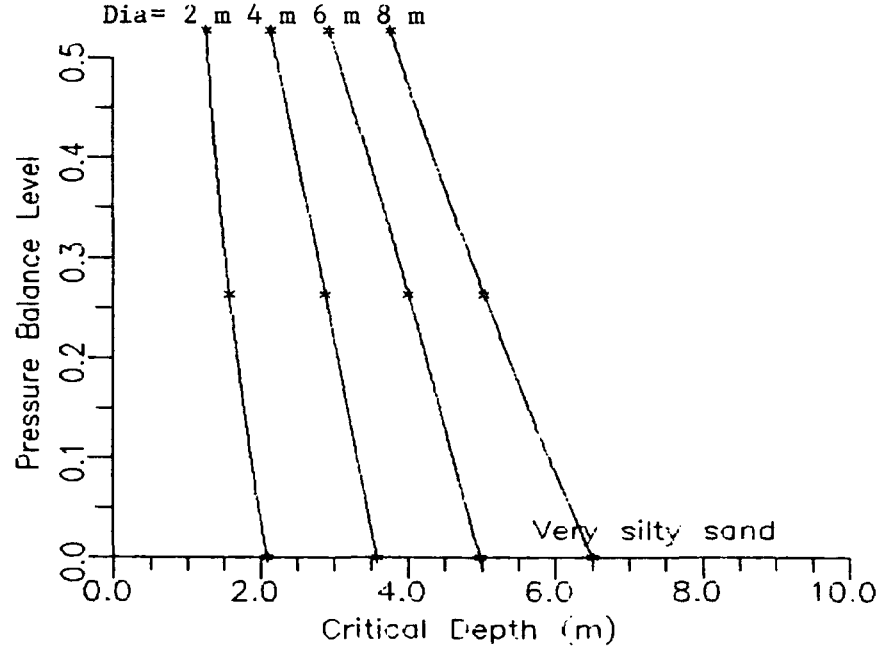
Dia= 2 m 4 m 6 m 8 m
Pressure Balance Level
0.0
0.1
0.2
0.3
0.4
0.5
0.0
2.0
4.0
6.0
8.0
10.0
Critical Depth (m)
Very silty sand

Appendix E

Design nomographs

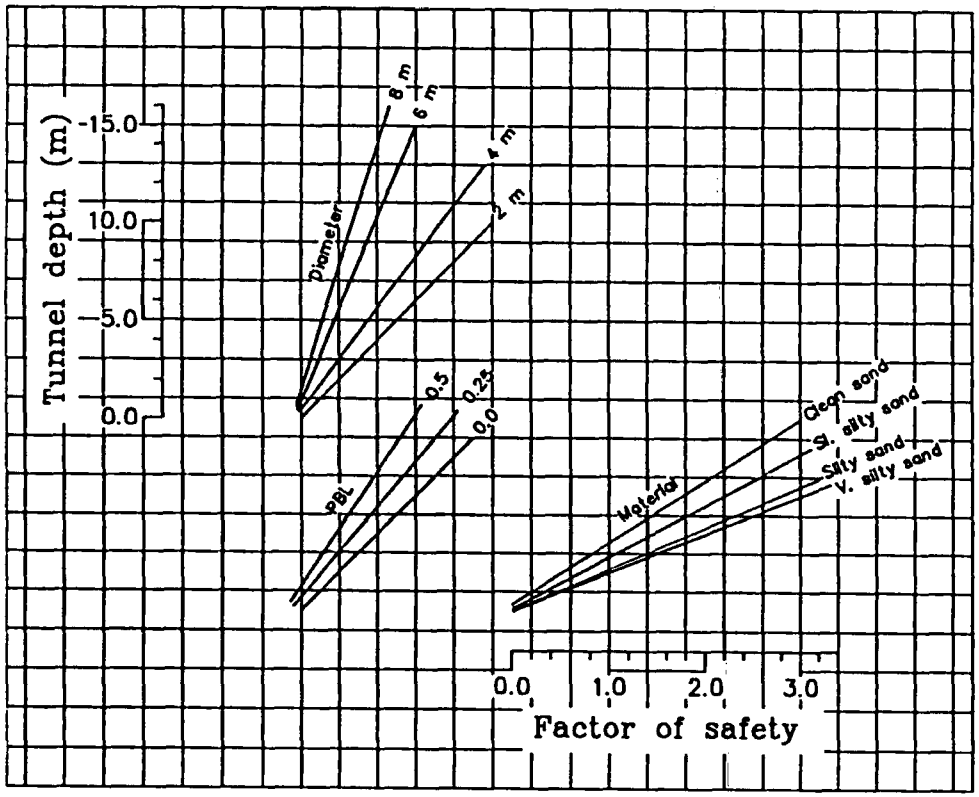

Tunnel design nomograph. Stability against blowouts. Standard shield.

Factor of safety = C/Ccr
C: Depth of cover to crown
Ccr: Critical depth to crown
PBL: Pressure balance level
(Level at which air and water pressure balance out in the face measured from the invert relative to diameter)

Route:

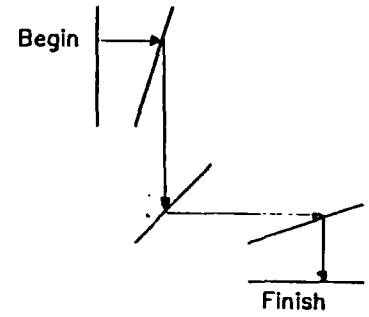

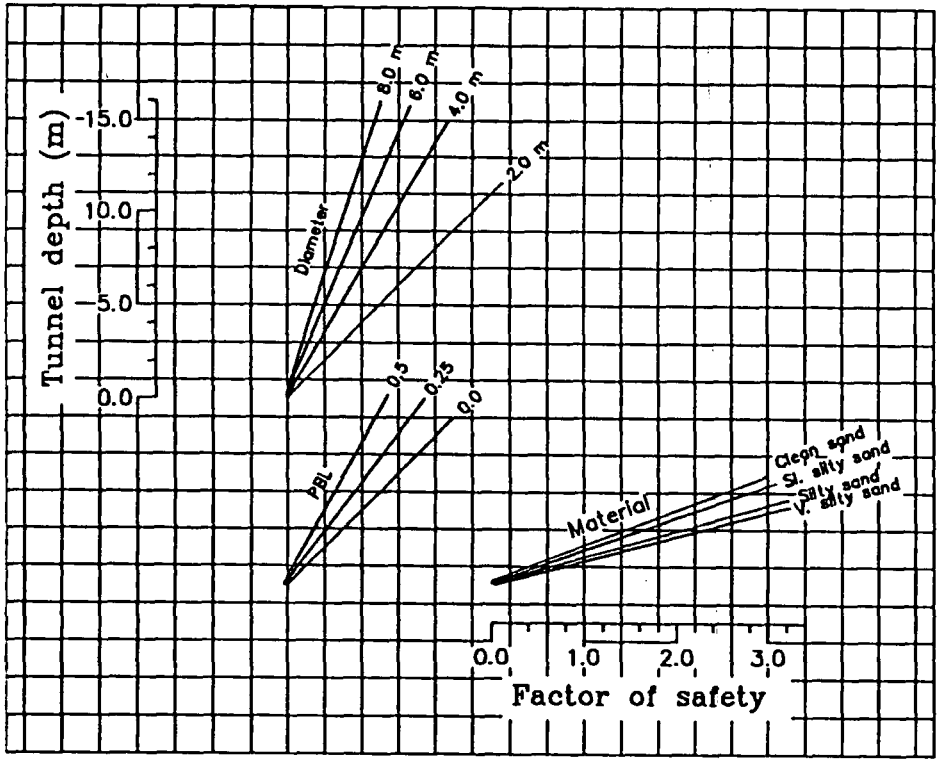

Tunnel design nomograph.
Stability against blowouts.
Hooded shield (L. of Hood=1/8 Dia.)

Factor of safety = C/Ccr
C: Depth of cover to crown
Ccr: Critical depth to crown
PBL: Pressure balance level
(Level at which air and water pressure balance out in the face measured from the invert relative to diameter)

Route:

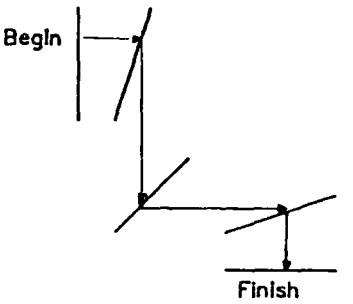

E2

Appendix F

FEM program listing

```
C
C      FEM PROGRAM FOR COMPRESSIBLE POTENTIAL FLOW
C
       LOGICAL FIRST
       REAL DETJAC, TOTG
       INTEGER BNDNOD, BNODE, DIF, DIMEN, DOFEL, DOFNOD, ELNUM,
      *      ELTOP, ELTYP, HBAND, I, IABSS, ICOORD, IDTPD, IELK,
      *      IELTOP, IELQ, IFUN, IGDER, IGDERT, IGEOM, IJAC,
      *      IJACIN, ILDER, INF, IP, IPD, IQUAD, IRHS, ISCVEC,
      *      ISTEER, ISYSK, ITEST, IWGHT, J, JABSS, JCOORD, JDTPD,
      *      JELK, JELTOP, JGDER, JGDERT, JGEOM, JJAC, JJACIN,
      *      JLDER, JNF, JP, JPD, JSYSK, NELE, NELTYP, NF, NIN,
      *      NODEL, NODNUM, NOUT, NQP, STEER, TOTDOF, TOTELS,
      *      TOTNOD
       DOUBLE PRECISION ABSS, B, BVAL, COORD, DET, DTPD, ELK, ELQ,
      *      ETA, FUN, GDER, GDERT, GEOM, GRAD, JAC, JACIN, LDER, P,
      *      PD, PHI, QUOT, RHS, SCALE, SCVEC, SOURCE, STRGTH, SYSK,
      *      WGHT, X, XI, Y
C
C                    VARIABLES USED TO DETERMINE ELEMENT AREA
C
       REAL ALPHA1, ALPHA2, H1, H2, LS1, LS2, LS3, LS4, LDIAG
       DIMENSION AREA(500)
       DOUBLE PRECISION AREA
C
C                    VARIABLES USED IN DESATURATION
C
       INTEGER FTEST
       REAL MAXFOS, PAR, PARA, PARB, PARC, PBL, SCAFAC
       DOUBLE PRECISION FS, XC, YC, K, SR, SRPAR
       DIMENSION FTEST(500), K(500), SR(500)
C
C                    VARIABLES USED FOR COMPRESSIBLE ELEMENT EQUATION
C
       INTEGER CBNDS, CBNODE, FACEL, FACNOD, ICSOL, IECOMP, IEINC,
      *      IGCOMP, IGDER2, IH, IHT, IHV, IIDN, IM, IMH, IMHHT, IMHHTM,
      *      IM2HMH, JECOMP, JGCOMP, JGDER2, JH, JHT, JIDN, JM, JMH,
      *      JMHHT, JMHHTM, NFACND, NN
       DOUBLE PRECISION AE, AX, AY, CD, E, EQUIL, EP, EQ, ER, ES, FOS1,
      *      FOS2, HF, HFN, IC, PCBVAL, P1, P2I, QF, QT, QX, QY, CPOTL,
      *      SDATUM, WDEPTH, ZW
       DIMENSION CBNODE(100), CBVAL(100), CPOTL(500), CSOL(500),
      *      ECOMP(8,8), EINC(8), FACEL(50), FACNOD(50), FOS1(500),
      *      FOS2(500), GCOMP(500,500),GDER2(8,8), H(8,1), HF(500),
      *      HT(1,8), HV(8), IDN(8,8),M(8,8), MH(8,1), MHHT(8,8),
      *      MHHTM(8,8), M2HMH(8), PCBVAL(50)
       DOUBLE PRECISION CSOL, ECOMP, EINC, GCOMP, GDER2, IDN, M, HV,
      *      H, HT, MH, MHHT, MHHTM, M2HMH
       DATA ICSOL/500/, IECOMP/8/, IEINC/8/, IGCOMP/500/, IGDER2/8/,
      *      IH/8/, IHT/8/, IHV/8/, IIDN/8/, IM/8/, IMH/8/, IMHHT/8/,
      *      IMHHTM/8/, IM2HMH/8/, JECOMP/8/, JGCOMP/500/, JGDER2/8/,
      *      JH/1/, JHT/8/, JIDN/8/, JM/8/, JMH/8/, JMHHT/8/, JMHHTM/8/
C
       DIMENSION ABSS(3,9), B(2,4), DTPD(8,8), ELK(8,8), ELQ(8),
      *      FUN(8), GDER(3,8), GDERT(8,3), GEOM(8,3), GRAD(2,1),
      *      JAC(3,3), JACIN(3,3), LDER(3,8), P(3,3), PD(3,8), PHI(4),
      *      PP(3,3), PQ(3,3), PR(3,3), PS(3,3), SCVEC(8),
      *      STEER(8), WGHT(9)
C
```

```
C                                PROBLEM SIZE DEPENDENT ARRAYS
C
      DIMENSION BNODE(50), BVAL(50), COORD(500,3),
     *     ELTOP(500,10), NF(500,1), RHS(500), SYSK(500,100)
C
      DATA IABSS /3/, IDTPD /8/, IELK /8/, IELQ /8/, IFUN /8/,
     *     IGDER /3/, IGDERT /8/, IGEOM /8/, IJAC /3/, IJACIN /3/,
     *     ILDER /3/, IP /3/, IPD /3/, ISCVEC /8/, ISTEER /8/,
     *     IWGHT /9/, JABSS /9/, JCOORD /3/, JDTPD /8/,
     *     JELK /8/, JGDER /8/, JGDERT /3/, JGEOM /3/, JJAC /3/,
     *     JJACIN /3/, JLDER /8/, JNF /1/, JP /3/, JPD /8/,
     *     SCALE /1.0D+10/
C
C                                PROBLEM SIZE DEPENDENT DATA STATEMENTS
C
      DATA ICOORD /500/, IELTOP /500/, INF /500/, IRHS /500/,
     *     ISYSK /500/, JELTOP /10/, JSYSK /100/
C
      DATA NIN /5/, NOUT /6/
C
C                                SET ITEST FOR FULL CHECKING
C
      ITEST = 0
C
C*                               **********************
C*                               *                    *
C*                               * INPUT DATA SECTION *
C*                               *                    *
C*                               **********************
C
C
C                                INPUT OF NODAL GEOMETRY
C
C     WRITE (NOUT,9010)
      READ (NIN, 8030) SCAFAC
      WRITE (NOUT, 9060) SCAFAC
      READ (NIN,8010) TOTNOD, DIMEN
      DO 1010 I=1,TOTNOD
      READ (NIN,8020) NODNUM, (COORD(NODNUM,J),J=1,DIMEN)
      DO 1015 J=1, DIMEN
      COORD(NODNUM,J)=COORD(NODNUM,J)*SCAFAC
 1015 CONTINUE
 1010 CONTINUE
C
C                                INPUT OF ELEMENT TOPOLOGY
C
C     WRITE (NOUT,9040)
      READ (NIN,8010) NELTYP, TOTELS, NODEL
      DO 1020 I=1,TOTELS
      READ (NIN,8010) ELNUM, ELTYP, (ELTOP(ELNUM,J+2),J=1,NODEL)
      ELTOP(ELNUM,1) = ELTYP
      ELTOP(ELNUM,2) = NODEL
 1020 CONTINUE
C
C                                INPUT OF SOIL AND WATER DATUM
C                                INPUT SOURCE STRENGTH
C
      READ(NIN, 8030) SDATUM, WDEPTH
      SDATUM=SDATUM*SCAFAC
```

```
      READ (NIN,8030) STRGTH
C
C                                INPUT OF NUMBER OF DEGREES OF FREEDOM
C                                PER NODE, GENERATION OF BOUNDARY CON-
C                                DITIONS AND CONSTRUCTION OF NODAL
C                                FREEDOM ARRAY NF
C
C     WRITE (NOUT,9080)
      READ (NIN,8010) DOFNOD
      WRITE (NOUT,9020) DOFNOD
      BNDNOD=0
      CBNDS=0
C
C                                INITIALISE BOUNDARY CONDITIONS AT
C                                THE GROUND SURFACE
C
      DO 1025 I=1, TOTNOD
      IF (COORD(I,2).EQ.SDATUM) THEN
      BNDNOD=BNDNOD+1
      CBNDS=CBNDS+1
      BNODE(BNDNOD)=I
      CBNODE(BNDNOD)=I
      BVAL(BNDNOD)=0.0
      CBVAL(BNDNOD)=0.0
      END IF
 1025 CONTINUE
      READ (NIN, 8020) NFACND, PBL
      READ (NIN, 8010) (FACNOD(J), J=1, NFACND)
      WRITE(NOUT, 9030) NFACND, PBL
      WRITE(NOUT, 9020) (FACNOD(J), J=1, NFACND)
      DO 1026 I=1, NFACND
      BNDNOD=BNDNOD+1
      BNODE(BNDNOD)=FACNOD(I)
      BVAL(BNDNOD)=COORD(FACNOD(I),2)-(8*PBL+2)*SCAFAC
      CD=0.61
      PCBVAL(J)=(1-SQRT(((1+CD**2)*BVAL(BNDNOD)+2*ZW+20.6)/
     *             (2*BVAL(BNDNOD)+2*ZW+20.6)))*CD**2
 1026 CONTINUE
C
      TOTDOF = 0
      DO 1050 I=1,TOTNOD
      DO 1040 J=1,DOFNOD
      TOTDOF = TOTDOF + 1
      NF(I,J) = TOTDOF
 1040 CONTINUE
 1050 CONTINUE
C
C                                INITIALISE VOID RATIO VALUES
C
      EP=0.74
      EQ=0.71
      ER=0.57
      ES=0.52
      MAXFOS=0.0
C
C                                ITERATION LOOP FOR DESATURATION
C
      DO 9999 LMNO=1,3
C
```

```
C                                CALCULATION OF SEMI-BANDWIDTH
C
      FIRST = .TRUE.
      DO 1060 NELE=1,TOTELS
      CALL FREDIF(NELE, ELTOP, IELTOP, JELTOP, NF, INF, JNF,
     *     DOFNOD, FIRST, DIF, ITEST)
 1060 CONTINUE
      HBAND = DIF + 1
C
      DO 1072 NELE=1, TOTELS
      FTEST(NELE)=0
      SR(NELE)=1.0
      FOS1(NELE)=1.1
      CALL ELGEOM(NELE, ELTOP, IELTOP, JELTOP, COORD, ICOORD,
     *     JCOORD, GEOM, IGEOM, JGEOM, DIMEN, ITEST)
      YC=(GEOM(1,2)+GEOM(2,2)+GEOM(3,2)+GEOM(4,2))/4
      ZW=SDATUM+WDEPTH-YC
      IF (ELTOP(NELE,1).EQ.1) THEN
      K(NELE)=(2.31E-5)*(ZW+10.3)
      ELSEIF (ELTOP(NELE,1).EQ.2) THEN
      K(NELE)=(3.18E-5)*(ZW+10.3)
      ELSEIF (ELTOP(NELE,1).EQ.3) THEN
      K(NELE)=(1.94E-5)*(ZW+10.3)
      ELSEIF (ELTOP(NELE,1).EQ.4) THEN
      K(NELE)=(2.69E-5)*(ZW+10.3)
      END IF
 1072 CONTINUE
C
C*                               ****************************************
C*                               *                                      *
C*                               * INCOMPRESSIBLE SYSTEM MATRIX ASSEMBLY *
C*                               *                                      *
C*                               ****************************************
C
      CALL VECNUL(RHS, IRHS, TOTDOF, ITEST)
      CALL MATNUL(SYSK, ISYSK, JSYSK, TOTDOF, HBAND, ITEST)
      DOFEL = NODEL*DOFNOD
      CALL QQUA4(WGHT, IWGHT, ABSS, IABSS, JABSS, NQP, ITEST)
      DO 1100 NELE=1,TOTELS
      CALL ELGEOM(NELE, ELTOP, IELTOP, JELTOP, COORD, ICOORD,
     *     JCOORD, GEOM, IGEOM, JGEOM, DIMEN, ITEST)
C
C                               INTEGRATION LOOP FOR ELEMENT STIFFNESS
C                               USING NQP QUADRATURE POINTS
C
      CALL MATNUL(ELK, IELK, JELK, DOFEL, DOFEL, ITEST)
      CALL VECNUL(ELQ, IELQ, DOFEL, ITEST)
      DO 1090 IQUAD=1,NQP
C
C                               FORM LINEAR SHAPE FUNCTION AND SPACE
C                               DERIVATIVES IN THE LOCAL CORRDINATES.
C                               TRANSFORM LOCAL DERIVATIVES TO GLOBAL
C                               COORDINATE SYSTEM
C
      XI = ABSS(1,IQUAD)
      ETA = ABSS(2,IQUAD)
      CALL QUAM4(FUN, IFUN, LDER, ILDER, JLDER, XI, ETA, ITEST)
C
      CALL SCAPRD(GEOM(1,1), IGEOM, FUN, IFUN, NODEL, X, ITEST)
```

```
      CALL SCAPRD(GEOM(1,2), IGEOM, FUN, IFUN, NODEL, Y, ITEST)
C
      CALL MATMUL(LDER, ILDER, JLDER, GEOM, IGEOM, JGEOM, JAC,
     *     IJAC, JJAC, DIMEN, NODEL, DIMEN, ITEST)
      CALL MATINV(JAC, IJAC, JJAC, JACIN, IJACIN, JJACIN, DIMEN,
     *     DET, ITEST)
      CALL MATMUL(JACIN, IJACIN, JJACIN, LDER, ILDER, JLDER, GDER,
     *     IGDER, JGDER, DIMEN, DIMEN, NODEL, ITEST)
C
C                              FORMATION OF ELEMENT STIFFNESS ELK
C
      CALL MATNUL(P, IP, JP, DIMEN, DIMEN, ITEST)
       DO 1075 I=1,DIMEN
       P(I,I)=K(NELE)
 1075 CONTINUE
      CALL MATMUL(P, IP, JP, GDER, IGDER, JGDER, PD, IPD, JPD,
     *     DIMEN, DIMEN, DOFEL, ITEST)
      CALL MATRAN(GDER, IGDER, JGDER, GDERT, IGDERT, JGDERT,
     *     DIMEN, DOFEL, ITEST)
      CALL MATMUL(GDERT, IGDERT, JGDERT, PD, IPD, JPD, DTPD,
     *     IDTPD, JDTPD, DOFEL, DIMEN, DOFEL, ITEST)
      QUOT = DABS(DET)*WGHT(IQUAD)
      DO 1080 I=1,DOFEL
      DO 1070 J=1,DOFEL
      DTPD(I,J) = DTPD(I,J)*QUOT
 1070 CONTINUE
      SCVEC(I) = FUN(I)*SOURCE(X,Y,STRGTH)*QUOT
 1080 CONTINUE
      CALL MATADD(ELK, IELK, JELK, DTPD, IDTPD, JDTPD, DOFEL,
     *     DOFEL, ITEST)
      CALL VECADD(ELQ, IELQ, SCVEC, ISCVEC, DOFEL, ITEST)
 1090 CONTINUE
C
C                              ASSEMBLY OF SYSTEM STIFFNESS MATRIX
C
      CALL DIRECT(NELE, ELTOP, IELTOP, JELTOP, NF, INF, JNF,
     *     DOFNOD, STEER, ISTEER, ITEST)
      CALL ASSYM(SYSK, ISYSK, JSYSK, ELK, IELK, JELK, STEER,
     *     ISTEER, HBAND, DOFEL, ITEST)
      CALL ASRHS(RHS, IRHS, ELQ, IELQ, STEER, ISTEER, DOFEL, ITEST)
 1100 CONTINUE
C
C*                             **********************
C*                             *                    *
C*                             * EQUATION SOLUTION  *
C*                             *                    *
C*                             **********************
C
C                              MODIFICATION OF STIFFNESS MATRIX AND
C                              RIGHT-HAND SIDE TO IMPLEMENT BOUNDARY
C                              CONDITIONS
C
      DO 1110 I=1,BNDNOD
      J = BNODE(I)
      SYSK(J,HBAND) = SYSK(J,HBAND)*SCALE
      RHS(J) = SYSK(J,HBAND)*BVAL(I)
 1110 CONTINUE
C
C                              SOLUTION OF SYSTEM MATRIX FOR THE
```

```
C                               NODAL VALUES OF THE POTENTIAL
C
      CALL CHOSOL(SYSK, ISYSK, JSYSK, RHS, IRHS, TOTDOF, HBAND,
     *     ITEST)
C
C*                              ********************************
C*                              *                              *
C*                              * COMPRESSIBILITY CORRECTION *
C*                              *                              *
C*                              ********************************
C
      DO 6000 NELE=1,TOTELS
      CALL ELGEOM(NELE, ELTOP, IELTOP, JELTOP, COORD, ICOORD,
     *     JCOORD, GEOM, IGEOM, JGEOM, DIMEN, ITEST)
C
C                               INTEGRATION LOOP FOR ELEMENT STIFFNESS
C                               USING NQP QUADRATURE POINTS
C
      CALL MATNUL(GDER, IGDER, JGDER, DIMEN, NODEL, ITEST)
      CALL MATNUL(GDERT, IGDERT, JGDERT, NODEL, DIMEN, ITEST)
      CALL MATNUL(IDN, IIDN, JIDN, DOFEL, DOFEL, ITEST)
      CALL MATNUL(GDER2, IGDER2, JGDER2, DOFEL, DOFEL, ITEST)
      CALL MATNUL(M, IM, JM, DOFEL, DOFEL, ITEST)
      CALL MATNUL(H, IH, JH, DOFEL, 1, ITEST)
      CALL MATNUL(HT, IHT, JHT, 1, DOFEL, ITEST)
      CALL MATNUL(MH, IMH, JMH, DOFEL, 1, ITEST)
      CALL MATNUL(MHHT, IMHHT, JMHHT, DOFEL, DOFEL, ITEST)
      CALL MATNUL(MHHTM, IMHHTM, JMHHTM, DOFEL, DOFEL, ITEST)
      DO 6010 IQUAD=1,NQP
C
C                               FORM LINEAR SHAPE FUNCTION AND SPACE
C                               DERIVATIVES IN THE LOCAL CORRDINATES.
C                               TRANSFORM LOCAL DERIVATIVES TO GLOBAL
C                               COORDINATE SYSTEM
C
      XI = ABSS(1,IQUAD)
      ETA = ABSS(2,IQUAD)
      CALL QUAM4(FUN, IFUN, LDER, ILDER, JLDER, XI, ETA, ITEST)
C
      CALL SCAPRD(GEOM(1,1), IGEOM, FUN, IFUN, NODEL, X, ITEST)
      CALL SCAPRD(GEOM(1,2), IGEOM, FUN, IFUN, NODEL, Y, ITEST)
C
      CALL MATMUL(LDER, ILDER, JLDER, GEOM, IGEOM, JGEOM, JAC,
     *     IJAC, JJAC, DIMEN, NODEL, DIMEN, ITEST)
      CALL MATINV(JAC, IJAC, JJAC, JACIN, IJACIN, JJACIN, DIMEN,
     *     DET, ITEST)
      CALL MATMUL(JACIN, IJACIN, JJACIN, LDER, ILDER, JLDER, GDER,
     *     IGDER, JGDER, DIMEN, DIMEN, NODEL, ITEST)
      CALL MATRAN(GDER, IGDER, JGDER, GDERT, IGDERT, JGDERT,
     *     DIMEN, DOFEL, ITEST)
 6010 CONTINUE
C
C                               DETERMINE AREA OF NELE
C
      LS1=((GEOM(2,1)-GEOM(1,1))**2+(GEOM(2,2)-GEOM(1,2))**2)**0.5
      LS2=((GEOM(3,1)-GEOM(2,1))**2+(GEOM(3,2)-GEOM(2,2))**2)**0.5
      LS3=((GEOM(4,1)-GEOM(3,1))**2+(GEOM(4,2)-GEOM(3,2))**2)**0.5
      LS4=((GEOM(1,1)-GEOM(4,1))**2+(GEOM(1,2)-GEOM(4,2))**2)**0.5
      H1=(LS1+LS3)/2
```

```
      H2=(LS2+LS4)/2
      AREA(NELE)=H1*H2
C
C                                FORMATION OF ELEMENT COMPRESSIBLE
C                                STIFFNESS MATRIX
C
      CALL MATMUL(GDERT, IGDERT, JGDERT, GDER, IGDER, JGDER, GDER2,
     *     IGDER2, JGDER2, DOFEL, DIMEN, DOFEL, ITEST)
      CALL MATIDN(IDN, IIDN, JIDN, DOFEL, DOFEL, ITEST)
      CALL MATMUL(IDN, IIDN, JIDN, GDER2, IGDER2, JGDER2, M, IM, JM,
     *     DOFEL, DOFEL, DOFEL, ITEST)
      DO 6030 I=1, NODEL
      HV(I)=RHS(ELTOP(NELE,I+2))
      H(I,1)=RHS(ELTOP(NELE,I+2))
 6030 CONTINUE
      CALL MATRAN(H, IH, IH, HT, IHT, JHT, NODEL, 1, ITEST)
      CALL MATMUL(M, IM, JM, H, IH, JH, MH, IMH, JMH, DOFEL, DOFEL, 1,
     *     ITEST)
      CALL MATMUL(MH, IMH, JMH, HT, IHT, JHT, MHHT, IMHHT, JMHHT,
     *     DOFEL, 1, DOFEL, ITEST)
      CALL MATMUL(MHHT, IMHHT, JMHHT, M, IM, JM, MHHTM, IMHHTM, JMHHTM,
     *     DOFEL, DOFEL, DOFEL, ITEST)
      CALL VECMAT(HV, IHV, MHHTM, IMHHTM, JMHHTM, DOFEL, DOFEL, M2HMH,
     *     IM2HMH, ITEST)
      DO 6040 I=1, DOFEL
      ECOMP(I,I)=AREA(NELE)*M(I,I)
      EINC(I)=-AREA(NELE)*M2HMH(I)/2
 6040 CONTINUE
      CALL DIRECT(NELE, ELTOP, IELTOP, JELTOP, NF, INF, JNF,
     *     DOFNOD, STEER, ISTEER, ITEST)
      CALL ASSYM(GCOMP, IGCOMP, JGCOMP, ECOMP, IECOMP, JECOMP, STEER,
     *     ISTEER, HBAND, DOFEL, ITEST)
      CALL ASRHS(CSOL, ICSOL, EINC, IEINC, STEER, ISTEER, DOFEL, ITEST)
 6000 CONTINUE
C
C                                IMPLEMENTATION OF BOUNDARY CONDITIONS
C
C     AT SURFACE:
C
      DO 6050 I=1, CBNDS
      J=CBNODE(I)
      GCOMP(J,HBAND)=GCOMP(J,HBAND)*SCALE
      CSOL(J)=GCOMP(J,HBAND)*CBVAL(I)
 6050 CONTINUE
C
C     AT FACE:
C
      DO 6055 II=1, NFACND
      J=FACNOD(II)
      GCOMP(J,HBAND)=GCOMP(J,HBAND)*SCALE
      CSOL(J)=GCOMP(J,HBAND)*PCBVAL(II)
 6055 CONTINUE
C
C                                SOLUTION OF SYSTEM MATRIX FOR THE
C                                NODAL VALUES OF THE COMPRESSIBLE
C                                FLUID POTENTIALS
C
      CALL CHOSOL(GCOMP, IGCOMP, JGCOMP, CSOL, ICSOL, TOTDOF, HBAND,
     *     ITEST)
```

```
C
      DO 6060 I=1, TOTNOD
      CPOTL(I)=RHS(I)+CSOL(I)
C
C     WRITE (NOUT,8035) (COORD(I,J), J=1,DIMEN), RHS(I), CSOL(I),
     *       CPOTL(I)
C
 6060 CONTINUE
C
C                                SOLUTION FOR GRADIENTS
C
      DO 7000 NELE=1,TOTELS
      CALL ELGEOM(NELE, ELTOP, IELTOP, JELTOP, COORD, ICOORD,
     *     JCOORD, GEOM, IGEOM, JGEOM, DIMEN, ITEST)
      DO 7010 IQUAD=1,NQP
      XI = ABSS(1,IQUAD)
      ETA = ABSS(2,IQUAD)
      CALL QUAM4(FUN, IFUN, LDER, ILDER, JLDER, XI, ETA, ITEST)
C
      CALL SCAPRD(GEOM(1,1), IGEOM, FUN, IFUN, NODEL, X, ITEST)
      CALL SCAPRD(GEOM(1,2), IGEOM, FUN, IFUN, NODEL, Y, ITEST)
C
      CALL MATMUL(LDER, ILDER, JLDER, GEOM, IGEOM, JGEOM, JAC,
     *     IJAC, JJAC, DIMEN, NODEL, DIMEN, ITEST)
 7010 CONTINUE
      DETJAC=JAC(1,1)*JAC(2,2)-JAC(2,1)*JAC(1,2)
      B(1,1)=(GEOM(2,2)-GEOM(4,2))/(8*DETJAC)
      B(1,2)=(GEOM(3,2)-GEOM(1,2))/(8*DETJAC)
      B(1,3)=(GEOM(4,2)-GEOM(2,2))/(8*DETJAC)
      B(1,4)=(GEOM(1,2)-GEOM(3,2))/(8*DETJAC)
      B(2,1)=(GEOM(4,1)-GEOM(2,1))/(8*DETJAC)
      B(2,2)=(GEOM(1,1)-GEOM(3,1))/(8*DETJAC)
      B(2,3)=(GEOM(2,1)-GEOM(4,1))/(8*DETJAC)
      B(2,4)=(GEOM(3,1)-GEOM(1,1))/(8*DETJAC)
      PHI(1)=RHS(ELTOP(NELE,3))
      PHI(2)=RHS(ELTOP(NELE,4))
      PHI(3)=RHS(ELTOP(NELE,5))
      PHI(4)=RHS(ELTOP(NELE,6))
      GRAD(1,1)=B(1,1)*PHI(1)+B(1,2)*PHI(2)+B(1,3)*PHI(3)+B(1,4)*PHI(4)
      GRAD(2,1)=B(2,1)*PHI(1)+B(2,2)*PHI(2)+B(2,3)*PHI(3)+B(2,4)*PHI(4)
      TOTG=((GRAD(1,1))**2+(GRAD(2,1)**2))**0.5
C
C                              CALCULATION OF SOIL AND WATER OVERBURDEN
C
      XC=(GEOM(1,1)+GEOM(2,1)+GEOM(3,1)+GEOM(4,1))/4
      YC=(GEOM(1,2)+GEOM(2,2)+GEOM(3,2)+GEOM(4,2))/4
      ZS=SDATUM-YC
      ZW=WDEPTH+ZS
C
C                               DETERMINE EXCESS AIR PRESSURE
C                               IN SOIL ELEMENT NELE
C
      FS=0.0
      DO 7007 I=1, NODEL
      FS=FS+CPOTL(ELTOP(NELE,I+2))/NODEL
 7007 CONTINUE
C
C                               DETERMINE VOID RATIO, EFFECTIVE PERMEABIL
C                               AND DEGREE OF SATURATION OF SOIL ELEMENT
```

```
C
      IF (ELTOP(NELE,1).EQ.1) THEN
      E=EP
      IF (FS.LE.0.1272) THEN
      SRPAR=1.0
      ELSEIF (FS.GT.0.1272) THEN
      SRPAR=(FS**(-1.50048))*0.043258
      END IF
      IF (SRPAR.LT.SR(NELE)) THEN
      SR(NELE)=SRPAR
      END IF
      K(NELE)=(2.31E-5)*(SR(NELE)**(-0.552199))*(FS+ZW+10.3)
      ELSEIF (ELTOP(NELE,1).EQ.2) THEN
      E=EQ
      IF (FS.LE.0.08363) THEN
      SRPAR=1.0
      ELSEIF (FS.GT.0.08363) THEN
      SRPAR=(FS**(-0.79927))*0.13763
      END IF
      IF (SRPAR.LE.SR(NELE)) THEN
      SR(NELE)=SRPAR
      ENDIF
      K(NELE)=(3.18E-5)*(SR(NELE)**(-1.43418))*(FS+ZW+10.3)
      ELSEIF (ELTOP(NELE,1).EQ.3) THEN
      E=ER
      IF (FS.LE.0.374109) THEN
      SRPAR=1.0
      ELSEIF (FS.GT.0.374109) THEN
      SRPAR=(FS**(-0.60115))*0.553745
      END IF
      IF (SRPAR.LT.SR(NELE)) THEN
      SR(NELE)=SRPAR
      END IF
      K(NELE)=(1.94E-5)*(SR(NELE)**(-1.61379))*(FS+ZW+10.3)
      ELSEIF (ELTOP(NELE,1).EQ.4) THEN
      E=ES
      IF (FS.LE.0.1) THEN
      SRPAR=1.0
      ELSEIF (FS.GT.0.1) THEN
      SRPAR=(FS**(-0.22292))*0.598566
      END IF
      IF (SRPAR.LT.SR(NELE)) THEN
      SR(NELE)=SRPAR
      END IF
      K(NELE)=(2.69E-5)*(SR(NELE)**(-2.78293))*(FS+ZW+10.3)
      END IF
C
C                              SET PERMEABILITIES OF FAILED ELEMENTS
C
      IF (FTEST(NELE).EQ.1) THEN
      IF (ELTOP(NELE,1).EQ.1) THEN
      K(NELE)=(7.90E-4)*(FS+ZW+10.3)
      ELSEIF (ELTOP(NELE,1).EQ.2) THEN
      K(NELE)=(7.38E-4)*(FS+ZW+10.3)
      ELSEIF (ELTOP(NELE,1).EQ.3) THEN
      K(NELE)=(5.72E-4)*(FS+ZW+10.3)
      ELSEIF (ELTOP(NELE,1).EQ.4) THEN
      K(NELE)=(4.87E-4)*(FS+ZW+10.3)
      END IF
```

```
      END IF
C
C                              DETERMINE INCOMPRESSIBLE HEAD LOSS AT FACE
C                              FOR THE COMPRESSIBILITY CORRECTION
C
C                              DETERMINE FOS FOR FAILURE
C
      FOS1(NELE)=((2.65+SR(NELE)*E)/(1+E)*ZS+ZW-ZS)/(ZW+FS+TOTG)
      IF (FOS1(NELE).LE.1.0) THEN
      FTEST(NELE)=1
      END IF
      IF (YC.GT.10*SCAFAC) THEN
      IF (XC.EQ.13.5*SCAFAC) THEN
      PARA=FOS1(NELE-2)
      PARB=FOS1(NELE-1)
      PARC=FOS1(NELE)
      PAR=AMIN1(PARA,PARB,PARC)
      END IF
      IF (PAR.GT.MAXFOS) THEN
      MAXFOS=PAR
      END IF
      END IF
      WRITE(NOUT,8030) XC, YC, FOS1(NELE)
C
 7000 CONTINUE
C
      IF (MAXFOS.LT.1.0) THEN
      STOP
      END IF
C
 9999 CONTINUE
C
      STOP
C
 8010 FORMAT (16I5)
 8020 FORMAT (I5, 6F10.5)
 8030 FORMAT (4F10.2)
 8034 FORMAT (F10.2, 2E10.2)
 8035 FORMAT (2F10.1, F10.3, F12.5, F10.3)
 8040 FORMAT (I5, 6F10.0)
 9010 FORMAT (//25H **** NODAL GEOMETRY ****//1H )
 9020 FORMAT (1H , 16I5)
 9030 FORMAT (1H , I5, 6F10.5)
 9035 FORMAT (1H , I5, 5F10.2, E10.2, 4F10.2)
 9040 FORMAT (//27H **** ELEMENT TOPOLOGY ****//1H )
 9050 FORMAT (//25H **** PERMEABILITIES ****//1H )
 9060 FORMAT (1H , 2F10.5)
 9065 FORMAT (1H , 4E10.2)
 9070 FORMAT (//26H **** SOURCE STRENGTH ****//1H )
 9080 FORMAT (//30H **** BOUNDARY CONDITIONS ****//1H )
 9084 FORMAT (//37H **** C CORR BOUNDARY CONDITIONS ****//1H )
 9085 FORMAT (//25H **** FLOW GRADIENTS ****//1H )
 9090 FORMAT (//27H **** NODAL POTENTIALS ****//1H )
 9091 FORMAT (//28H **** NODAL SOLUTIONS - ****,1H )
 9092 FORMAT (/45H **** X, Y, INCOMP, COMP CORR, COMP POTL ****//1H )
      END
C
      DOUBLE PRECISION FUNCTION SOURCE(X, Y, STRGTH)
      DOUBLE PRECISION STRGTH, X, Y
```

```
      SOURCE = 0.0D0
      IF ((X.GE.1.0D0) .AND. (X.LE.2.0D0) .AND. (Y.GE.1.0D0) .AND.
     *     (Y.LE.2.0D0)) SOURCE = STRGTH
      RETURN
      END
C
C*                          **********************
C*                          *                    *
C*                          * LIST OF VARIABLES  *
C*                          *                    *
C*                          **********************
C
C       ABSS:    ABSCISSAE OF QUADRATURE POINTS
C       AREA:    ELEMENT AREA
C       B:       ELEMENT POTENTIAL MATRIX
C       BNDNOD:  NUMBER OF BOUNDARY NODES (INCOMPRESSIBLE POTENTIAL)
C       BNODE:   BOUNDARY NODES
C       BVAL:    BOUNDARY CONDITION OF COMPRESSIBILITY CORRECTION AT SUR

C       CBNDS:   NUMBER OF BOUNDARY NODES (COMPRESSIBILITY CORRECTION)
C       CBNODE:  COMPRESSIBLE BOUNDARY NODE
C       COORD:   X,Y COORDINATES OF NODE
C       CPOTL:   NODAL COMPRESSIBILITY POTENTIAL SOLUTION
C       CSOL:    NODAL COMPRESSIBILITY CORRECTION
C       DET:     DETERMINANT MATRIX
C       DETJAC:  DETERMINANT OF THE JACOBIAN J
C       DIF:     MAXIMUM DIFFERENCE IN ELEMENT NODAL ARRAY
C       DIMEN:   NUMBER OF SYSTEM DIMENSIONS
C       DOFEL:   DEGREES OF FREEDOM PER ELEMENT
C       DOFNOD:  DEGREES OF FREEDOM PER NODE
C       DTPD:    ELEMENT STIFFNESS MATRIX
C       E:       ELEMENT VOID RATIO
C       ECOMP:   ELEMENT COMPRESSIBILITY CORRECTION
C       EINC:    ELEMENT INCOMPRESSIBLE POTENTIAL
C       ELK:     ELEMENT STIFFNESS MATRIX
C       ELNUM:   ELEMENT NUMBER
C       ELQ:     ELEMENT SOURCE VECTOR
C       ELTOP:   ELEMENT TOPOLOGY
C       ELTYP:   ELEMENT TYPE
C       EP,Q,R,S: VOID RATIO OF MATERIAL TYPES
C       ETA:     LOCAL COORDINATE IN Y DIRECTION
C       FACEL:   NUMBER OF ELEMENTS ALONG TUNNEL FACE
C       FACNOD:  NUMBER OF NODES ALONG TUNNEL FACE
C       FOS1:    ELEMENT FACTOR OF SAFETY
C       FTEST:   FAILURE CRITERIA FLAG
C       FUN:     INTERPOLATION FUNCTION ARRAY
C       GCOMP:   GLOBAL COMPRESSIBLE CORRECTON MATRIX
C       GDER:    GLOBAL DERIVATIVE OF INTERPOLATION FUNCTIONS
C       GDERT:   TRANSPOSE OF GLOBAL DERIVATIVE
C       GDER2:   SECOND DERIVATIVE OF GLOBAL SYSTEM MATRIX
C       GEOM:    GEOMETRY OF ELEMENT TOPOLOGY
C       GRAD:    DIRECTIONAL GRADIENT
C       H1,H2:   AVERAGE LENGTHS OF ELEMENT
C       LS#:     ELEMENT SIDE LENGTHS
C       H:       COMPRESSIBILITY CORRECTION HEAD
C       HT:      TRANSPOSE OF H
C       HBAND:   SEMI-BANDWIDTH
C       I(VAR):  NUMBER OF ROWS IN VAR MATRIX
C       IDN:     IDENTITY MATRIX
C       J(VAR):  NUMBER OF COLUMNS IN VAR MATRIX
```

```
C       JAC:     JACOBIAN MATRIX
C       JACIN:   INVERSE OF JACOBIAN
C       K:       ELEMENT PERMEABILITY
C       LDER:    LINEAR DERIVATIVE
C       MAXFOS:  MAXIMUM FACTOR OF SAFETY FOR SYSTEM
C       NELE:    ELEMENT NUMBER
C       NELTYP:  TOTAL NUMBER OF ELEMENT TYPES
C       NF:      NODAL FREEDOM ARRAY
C       NFACND:  NUMBER OF FACE NODES
C       NIN:     INPUT FILE
C       NODEL:   NODES PER ELEMENT
C       NODNUM:  NODE NUMBER
C       NOUT:    OUTPUT FILE
C       NQP:     NUMBER OF QUADRATURE POINTS
C       P:       PERMEABILITY MATRIX
C       PAR:     FACTOR USED IN CALCULATING MAXFOS
C       PARA:    FACTOR USED IN CALCULATING MAXFOS
C       PARB:    FACTOR USED IN CALCULATING MAXFOS
C       PARC:    FACTOR USED IN CALCULATING MAXFOS
C       PBL:     PRESSURE BALANCE LEVEL
C       PCBVAL:  BOUNDARY CONDITION FOR COMPRESSIBILITY CORRECTION AT FA

C       PD:      DETERMINANT OF PERMEABILITY
C       PHI:     POTENTIAL
C       RHS:     NODAL INCOMPRESSIBLE POTENTIAL SOLUTION
C       SCAFAC:  SCALED FACTOR FOR TUNNEL DIAMETER
C       SCALE:   BIAS FACTOR FOR BOUNDARY VALUES
C       SCVEC:   SCALED VECTOR
C       SOURCE:  SOURCE VECTOR
C       SDATUM:  DEPTH BELOW GROUND SURFACE
C       SR:      DEGREE OF SATURATION
C       STEER:   STEERING VECTOR FOR SYSTEM ASSEMBLY
C       STRGTH:  SOURCE SRENGTH
C       SYSK:    SYSTEM STIFFNESS MATRIX
C       TOTDOF:  TOTAL DEGREES OF FREEDOM
C       TOTEL:   TOTAL NUMBER OF ELEMENTS
C       TOTG:    TOTAL GRADIENT
C       TOTNOD:  TOTAL NUMBER OF NODES
C       WDEPTH:  DEPTH BELOW RIVER
C       WGHT:    QUADRATURE WEIGHT FOR NUMERICAL INTEGRATION
C       X,Y:     GLOBAL COORDINATES
C       XC,YC:   COORDINATES OF CENTER OF ELEMENT
C       XI:      LOCAL COORDINATE IN X DIRECTION
C       ZW:      DEPTH BELOW WATER TABLE
C
C
C*                          ****************************
C*                          *                          *
C*                          * LIST OF NAG SUBROUTINES  *
C*                          *                          *
C*                          ****************************
C
C       ASRHS:   ASSEMBLES RIGHT HAND SIDE OF A MATRIX SYSTEM
C       ASSYM:   ASSEMBLES SYMMETRIC SYSTEM MATRIX
C       CHOSOL:  SOLVES LINEAR SYSTEMS USING CHOLESKI REDUCTION
C       DIRECT:  CONSTRUCTS STEERING VECTOR USED IN ASSEMBLING SYSTEM MA

C       ELGEOM:  CONSTRUCTS ELEMENT GEOMETRY ARRAY
C       FREDIF:  CALCULATES MAXIMUM FREEDOM NUMBER
C       MATADD:  ADDS TWO MATRICES TOGETHER
C       MATION:  INITIALISES MATRIX TO THE IDENTITY MATRIX
```

```
C       MATINV: INVERTS A MATRIX
C       MATMUL: MULTIPLIES TWO MATRICES
C       MATNUL: SETS ALL VALUES TO ZERO IN A MATRIX
C       MATRAN: FORMS THE TRANSPOSE OF A MATRIX
C       QQUA4:  FOUR POINT QUADRATURE RULE
C       QUAM4:  FORMS INTERPOLATION FUNCTIONS FOR QUADRATIC ELEMENT
C       SCAPRD: FORMS THE PRODUCT OF TWO VECTORS
C       VECADD: ADDS TWO VECTORS TOGETHER
C       VECMAT: MULTIPLIES A MATRIX BY A VECTOR
C       VECNUL: SETS ALL VALUES TO ZERO IN A VECTOR
```

Appendix G

List of credits for figures

Figure	Source
1.1	Haswell & Gutteridge, 1990
1.2	Harris, 1983
1.3	Harris, 1983
1.4	Harris, 1983
1.5	Pequignot, 1963
1.6a	Megaw & Bartlett, 1981
1.6b	Haxton & Whyte, 1965
1.7	Megaw & Bartlett, 1981
1.8	Hagimoto & Kashima, 1984
2.1	After Szechy, 1973
2.2	Davis et.al., 1980
2.3	Davis et.al., 1980
2.4	Davis et.al., 1980
2.5	Davis et.al., 1980
2.6	Atkinson, 1981
2.7	Atkinson, 1981
2.8	Szechy, 1973
3.1	Craig, 1987
3.2	Craig, 1987
3.3	After Rouse, 1946
3.4	After Rouse, 1946
3.5	After Toll & Hight, 1990
3.6	After Marle, 1981
3.7	Craig, 1987
4.1	Craig, 1987
4.2	Blight, 1971
4.3	Topp & Miller, 1966
4.4	After Marle, 1981
5.1	Ruska Instrument Corp.
5.2	After Craig, 1987
6.1	After Rouse, 1946

Appendix H

Bibliography

Bibliography

Atkinson, J.H., "Soil mechanics aspects of soft ground tunnelling", *Ground Engineering*, July 1981.

Atkinson, J.H. and Potts, D.M., "Stability of a shallow circular tunnel in cohesionless soil", *Geotechnique*, **27**, 1977, No. 2, pp 397-416.

Bishop, A.W., "The principles of effective stress", *Tecknisk Ukrblad*, **106**, 1959, No.39, pp 859-863.

Blight, G.E., "Flow of air through soils", *J. Soil Mech. Fnd. Div. ASCE*, **97**, 1971, SM4, pp 607-624.

British Standard 5930, "Code of practice for site investigations", *British Standards Institution, London*, 1981.

Broms, B.B. and Bennermark, H., "Stability of clay in vertical openings", *J. Soil Mech. Fnd. Div. ASCE*, **93**, 1967, SM1, pp 71-94.

Carey, G.F., "A dual Perturbation Expansion and Variational Solution for Compressible Flows using Finite Elements", *Finite Elements of Fluids, chap. 9*, John Wiley and Sons, N.Y., 1975.

Craig, R.F., "Soil Mechanics", *Van Nostrand Reinhold Co Ltd.*, 4rth edition 1987.

Davidson, J.H. and Harrison, D., "Fluidised particles", *Cambridge University Press*, 1963.

Davis, E.H., Gunn, M.J., Mair, R.J. and Senevirantne H.N., "The stability of shallow tunnels and underground openings in cohesive materials", *Geotechnique*, **30**, 1980, No. 4, pp 397-416.

Desai, C.S., "Elementary Finite Element Method", *Prentice Hall, N.J.*, 1979.

Falkiner, R.H. and Tough, S.G. "The Tyne Tunnel 2: Construction of the main tunnel", *Proceedings ICE*, **39**, Feb. 1968, pp 213-234.

Fredlund, D.G., Morgenstern, N.R. and Widger, R.A., "The shear strength of unsaturated soils", *Can. Geotech. J.*, **15**, 1978, pp 313-321.

Glossop, R. "The invention and early use of compressed air to exclude water from shafts and tunnels during construction", *Geotechnique*, **26**, 1976, No. 2, pp 253-280.

Hagimoto, H. and Kashima, Y., "D.K. shield method", *Tunnelling in soft and water bearing ground, Lyon*, 1984.

Harris, F., "Ground Engineering Equuipment and Methods", *Granada Publishing, U.K.*, 1983.

Haswell, C.K. and Gutteridge, D.R., "Specialist tunnelling processes", *Tunnel Construction '90, IMM*, 1990.

Haxton, A.F. and Whyte, H.E., "Clyde Tunnel: Constructional Problems", *Proceedings ICE*, **30**, Feb 1965, pp 323-346.

Hewett, B.H.M., and Johannesson, S., "Shield and Compressed air tunnelling", *McGraw Hill, New York*, 1922.

Hirokawa, H. and Nishthitake, S., "Slurry Shield Machine (Automatic Operation and Control)", *Tunnelling in soft and Water Bearing Ground, Lyon*, 1984.

Kell, J., "The Dartford Tunnel", *Proceedings ICE*, **24**, March 1963, pp 359-371.

Kimura, T. and Mair, R.J., "Centrifugal testing of model tunnels in soft clay', *Proc. 10th International Conference on Soil Mechanics and Foundation Engineering*, Stockholm, 1981.

Klinkenberg, L.J., "API Drilling Production and Practice", *Oil Weekly*, **104**, 24.

Kurosawa, S., "Up-to-date state of the art of Japanese shield: The selection

criteria of slurry shield and earth pressure balance shield", *Tunnelling in soft and water bearing ground, Lyon*, 1984.

Langfelder, A.M., Chen, A.M. and Justice, J.A., "Air permeability of compacted cohesive soils", *J. Soil Mech. Fnd. Div., ASCE*, **94**, 1968, SM4, pp 981-1001.

Lohner, R., Morgan, K. and Zienkiewicz. O.C., *Comp Meth Appl Mech Engr*, **51**, 441.

Marle, C.M., "Multiphase flow in porous media", *Technip, Paris*, 1981.

Matyas, E.L., "Air and Water Permeability of Compacted Soils", *Symposium on Permeability and Capillarity of Soils*, ASTM STP 417, 1968.

Megaw, T.M. and Bartlett, J.V., "Tunnels: Planning, Design, Construction", Vol. 1 & 2, *Ellis Horwood Ltd.*, 1981.

Michell, S.J., "Fluid and Particle Mechanics", *Pergamon Press, Oxford*, 1970.

Muskat, M., "The flow of Homogeneous Fluids Through Porous Media", *International Human Resources Development Corporation*, 1982 by copyright, McGraw Hill Book Co., Inc. 1937.

Nussbaumer, M., "Pipejacking in Water Saturated Ground", *Tunnel Construction '90, IMM*, 1990.

Olson, R.E. and Daniel, D.E., "Measurement of the hydrostatic conductivity of fine grained soils", *Permeability and groundwater containment transport*, ASTM STP 746, 1981, pp 18-64.

Othmer, D.F., "Fluidization", *Reinhold Publishing Co., NY*, 1956.

Pequignot, C.A., "Tunnels and Tunnelling", *Hutchinson & Co., Ltd.*, 1963.

Peraire, J., Vahadati, M., Morgan, K. and Zienkiewicz, O., "Adaptive Remeshing for Compressible Flow Computation", *Jnl Comp Phys*, **72**, 1987, No. 2.

Rouse, H., "Elementary Mechanics of Fluids", *Dover Publications, Inc., New York*, 1946.

Ruska Instrument Corporation, "Operating Manual for Ruska Porometer and Permeameter", Houston Texas.

Scenck, W. and Wagner, H., "Luftuerbrauch v. Uberdeckung beim Tunnelvortrieb mit Druckluft", *Bautechnik*, **2**, 1963.

Scherle, "Rohrvortrieb", Vol 1-4, *Bauverlage Wiesbaden und Berlin.*

Schreier, S., "Compressible Flow", *John Wiley and Sons, N.Y.*, 1982.

Shapiro, A.H., "The Dynamics and Thermodynamics of Compressible Fluid Flow", *Ronald Press Co., N.Y.*, 1953.

Smith, I.M. and Griffiths, D.V., "Programming the Finite Element Method", *2nd ed, John Wiley and Sons, U.K.*, 1988.

Smith, G.N. and Pole, E.C., "Elements of Foundation Design", *Granada Publishing Ltd., U.K.* 1980.

Sullivan, R.R. and Hertel, K.L., "The flow of air through porous media", *Jounal of applied Physics*, 1940, Vol. II, pp 761-765.

Szechy, K., "The art of tunnelling", *Akademiai Kiado, Budapest*, 1973.

Toll, D.G., "Framework for unsaturated soil behavior", *Geotechnique*, **40**, 1990, No.1, pp 31-44.

Toll, D.G. and Hight, D.W., "On the Desaturation and Drying of Soil", *unpublished*, 1990.

Topp, G.C. and Miller, E.E., "Hysteretic moisture characteristics and hydraulic conductivities for glass-bead media", *Soil Sci. Amer. Proc.*, **30**, 1966, pp 156-162.

Yoshimi, V. and Osterberg, J.O. "Compression of partially saturated cohesive soils", *J. Soil Mech. Fnd. Div., ASCE*, **89**, 1963, SM4, pp 1-24.